



PHD

Synthesis of novel sialidase inhibitors to target influenza A virus and Chagas' disease

Resende, Ricardo

Award date:
2010

Awarding institution:
University of Bath

[Link to publication](#)

Alternative formats

If you require this document in an alternative format, please contact:
openaccess@bath.ac.uk

Copyright of this thesis rests with the author. Access is subject to the above licence, if given. If no licence is specified above, original content in this thesis is licensed under the terms of the Creative Commons Attribution-NonCommercial 4.0 International (CC BY-NC-ND 4.0) Licence (<https://creativecommons.org/licenses/by-nc-nd/4.0/>). Any third-party copyright material present remains the property of its respective owner(s) and is licensed under its existing terms.

Take down policy

If you consider content within Bath's Research Portal to be in breach of UK law, please contact: openaccess@bath.ac.uk with the details. Your claim will be investigated and, where appropriate, the item will be removed from public view as soon as possible.

Synthesis of novel sialidase inhibitors to target influenza A virus and Chagas' disease

Ricardo Resende

A thesis submitted for the degree of Doctor of Philosophy

University of Bath

Department of Pharmacy and Pharmacology

September 2010

COPYRIGHT

Attention is drawn to the fact that copyright of this thesis rests with its author. A copy of this thesis has been supplied on condition that anyone who consults it is understood to recognise that its copyright rests with the author and they must not copy it or use material from it except as permitted by law or with the consent of the author.

This thesis may be available for consultation within the University Library and may be photocopied or lent to other libraries for the purposes of consultation

Signed

Date

Abstract

This thesis is divided into two parts. Part One describes inhibitors towards influenza neuraminidase and Part Two describes inhibitors towards *Trypanosoma cruzi* *trans*-sialidase.

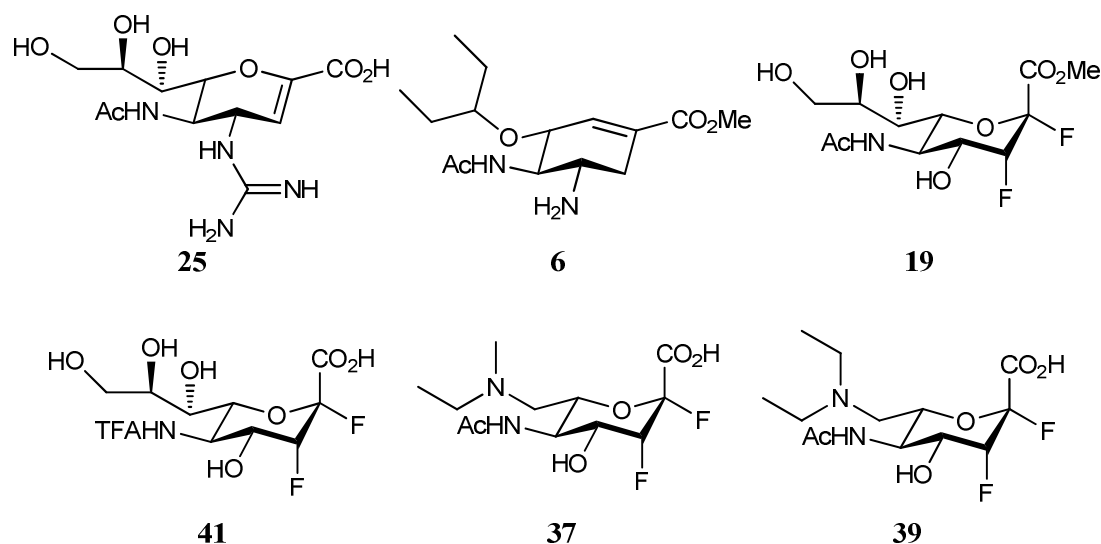
In Part One, a description of the influenza virus is given followed by details of the current approved therapies and our approach.

Influenza is a virus that has the ability to cause a pandemic with a possible high mortality rate. The life cycle of the influenza virus exhibits several key stages that, if inhibited, would hinder its replication and have potential as therapeutic targets. The two currently approved drugs on the market (zanamivir (**25**) and oseltamivir (**6**)) target influenza neuraminidase. Influenza neuraminidase has the function of cleaving terminal sialic acid groups from glycoconjugates present at the surface of cells, enabling the release of the newly formed viral particles.

Our strategy towards the syntheses of novel inhibitors against influenza neuraminidase is based on 2,3-difluorosialic acid (**19**). Modifications were made at position C-5 of sialic acid to replace the 5-*N*-acetamido with a 5-*N*-trifluoroacetamido group. The formation of 5-*N*-trifluoroacetamido-2,3-difluorosialic acid (**41**) was achieved by deprotecting 5-*N*-acetamido-2,3-difluorosialic acid (**52**) using methanesulfonic acid. Modifications were also performed at position C-7, introducing a series of 7-*N*-alkylamines on 2,3-difluorosialic acid (**47**) by oxidative cleavage of the glycerol side chain and reductive amination.

A series of 4-*epi-N*-alkylamines were introduced onto the Neu5Ac2ene moiety, with the intention of probing the size of the enzyme pocket available in the surroundings of position C-4.

The C-4, C-5 and C-7 modified compounds were tested against a panel of influenza viruses (CSIRO). Furthermore, 7-*N,N*-diethylamino-2,3-difluorosialic acid (**39**) was tested against influenza neuraminidase N9. The compounds showed poor levels of inhibition, with the IC₅₀'s referring to the influenza neuraminidase N9 wild type, being 326 and 68 mM for the 7-*N*-ethyl-*N*-methylamino (**37**) and 7-*N,N*-diethylamino-2,3-difluorosialic acid (**39**), respectively.

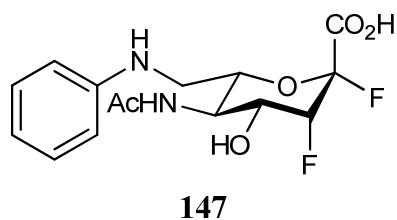
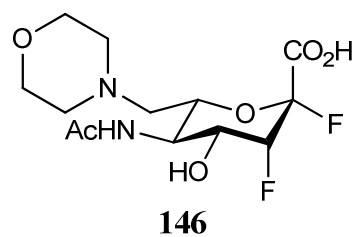
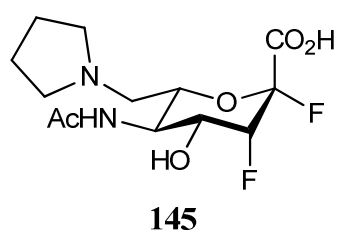


In Part Two, a description of Chagas' disease is given followed by the currently approved therapies and our approach.

Chagas' disease is endemic in Central and South America and is caused by a parasite, *Trypanosoma cruzi*. There are currently two approved drugs to treat Chagas's disease, and both have a similar mode of action, inducing oxidative stress in the parasite.

Our approach is to target *Trypanosoma cruzi* *trans*-sialidase (TcTS), which has two important roles in the life cycle of the parasite. TcTS cleaves sialic acid from glycoconjugates present at the host cell surface and transfers them to mucin like receptors present on the parasite. This action allows the parasite to evade the host defence mechanisms. In addition, TcTS enables the parasite to enter the host cell during the infection process.

Our strategy towards the synthesis of novel inhibitors against *Trypanosoma cruzi* *trans*-sialidase is based on 2,3-difluorosialic acid (**19**), akin to the inhibitors developed in Part One. Several modifications were made at position C-7 via cleavage of the glycerol side chain and introducing a series of cyclic 7-*N*-alkylamines by reductive amination.



The synthesised compounds were then tested against trypomastigotes, the infectious form of the parasite. The inhibitory results showed an IC_{50} of 3.1 mM for 7-*N*-pyrrolidino-2,3-difluorosialic acid (**145**); 35.5 mM for 7-*N*-morpholino-2,3-difluorosialic acid (**146**); and 4.2 mM for 7-*N*-anilino-2,3-difluorosialic acid (**147**).

Acknowledgements

I would like to say thank you to the University of Bath for the PhD scholarship that was awarded to me.

I would like to say thank you to Abbey Santander for the travel grant that was awarded to me and allowed me to travel to Argentina and have a glimpse to the biological side of medicinal chemistry.

I would like to say thank you to my supervisor, Dr. Andrew Watts for the support and patience (lots of it) throughout these long years, specially during this last year.

I would also like to thank Dr. Jenny Mckimm-Breschkin for testing our inhibitors against a series of influenza virus as well as providing the crystal structure of one inhibitor.

I would like to say thank you to Dr Frasci for allowing me to go to his laboratory in Argentina and learn how to set up a biological assay. Laura Ratier helped me greatly whilst my stay in Buenos Aires, teaching me the basis of a biological assay.

I would like to acknowledge all the input that Dr. Tim Woodman gave with my NMR spectra, the helping hand by proof reading my thesis and for convincing me that it is possible to run, up!, the hills in Bath! Dr. Anneka Lubben for her contribution and technical help regarding mass spectrometry instrumentation and data processing.

To my group (Benjamin, Christian, Patricia, Stefan and Terrence) for being such great company and for dealing (very well) with my blindness when it comes to search for chemicals.

I would like to thank all the people that have belonged to the research laboratory of 3.11 during the last four years. It has been a long and interesting journey that you all made fun and enjoyable.

I would like as well to say thank to the people in the department that I got to know during these four years.

I would like to give a big thank you to my family for all the love, support, encouragement, ..., that they gave me during all these years! Há coisas que não se demonstram com palavras mas sim com gestos.. Muito obrigado!

I will not name individual people, instead will just leave a big hug to all of my friends that, wherever they are now, gave me the strength to start my PhD and in particular to survive the period of writing up. Thank you!

Contents

Abstract	i
Acknowledgements	v
Contents	vii
List of Figures	xi
List of Graphs	xv
List of Schemes	xvi
List of Tables	xix
Glossary	xx
Functional group structures	xxiii

Chapter 1 - General Introduction

1.1 Sialic acids in Nature: structures and roles	1
1.2 Carbohydrate processing enzymes	3
1.2.1 Inverting glycosidases	4
1.2.2 Retaining glycosidases	5
1.3 Inhibitors of retaining glycoside hydrolases	9
1.3.1 Competitive glycosidase inhibitors	9
1.3.2 Covalent inhibitors	10
1.3.3 Fluorinated carbohydrates as mechanism-based inhibitors of retaining glycosidases	12
1.4 Thesis overview	15

Part One

Chapter 2 - Introduction to influenza A virus

2.1 Prelude	17
2.2 The influenza A virus family	18
2.3 Structure and life cycle of influenza A virus	18
2.4 Nomenclature of influenza A viruses and their sub-types	21
2.5 Therapeutic targets for the clinical treatment of influenza A infection	22
2.5.1 M2 ion-channels	22

2.5.2 RNA transcription	23
2.5.3 Influenza neuraminidase	24
2.6 Overview of competitive inhibitors of influenza neuraminidase	27
2.6.1 Zanamivir	27
2.6.2 Oseltamivir	30
2.6.3 Novel clinical candidates	33
2.7 Aims of the present project	35
 Chapter 3 - Synthesis of C-7 modified 2,3 difluorosialic acids	 43
3.1 Prelude	43
3.2 Retrosynthetic analysis	44
3.3 The synthesis of 2,3-difluorosialic acid (47)	45
3.4 Investigation the conditions for the synthesis of the anomeric fluoride	51
3.5 Preliminary investigations into the oxidative cleavage and reductive amination synthesis of a series of 7- <i>N,N</i> -dialkylamino 2,3-difluorosialic acids	55
3.5.1 Formation of the methyl sialoside (70)	59
3.5.2 Formation of the benzyl sialoside (75)	61
3.5.3 Formation of the <i>para</i> -methoxybenzyl sialoside (82)	64
3.6 Synthesis of a series of 7- <i>N</i> -alkylamino 2,3-difluorosialic acids	65
 Chapter 4 - Synthesis of 5-<i>N</i>-trifluoroacetamido-2,3-difluorosialic acid (94)	 69
4.1 Rationale	69
4.2 Synthesis of the 5- <i>N</i> -trifluoroacetamido-2,3-difluorosialic acid (94)	70
 Chapter 5 - Synthesis of C-4 <i>N</i>-alkylamino Neu5Ac2ene derivatives	 75
5.1 Prelude	75
5.2 Rationale	76
5.3 Retrosynthetic analysis of the formation of the series of 4- <i>epi-N</i> -alkylamines (97)	77
5.4 Synthesis of the common precursor, oxazoline (99)	78
5.5 Overview of the use of palladium for the formation of C-C bonds	80
5.6 Palladium-catalysed allylic amination for the direct synthesis of <i>epi</i> -4- <i>N</i> -alkylamino Neu5Ac2ene derivatives	85

5.7 Synthesis of 4-epi-azido (131) and 4-epi- <i>N</i> -amino Neu5Ac2ene (126)	91
5.7.1 Studies towards the introduction of an azide at C-4 of oxazoline (99)	92
5.7.2 Synthesis of the 4-epi-azido Neu5Ac2ene (131)	94
5.7.3 Synthesis of the 4-epi- <i>N</i> -amino Neu5Ac2ene (126)	95

Chapter 6 - Inhibitory activity of a series of 7-*N*-alkylamino

2,3-difluorosialic acids against a panel of influenza viruses	97
6.1 Crystal structure obtained with 7- <i>N,N</i> -diethylamino-2,3-difluorosialic acid (39) and influenza neuraminidase N9	98
6.2 Point mutations conferring resistance towards influenza neuraminidase inhibitors	99
6.3 Inhibition of a panel of influenza viruses with 7- <i>N</i> -alkylamine 2,3-difluorosialic acids	103
6.3.1 IC ₅₀ results obtained against a panel of influenza viruses (CSIRO)	103
6.3.2 Determination of the <i>K_i</i> for 7- <i>N,N</i> -diethylamino-2,3-difluorosialic acid (39)	107
6.4 Inhibition results obtained for the 4-epi- <i>N</i> -alkylamino Neu5Ac2ene derivatives (42), (43) and (131) against a panel of influenza viruses (CSIRO)	109

Chapter 7 - Conclusions **113**

Part Two

Chapter 8 - Introduction to Chagas' disease and *Trypanosoma cruzi* **117**

8.1 Historical perspectives, prevalence and modes of infection	117
8.2 Life-cycle of the <i>Trypanosoma cruzi</i> parasite and the progression of Chagas' disease	118
8.3 Current treatments for Chagas' disease	120
8.3.1 Mode of action of currently approved drugs	121
8.3.2 Side-effects associated with current therapies	122
8.4 Novel therapeutic targets for inhibition of <i>Trypanosoma cruzi</i>	122
8.5 <i>Trypanosoma cruzi</i> trans-sialidase	123
8.5.1 Catalytic mechanism	125

8.5.2 Active site architecture of TcTS	127
8.6 The development of novel inhibitors of <i>Trypanosoma cruzi</i> trans-sialidase	129
8.7 Aims of the present project	132
Chapter 9 - Synthesis of 7-<i>N</i>-alkylamino modified 2,3 difluorosialic acids and their biological evaluation against TcTS and trypomastigotes	135
9.1 Prelude	135
9.2 IC ₅₀ determination of the inhibitors (145 – 147)	138
9.3 Evaluation of the ability of the inhibitors to prevent the infection of cells by trypomastigotes	142
Chapter 10 - Conclusions	147
Chapter 11 - Experimental	149
11.1 General	149
11.2 Synthesis	150
11.3 Biology	201
11.3.1 Inhibition of influenza neuraminidase	201
11.3.2 Inhibition of <i>Trypanosoma cruzi</i> trans-sialidase	201
11.3.2.1 IC ₅₀ determination	201
11.3.2.2 Inhibition of the infection of cells by trypomastigotes	202
Chapter 12 - References	204

List of Figures

Figure 1: General structures of the major sialic acid classes, with the numbering of the carbon backbone indicated. Substituents at C-5 generally include a -hydroxyl, -amino, *N*-glycol or an *N*-acetamido group (**1 – 4**). 1


Figure 2: The role of sialic acid of masking an erythrocyte and the mechanism of binding to a macrophage. \ominus sialic acid; ■ galactose; ○ and ▽ other residues;  galactose specific receptor on the macrophage surface. 2

Figure 3: Two examples of mechanism-based inhibitors (**9** and **10**) towards yeast- α -glucosidase and almond- β -glucosidase, and the mechanism of formation of the reactive aglycones (**13** and **14**). 12

Figure 4: Structures of some fluorinated glycosides. DNP – 2,4-dinitrophenyl, TNP 2,4,6 trinitrophenyl. 14

Figure 5: Cartoon illustration of an influenza virus particle. Details of hemagglutinin, neuraminidase, the M2 ion channels and the RNA material (RNP) are shown. 19

Figure 6: Schematic representation of the replication cycle of influenza A virus. 20

Figure 7: Cartoon representation of the different stages involved with an influenza virion proceeding across the human airway epithelium to reach a suitable endocytic site. 21

Figure 8: Illustration of the process of antigenic drift and shift in influenza virus. a) Small mutations occurring during replication; b) Genetic information exchange between different strains of influenza virus. 22

Figure 9: Interactions of 4-guanidino Neu5Ac2ene (**25**) with the different residues present at the active site of influenza A N1. Generated with LigPlot⁺ (PDB 2HTQ). 29

Figure 10: a) Interactions of oseltamivir (**33**) with the catalytic amino acid residues of neuraminidase subtype N8. b) Superimposed view of the active site of influenza neuraminidase, subtype N9 (blue) with Neu5Ac2ene (**27**) and subtype N8 (green) with oseltamivir (**33**) where it is possible to observe the movement of Glu276 and Arg224. Generated with PyMOL and LigPlot⁺ (PDB's 1F8B, blue, and 2HT8, green). 32

Figure 11: Overview of the aldolase reaction over 5 days, showing the consumption of β -fluoropyruvic acid (δ -233.3 ppm) and the formation of the product,

3-fluorosialic acid (δ -208.3 ppm). t - time; A – β -fluoropyruvic acid; B – C-3 equatorial fluorine; C – C-3 axial fluorine (desired product). 46

Figure 12: ^1H NMR spectrum of the oxidative cleavage reaction, showing the formation of a signal at δ 8.06 ppm after 15 min. 57

Figure 13: Mass spectrum of the C-7 aldehyde 2,3-difluorosialic acid (**46**). 58

Figure 14: Interactions of the *N*-acetyl group with Arg152, Ile222 and Trp178. Generated with LigPlot⁺ (PDB 2C4A). 70

Figure 15: Possible interactions with glutamate or aspartate residues around C-4 position of sialic acid bound in the active site of influenza neuraminidase N2 with an axial or equatorial amino substituent at this position, respectively. Generated with PyMOL (PDB 2BAT). 76

Figure 16: Example of an oxidative addition between $\text{Pd}(\text{PPh}_3)_4$ and a general molecule X-Y. 81

Figure 17: Structures of the different catalyst (**109** - **113**) used for the opening of the oxazoline (**99**) with a series of *N*-alkylamines (**114** - **116**). 85

Figure 18: NOESY spectrum of 4-*epi-N*-sulfonamide (**120**) where the interaction between H-6 and the methylamine can be observed (highlighted with a circle). 89

Figure 19: Mass spectrum showing the sodium peak (479.1379 m/z) of the per-*O*-acetylated-4-*epi*-azido Neu5Ac2ene (**128**). 94

Figure 20: Superimposition of the view of 7-*N,N*-diethylamino-2,3-difluorosialic acid (**39**) covalently bound in the active site of influenza neuraminidase N9 (green) with the uncomplexed influenza neuraminidase N9 (blue). Only the residues interacting with the diethylamino side chain are shown. Generated with PyMOL (PDB unpublished, green, and 2C4A, blue). 98

Figure 21: Mutants of influenza neuraminidase known to confer resistance to the currently approved drugs and their interactions with C-4, C-5 and glycerol side chain of Neu5Ac2ene. 99

Figure 22: Superimposition of the active site of wild type N9 (blue) with Neu5Ac2ene (**27**) present in the active site and Glu119Gly N9 (green). Generated with PyMOL (PDB 1F8B, blue, and 1L7G, green). 100

Figure 23: Superimposition of the active site of wild type N9 (blue) with Neu5Ac2ene (**27**) bound in the active site, and the active site of N9, with the Arg292Lys mutation (green). Generated with PyMOL (PDB 1F8B, blue, and 2QWB, green). 101

Figure 24: Superimposition of the active sites of the wild type N9 (blue) and the His274Tyr N1 (green) with Neu5Ac2ene bound in the active site. Generated with PyMOL (PDB 1F8B, blue, and 3CKZ, green).	102
Figure 25: Geographical distribution of Chagas' disease in Central and South America.	117
Figure 26: Reduviid insect, the natural reservoir for the <i>Trypanosoma cruzi</i> parasite.	118
Figure 27: Life-cycle of the <i>Trypanosoma cruzi</i> parasite in the reduviid insect (red arrows) and in a human host (blue arrows).	119
Figure 28: Characteristic sign of a reduviid insect bite, called the Romañas' sign.	120
Figure 29: Mode of action of a molecule containing a nitro group.	121
Figure 30: The role of TcTS on the transfer of sialic acid from a host cell glycoconjugate (blue sphere) to a mucin receptor at the surface of the parasite (orange sphere).	124
Figure 31: Role of <i>Trypanosoma cruzi</i> trans-sialidase on transferring sialic acid from host glycoconjugates and its biological effects when it is free from the parasitic surface.	125
Figure 32: A monomeric subunit of TcTS (in Corey-Pauling-Kolton form). Generated with PyMol (PDB 1MS4).	127
Figure 33: Representation of the catalytic site of <i>Trypanosoma cruzi</i> trans-sialidase with Neu5Ac2en (27) binding to the key amino acids. Generated with LigPlot ⁺ (PDB 1MS8).	128
Figure 34: Cartoon representation of <i>Trypanosoma cruzi</i> trans-sialidase.	129
Figure 35: Structures of inhibitors towards the donor active site.	130
Figure 36: Structures of inhibitors towards the lactose binding site as well as both binding sites.	131
Figure 37: Structures of novel fluorinated inhibitors of <i>Trypanosoma cruzi</i> trans-sialidase.	131
Figure 38: Representation of the interactions within the active site with the C-9 benzoylamide (143) and the amino acid residues. Generated with LigPlot ⁺ (PDB 3B69).	132
Figure 39: Illustration of the procedure for the determination of the IC ₅₀ .	139
Figure 40: Illustration of the assay for the inhibition of trypomastigotes assay, with the key steps shown.	143

Figure 41: Example of an image from one of the experiments. The presence of infected cells (circle) and healthy cells (square) is evident. The dots inside the cell are amastigotes

144

List of Graphs

Graph 1: Plotting the residual activity <i>versus</i> time, giving the initial rate of the reaction and the time at which the inhibitor has inhibited the enzyme (steady-state). \square – 100 μM ; \diamond – 250 μM ; \circ – 2.5 mM of inhibitor (39).	108
Graph 2: Lineweaver-Burk plot, where the intercept at y axis gives the inverse of V_{\max} and the gradient gives K_i/V_{\max} .	109
Graph 3: IC_{50} determination for inhibitor 7- <i>N</i> -pyrrolidino-2,3-difluorosialic acid (145).	140
Graph 4: IC_{50} determination for inhibitor 7- <i>N</i> -morpholino-2,3-difluorosialic acid (146).	140
Graph 5: IC_{50} determination for inhibitor 7- <i>N</i> -anilino-2,3-difluorosialic acid (147).	141
Graph 6: Rate of infection at different concentrations of the inhibitors (145) – (147).	145

List of Schemes

Scheme 1: Proposed mechanism of action for inverting α -glycosidases. R - Glycoconjugate.	5
Scheme 2: Proposed mechanism of action for retaining β -glycosidases. R - Glycoconjugate.	6
Scheme 3: Proposed mechanism of action for substrate assisted α -glycosidases. R - Glycoconjugate.	8
Scheme 4: General proposed mechanism of inactivation of retaining β -glycosidase by a fluorinated- β -glucoside. HLG – Protonated leaving group	13
Scheme 5: Proposed mechanism of hydrolysis of the sialic acid from the glycoconjugate (R) by influenza neuraminidase.	26
Scheme 6: Proposed catalytic mechanism for <i>Trypanosoma cruzi</i> trans-sialidase. R - Glycoconjugate.	37
Scheme 7: Neuraminidase catalytic reaction with 2,3-difluorosialic acid (19).	39
Scheme 8: Retrosynthetic scheme outlining the strategy for the synthesis of a series of 7- <i>N,N</i> -dialkylamino 2,3-difluorosialic acids.	44
Scheme 9: Aldolase reaction. Neu5Ac aldolase, H ₂ O, r.t., 5 days.	45
Scheme 10: Aldol reaction between <i>N</i> -acetylmannosamine (48) and β -fluoropyruvic acid (49) catalysed by Neu5Ac aldolase. The numbering of the carbon backbone is indicated corresponding to the final compound, 3-fluorosialic acid (51).	47
Scheme 11: Formation of per- <i>O</i> -acetylated 3-fluorosialic acid (53) a) TFA, MeOH, r.t., O/N; b) Ac ₂ O, Pyr, r.t., 5 days. 72% from the aldolase reaction.	48
Scheme 12: Anomeric deprotection of per- <i>O</i> -acetylated (53). Hydrazine acetate, DCM/MeOH 1:1, 4 °C, 3h, 65%.	49
Scheme 13: Mechanism of fluorination of the hemiketal (54) using DAST (55) as the fluorinating agent. DAST, DCM, -30 °C, 30 min, 45%.	50
Scheme 14: Deacetylation of per- <i>O</i> -acetylated 2,3-difluorosialic acid (58). NaOMe, MeOH, 4 °C → r.t., 1h, 100%.	50
Scheme 15: Proposed mechanism for the formation of the 2,3-difluorosialic acid methyl ester (59).	51
Scheme 16: Possible mechanism towards the formation of compound 59 and 64 with DAST (55) in the presence of THF (63).	54

- Scheme 17: Oxidative cleavage of 2,3-difluorosialic acid (**47**). NaIO₄, H₂O, r.t., 1h30 min. 55
- Scheme 18: Proposed mechanism for the oxidative cleavage of the glycerol side chain of 2,3-difluorosialic acid methyl ester (**47**) using sodium periodate. 56
- Scheme 19: Reductive amination of the aldehyde (**46**). Diethylamine, NaCNBH₃, AcOH, MeOH, r.t., O/N. 58
- Scheme 20: Formation of 3-fluorosialic acid methyl sialoside. a) NaH, MeI, DMF, r.t., 2h, 68%; b) NaOMe, MeOH, r.t. O/N, 100%. 59
- Scheme 21: Formation of 7-*N*-ethylamine-3-fluorosialic acid. a) 0.4 M NaIO₄, H₂O, r.t., 30 min; b) Ethylamine, NaCNBH₃, AcOH, MeOH, r.t., O/N; c) 1 M HCl, H₂O, r.t. 60
- Scheme 22: Formation of 7-*N*-ethylacetamido (**70**) and diethylamine (**78**) 3-fluorosialic acid benzyl sialoside. a) NaH, BnBr, DMF, r.t., 1 day, 95%; b) NaOMe, MeOH, r.t., 1h, 95%; c) NaIO₄, H₂O, r.t., 30 min; d) i) Amine, AcOH, NaCNBH₃, MeOH, r.t., O/N; ii) Ac₂O, Pyr, r.t., O/N. 36% for 7-*N*-ethyl-*N*-acetamido (**77**) (over 3 steps); 2% for 7-*N,N*-diethylamino (**78**) (over 3 steps). 62
- Scheme 23: Formation of 7-*N*-ethylacetamido-2,3-difluorosialic acid (**80**). a) H₂, Pd/C (10%), THF, AcOH, r.t., 10 days, 48%; b) DAST, DCM, -30 °C, 30 min, 50%. 63
- Scheme 24: Formation of 4,7-di-*O*-acetyl-3-fluorosialic acid *p*MB sialoside (**83**). a) NaH, *p*MBCl, DMF, r.t., 1 day, 86%; b) NaOMe, MeOH, r.t., O/N, 81%; c) NaIO₄, H₂O, r.t., 30 min; d) i) Diethylamine, AcOH, NaCNBH₃, MeOH, r.t., O/N; ii) Ac₂O, Pyr, r.t., O/N, 10% from the C-7 aldehyde. 65
- Scheme 25: Formation of 5-*N*-trifluoroacetamido-3-fluorosialic acid (**90**). a) MsOH, MeOH, reflux, 1 day; b) TFA₂O, Et₃N, MeOH, 4 °C, 1h; c) Ac₂O, Pyr, r.t., 5 days, 20 % (over 3 steps). 71
- Scheme 26: Formation of 5-*N*-trifluoroacetamido-2,3-difluorosialic acid (**94**). a) Hydrazine acetate, DCM/MeOH 4:1, 4 °C, 3h, 67%; b) DAST, DCM, -30 °C, 30 min, 44%; c) NaOMe, MeOH, 4 °C → r.t., 1h, 100%; d) NaOH, H₂O, 4 °C, 1h, 100%. 72
- Scheme 27: Retrosynthetic pathway for the formation of a series of 4-*epi-N,N*-alkylamino Neu5Ac2ene (**97**). 78
- Scheme 28: Acetylation of sialic acid (**102**). i) TFA, MeOH, r.t., O/N; ii) Ac₂O, Pyr, r.t., 4 days, 81% (over 2 steps). 78

Scheme 29: Mechanism of formation of the per- <i>O</i> -acetylated Neu5Ac2ene (100). TMSOTf, MeCN, r.t., O/N, 75%.	79
Scheme 30: Mechanism for the formation of oxazoline (99). TMSOTf, MeCN, 50 °C, O/N, 76%.	80
Scheme 31: General method for the formation of π -allylpalladium complexes.	82
Scheme 32: Opening of the oxazoline with the aid of a palladium (0) complex.	83
Scheme 33: The two different pathways that the nucleophilic <i>N</i> -alkylamine can use to attack the palladium complex, in both cases from the <i>re</i> -face.	84
Scheme 34: Formation of sulfonamides (120 and 121). TsCl, DCM, r.t., O/N, 38% for 120 and 29% for 121 .	89
Scheme 35: Retrosynthetic analysis towards 4- <i>epi-N</i> -amino Neu5Ac2ene (126).	92
Scheme 36: Formation of 4-azido Neu5Ac2ene (131). a) NaOMe, MeOH, 4 °C, 2h, 92%; b) 1M NaOH, H ₂ O, 4 °C, 1h, 100%.	94
Scheme 37: Formation of 4-amino Neu5Ac2ene (126). a) Pd ₂ (dba)(PPh ₃) ₂ , TMSN ₃ , THF, 50 °C, O/N, 30%; b) 1,3-propanedithiol, Et ₃ N, MeOH, 4 °C → r.t., 2h, 63%; c) NaOMe, MeOH, 4 °C, 2h, 54%; d) 1M NaOH, H ₂ O, 4 °C, 1h, 100%.	95
Scheme 38: Catalytic mechanism of <i>Trypanosoma cruzi</i> <i>trans</i> -sialidase.	126

List of Tables

Table 1: Overview of the different conditions used for the fluorination step. Ratios of isomers determined by ^{19}F NMR. ^a Supplied in THF; ^b Supplied in toluene; a Not isolated.	53
Table 2: Combine yields of the different 7- <i>N</i> -alkylamines synthesised.	67
Table 3: Yields for the saponified final compounds, 7- <i>N</i> -alkylamine 2,3-difluorosialic acids.	68
Table 4: Resume of the conditions used to synthesise the series of 4- <i>N</i> -alkylamines with an axial orientation.	86
Table 5: The series of 4- <i>epi-N</i> -alkylamines (117 - 119) synthesised.	88
Table 6: Yields of the different 4- <i>epi-N</i> -alkylamines (123 - 125) synthesised.	90
Table 7: Yields for the saponified final compounds, 4- <i>epi-N</i> -alkylamino Neu5Ac2ene (42 - 44)	91
Table 8: Different conditions used in order to introduce the azide in an equatorial orientation. ^a Stereochemistry of the OH group is undetermined; ^b Microwave reaction set at 100 °C.	93
Table 9: Comparison of the ^{13}C NMR chemical shifts for the 4- <i>epi</i> -azido and 4-azido Neu5Ac2ene derivatives (128 and 129).	93
Table 10: IC ₅₀ values obtained for the inhibitors given in μM . wt – wild type.	105
Table 11: IC ₅₀ values obtained for the inhibitors are given in μM . wt – wild type, ^a No data available.	106
Table 12: IC ₅₀ values obtained for the inhibitors are given in μM . wt - wild type.	111
Table 13: IC ₅₀ values obtained for the inhibitors are given in μM . wt – wild type.	111
Table 14: Yields of the different 7- <i>N</i> -alkylamines synthesised (148 – 150).	137
Table 15: Yields for the saponified final compounds (145 - 147).	138
Table 16: IC ₅₀ values for the inhibitors (145 – 146).	141

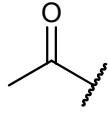
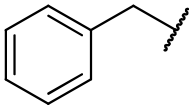
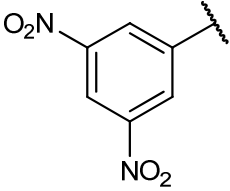
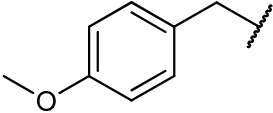
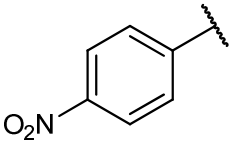
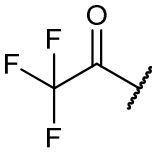
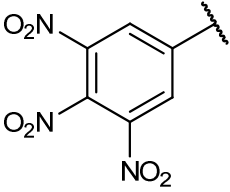
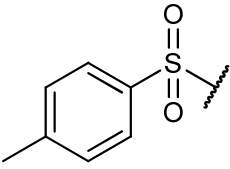
Glossary

Abbreviation	Meaning
δ	Chemical shift
$^{\circ}\text{C}$	Degree(s) Celsius
Ac_2O	Acetic anhydride
AcOH	Acetic acid
Arg	Arginine
CRP	Complement regulatory protein
Ax	Axial
Bn	Benzyl
br	Broad
Brine	Saturated solution of sodium chloride
BSA	Bovine serum albumin
CD_3OD	Deuterated methanol
CDCl_3	Deuterated chloroform
d	Doublet
D_2O	Deuterium oxide
DAST	(Diethylamino)sulphur trifluoride
dba	Dibenzylideneacetone
DCM	Dichloromethane
dd	Doublet of doublets
ddd	Doublet of doublet of doublets
Deoxo-fluor	Bis(2-methoxyethyl)aminosulfur trifluoride
DMF	Dimethylformamide
DNA	Deoxyribonucleic acid
DNP	2,4-dinitrophenyl
<i>e.g.</i>	<i>Exempli gratia</i> (As an example)
Eq	Equatorial
ESI	Electrospray ionisation
ESR	Electron spin resonance

Abbreviation	Meaning
Et ₃ N	Triethylamine
EtOAc	Ethyl acetate
Et ₃ P	Triethylphosphine
FBS	Fetal bovine serum
Gln	Glutamine
Glu	Glutamic acid
Gly	Glycine
GPI	Glycosylphosphatidylinositol
H	Hour(s)
Hepes-Na	4-(2-hydroxyethyl)-1-Piperazineethanesulfonic acid sodium salt
His	Histidine
HMBC	Heteronuclear multiple bond coherence
HMQC	Heteronuclear multiple quantum coherence
HRMS	High resolution mass spectrometry
Hz	Hertz
IC ₅₀	Half maximal (50%) inhibitory concentration (IC)
<i>i.e.</i>	<i>Id est</i> (That is)
<i>J</i>	Coupling constant
<i>K_i</i>	Inhibition constant
Lys	Lysine
M	Multiplet
MeCN	Acetonitrile
MeOH	Methanol
MHz	Megahertz
Min	Minute(s)
mM	Millimolar
m.p.	Melting point
MsOH	Methanesulfonic acid
NMR	Nuclear magnetic resonance

Abbreviation	Meaning
NOESY	Nuclear Overhauser effect spectroscopy
<i>p</i>	<i>Para</i>
PI-PLC	Phosphatidylinositol-phospholipase C
Pd ₂ (π -allyl) ₂ Cl ₂	Allylpalladium (II) chloride dimer
Pd ₂ (dba) ₃	Tri(dibenzylideneacetone)dipalladium
Pet Ether	Petroleum ether (40 – 60 °C)
<i>p</i> MBCl	<i>para</i> -Methoxybenzyl chloride
<i>p</i> NP	<i>para</i> -Nitrophenyl
ppm	Parts per million
Pyr	Pyridine
q	Quartet
RNA	Ribonucleic acid
r.t.	Room temperature
s	Singlet
SAPA	Shed acute phase antigen
SOD	Superoxide dismutase
t	Triplet
TcTS	<i>Trypanosoma cruzi trans</i> -sialidase
TFA	Trifluoroacetic acid
THF	Tetrahydrofuran
t.l.c.	Thin layer chromatography
TMSN ₃	Azidotrimethylsilane
TMSOTf	Trimethylsilyl trifluoromethanesulfonate
TNP	2,4,6-Trinitrophenyl
Tol	Toluene
Ts	<i>para</i> -Toluenesulfonyl chloride
Tyr	Tyrosine
Val	Valine
WHO	World Health Organization
Wt	Wild type

Functional group structures

Symbol	Structure
Ac	
Bn	
DNP	
<i>p</i> MB	
<i>p</i> NP	
TFA	
TNP	
Ts	

Chapter 1 - General Introduction

1.1 Sialic acids in Nature: structures and roles

Sialic acid is the generic name given to a family of carboxylic acid containing monosaccharides. This family comprises over 40 different compounds with common characteristics that include a 9-carbon backbone and a carboxylic acid at C-1 (pKa ~2.2) conferring a negative charge to the molecule under physiological conditions (Figure 1).¹

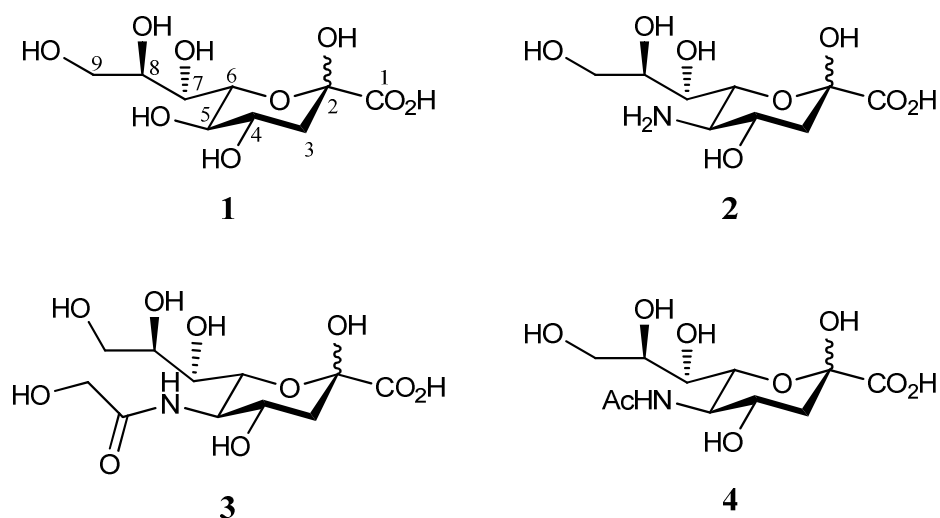


Figure 1 General structures of the major sialic acid classes, with the numbering of the carbon backbone indicated. Substituents at C-5 generally include a -hydroxyl, -amino, *N*-glycol or an *N*-acetamido group (1 – 4).

There are several possible substituents commonly found at C-5, such as a hydroxyl, amino, *N*-glycol or *N*-acetamido group, which define the four major classes in the sialic acid family: deaminoneuraminic acid (KDN) (1), neuraminic acid (2), *N*-glycolylneuraminic acid (Neu5Gc) (3) and *N*-acetylneuraminic acid (Neu5Ac) (4).¹⁻³ Guntar Blix, Ernst Klenk and Alfred Gottschalk were the pioneers of sialic acid research, with Gottschalk publishing the first book on sialic acids, Klenk the first to introduce the term neuraminic acid, and Blix the first to crystallise a number of sialic acid derivatives.^{4,5} As a group, the three collectively agreed on a common term to define the family generally as sialic acids, and the individual members of the family, defined as derivatives of neuraminic acid (2).^{4,5}

The vast numbers of sialic acids found in nature result from the numerous modifications that are observed on the hydroxyl groups present at C-7, 8 and 9 of the glycerol side chain, where they are often found to be acetylated.¹

Sialic acids are commonly present as the terminal carbohydrate moieties on glycoproteins and gangliosides, which are frequently expressed at the outer cell membrane. Sialic acids are therefore exposed to the blood plasma and due to their inherent negative charge (carboxylate) they are associated with influencing the mobility of cells and cations (for instance Ca^{2+}).¹ Sialic acids are associated with several important roles in human biology, such as having a possible interaction with neuronal plasticity, and maintaining a normal filtering function of the glomerular epithelium.⁶⁻¹¹ In addition to the previous features, sialic acids are also involved in the masking of cells, such as erythrocytes, from target receptors (Figure 2). Erythrocytes are covered with a layer of sialic acid containing glycoconjugates, and throughout their life span, sialic acids are slowly cleaved from the surface by the action of serum sialidases and spontaneous hydrolysis.¹ This cleavage unmasks the penultimate sugar residue of the glycoconjugate, a galactose, which signals the cell for degradation.¹ Ultimately, the unmasked galactose will bind to macrophages and the erythrocyte phagocytise. Therefore, the presence of sialic acids on the surface of erythrocytes prevents degradation by masking the underlying galactose residues.⁵

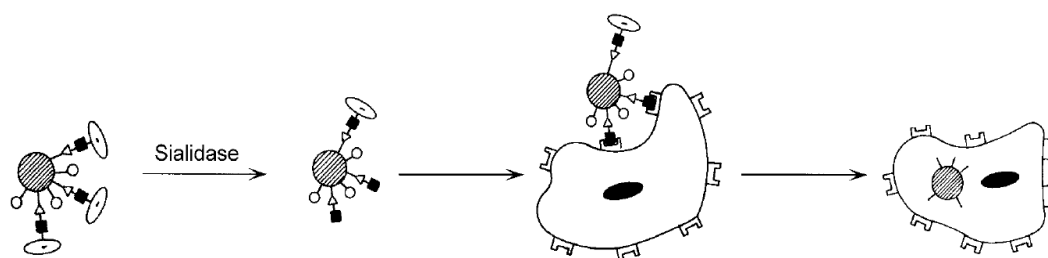


Figure 2 The role of sialic acid of masking an erythrocyte and the mechanism of binding to a macrophage. \ominus sialic acid; \blacksquare galactose; \circ and ∇ other residues; T galactose specific receptor on the macrophage surface.¹

Sialic acids have also been found to be involved in the proliferation of cancer cells, where they are usually over-expressed on the surface glycoproteins of some cancer cell lines.¹²⁻¹⁷ Gangliosides, present on the plasma membrane of cancer cells, play an important role in the regulation of these cells. It has been shown by Miyagi's group that the action of a specific human sialidase (NEU3) on gangliosides induces

inhibition of apoptosis and promotes cancer cell mobility (metastasis) in some colon and rectal cancer cells.^{17,18}

In parallel to the important roles that sialic acids play in numerous biological processes in the human body, many pathogens (viruses, bacteria and parasites) have also evolved to rely on sialic acids for a number of processes, such as evading the host immune response, cell targeting and infection. By sialylating their external glycoconjugates, pathogens can increase their chance of passing undetected through the host immune system, as well as enhancing their ability to target specific host cells. Two such examples, which make up the focus of this thesis, include the parasite *Trypanosoma cruzi* and the influenza A virus. Both of these pathogens interact with sialic acid containing glycoconjugates in order to evade the host immune response, and to target specific cells thus aiding the infection process. This thesis will focus on sialic acid modifying enzymes, discussing their roles in the infection processes and life cycles, as well as the current therapeutic targets associated with *Trypanosoma cruzi* and influenza A virus.

1.2 Carbohydrate degrading enzymes

As monosaccharides, carbohydrates do not generally exhibit a strong cellular function in living organisms; however, when linked to other carbohydrates to form complex oligosaccharides, polysaccharides or glycoconjugates, they then become relevant in a diverse range of biological functions.¹⁹ These include cell-cell communication; maintenance of the physical tissue structure, integrity and porosity; and being present during the folding of polypeptides in rough endoplasmic reticulum, and in the subsequent maintenance of protein solubility and conformation.²⁰ As a consequence of the important roles played by carbohydrates, the enzymes responsible for the selective formation (glycosyltransferases) or cleavage (glycoside hydrolases) of glycosidic bonds hold the key to a vast number of processes occurring in the human body.¹⁹ For the purpose of this work, we shall focus on glycoside hydrolases, their mechanism of action and inhibitors.

Glycoside hydrolases are a group of enzymes that are characterized by their ability to catalyse the hydrolysis of glycosidic linkages. Some important representative

examples of glycosidases include those necessary for the correct assembly of mammalian glycoproteins, such as α -glucosidases I and II; the metabolism of lactose by β -galactosidase; and the catabolism of starch and various carbohydrates present in aliments by α - and β -amylases.²¹⁻²³

Glycosidases can be classified into different classes, depending on the stereochemistry of the initial glycosidic linkage being processed (α - or β -); comparison of the anomeric stereochemistry of the product to that of the substrate (retaining or inverting); whether the glycosidic cleavage occurs internally in the oligosaccharide (*endo*-), or at the terminus (*exo*-); and the identity of the substrate carbohydrate towards which each glycosidase is selective (*e.g.* mannosidase, glucosidase).²⁴ Furthermore, glycosidases can be divided into different families based upon sequence homology, and further divided into clans, based upon similarities of their three-dimensional (tertiary) structures.²⁴⁻²⁸ This method is the basis of the CAZy classification system.²⁵ Within each CAZy family there is also found the conservation of the catalytic mechanism and the class of catalytic process involved.²⁴⁻²⁸

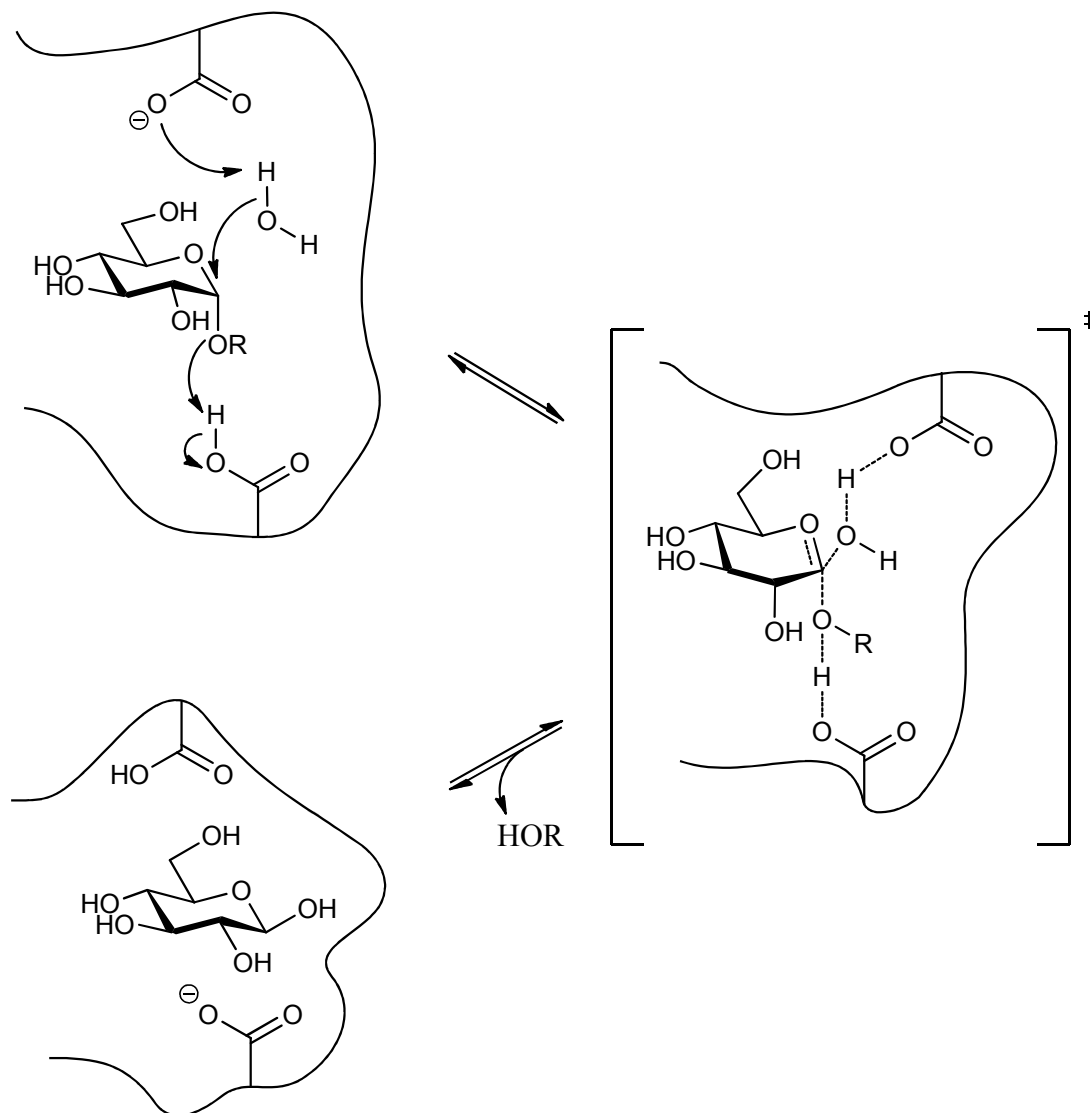
The chemical mechanisms employed by glycosidases to catalyse the cleavage of glycosidic linkages have been well studied over the years, and the subject of several reviews.^{26,29,30} In 1953, Koshland first postulated a mechanistic model to rationalise the anomeric configuration of the hemiacetal produced upon hydrolysis of a glycoside by a hydrolase.³¹ Since then, several techniques have been employed (individually or in combination) in order to study, and ultimately prove, the mechanisms originally proposed by Koshland.³²⁻³⁴

Glycosidases can cleave the glycosidic bond *via* two pathways, either with inversion or overall retention of configuration at the anomeric centre.

1.2.1 Inverting glycosidases

Inverting glycosidases are thought to operate through a concerted mechanism, where cleavage of the glycosidic bond is accompanied by general base assisted nucleophilic attack of water at the anomeric carbon, passing through an oxocarbenium ion-like

transition state (Scheme 1).³⁵ This process is aided by the general acid assisted protonation of the glycosidic oxygen by a second catalytic amino acid. The two catalytic amino acid residues are generally separated by a distance of ~ 11 Å, to enable access of the participating water molecule.³⁵

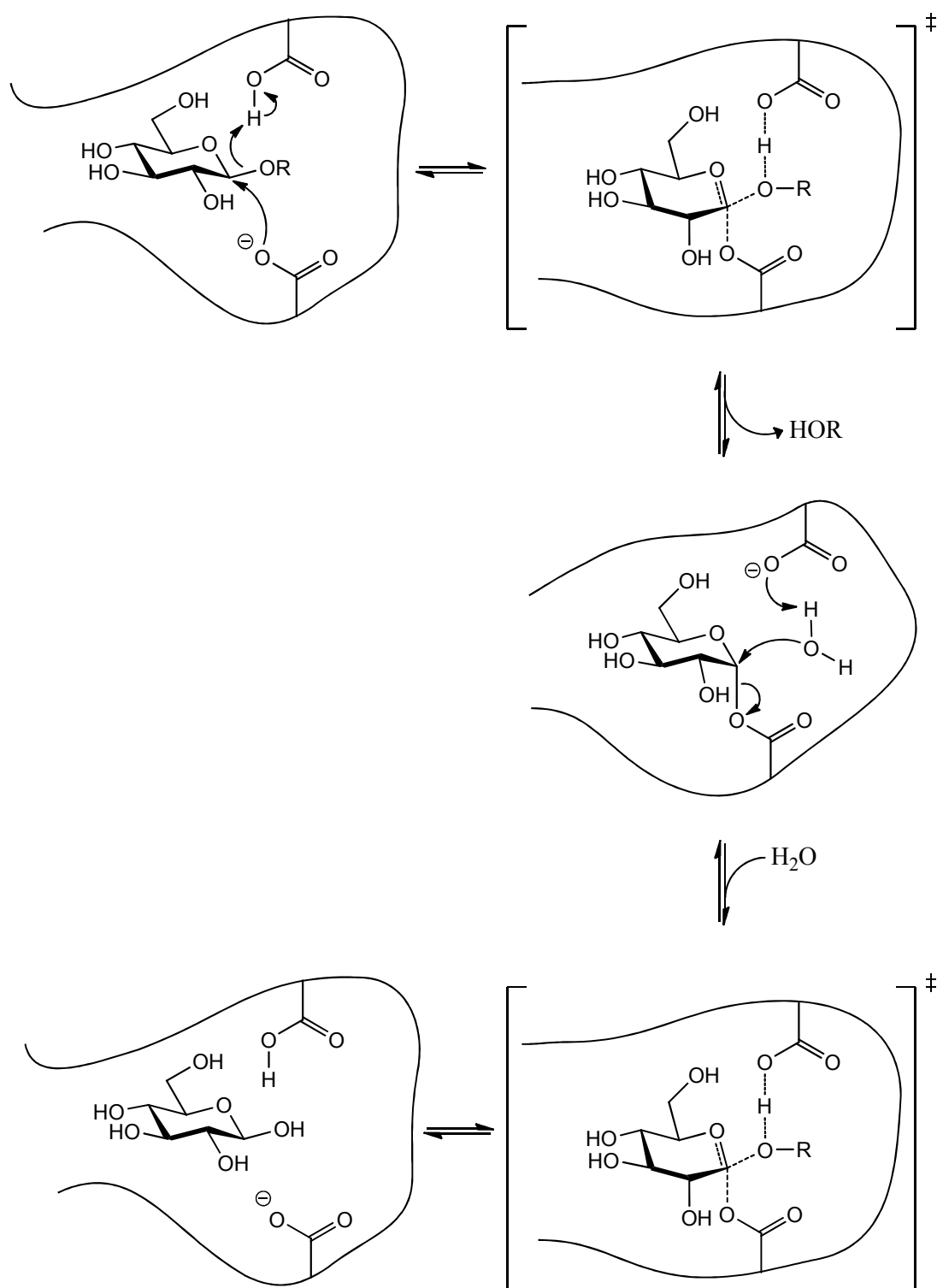


Scheme 1 Proposed mechanism of action for inverting *exo-α*-glycosidases.³⁵ R – Glycoconjugate.

1.2.2 Retaining glycosidases

Retaining glycosidases, usually proceed through a double displacement mechanism involving the formation, and subsequent hydrolyses, of a covalent glycosyl-enzyme intermediate (Scheme 2).³⁵ Within the active site, there are two catalytic amino acid residues generally separated by ~ 5.5 Å that act as acid/base catalysts, namely aspartate and glutamate.³⁶ Unlike inverting glycosidases, one of the catalytic amino

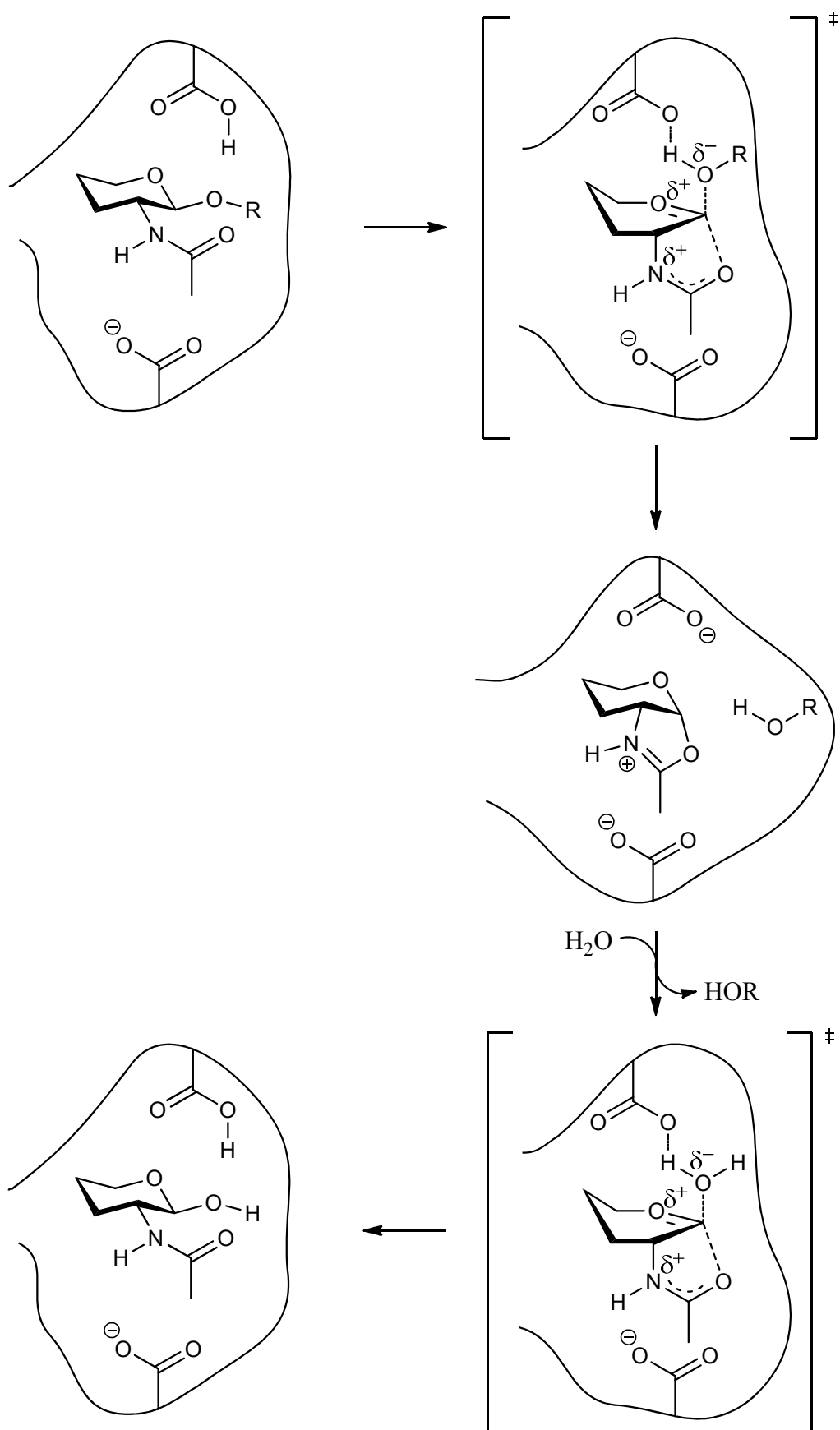
acid residues will have both functions, acting as acid catalyst for the first step (glycosylation) and as base catalyst on the second step (deglycosylation).³⁵



Scheme 2 Proposed mechanism of action for retaining *exo*- β -glycosidases.³⁷ R – Glycoconjugate.

Firstly there is the protonation of the glycosidic oxygen by the general acid/base residue, followed by nucleophilic attack to the anomeric position from the nucleophilic residue which will generate the covalent glycosyl-enzyme intermediate.³⁵ An incoming water molecule is deprotonated by the general acid/base residue, and performs a nucleophilic attack at the anomeric position, resulting in the cleavage of the covalent glycosyl-enzyme intermediate. One key aspect of this mechanism is the importance of the nucleophilic amino acid residue, where studies have shown that a point mutation in this residue originates a reduction in the activity of the glycosidase.³⁸

Another explanation for the mechanism of retaining glycosidases could be through a substrate assisted mechanism, where the group present at the adjacent position to the anomeric centre acts as the nucleophilic species.



Scheme 3 Proposed mechanism of action for substrate assisted *exo*-glycosidases.³⁹
R - Glycoconjugate.

The glycosidic oxygen is protonated by the general acid/base residue, and the adjacent group to the anomeric position performs a nucleophilic attack at the anomeric centre (Scheme 3). An incoming water molecule is deprotonated by the general acid/base amino acid residue, which then performs a nucleophilic attack at the anomeric centre. The role of the catalytic amino acid residues is to act as general acid/base and orientate the nucleophilic attack of the neighbouring group as well as stabilizing the transition states.³⁹

1.3 Inhibitors of retaining glycoside hydrolases

Owing to the importance of glycoside hydrolases in many biological processes, the ability to regulate their enzymatic function is associated with numerous medical applications, ranging from treatment of type II diabetes to antiviral and cancer therapeutics.⁴⁰⁻⁴³

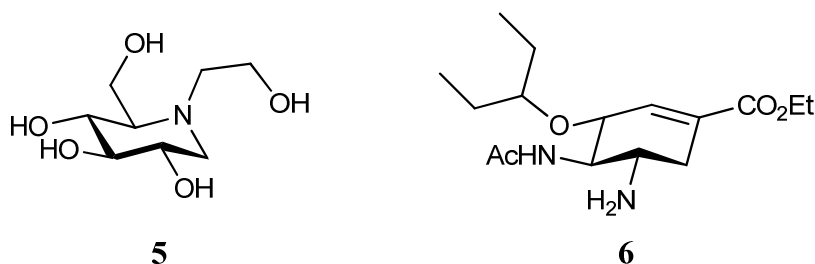
Broadly, glycosidase inhibitors can be divided into two different categories, non-covalent (competitive) and covalent inhibitors, depending on their mode of action.

1.3.1 Competitive glycosidase inhibitors

A strategy to develop potent competitor inhibitors towards a specific glycosidase is to target the transition state that is formed during the catalytic cycle of the enzyme. The rationale for this approach is due to the fact that the transition state is the species with the highest energy formed during the catalytic cycle and enzymes have evolved to form strong binding interactions with such species.⁴⁴ During the development of a competitive inhibitor the charge distribution in the transition state is taken into account as well as the geometry adopted in the catalytic site.⁴⁴ Transition state theory has proven successful, and has been applied in different areas ranging from agrochemical (insecticides), anti-diabetic, antiviral and molecular therapy for human genetic disorders.^{45,46} Two examples of different competitive inhibitors, in this case compounds that were developed to inhibit type II diabetes and influenza A virus are shown. Miglitol (**5**) is a second-generation α -glucosidase inhibitor prescribed towards type II diabetes, whilst Tamiflu[®] (**6**) was developed as a competitive

inhibitor of influenza neuraminidase, a key enzyme in the life cycle of influenza A virus.⁴⁵

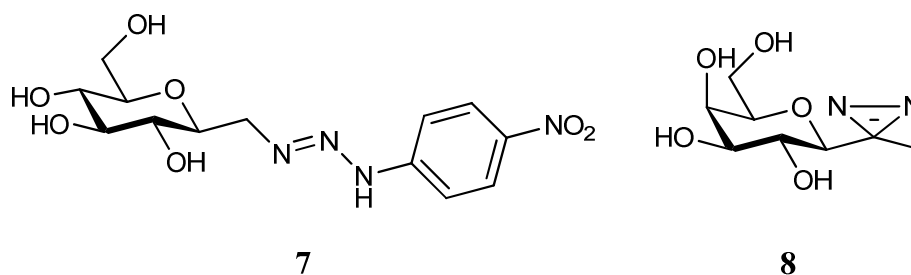
Both compounds attempt to mimic the charge distribution that occurs during the catalytic cycle, as well as the geometry of the sugar ring at the transition state.



1.3.2 Covalent inhibitors

Covalent inhibitors are a class of molecules that inactivate the enzyme through the formation of a covalent bond between the inhibitor and the enzyme.⁴⁷ The enzyme activity is reduced as the inhibitor may either physically block the access of the substrate to the active site, or may modify an important active site residue, which is essential in the catalytic cycle.⁴⁷ The covalent bond formed between enzyme and inhibitor is usually a result of a nucleophilic residue present in the enzyme attacking an electrophilic centre of the inhibitor. Covalent inhibitors have been used for a myriad of applications, such as to identify the residues within the active site and their function; and to determine the role of an enzyme in a complex biological system by inhibiting it and measuring the effects of this inhibition in the system.⁴⁷

Covalent inhibitors can be separated into two broad classes, affinity probes and mechanism-based inhibitors.⁴⁷ Affinity probes are molecules that are divided in two regions, one that is designed to afford specificity towards a given enzyme and a reactive functionality that irreversibly binds to a neighbouring region of the enzyme.⁴⁷ This irreversible bond will not necessarily be formed in the active site, since the reactive functionality does not possess any specificity to any amino acid residue in the active site. Affinity probes can be divided in two classes, ones that are inherently reactive as a consequence of their chemical structure (7); and photo-affinity labels (8), which require external energy (such as light) to be activated towards reacting with the enzyme.^{47,48}



A mechanism-based inhibitor, as opposed to affinity labels, is a molecule that is chemically inert and requires specific activation by processing through the catalytic process of the enzyme to become activated.⁴⁷ Regarding glycoside hydrolases, this activation can occur either by the hydrolytic cleavage of a glycosidic bond to release a reactive aglycone that can bind with a protein residue. Looking firstly at the class of inhibitors with a reactive aglycone, two compounds (**9** – **10**) are shown that were tested against yeast- α -glucosidase and almond- β -glucosidase (Figure 3).⁴⁷ The α -glucoside (**9**) was tested against yeast α -glucosidase inhibiting it ($K_i = 0.7$ mM) through its reactive aglycone (**13**), whilst the β -glucoside (**10**) was tested against almond β -glucosidase inhibiting it ($K_i = 1.7$ mM) also via its reactive aglycone (**14**).^{49,50} After the enzymatic cleavage of the glycosidic bonds, the aglycones (**11** and **12**) rapidly decompose, releasing an HF molecule and generating a reactive species (**13** and **14**).

Alternatively a nucleophilic residue attacks a position in the inhibitor that has been activated by the general acid residue.⁴⁷ We will focus our attention on mechanism-based inhibitors of glycoside hydrolases, their mode of action and applications.

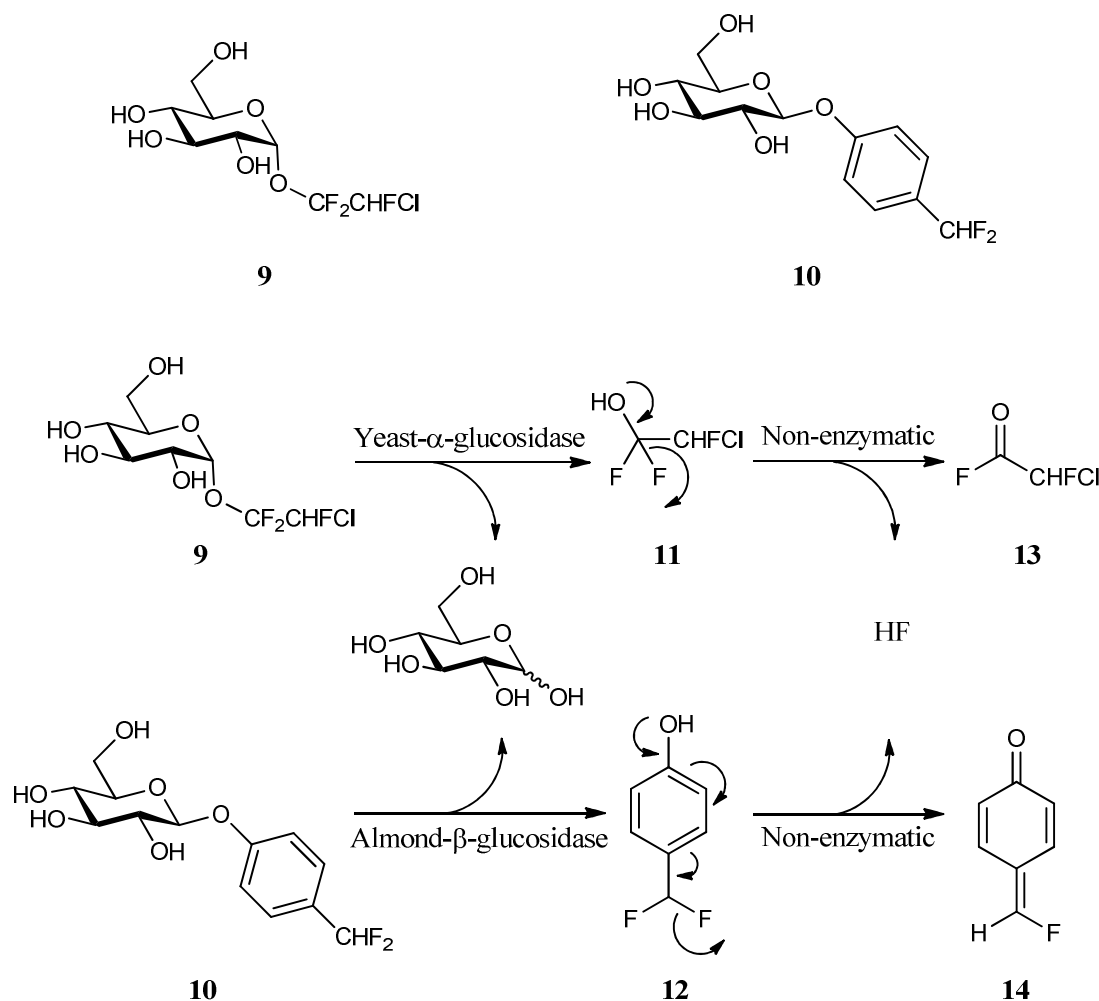


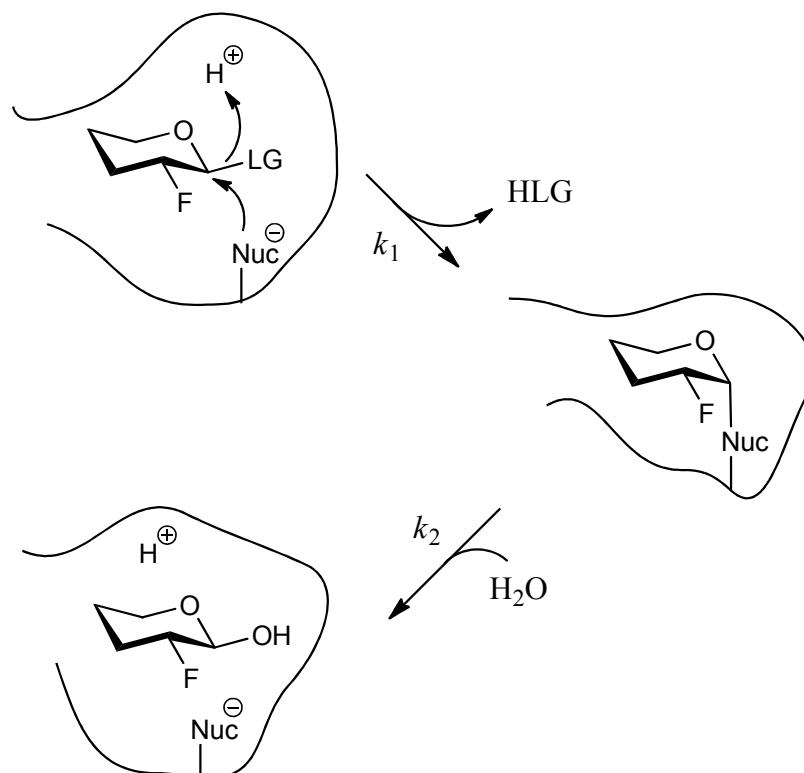
Figure 3 Two examples of mechanism-based inhibitors (**9** and **10**) towards yeast- α -glucosidase and almond- β -glucosidase, and the mechanism of formation of the reactive aglycones (**13** and **14**).⁴⁷

1.3.3 Fluorinated carbohydrates as mechanism-based inhibitors of retaining glycosidases

Fluorinated glycosides have found much use as a class of mechanism-based inhibitor, specific to retaining glycosidases owing to their mode of action. These inhibitors rely on the differentiation of rates between the two key steps involved in the catalytic mechanism, the glycosylation and deglycosylation rates (Scheme 2).

The presence of a fluorine at the carbon adjacent to the anomeric centre leads to the destabilization of the formation of positive charges at the anomeric centre during the transition states due to the electronegativity of fluorine. This destabilization leads to a reduction in the rate of formation of the glycosyl-enzyme intermediate (glycosylation) and its subsequent hydrolysis (deglycosylation) (Scheme 4).⁴⁷ The incorporation of a good leaving group at the anomeric carbon enables the

glycosylation step to still occur at an appreciable rate. Owing to the difference in relative rates between both steps, the covalent intermediate will accumulate, leading to enzyme inhibition.^{51,52}



Scheme 4 General proposed mechanism of inactivation of retaining *exo*- β -glycosidase by a fluorinated- β -glucoside.⁴⁷ HLG – Protonated leaving group.

The enzymatic activity can be regained by hydrolysis of the glycosyl-enzyme intermediate.⁴⁷

A range of fluorinated glycosides have been synthesised (**15** - **18**) and tested against a myriad of α - and β -retaining glycosidases (Figure 4).^{37,47,52-55} Although these compounds do not render the enzyme inactive *per se*, the intermediate that is formed between the inhibitor and the catalytic nucleophile is stable enough to inhibit the enzyme through accumulation of the glycosyl-enzyme intermediate.

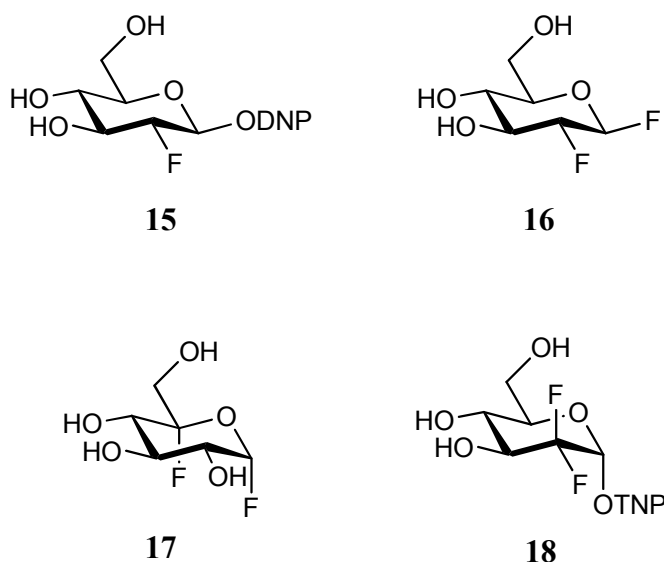


Figure 4 Structures of some fluorinated glycosides. DNP – 2,4-dinitrophenyl, TNP – 2,4,6-trinitrophenyl.⁴⁷

One of the uses of mechanism-based inhibitors is to label and identify the nucleophilic amino acid residues, since a covalent glycosyl-enzyme bond is formed.⁵¹ There are several examples in the literature that use this class of compounds to determine which of the catalytic amino acid residues is responsible for the nucleophilic attack, such as *E. coli lacZ* β -galactosidase, CGTase, almond β -glucosidase; identification of threonine as the nucleophilic residue in *Ferroplasma acidiphilum* and tyrosine in *trans*-sialidases.^{35,56-60}

Moreover, the rationale behind the mode of action of the fluorinated inhibitors has been applied to study different enzymes in order to identify the amino acid residue that is involved in the nucleophilic attack.⁶¹ For example, the nucleophilic amino acid residues present in xylanases and galactosidases were identified as a glutamate and aspartate residues respectively.^{62,63}

The mode of action of the mechanism-based inhibitors to halt the enzyme is intertwined with the catalytic mechanism and catalytic residues used naturally by the enzyme. This class targets the nucleophilic amino acid residue, and as it was shown this amino acid is of paramount importance to the activity of the enzyme. Such an approach is of use when developing new inhibitors against pathogenic enzymes. Pathogenic enzymes are able to mutate their catalytic amino acid residues; however, if such a mutation occurs with a nucleophilic residue, the activity of the enzyme

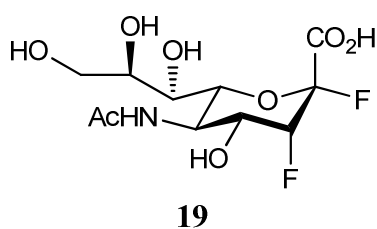
would be compromised, losing efficacy and ultimately, the mutated enzyme would not be functional.

1.4 Thesis overview

This thesis is presented in two parts. Part One is concerned with the development of 2,3-difluorosialic acid derivatives as mechanism-based inhibitors of influenza neuraminidases, a crucial enzyme in the life cycle of the influenza virus. A brief introduction to the influenza virus is presented, followed by a description of the synthesis of the target compounds and the inhibition results of these compounds against a panel of strains of influenza virus.

Part Two is dedicated to the development of 2,3-difluorosialic acid derivatives as mechanism-based inhibitors towards *Trypanosoma cruzi* trans-sialidase, an enzyme that has an important role in the life cycle of *Trypanosoma cruzi* parasite, which is the causative agent of Chagas' disease. An overview of Chagas' disease will be presented followed by a description of the synthetic methods employed to synthesise the target compounds, as well as results of biological testing against the parasite.

The general strategy for both projects is based on a series of modifications to the parent compound, 2,3-difluorosialic acid (**19**), in order to generate potent and specific inhibitors to influenza neuraminidase and *Trypanosoma cruzi* trans-sialidase (TcTS).



Chapter 2 - Introduction to influenza A virus

2.1 Prelude

Historically, there are a number of reliable recordings of influenza pandemics dating back to the 18th century, although it was not until 1918-20 that the first well documented account of an influenza pandemic was recorded.⁶⁴ This pandemic became known as the “Spanish flu” and it is considered that half of the world’s human population at the time was infected, with the death toll estimated to be between 50 and 100 million people.^{65,66}

Following the “Spanish flu” of 1918, caused by a strain of H1N1 influenza A virus, there were two more influenza pandemics in the last century, arising in 1957-58 and 1968, with the appearance of two new strains of influenza A virus, those being H2N2 and H3N2 respectively. Both of these strains were originally of avian origin, but underwent a genomic reassortment with a circulating strain of human H1N1.⁶⁷ The next major outbreak of influenza A virus occurred in 1997, where a new strain, H5N1, (commonly referred to as “bird flu”) emerged in the human population. This subtype is still active, with a new outbreak occurring in 2005; however, it has not reached pandemic status.⁶⁵ The World Health Organization (WHO) continues to monitor this H5N1 strain of influenza A virus and, in the beginning of 2010, there were further cases recorded of infection by this strain.⁶⁸

In 2009, when the world was vigilant towards H5N1 and expecting the next pandemic to arise from this strain, the WHO announced the first pandemic of the 21st century caused by an H1N1 strain which originated from pigs (commonly referred to as “swine flu”). This H1N1 strain had been endemic in pigs since 1918, when the virus crossed the species barrier to infect them and had remained virtually unmodified until recently.⁶⁹

The drugs currently available for the treatment of the influenza virus proved effective towards the outbreak of H5N1 and H1N1, although some serious setbacks emerged. One of the most worrying factors was the rapid development of resistance towards the approved drugs. These high levels of resistance are derived from a number of point-mutations in key enzymes, with one mutation in particular found to be present

in virtually all of the isolates of seasonal influenza H1N1 of 2009, making the front line drug against influenza virus virtually ineffective.⁷⁰ As a consequence, there is an urgent need to develop new inhibitors towards the influenza virus that are less susceptible to drug induced resistance.

2.2 The influenza A virus family

The influenza virus belongs to the *Orthomyxoviridae* family, which is characterised by having six or eight single-stranded negative-sense RNA segments and includes six genera, *Influenzavirus A*, *Influenzavirus B*, *Influenzavirus C*, *Isavirus*, *Thogotovirus* and *Quarjavirus*.⁷¹ The genus *Isavirus* consists only of the salmon anaemia virus, whilst the *Thogotovirus* has three different viruses: Thogoto; Dhori; and Araguari virus. *Quarjavirus* was the last genera to be classified into the *Orthomyxoviridae* family and it is comprised of three different viruses: Quaranfil; Johnston Atoll; and Lake Chad virus. Due to the genetic capacity of the *Orthomyxoviruses* to undergo reassortment within a specific genus, new virus strains can emerge that continue to elude the immune response and infect humans, poultry and livestock.⁷¹⁻⁷³ By far the most important virus from this family in terms of infection and mortality to humans is influenza A virus.

2.3 Structure and life cycle of influenza A virus

As mentioned previously, influenza A viruses are single-stranded negative-sense RNA viruses. Their genome is divided into eight segments which encode for 10 viral proteins: the polymerases PA, PB1 and PB2; hemagglutinin (HA); nucleoprotein (NP); neuraminidase (NA); ion-channel proteins M1 and M2; and finally non-structural proteins NS1 and NS2 (Figure 5).^{65,74-76}

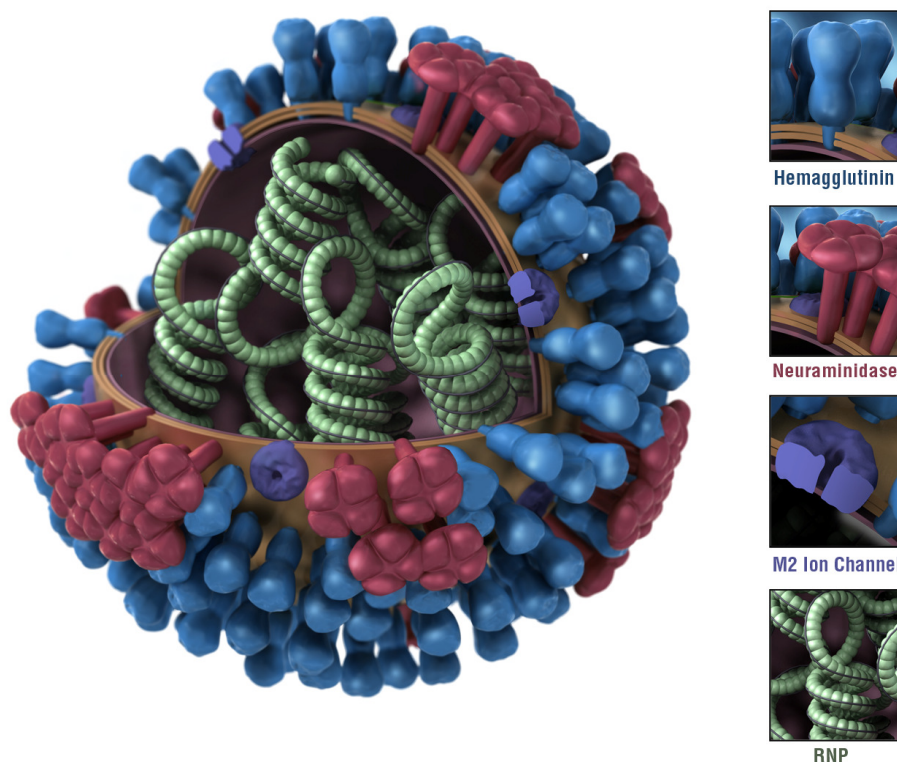


Figure 5 Cartoon illustration of an influenza virus particle. Details of hemagglutinin, neuraminidase, the M2 ion channels and the RNA material (RNP) are shown.⁷⁴

The first step in the infection process involves the binding and fusion of the viral particle onto the host cell (Figure 6).⁷⁷ This process is facilitated by hemagglutinin proteins present on the virion surface, binding to terminal sialic acid residues present on glycoproteins, or glycolipid, receptors located on the host cell surface.⁷⁸ Following binding to the host cell surface, the viral particle is internalised via endocytosis to produce an endosome within the cell cytoplasm. The M2 ion-channel, present in the viral lipid bilayer, facilitates fusion of the viral membrane with the endosome, by allowing the passage of H^+ from the endosome to the interior of the viral particle. This leads to a structural modification of hemagglutinin, which extends a fusion peptide towards the endosome membrane in order to fuse both membranes, liberating the viral RNA into the host cell cytoplasm.⁷⁹⁻⁸¹ Additionally, the M2 protein controls the pH in the Golgi apparatus during hemagglutinin biosynthesis.^{76,78} Viral RNA is then transported to the nucleus, where transcription occurs. The M1 matrix protein forms a protective layer within the viral particle for the RNA material, and once the viral and cellular membranes have been fused it will interact with the host cell genome, nuclear export factor and initiating progeny viral assembly.^{76,78}

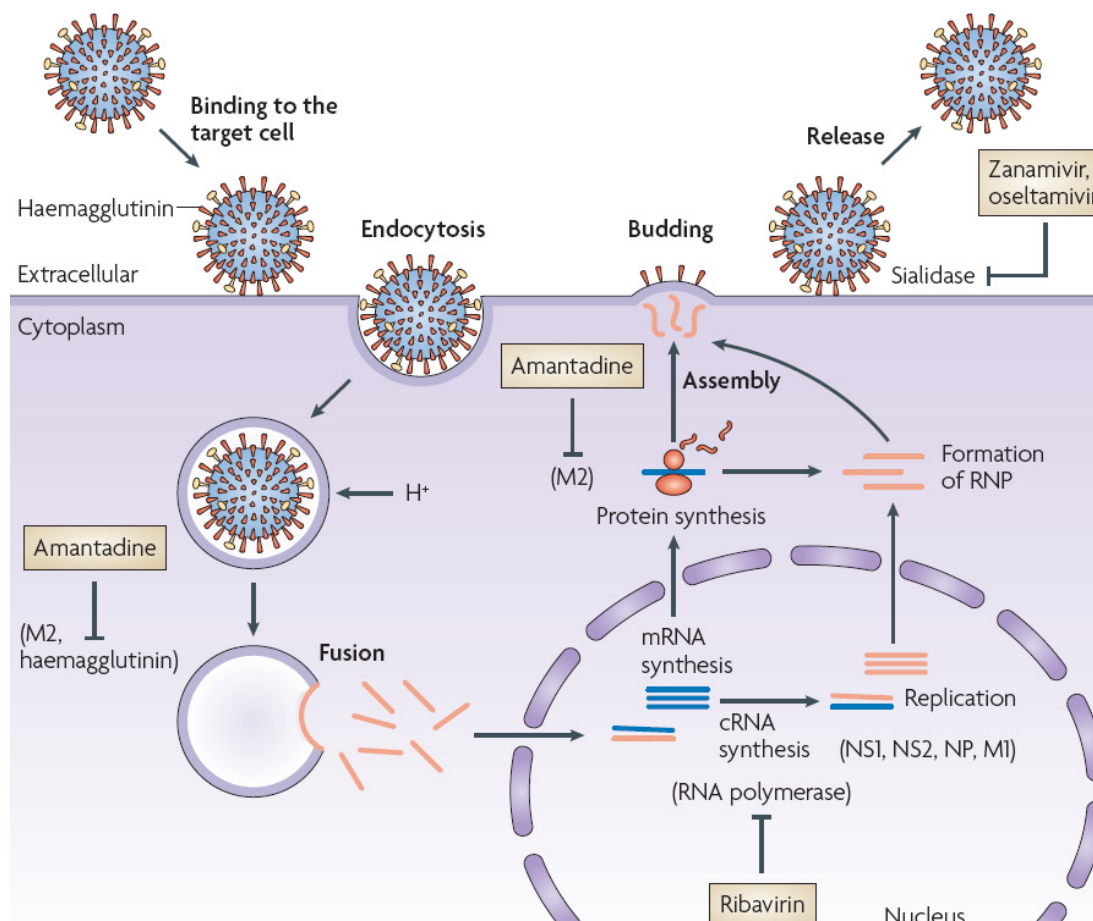


Figure 6 Schematic representation of the replication cycle of influenza A virus.⁷⁷

The role of the nucleoprotein, NP, is to encapsulate the viral RNA once in the nucleus of the host cell, whilst the non-structural proteins NS1 and NS2, the PB1, PB2 and PA polymerases are involved in the process of viral RNA transcription.^{65,76,78} The newly transcribed viral RNA is then released from the nucleus into the cytoplasm where it can migrate to the inner cell membrane. Furthermore, mRNA transcribed from the viral RNA is translated into the various viral proteins which also begin to aggregate near the host cell membrane. The aggregation of the viral material near the host cell membrane gives rise to the formation of a capsule, or envelope, utilizing the host cell membrane and is aided by the M1 protein. Once the budding process is complete, the newly formed viral membrane detaches from the host membrane, forming a new viral particle. Once the new viral particle is formed, it first remains attached to the host cell membrane through binding of its hemagglutinin protein to the terminal sialic acid present on cell surface glycoconjugates. The neuraminidase enzyme now plays a crucial role at this late stage of viral replication, as it is required to hydrolyse the terminal sialic acid

residues on the host cell surface receptors in order to liberate the new viral particle from the infected cell.^{76,82} More recently, it has been reported that neuraminidase also has an active role in the initiation of influenza virus infection in the human airway epithelium, where it is thought that the existence of mucins and cilia, amongst other glycoconjugates with terminal sialic acids, could hinder access of the virus to the target cells.⁸³ Therefore, neuraminidase aids the virus in proceeding through the human airway epithelium by cleaving the terminal sialic acids present on glycoconjugates, enabling the virus to reach the lower respiratory tract (Figure 7).⁸⁴

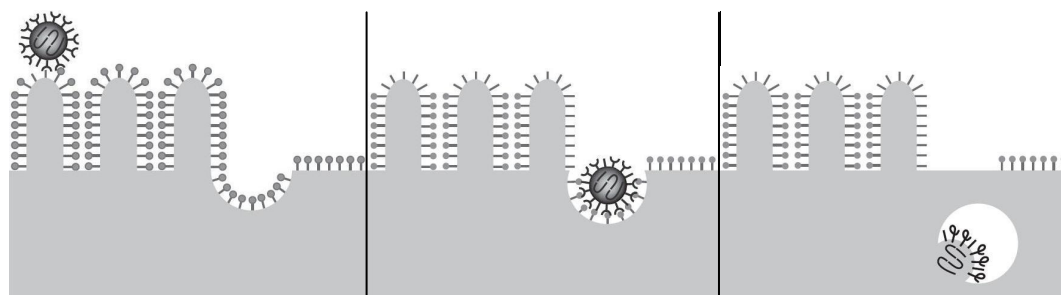


Figure 7 Cartoon representation of the different stages involved with an influenza virion proceeding across the human airway epithelium to reach a suitable endocytic site.⁸⁴

2.4 Nomenclature of influenza A viruses and their sub-types

The nomenclature (HxNy) of the different subtypes of influenza A virus relates to the immunological characteristics of the hemagglutinin and neuraminidase surface proteins. Presently, there are 16 different hemagglutinin subtypes (H1-H16) identified, and nine different subtypes of neuraminidase (N1-N9).^{85,86}

The large diversity of subtypes of hemagglutinin and neuraminidase is a result of two different processes known as antigenic drift and antigenic shift (Figure 8).⁸⁷ Antigenic drift occurs as a result of random errors during polymerisation of the viral RNA (where the rate of mutation is about 1 in 10^4 bases per replication) (Figure 8, a)).⁸⁸ If a host cell is infected with two strains of influenza virus, a process called antigenic shift can occur. The viral RNA is divided into segments, with each carrying genetic information; therefore, when two different strains infect the same host cell the probability of the genetic information from strain X being exchanged with strain Y is elevated (Figure 8, b)).^{65,85} In combination, these two processes are capable of continually generating new subtypes of influenza viruses with the potential to initiate a new pandemic.

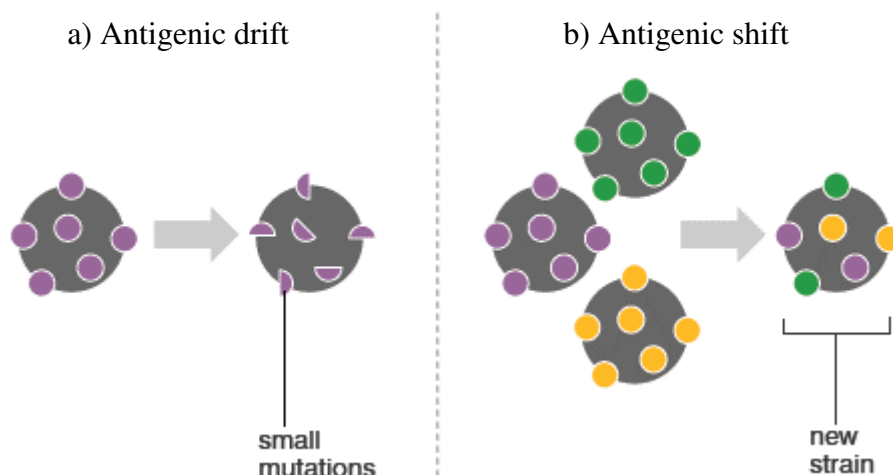


Figure 8 Illustration of the process of antigenic drift and shift in influenza virus.⁸⁷ a) Small mutations occurring during replication; b) Genetic information exchange between different strains of influenza virus.

2.5 Therapeutic targets for the clinical treatment of influenza A infection

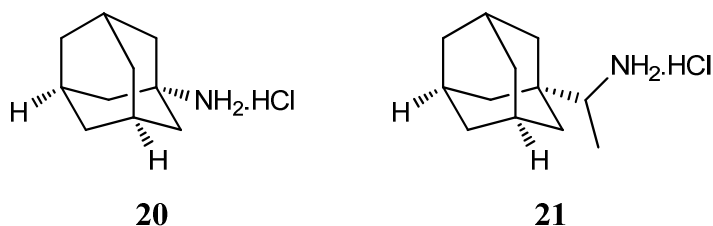
Looking closely at the life cycle of influenza virus there are several key stages that, if inhibited, would hinder its replication and have the potential to act as therapeutic targets. These stages include the viral uncoating process, where the role of the M2 ion-channel is of prime importance for effective release of the viral RNA into the host cytoplasm; the RNA transcription process, where inhibition of the RNA polymerase would halt the replication of the viral RNA; and finally, the viral release process, where the action of neuraminidase is of paramount importance for the efficient release of new viral particles from the host cell surface (Figure 6).

For the past several decades, numerous small molecules have been developed to inhibit these processes with reasonable success; however, the rapid development of resistance by the virus or the toxicity associated with the inhibitors has been a serious handicap, significantly impairing their long-term effectiveness and use.

2.5.1 M2 ion-channels

A class of compounds called adamantamines were developed in order to inhibit the M2 ion-channel, which is closely linked to the viral uncoating process. Two compounds have been approved onto the market, amantadine (Symmetrel®) (**20**) and

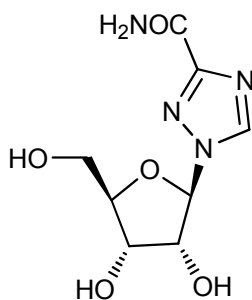
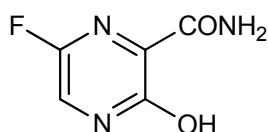
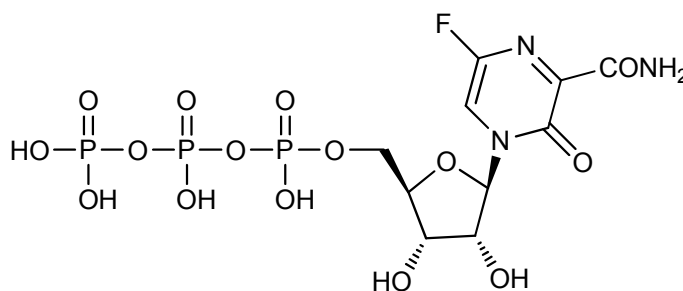
rimantadine (Flumadin[®]) (**21**) and are specific towards influenza A virus, since influenza B virus does not possess the M2 protein.



Resistance arose rapidly towards both of these two compounds, which was a major setback to their use as stand-alone therapeutics. As such, they are now only used as a component of combination therapy in the presence of other inhibitors.⁸⁹⁻⁹¹

2.5.2 RNA transcription

The inhibition of viral RNA transcription and genome replication can be achieved by using ribavirin (Virazole[®]) (**22**), which lowers the intracellular GTP levels via the inhibition of inosine 5'-monophosphate dehydrogenase as well as through interference with transcription and genome replication.⁹² Although ribavirin (**22**) has so far only been approved for the treatment of hepatitis C, it has been tested against wild type H5N1 *in vivo*.⁹³ The treatment of H5N1 infected mice with either ribavirin (**22**), oseltamivir (**6**) or amantadine (**20**) at a dose of 20 or 40mg/kg/day showed an average survival rate of 30% for each. However, when ribavirin (**22**) was used in a combination therapy with either oseltamivir (**6**) or amantadine (**20**), the survival rate increased to 90%, showing a significant synergetic effect for these combinations.⁹³ So far however, the use of ribavirin (**22**) is limited due to the severity of side effects that it causes, which in extreme cases can include haemolytic anaemia and the possibility of teratogenic effects in pregnant women.⁹² Another inhibitor of RNA transcription that has shown promising results is the pyrazine derivative, T-705 (Favipiravir) (**23**) which is now in phase II clinical trials.⁹⁴ Once T-705 (**23**) enters the cell it is converted into its active form, ribofuranosyl triphosphate, T-705RTP (**24**) by the host's cellular glycosylation, phosphorylation and kinase pathways.^{94,95}

**22****23****24**

T-705RTP (**24**) is a general inhibitor of RNA type viruses, acting by selectively inhibiting the viral RNA polymerase.^{92,95} Smee *et al* have studied the therapeutic effects of using T-705 (**24**) as a single drug and in combination with oseltamivir (**6**) and zanamivir (**25**) to treat mice infected with the H1N1, H3N2 and H5N1 strains of influenza A.⁹⁴ The results observed illustrate that used as a stand-alone therapy; T-705 (**24**) does not have a significant effect on the survival rate of the animals. However, when used in a combined therapy with either oseltamivir (**6**) or zanamivir (**25**), survival rates increase dramatically, from an average of 20% survival in monotherapy to an average of 90% in the combination therapy, irrespective of the strain under analysis.⁹⁴ T-705 (**24**) has also shown minor interactions with human DNA polymerase, resulting in a small number of side effects in humans during clinical trials.⁹⁶

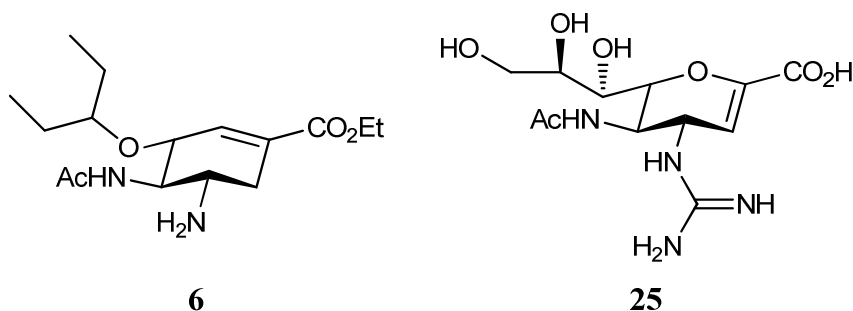
2.5.3 Influenza neuraminidase

Influenza neuraminidase (EC 3.2.1.18) is an *exo*-glycohydrolase which catalyses the hydrolysis of α -ketosidically-linked terminal sialic acids from glycoconjugates.⁹⁷ As mentioned previously (Chapter 2.3) the hydrolysis of sialic acid from the

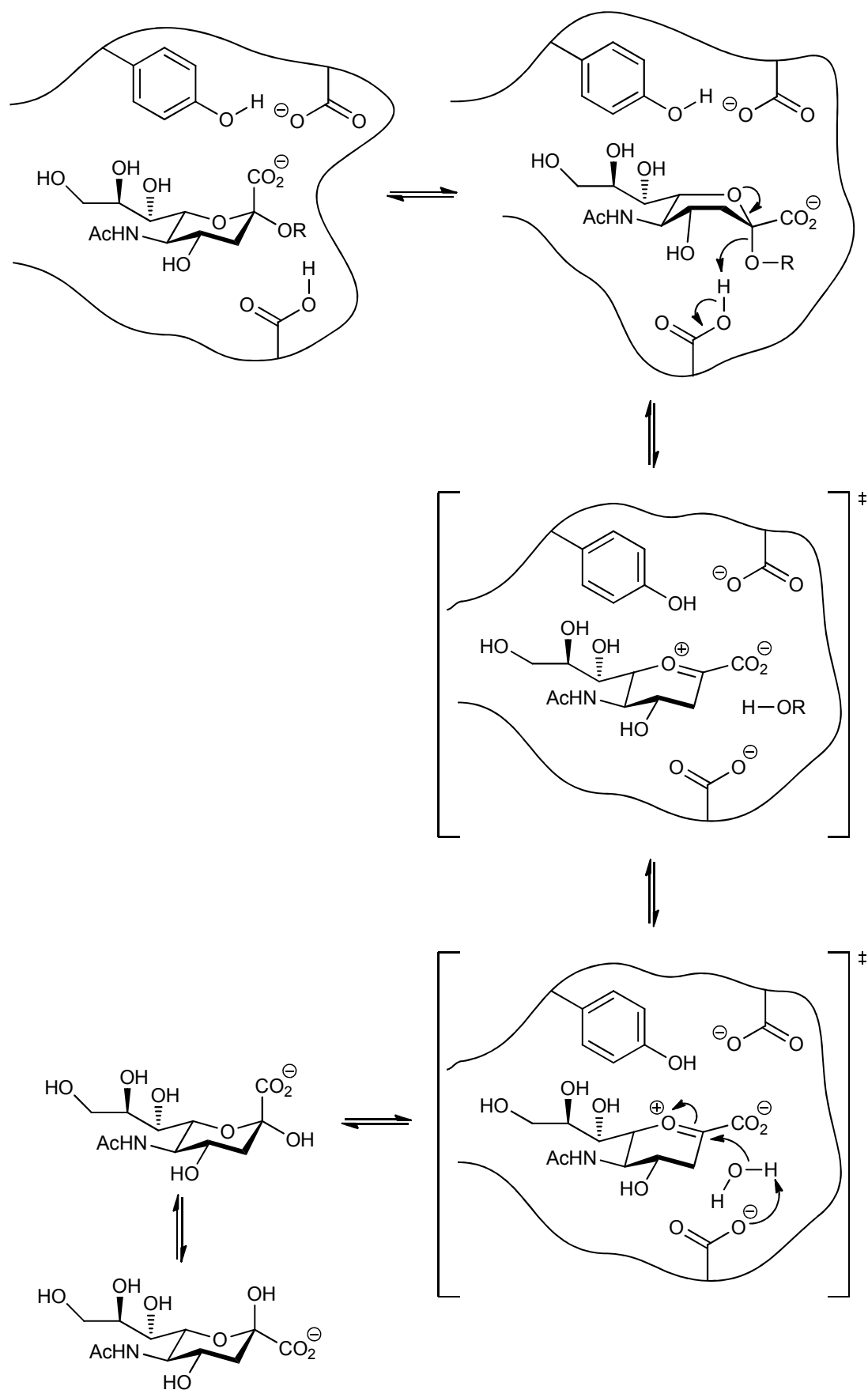
glycoconjugates can facilitate the progression of the virus in the upper respiratory tract, as well as the release of the progeny viral particles that would otherwise remain bound to the host cell surface via sialic acid-hemagglutinin interactions and be phagocytised by the host immune system.^{77,98}

Over the past few decades, the determination of the X-ray crystal structure of influenza neuraminidase, allied with the study of its biochemical properties, has provided new opportunities for the development of several novel therapeutics.^{99,100}

The study of the catalytic mechanism of influenza neuraminidase greatly assisted the development of the two neuraminidase inhibitors currently approved for the treatment of influenza, Relenza[®] (**25**) and Tamiflu[®] (**6**). A detailed explanation of both inhibitors is given in subsection 2.6.



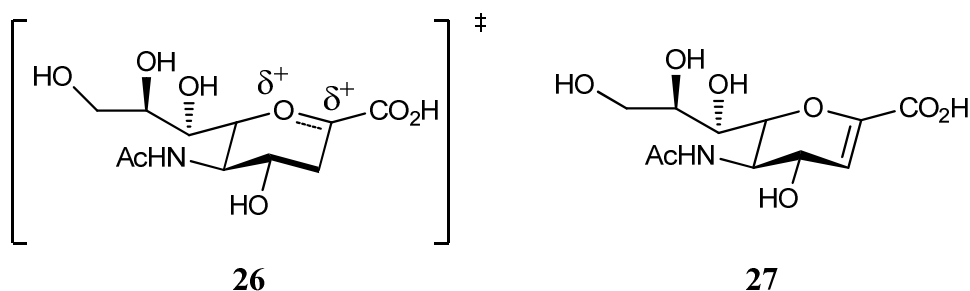
The current accepted catalytic mechanism of influenza neuraminidase is composed of four major steps. These involve the binding of the sialic acid substrate, protonation of the anomeric oxygen and subsequent formation of the oxocarbenium-ion transition state, followed by hydrolysis of the glycosidic linkage and liberation of sialic acid (Scheme 5).¹⁰¹ Sialic acid needs to shift from the stable chair conformation to a pseudo boat conformation in order to interact with the arginine triad present in the active site of neuraminidase.⁷⁷ The glycosidic hydroxyl is then protonated by the Asp151, with the subsequent hydrolysis of the glycosidic bond, forming the oxocarbenium ion transition state.⁷⁷ The negative charges from Asp151 and Glu277 are considered to stabilize the oxocarbenium ion.¹⁰² An incoming water molecule is then deprotonated by the same Asp151 residue, and is then able to perform a nucleophilic attack onto the anomeric carbon of sialic acid affording the free sialic acid.



Scheme 5 Proposed mechanism of hydrolysis of the sialic acid from the glycoconjugate (R) by influenza neuraminidase.⁷⁷

2.6 Overview of competitive inhibitors of influenza neuraminidase

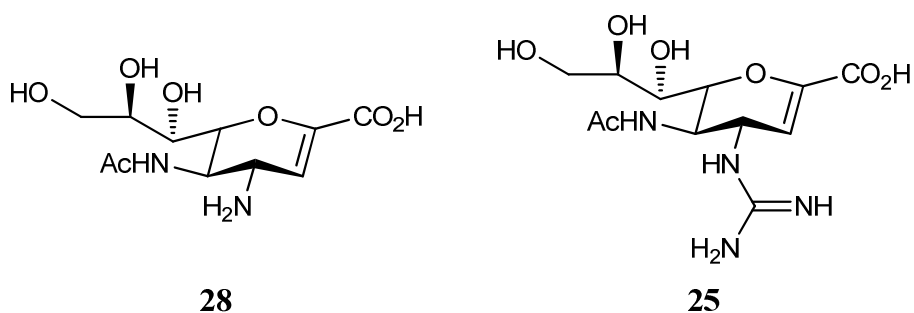
The first competitive inhibitors of influenza neuraminidase were designed to mimic the flattened conformation adopted by the sugar ring at the transition state (**26**). This led to the development of a series of 2,3-ene derivatives based on the structure of 2-deoxy-2,3-dehydro-*N*-acetylneuraminic acid (Neu5Ac2ene) (**27**), found to have a K_i of 4 μM against influenza A N2.¹⁰³



It is thought that the loss of binding energy derived by removing the hydroxyl present at C-2 (loss of a hydrogen bond interaction) is compensated for by the fact that no energy is required to distort the conformation of the ring, since it already exists in the geometry required to mimic the transition state.¹⁰³ Although Neu5Ac2ene (**27**) showed good inhibition towards influenza neuraminidase, it was also found to be a potent inhibitor against bacterial and mammalian neuraminidases both *in vitro* and *in vivo*.¹⁰³

2.6.1 Zanamivir

Molecular modelling, in addition to the information obtained from the crystal structure of influenza neuraminidase, was used in order to develop a new inhibitor. Several atomic probes (such as amino, carboxy and hydroxyl) were used in the molecular model studies, until an important interaction was discovered around the hydroxyl at C-4, where it was noticed that the introduction of a basic nitrogen group would benefit from interactions with neighbouring amino acid residues.^{97,101} Therefore, 4-*N*-amino Neu5Ac2ene (**28**) and subsequently 4-guanidino Neu5Ac2ene (**25**) were synthesised and tested *in vitro* and *in vivo* against influenza A and B virus strains.^{104,105}



Both compounds were tested against influenza A N2, with 4-*N*-amino Neu5Ac2ene (**28**) showing a 100 fold improvement in the K_i compared with the parent compound, Neu5Ac2ene (**27**), whilst 4-guanidino Neu5Ac2ene (**25**) showed an improvement of 10000 fold. The K_i value obtained for 4-*N*-amino Neu5Ac2ene (**28**) was 40 nM whilst for 4-guanidino Neu5Ac2ene (**25**) was 0.2 nM.⁷⁷ X-ray crystallographic structure determination of 4-guanidino Neu5Ac2ene (**25**) in the active site of influenza neuraminidase N2, showed that the guanidino group at C-4 made several binding interactions with glutamate, aspartate and tryptophan amino acid residues (Figure 9).¹⁰⁴ In addition to the good inhibition shown by 4-guanidino Neu5Ac2ene (**25**), this compound was also highly selective for influenza neuraminidases, showing only low levels of inhibition towards bacterial and mammalian neuraminidases.⁷⁷ 4-Guanidino Neu5Ac2ene (**25**) was selected as the lead drug candidate by Biota, now on the market as zanamivir (**25**). Zanamivir was the first approved drug to target influenza neuraminidase, under the name of Relenza[®] (**25**), in 1993.⁷⁷ Due to the highly polar nature of Zanamivir (**25**), it has a low bioavailability (< 5%); therefore, it was developed as an inhaled formulation, delivering the drug directly to the main site of infection.⁷⁷ Unfortunately this method of administration cannot be employed to people with impaired lung capacity. To address this problem new methods of administration are being investigated, such as an intravenous formulation; however, this formulation method is yet to be approved.¹⁰⁶⁻¹⁰⁸ Notwithstanding the difficulties associated with the administration of zanamivir (**25**), it is a very effective treatment against both influenza A and B viruses.

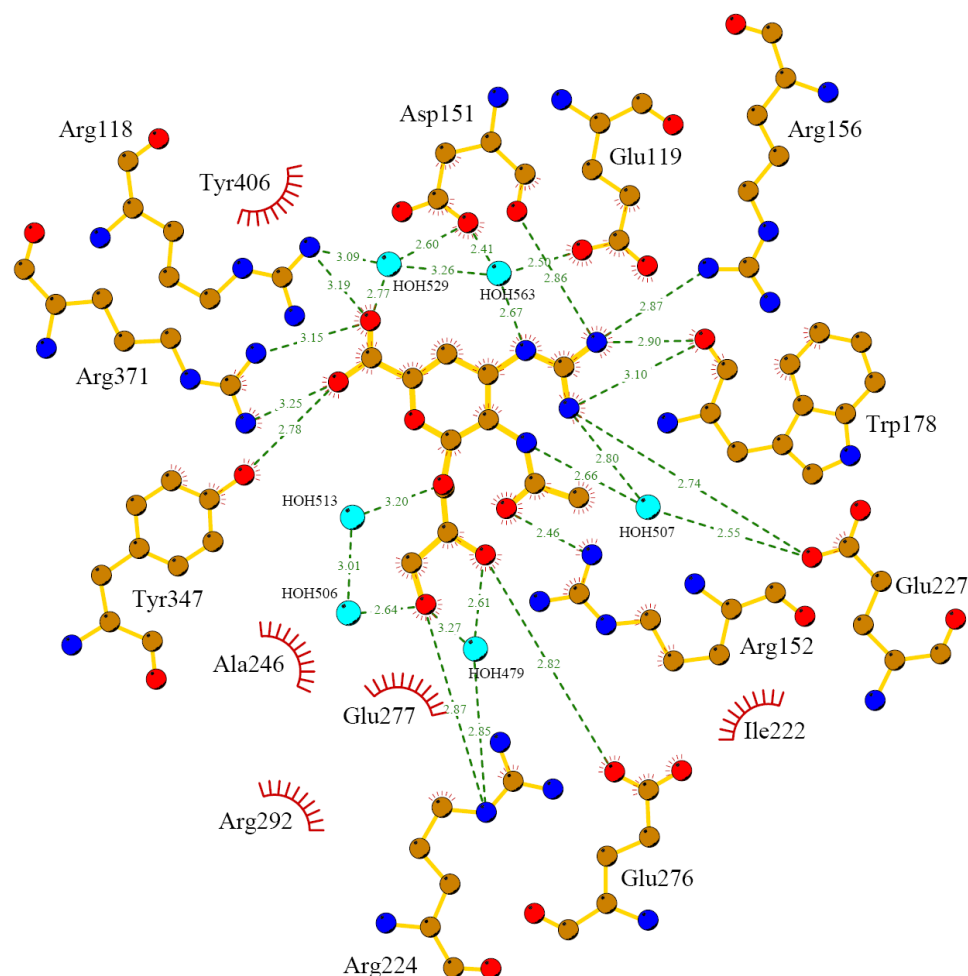
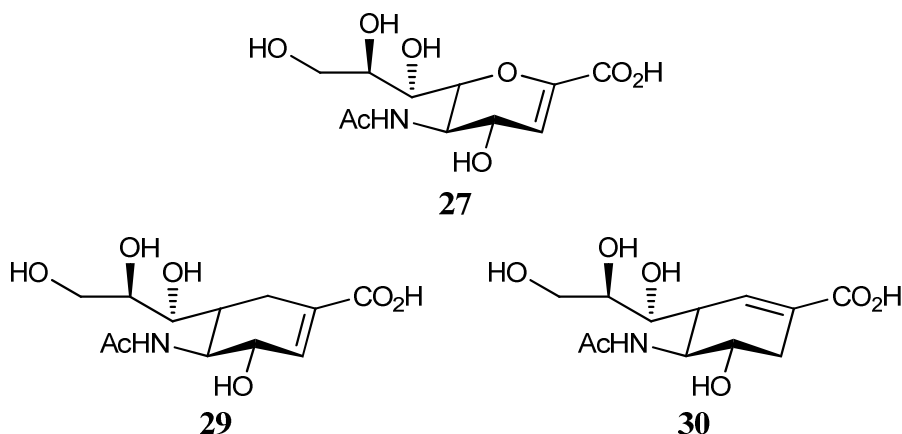


Figure 9 Interactions of 4-guanidino Neu5Ac2ene (**25**) with the different residues present at the active site of influenza A N1. Generated with LigPlot⁺ (PDB 2HTQ).¹⁰⁹

Zanamivir (**25**) has shown a low incidence of drug induced resistance, most likely as a consequence of its close similarity to the natural substrate sialic acid (**4**), with only one clinical case of resistance reported in the literature. This was detected in an 18 month old immunocompromised child after a long period of infection with influenza B virus.^{110,111} One other mutant with a lower sensitivity towards zanamivir (**25**) was identified in a study conducted between 2006 and 2008 and a detailed account on these mutations is given in Chapter 6.2.¹¹² The side effects associated with zanamivir (**25**) are very mild, and largely confined to the airways (*e.g.* cough, nasal symptoms), although episodes of bronchospasm have also been reported in patients with an underlying asthma conditions.^{113,114}

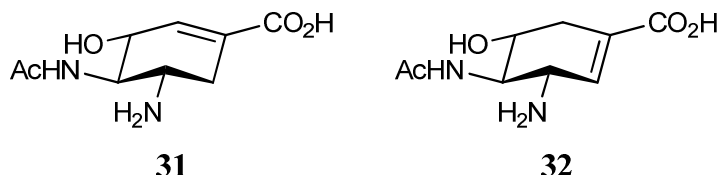
2.6.2 Oseltamivir

It was observed that the presence of the ring oxygen in Neu5Ac2ene (**27**) and zanamivir (**25**) does not contribute significantly to their binding in the active site, so it was considered that substituting this oxygen with a methylene isostere could help to increase hydrophobicity and potentially increase bioavailability, without introducing any loss of inhibitory activity.¹⁰³ The removal of the ring oxygen would also allow the development of cyclohexene analogues that more closely mimic the geometry of the transition state by changing the position of the alkene bond.¹⁰³ Two compounds were initially synthesised, **29** and **30**, and the inhibition against influenza A N2 results proved encouraging.¹¹⁵

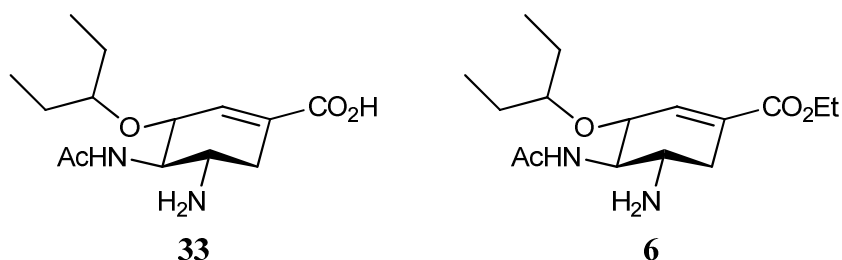


Both compounds adopt half chair conformations, although they differ from each other by the position of the double bond. The position of the double bond proved to be of paramount importance when the compounds were tested, with compound **30** (IC₅₀ of 20 μ M) observed to be 40 times more active than **29** (IC₅₀ of 850 μ M).¹¹⁵ In order to increase the binding of the compound it was planned to replace the hydroxyl at C-4 for an amino group and to increase the hydrophobicity it was planned to replace the glycerol moiety by an hydroxyl group.¹⁰³ The rationale for the introduction of an hydroxyl group at C-6 was that it could pose an inductive electron withdrawing effect, reducing the electron density of the double bond akin to the oxocarbenium ion which is a highly polarized species.¹⁰³ Furthermore, the C-6 hydroxyl could become the basis for the synthesis of ether analogues to further increase the hydrophobicity of the compound improving its potential to be orally

bioavailable.¹⁰³ Two further derivatives were then synthesised and the results supported the idea that the position of the double bond is of paramount importance, with compound **31** having an IC_{50} of 6.3 μM whilst compound **32** was found to be inactive, when tested against influenza A N1.^{103,116}



Taking compound **31** as a scaffold, several alkoxy analogues were then synthesised in an effort to optimize the hydrophobic interactions in the binding pocket, previously occupied by the glycerol side chain.¹⁰³ Ultimately, the pentyloxy side chain derivative in compound GS4071 (**33**) was found to be the most potent, with a IC_{50} of 1 nM against H1N1.^{116,117}



Although GS4071 (**33**) is more hydrophobic when compared to zanamivir (**25**), its oral bioavailability was still found to be poor.⁷⁷ Therefore, it was decided to produce the ethyl ester as a prodrug, oseltamivir (**6**), which is readily converted into the active form *in vivo* by the action of endogenous esterases present in the liver.¹¹⁸ This compound, marketed as Tamiflu[®], was approved in 1999 as the second drug targeting influenza neuraminidase.⁷⁷

Co-crystallization of GS4071 (**33**) with influenza neuraminidase, revealed that the alkoxy side chain is involved in several hydrophobic contacts in the space previously occupied by the glycerol side chain (Figure 10). Within this pocket, in order to create the additional space required by the alkoxy side chain, there is the movement of Glu276, being reoriented outwards, interacting with Arg224 creating a reasonable hydrophobic pocket that can accommodate the alkoxy side chain.⁷⁷

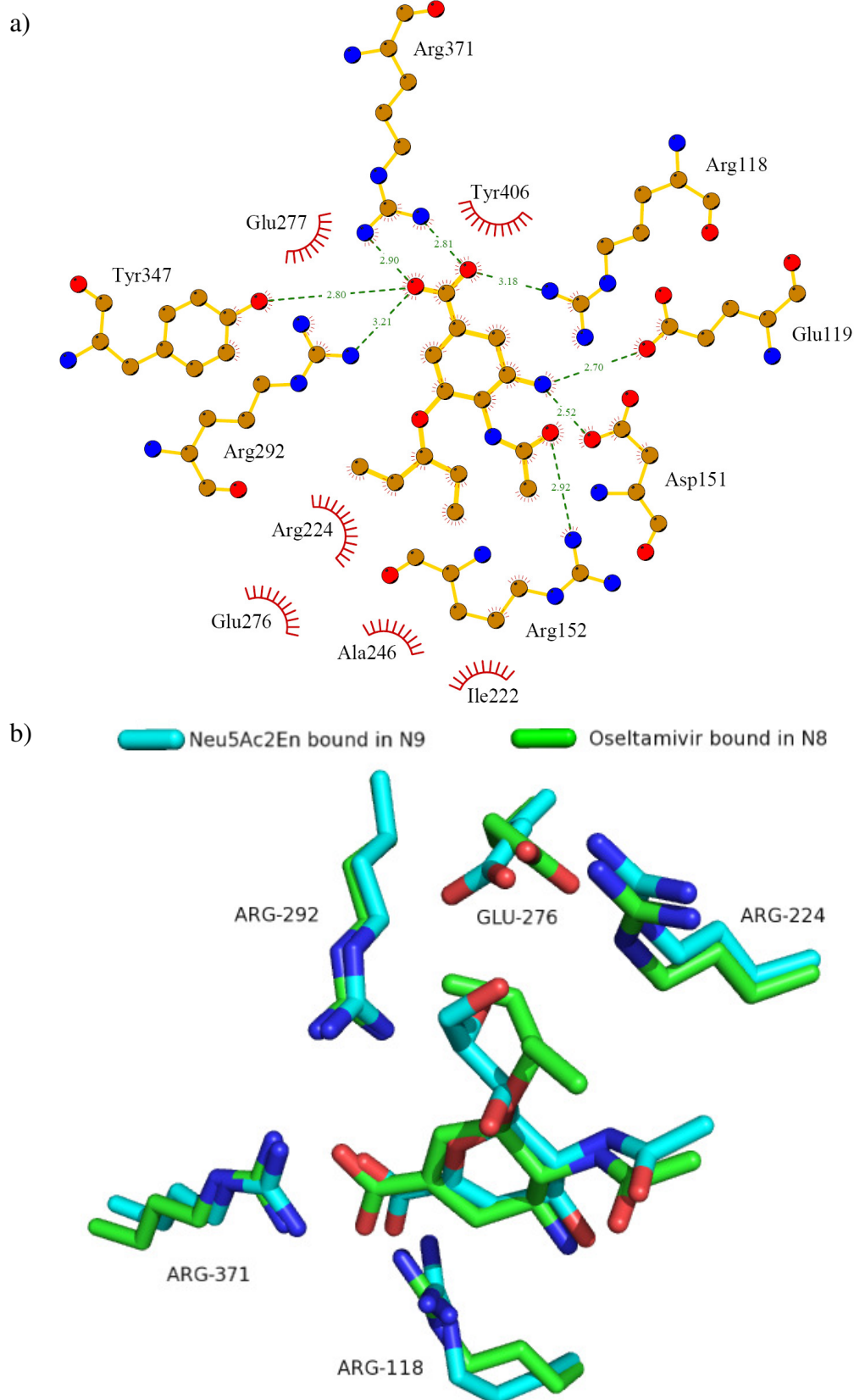


Figure 10 a) Interactions of oseltamivir (**33**) with the catalytic amino acid residues of neuraminidase subtype N8. b) Superimposed view of the active site of influenza neuraminidase, subtype N9 (blue) with Neu5Ac2ene (**27**) and subtype N8 (green) with oseltamivir (**33**) where it is possible to observe the movement of Glu276 and Arg224. Generated with PyMOL and LigPlot⁺ (PDB's 1F8B, blue, and 2HT8, green).¹¹⁹

Oseltamivir (**6**) can be administered orally and displays high systemic bioavailability. It is very likely that these two factors played a significant role in it being selected as the drug of choice towards the fight against the influenza virus, and being stockpiled by countries around the world in preparedness for a sudden influenza outbreak.⁹¹

In terms of side effects, oseltamivir (**6**), like zanamivir (**25**), produces very mild adverse effects (*e.g.* diarrhoea, cough); however, it has additionally been linked with some more serious conditions, such as an indication of mental instability and suicidal tendencies.¹²⁰⁻¹²² Although some cases of psychiatric incidents have been recorded in patients using oseltamivir (**6**), consensus as to whether these were caused by its use has not been reached.^{122,123} Owing to the potential for psychiatric interactions it is now mandatory for a warning to be present in the label of oseltamivir (**6**).¹²²

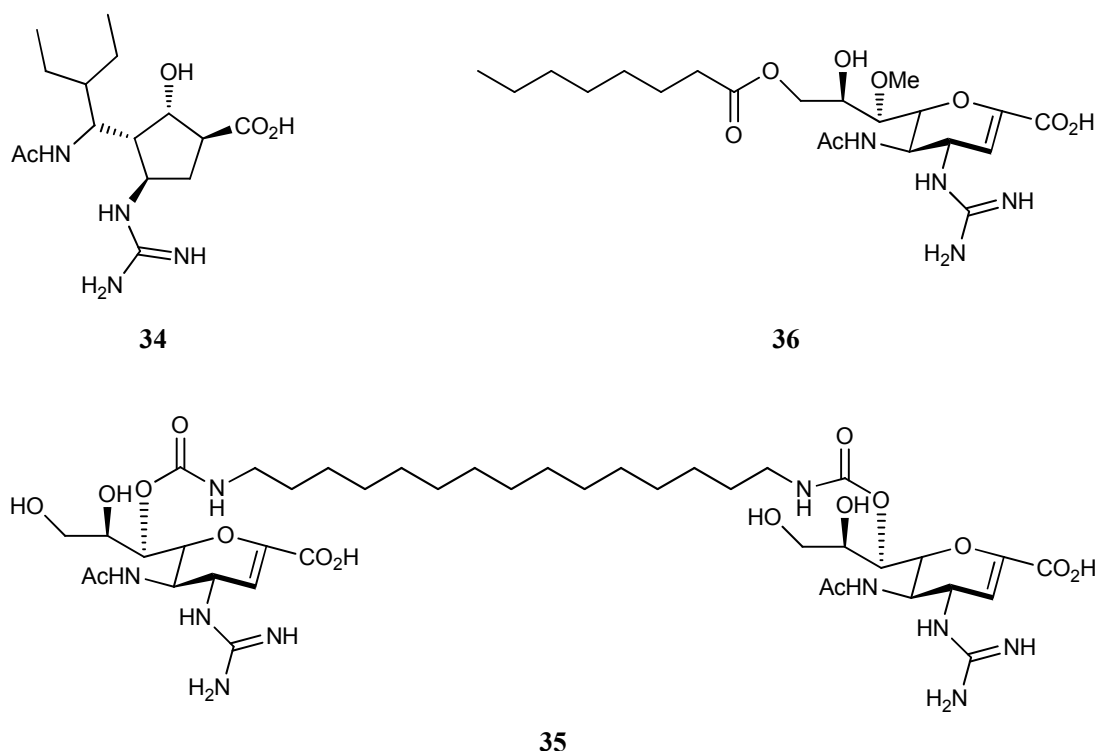
In drug design, one of the major risks that researchers undertake is to design an inhibitor that is structurally different from the natural substrate, targeting non-essential amino acids for catalysis. Non-essential amino acids for catalysis are more likely to suffer point-mutations than nucleophilic ones, since their mutation does not greatly influence the overall catalytic mechanism. Comparing oseltamivir (**6**) with the natural substrate, sialic acid (**4**), the differences are easily apparent, and once in the active site both compounds are capable of interacting with different amino acids. Oseltamivir (**6**) interacts with some non-nucleophilic amino acids; therefore, the probability of a mutant virus arising that is resistant towards oseltamivir is high. The number of mutated influenza viruses resistant to oseltamivir (**6**) that circulate in the human population is already alarming, with five specific point mutations identified so far; however, these mutants are still sensitive towards zanamivir (**25**).^{91,124,125} One particular mutation that has caused concern occurred in H1N1 where the percentage of resistance towards oseltamivir (**6**) passed from 0.4% in the 2007-2008 flu season to a virtually 100% in the following year.^{70,126} A description of each of the specific neuraminidase point mutations conferring resistance to the neuraminidase inhibitors will be given in Chapter 6.2.

2.6.3 Novel clinical candidates

In light of the alarming rate at which resistance is being observed towards the currently approved neuraminidase inhibitors, there is a critical need to design and develop new inhibitors for the treatment of the influenza A virus before the

emergence of a new, global influenza pandemic with more dramatic effects than the recent one.

In an effort to aid the development of new inhibitors towards influenza, the United States Federal Drug Administration created a fast track programme for the development of such drugs. Peramivir (**34**); a dimeric derivative of zanamivir (**35**); and CS-8958 (**36**) are currently in clinical trials as part of this programme.



Peramivir (**34**) was designed to take advantage of the hydrophobic pockets present in the active site. *In vitro* and *in vivo* testing showed that it is as active as zanamivir (**25**) and oseltamivir (**6**) *in vitro*, with the advantage of being highly specific towards viral neuraminidase over bacterial and mammalian neuraminidases.¹²⁷ In human clinical trials Peramivir (**34**) has been shown to have a low oral bioavailability; therefore, it has been tested by intramuscular injection *in vivo* in mice infected with H1N1 (and H3N2), affording the same survival rate as oseltamivir (**6**) (100% with a 10 or 20 mg/kg/day).¹²⁷ Dimeric zanamivir (**35**) and CS-8958 (**36**) are long lasting neuraminidase inhibitors, which offer the potential for a weekly administration instead of a daily dosing.^{128,129} Furthermore, the dimeric zanamivir (**35**) has been shown to be a 100-fold more potent inhibitor than the parent compound, zanamivir (**25**), against influenza virus H1N1 and H3N2.^{129,130} It is thought that the increased

inhibitory activity of the dimeric inhibitors is due to the ability to cross-link and possibly cause aggregation of several viral particles.¹²⁹

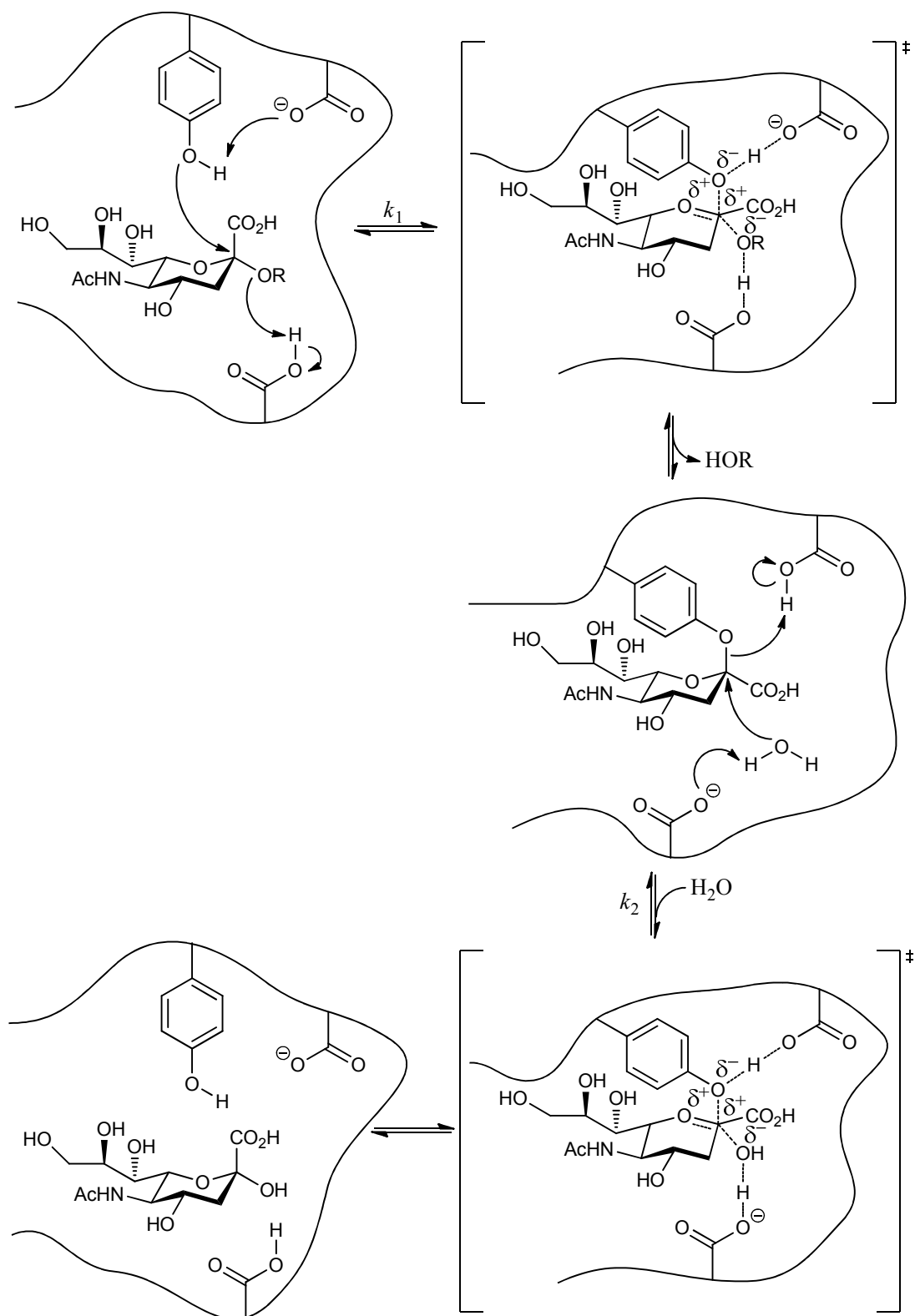
Also noteworthy is the development of a new influenza virus inhibitor, that does not target any of the viral replication pathways or even the two viral surface proteins, hemagglutinin and neuraminidase. DAS181 (Fludase[®]) is a broad-spectrum drug candidate for the prophylactic treatment of the influenza virus, and is presently undergoing Phase II clinical trials.¹³¹ DAS181 is a recombinant fusion protein with a molecular mass of 45kDa, composed of the catalytic domain of *Actinomyces viscosus* sialidase and an epithelial anchoring domain of human amphiregulin.¹³² This new approach is based on the concept of cleaving cell-surface terminal sialic acid residues present on the respiratory epithelium; removing these receptors leads to the influenza virus being unable to attach itself to the host cells.^{133,134} By targeting the epithelium cells instead of the influenza virus, DAS181 avoids the potential development of resistance.^{132,135}

2.7 Aims of the present project

The currently approved drugs, zanamivir (**25**) and oseltamivir (**6**), have already been observed to induce the generation of several drug resistant mutations within the influenza virus. This may be due to the fact that both inhibitors target the oxocarbenium ion-like transition state in the catalytic mechanism of neuraminidases, targeting non-essential amino acid residues for catalysis (Scheme 5, Chapter 2.5.3).

As an alternative mechanism for sialidases, it has been shown that bacterial and parasitic sialidases use a tyrosine/glutamate couple as the catalytic nucleophile, rather than the more common glutamate/tyrosine couple found in the majority of retaining glycosidases.⁵⁷ This is most likely to be due to the chemical nature of the substrate, sialic acid.⁵⁷ Watts *et. al.* postulated that since sialic acid possesses a carboxylate group adjacent to the anomeric position, a possible nucleophilic attack from a glutamate residue would be unfavourable due to electrostatic interactions between the incoming nucleophile and the carboxylate group.⁵⁷ Therefore, by employing a tyrosine/glutamate nucleophilic pair, the tyrosine residue is able to perform the nucleophilic attack without facing such repulsive electrostatic interactions, only achieving a considerable ionic character at the transition-state.⁵⁷

In the first step of this alternative mechanism, a glutamate residue acts as a general base catalyst, deprotonating the hydroxyl group of the catalytic tyrosine residue (Scheme 6).¹³⁶ The hydroxyl group of the tyrosine residue then acts as a nucleophile, attacking the anomeric position (C-2) of the sialic acid residue, forming a covalent sialyl-enzyme intermediate. Parallel to this action, the aglycone is protonated by an aspartate residue activating it towards leaving. During the glycosylation step, there is then the cleavage of the sialic acid from the host cell membrane glycoconjugate.



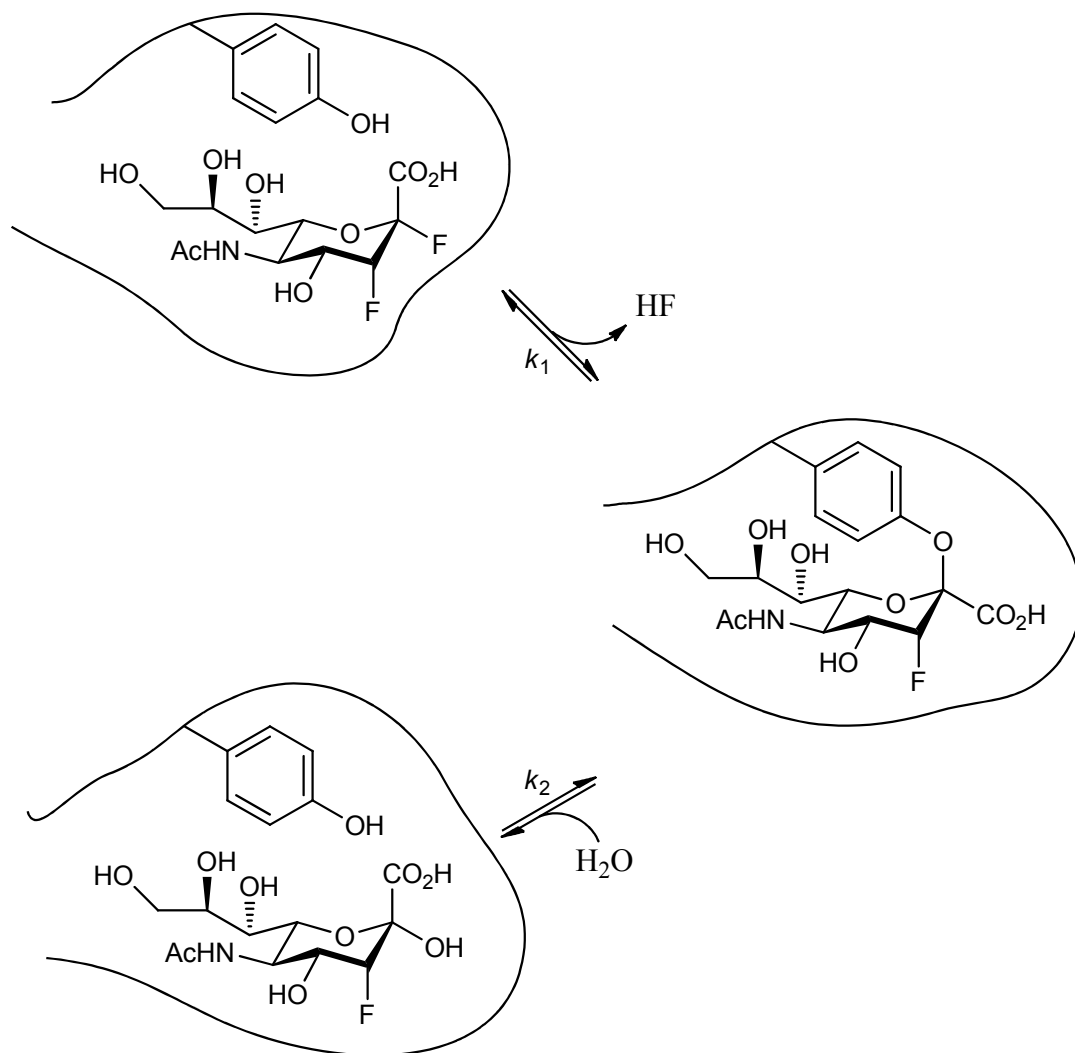
Scheme 6 Proposed catalytic mechanism for *Trypanosoma cruzi* trans-sialidase.¹³⁷
R - Glycoconjugate.

However, the sialidase enzyme needs to complete the catalytic cycle to regain enzymatic activity, as its tyrosine residue remains covalently bound to the sialic acid residue after the first (glycosylation) step.

In the second stage of the mechanism, an aspartate residue deprotonates a molecule of water, activating it towards nucleophilic attack on the sialosyl-enzyme intermediate. This step passes through a second oxocarbenium ion-like transition state with concomitant cleavage of the bond between the sialic acid (**4**) and the tyrosine residue. This second (deglycosylation) step is important for the recovery of enzymatic activity. The key aspect of this alternative mechanism for sialidases is that a covalent bond is formed between sialic acid and the catalytic tyrosine residue, ultimately yielding an overall retention of configuration at the anomeric centre of the sialic acid.

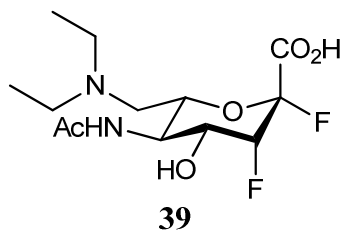
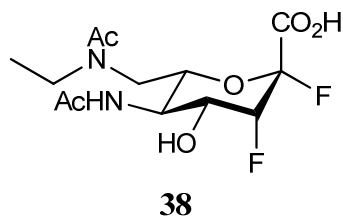
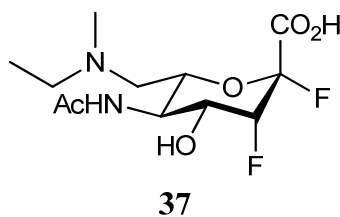
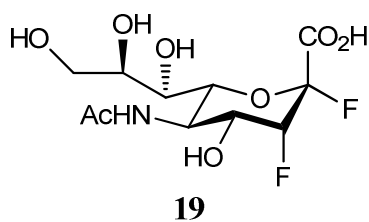
Recent unpublished work by the research groups of Dr. Andrew Watts and Prof Stephen Withers has observed that influenza neuraminidase also operates through a similar mechanism, with the presence of both oxocarbenium ion-like transition states and formation of the covalent sialyl-enzyme intermediate. This project aims to develop a novel class of inhibitors of influenza neuraminidase based on 2,3-difluorosialic acid (**19**), and evaluate these compounds as potential therapeutics for the treatment of the influenza virus. However, rather than targeting the transition state of the neuraminidase catalysed reaction like the current therapeutics, zanamivir (**25**) and oseltamivir (**6**), our strategy will target the covalent sialyl-enzyme intermediate formed during the catalytic cycle (Scheme 6). It is anticipated that these compounds, known as mechanism-based inhibitors, have the potential to be less susceptible to drug induced resistance. By targeting key residues essential for catalysis, evolutionary pressure for the enzyme to mutate these specific amino acid residues will be greatly reduced, as mutations to catalytically essential residues will result in the generation of non-viable influenza neuraminidase.

In order to achieve this, an approach based on 2,3-difluorosialic acid (**19**) was developed. It has been shown by Watts *et al* that 2,3-difluorosialic acid differentiates the rate constants of glycosylation (k_1) and deglycosylation (k_2) of *Trypanosoma rangeli* sialidase which has a similar catalytic cycle.¹³⁸ The electronegative substituent at C-3 destabilises the formation of the oxocarbenium ion formed in the transition states (slowing down k_1 and k_2), whilst the fluorine at C-2 allows the glycosylation step to occur, by acting as a leaving group (Scheme 7).^{137,138}

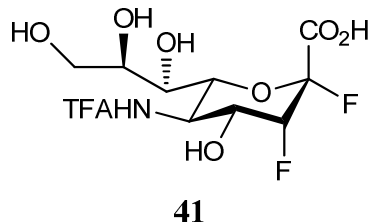
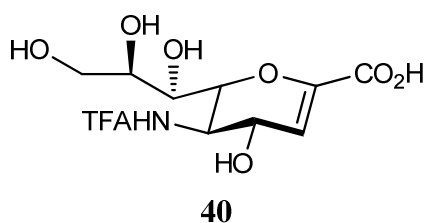


Scheme 7 Neuraminidase catalytic reaction with 2,3-difluorosialic acid (**19**).

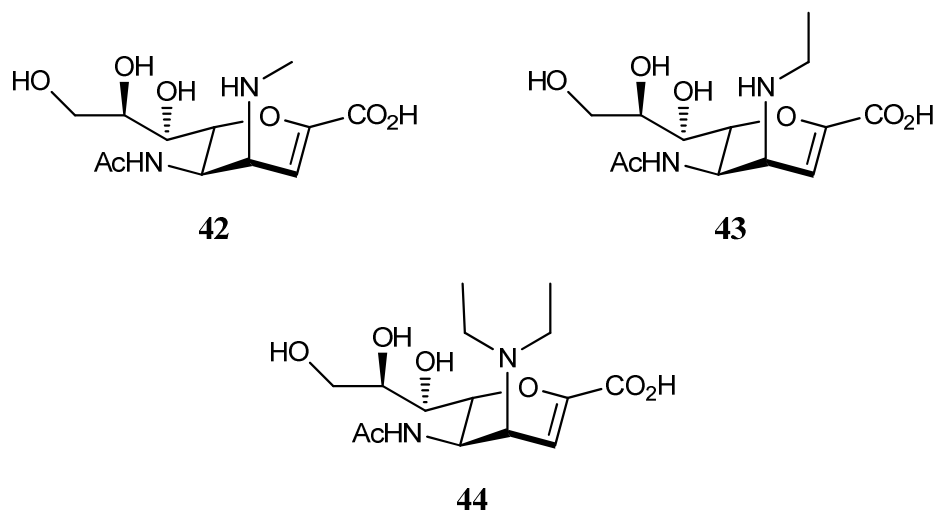
It was envisaged that the introduction of a series of *N*-alkyl amines at C-7 (namely 7-*N*-ethyl-*N*-methylamino (**37**), 7-*N*-ethylacetamido (**38**) and 7-*N,N*-diethylamino (**39**)) could result in an increase of hydrophobic and hydrophilic contacts with neighbouring amino acid residues around the pocket of the glycerol moiety akin to those observed in oseltamivir (**6**).¹³⁹



In addition, it was shown by Meindl that the 5-*N*-trifluoroacetamido-Neu5Ac2ene (**40**) had an IC_{50} of 8.6 μM ; therefore, it was decided to probe the change of the *N*-acetamido group to a *N*-trifluoroacetamido group in the 2,3-difluorosialic acid moiety (**41**).¹⁴⁰



In addition to the modifications at C-7 and C-5, a study to probe the interactions found around an *N*-alkylamine substituent at C-4 was undertaken.⁹⁷ For this reason a series of 4-*epi-N*-alkylamines Neu5Ac2ene derivatives were synthesised, namely 4-*epi-N*-methylamine (**42**), 4-*epi-N*-ethylamine (**43**) and 4-*epi-N,N*-diethylamine (**44**).

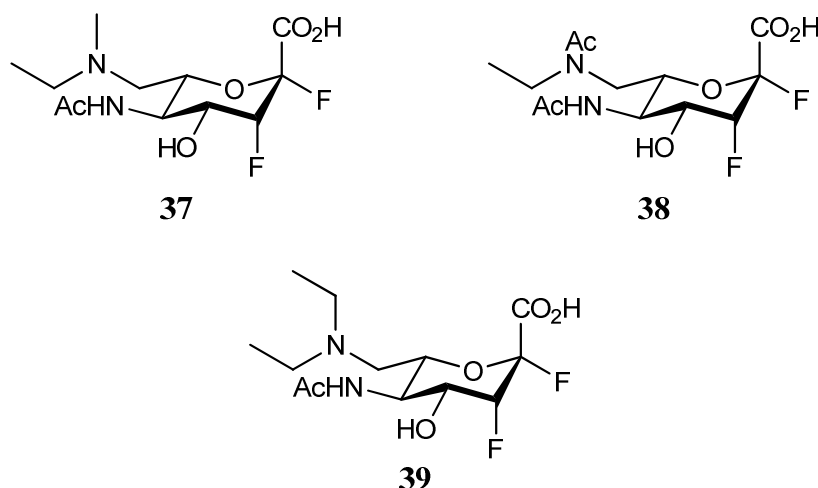


The reasons why it was decided to use the Neu5Ac2ene scaffold were due to the straightforward synthesis of the common precursor for the synthesis of the C-4 *N*-alkylamines, and once they were inserted, the introduction of the fluorines at C-2 and C-3 could be attempted.

Chapter 3 - Synthesis of C-7 modified 2,3-difluorosialic acids

3.1 Prelude

This chapter describes the synthesis of several 7-*N*-alkylamino 2,3-difluorosialic acids; 7-*N*-ethyl-*N*-methylamino (**37**), 7-*N*-acetamido-*N*-ethyl (**38**) and 7-*N,N*-diethylamino (**39**) 2,3-difluorosialic acids, as mechanism-based inhibitors of influenza neuraminidase. We aimed to probe the effect of these substitutions on the binding to Arg224 and Glu276, which are associated with hydrogen bond forming interactions with the glycerol side chain of sialic acid.



It was predicted that compound 7-*N*-ethyl-*N*-methylamino-2,3-difluorosialic acid (**37**) may represent an isosteric analogue of the glycerol side chain of sialic acid. It was hoped that this compound might provide information regarding the importance of the hydrogen bonds formed between the hydroxyl groups of the glycerol side chain and the amino acid residues (principally Arg224 and Glu276). Furthermore, by replacing the hydrophilic side chain with a hydrophobic one, the overall hydrophobicity of the compound could be also increased.

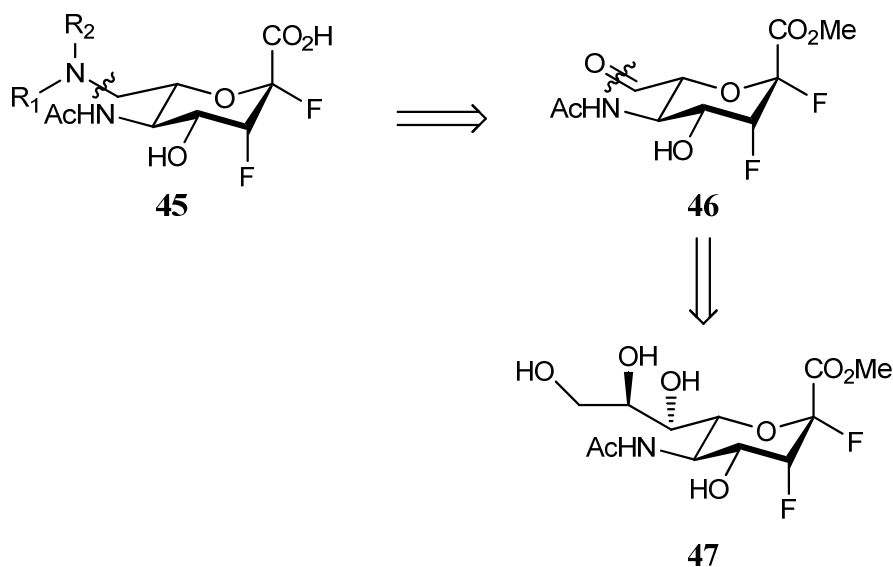
The 7-*N,N*-diethylamino derivative (**39**) was designed as an isostere of the pentyloxy ester side chain of oseltamivir (**6**). In addition to the presence of the diethyl side

chain, the presence of a nitrogen, instead of oxygen, may show further hydrogen bonding interactions to residues and this could improve the binding.

Compound 7-*N*-ethylacetamido-2,3-difluorosialic acid (**38**) was synthesised after the study of the crystal structure of influenza neuraminidase N2, where the presence of amino acid residues (Arg224 and Glu276) above the nitrogen atom that could interact with an acetate moiety was observed (A. Watts, unpublished results). Therefore, it was envisaged that the synthesis of the 7-*N*-ethyl-*N*-acetamido derivative could help to maximize this possible interaction.

3.2 Retrosynthetic analysis

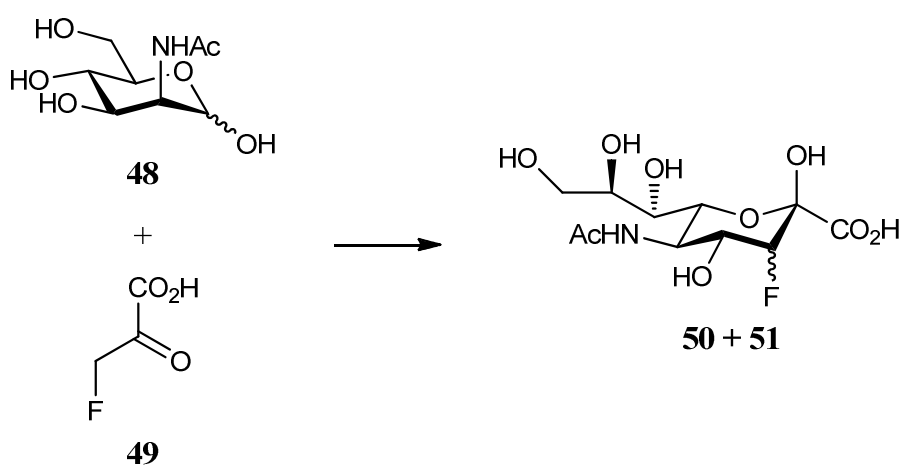
Our general strategy for the construction of the series of 7-*N*-alkylamino 2,3-difluorosialic acids was based on the retrosynthetic analysis shown in Scheme 8. Retrosynthetic cleavage of the bond indicated on the 7-*N,N*-dialkylamino (**45**) furnishes the C-7 aldehyde (**46**) as a viable precursor. This key intermediate contains the aldehyde, which could support the introduction of the *N,N*-dialkylamines via a reductive amination. It was anticipated that the aldehyde intermediate (**46**) could be derived from the 2,3-difluorosialic acid (**47**) through an oxidative cleavage of the glycerol side chain. The synthesis of 2,3-difluorosialic acid (**47**) has been reported previously by Watts *et al.*¹³⁷



Scheme 8 Retrosynthetic scheme outlining the strategy for the synthesis of a series of 7-*N,N*-dialkylamino 2,3-difluorosialic acids.

3.3 The synthesis of 2,3-difluorosialic acid (47)

The synthesis of 3-fluorosialic acid (**50**) was accomplished enzymatically using *N*-acetylneuraminic acid aldolase (Neu5Ac aldolase, EC 4.1.3.3) following the literature procedure of Watts *et al.*¹³⁷ A solution of *N*-acetylmannosamine (**48**) and β -fluoropyruvic acid (**49**) was treated with Neu5Ac aldolase for 5 days (Scheme 9).¹³⁷ The reaction mixture was purified by passing it through an ion-exchange column (formate form), followed by freeze-drying the eluent, to afford 3-fluorosialic acid (**50**).



Scheme 9 Aldolase reaction. Neu5Ac aldolase, H₂O, r.t., 5 days.

The reaction was followed using ¹⁹F NMR by monitoring the disappearance of the signal from β -fluoropyruvic acid (**49**) at δ -233.3 ppm, and the formation of a signal corresponding to the axial 3-fluorosialic acid (**50**) at δ -208.3 ppm (Figure 11).

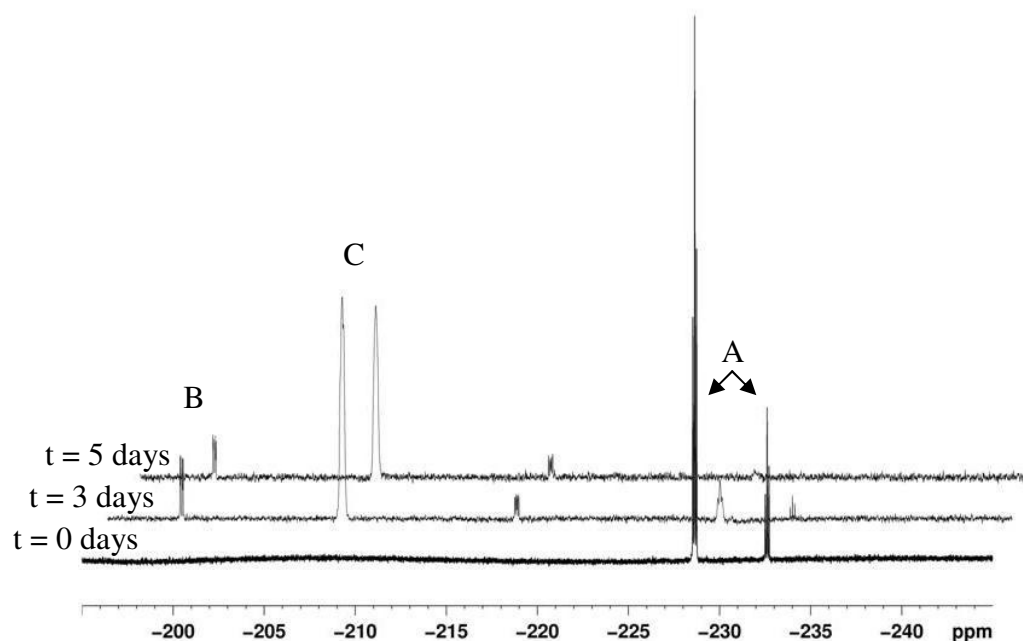
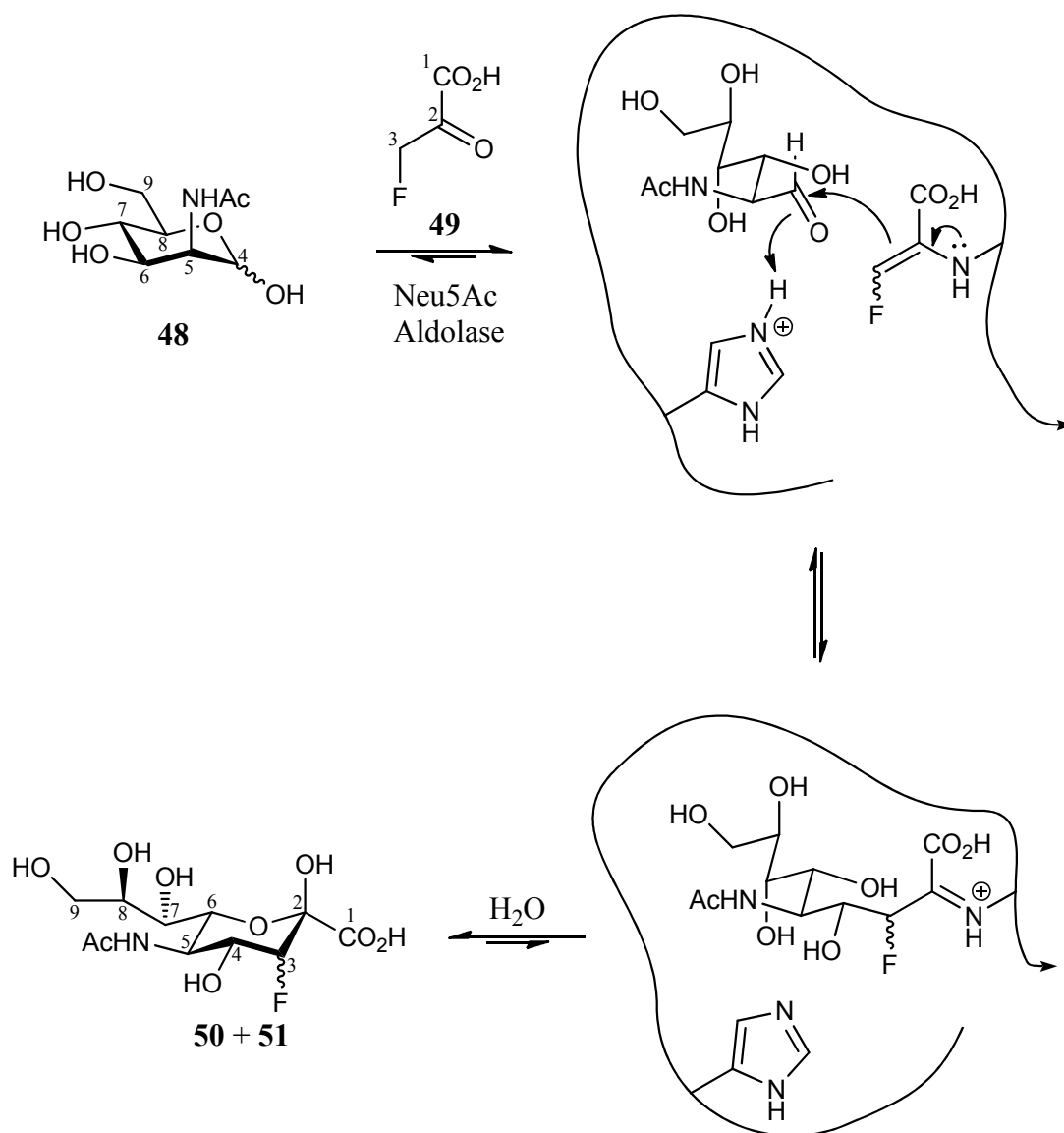


Figure 11 Overview of the aldolase reaction over 5 days, showing the consumption of β -fluoropyruvic acid (δ -233.3 ppm) and the formation of the product, axial 3-fluorosialic acid (**50**) (δ -208.3 ppm). t - time; A – β -fluoropyruvic acid; B – C-3 equatorial fluorine; C – C-3 axial fluorine (desired product).

The aldolase used in this reaction is a type I aldolase, which forms a Schiff base intermediate in the active site with β -fluoropyruvic acid (**49**), adding the β -fluoropyruvic acid stereospecifically to the acyclic form of *N*-acetylmannosamine (**48**). The β -fluoropyruvic acid (**49**) forms an enamine with an active site residue, Lys, subsequently reacting with the aldehyde of *N*-acetylmannosamine, which is activated by protonation from an active site residue, His, generating the new carbon-carbon bond (Scheme 10).^{141,142}



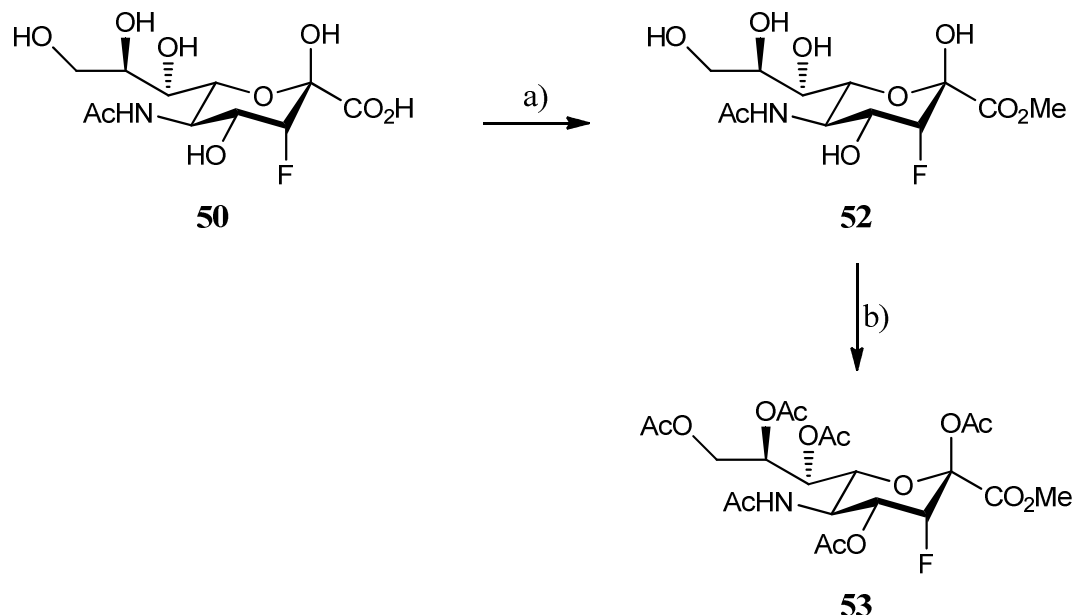
Scheme 10 Aldol reaction between *N*-acetylmannosamine (**48**) and β -fluoropyruvic acid (**49**) catalysed by Neu5Ac aldolase.¹⁴² The numbering of the carbon backbone is indicated corresponding to the final compound, 3-fluorosialic acid (**51**).

Under the experimental conditions used here, the axial isomer of the fluorine at C-3 was produced as the major product. The ratio between the fluorine having an axial or equatorial orientation depends on the relation between β -fluoropyruvic acid (**49**) and *N*-acetylmannosamine (**48**), with a ratio of 1:2 affording as the predominant isomer, the axial one. In the work developed by Beliczey *et al*, no specific reasons were given for this occurrence.¹⁴³

The optimal conditions for the aldolase reaction are at a pH 6-9 and at 37 °C.¹⁴¹ It has been shown that Neu5Ac aldolase, although being specific to the pyruvate donor group, can accept slight modifications to the molecule such as the presence of a

fluorine at the β carbon. On the other hand, the enzyme is able to accommodate a variety of modifications at C-4, 5 and 6 of the acceptor hexose moiety.^{137,141} However, modifications at the C-3 hydroxyl of the hexose moiety (labelled as C-6 in Scheme 10) are not tolerated by the aldolase, as this hydroxyl is crucial for the formation of the new nonulose ring, since this hydroxyl oxygen will ultimately become the endocyclic oxygen of the sialic acid formed.¹⁴² As a result of the subtle change of using β -fluoropyruvic acid as a substrate a large reduction in the rate of reaction was observed.

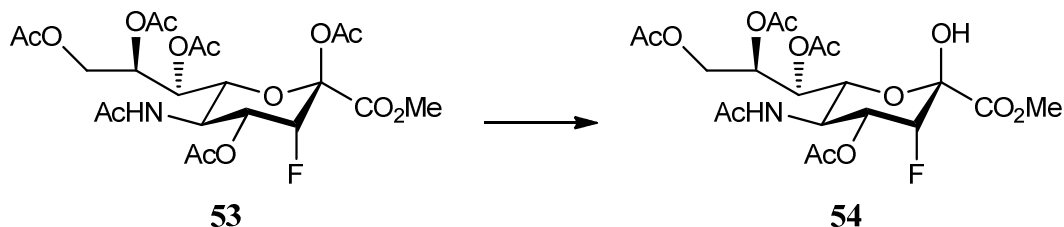
The 3-fluorosialic acid (**50**) was then esterified by treatment with trifluoroacetic acid in methanol to give the 3-fluorosialic acid methyl ester (**52**), which was used in the next step without further purification (Scheme 11). Global acetylation of the 3-fluorosialic acid methyl ester (**52**) was achieved using acetic anhydride in pyridine which proceeded slowly over 4 days (owing to the low reactivity of the anomeric hydroxyl) to give the per-*O*-acetylated-3-fluorosialic acid methyl ester (**53**) in good overall yield (72% from the aldolase reaction) (Scheme 11).¹³⁷



Scheme 11 Formation of per-*O*-acetylated 3-fluorosialic acid (**53**). a) TFA, MeOH, r.t., O/N; b) Ac_2O , Pyr, r.t., 5 days. 72% from the aldolase reaction.

The low reactivity observed for the anomeric hydroxyl is likely to be a consequence of the fluorine present at C-3, which will reduce the nucleophilicity of the hydroxyl. Furthermore, the anomeric hydroxyl is a tertiary hydroxyl and so sterically quite

hindered. The per-*O*-acetylated-3-fluorosialic acid methyl ester (**53**) was then selectively deprotected at C-2 using hydrazine acetate in a 1:1 mixture of DCM and MeOH, affording the hemiketal (**54**) in good yield (65%) (Scheme 12).¹³⁷



Scheme 12 Anomeric deprotection of per-*O*-acetylated sialic acid (**53**). Hydrazine acetate, DCM/MeOH 1:1, 4 °C, 3h, 65%.

Owing to a higher reactivity of the anomeric acetal (relative to the other hydroxyl groups) combined with a weak nucleophile, hydrazine acetate, the deacetylation reaction is selective for the anomeric acetal.¹⁴⁴

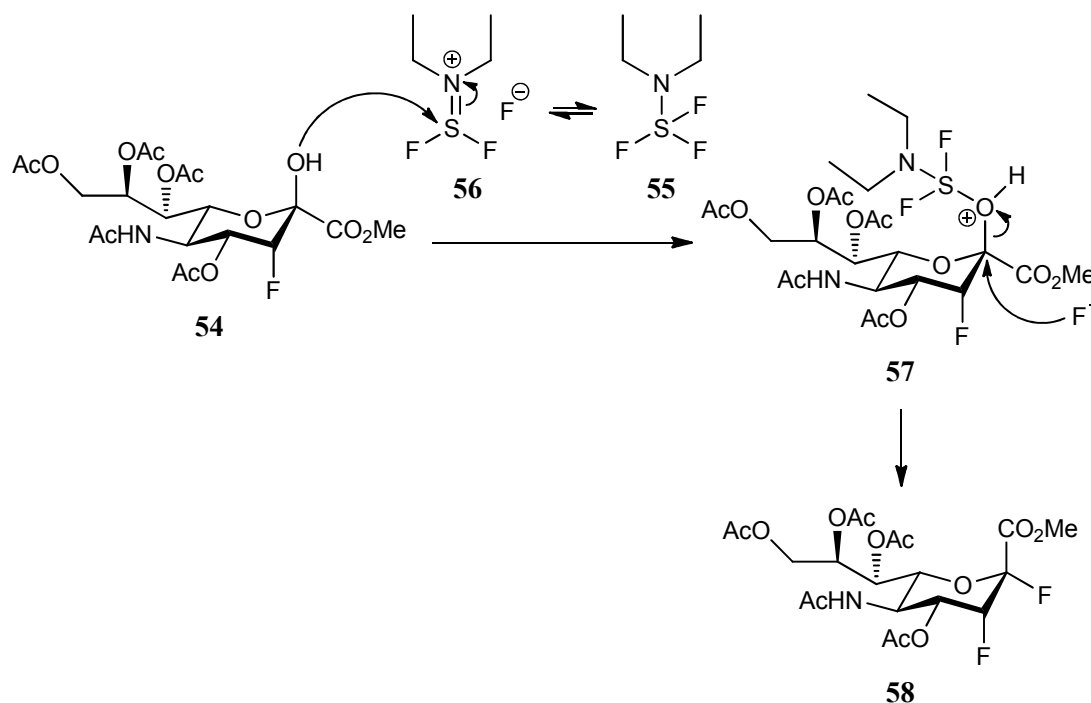
It was found that the ratio of DCM/MeOH had an effect on the yield of the reaction, where a ratio of 1:1 gave a yield of 65%. The ratio of 4:1 DCM/MeOH was found to improve the yield of reaction, increasing from 65 to 81%.

The next step in the synthesis was to introduce a fluorine atom into the anomeric position. Following the methodology employed by Watts *et al*, the hemiketal (**54**) was treated with DAST (**55**), in dichloromethane, at -30 °C, resulting in the fluorination at C-2 to give the desired 2,3-difluorosialic acid derivative (**58**) in modest yield (45%) (Scheme 13).¹³⁷ The mechanism for this reaction involves the nucleophilic attack on the sulfonium ion (**56**) by the anomeric hydroxyl of the hemiketal (**54**) to form the intermediate species (**57**) (Scheme 13). This intermediate activates the anomeric hydroxyl to become a good leaving group, which then undergoes S_N2 displacement by a fluoride ion.¹⁴⁵ This class of fluorination reaction usually occurs with stereochemical inversion of configuration at C-2.

The existence of such intermediate species has been supported by ¹⁹F NMR data obtained during a similar fluorination reaction, between DAST and a glucose derivative.¹⁴⁶

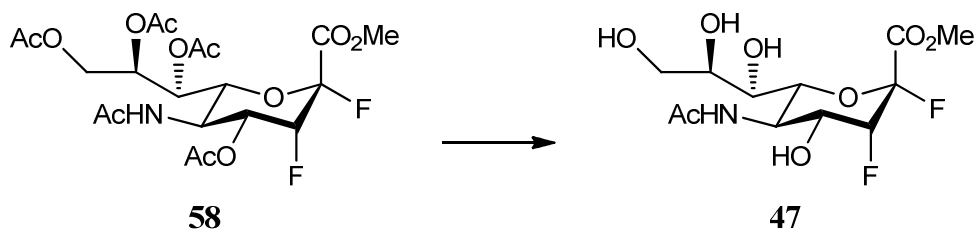
The equatorial orientation of the fluorine atom at C-2 of 2,3-difluorosialic acid (**58**) was confirmed using ¹⁹F NMR. The chemical shift and coupling constant for the fluorine at C-2 were compared with the literature. A coupling constant between F₂-F₃ of 12 Hz was observed, which is in agreement with literature.^{137,147} For the diaxial

2,3-difluorosialic acid methyl ester (**59**), the F_2 - F_3 coupling constant observed was 17 Hz, confirming a *trans*-diaxial relationship by comparing with values reported in the literature (Scheme 15).¹⁴⁷



Scheme 13 Mechanism of fluorination of the hemiketal (**54**) using DAST (**55**) as the fluorinating agent. DAST, DCM, -30 °C, 30 min, 45%.

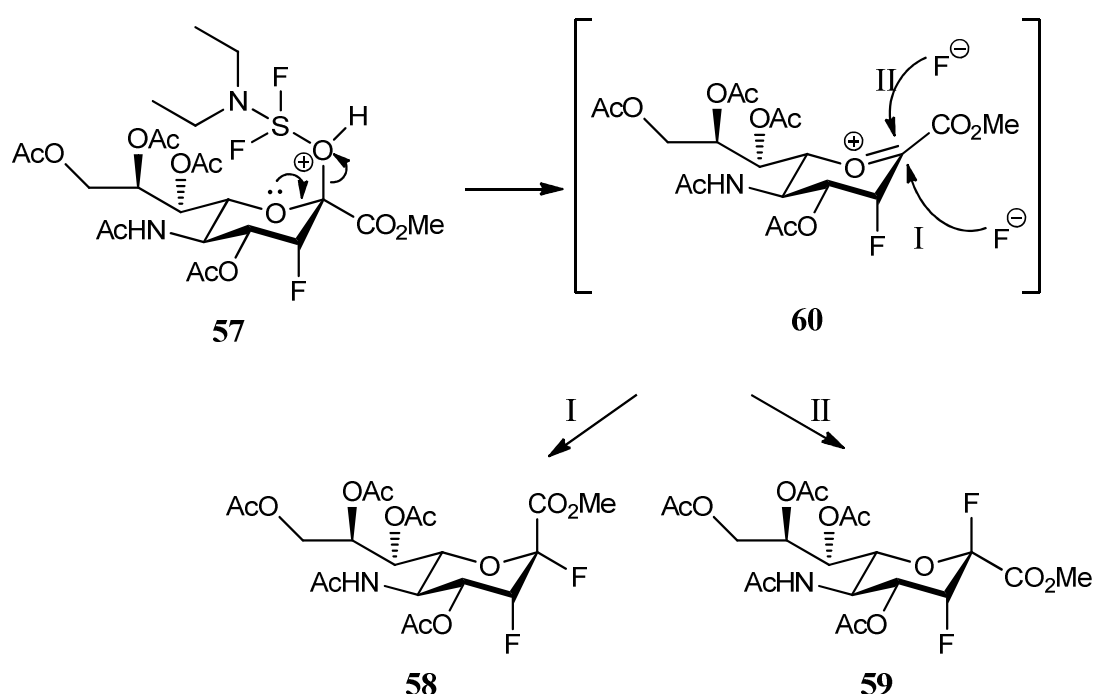
Global deacetylation of the per-*O*-acetylated 2,3-difluorosialic acid methyl ester (**58**) was performed following classic Zemplén conditions using a solution of sodium methoxide in methanol at 4 °C, to afford the desired 2,3-difluorosialic acid methyl ester (**47**) in quantitative yield (Scheme 14).¹⁴⁸



Scheme 14 Deacetylation of per-*O*-acetylated 2,3-difluorosialic acid (**58**). NaOMe, MeOH, 4 °C → r.t., 1h, 100%.

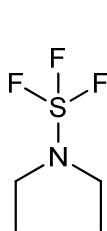
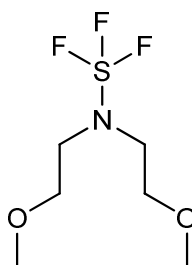
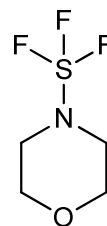
3.4 Investigation the conditions for the synthesis of the anomeric fluoride

The total yield obtained for the fluorination reaction (95%) was considered ideal; however, a mixture of axial (35%) and equatorial (45%) fluorines at C-2 was produced that proved difficult to separate. The mixture of fluorine anomers at C-2 can be rationalized if one postulates the existence of a oxocarbenium-ion (**60**) (Scheme 15). Once the oxocarbenium-ion is formed, the fluoride ion may attack the anomeric position at either the *si*-face, to form the axial isomer (**59**) (pathway I), or at the *re*-face, to form the equatorial isomer (**58**) (pathway II) (Scheme 15).



Scheme 15 Proposed mechanism for the formation of the 2,3-difluorosialic acid methyl ester (**59**).

A series of alternative fluorinating reagents were investigated, in addition to DAST (**55**) in an effort to improve the fluorination step in the synthetic pathway. These reagents included bis(2-methoxyethyl)aminosulfur trifluoride, Deoxo-fluor[®] (**61**) and morpholinosulfur trifluoride (**62**). The advantage of using such aminosulfur fluorinating reagents is that they are less reactive, potentially enabling a higher selectivity towards the fluorination at C-2 and reducing the possibility of undesired side reactions such as rearrangements and eliminations.¹⁴⁹

**55****61****62**

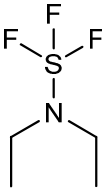
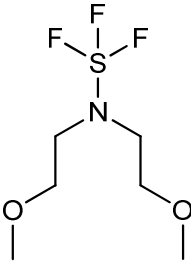
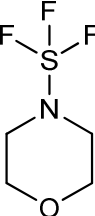
Moreover, these aminosulfur reagents do not require elaborate experimental conditions or apparatus for their use.¹⁴⁹

In addition to investigating different fluorinating reagents, a range of temperatures was also tried varying from -30 °C to reflux. The solvents employed included DCM (from the original conditions) and THF due to its ability to stabilize charged intermediates.

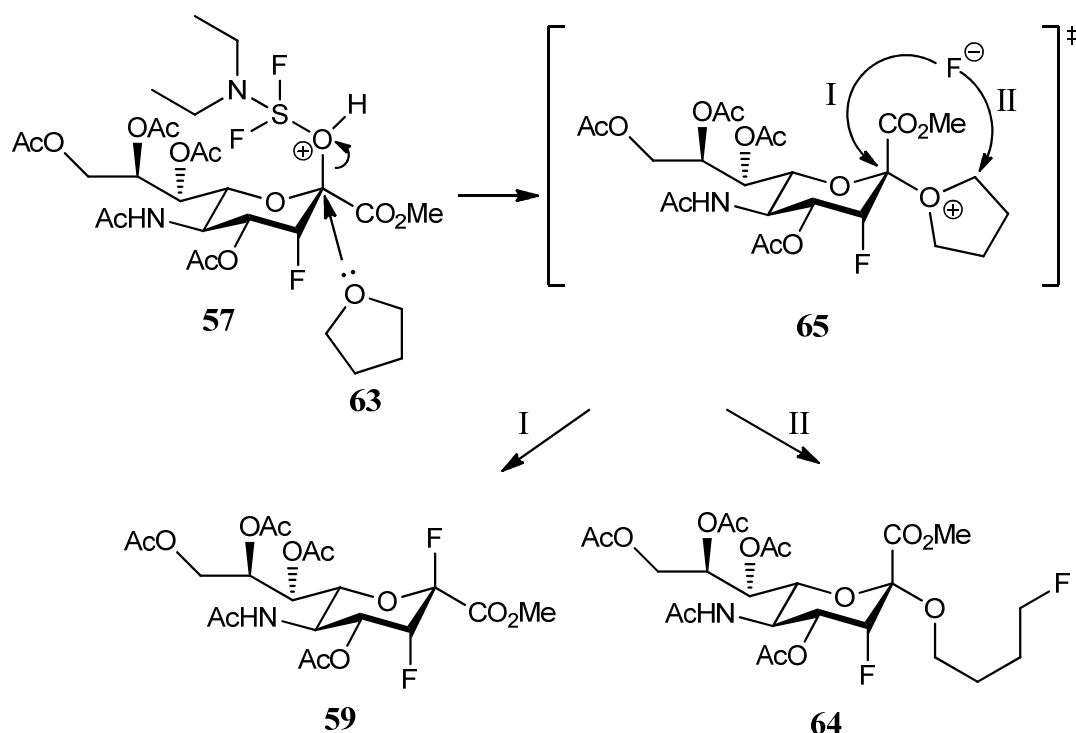
The original condition, DAST in DCM at -30 °C, was the starting point for the improvement of the yield (entry 1, Table 1). This condition afforded both anomers in a 1:1 ratio, and after purification gave the desired equatorial fluorine (**58**) in reasonable yield (45%), and the axial fluorine (**59**) obtained equally with a reasonable yield (30%).

The solvent was then changed from DCM to THF, using DAST as the fluorinating agent and the reaction was performed at -30 °C (entry 2, Table 1). This afforded the undesired axial fluorine exclusively in low yield (30%). An explanation for the predominant formation of the axial fluorination product (**59**), instead of a 1:1 ratio (entry 2, Table 1) when using THF as solvent of the reaction, could be if THF (**63**) is participating in the fluorination reaction by displacing the activated hydroxyl intermediate (**57**), which can then be attacked by the fluorine ion (Scheme 16).

Table 1 Overview of the different conditions used for the fluorination step. Ratio of isomers determined by ^{19}F NMR. ^a Supplied in THF; ^b Supplied in toluene; a Not isolated.

<div style="display: flex; justify-content: space-around; align-items: center;"> <div style="text-align: center;"> DAST  55 </div> <div style="text-align: center;"> Deoxo-fluor  61 </div> <div style="text-align: center;"> Morpholinosulfur trifluoride  62 </div> </div>						
Entry	Reagent	Solvent	Temp (°C)	F _{ax}	F _{eq}	Yield (%) of F _{eq}
1	(55)	DCM	-30	1	1	45
2	(55)	THF	-30	1	0	30
3	(61)^a	DCM	-30	1	0	30
4	(61)^a	DCM	r.t.	1	1	a
5	(61)^b	DCM	r.t. → reflux	5	1	40
6	(62)	DCM	0 → r.t.	2	1	a
7	(62)	DCM	reflux	1	0	20

The fluorine ion can attack the intermediate (**65**) either at the anomeric position, displacing the THF to form the diaxial fluorination product (**59**), or at the carbon adjacent to the THF ring oxygen, leading to the opening of the THF ring, generating the 4'-fluorobutoxy-3-fluorosialic acid (**64**) in low yield (26%). The observed formation of this product serves as confirmation of participation of THF in the reaction. The anomeric stereochemistry of the ether derivative (**64**) has not been confirmed; however, equatorial stereochemistry presented is inferred on the basis of the proposed mechanism (Scheme 16).



Scheme 16 Possible mechanism towards the formation of compound **59** and **64** with DAST (**55**) in the presence of THF (**63**).

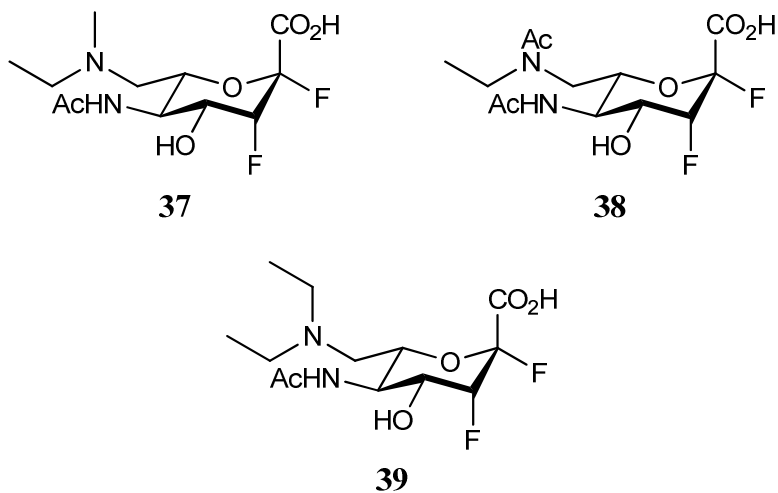
When the hemiketal (**54**) was treated with either Deoxo-fluor[®] (**61**) or morpholinosulfur trifluoride (**62**), a mixture of anomers was observed (entries 3-7). When the reaction was performed in DCM with morpholinosulfur trifluoride (**62**) at reflux, only the axial isomer (**59**) could be observed (entry 7).

Initially these findings seemed contradictory; however, further rationalization revealed that the ether oxygens present in the structures of both Deoxo-fluor[®] (**61**) and morpholinosulfur trifluoride (**62**) might be participating as a Lewis base, stabilizing the formation of an oxocarbenium-ion (**60**).

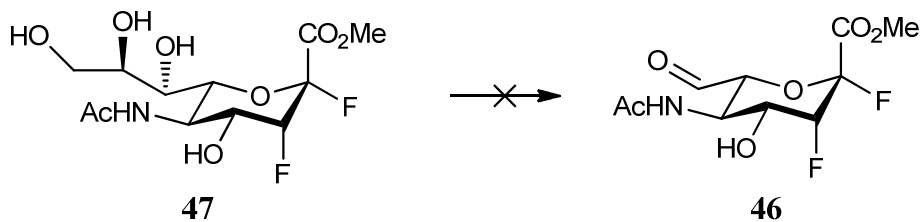
The conditions investigated did not provide a method that would afford the desired compound (fluorine in an equatorial orientation) as a pure isomer and in good yield. The conditions that proved to be the best in terms of yield and anomeric ratio were the ones initially used (entry 1); therefore, no improvement was attained.

3.5 Preliminary investigations into the oxidative cleavage and reductive amination synthesis of a series of 7-*N,N*-dialkylamino 2,3-difluorosialic acids

In order to synthesise the desired final compounds (**37** – **39**) an oxidative cleavage was performed on the glycerol side chain of the 2,3-difluorosialic acid methyl ester (**47**), affording the aldehyde (**46**) which was then treated with a series of *N*-alkyl or *N,N*-dialkylamines to afford the desired final compounds.

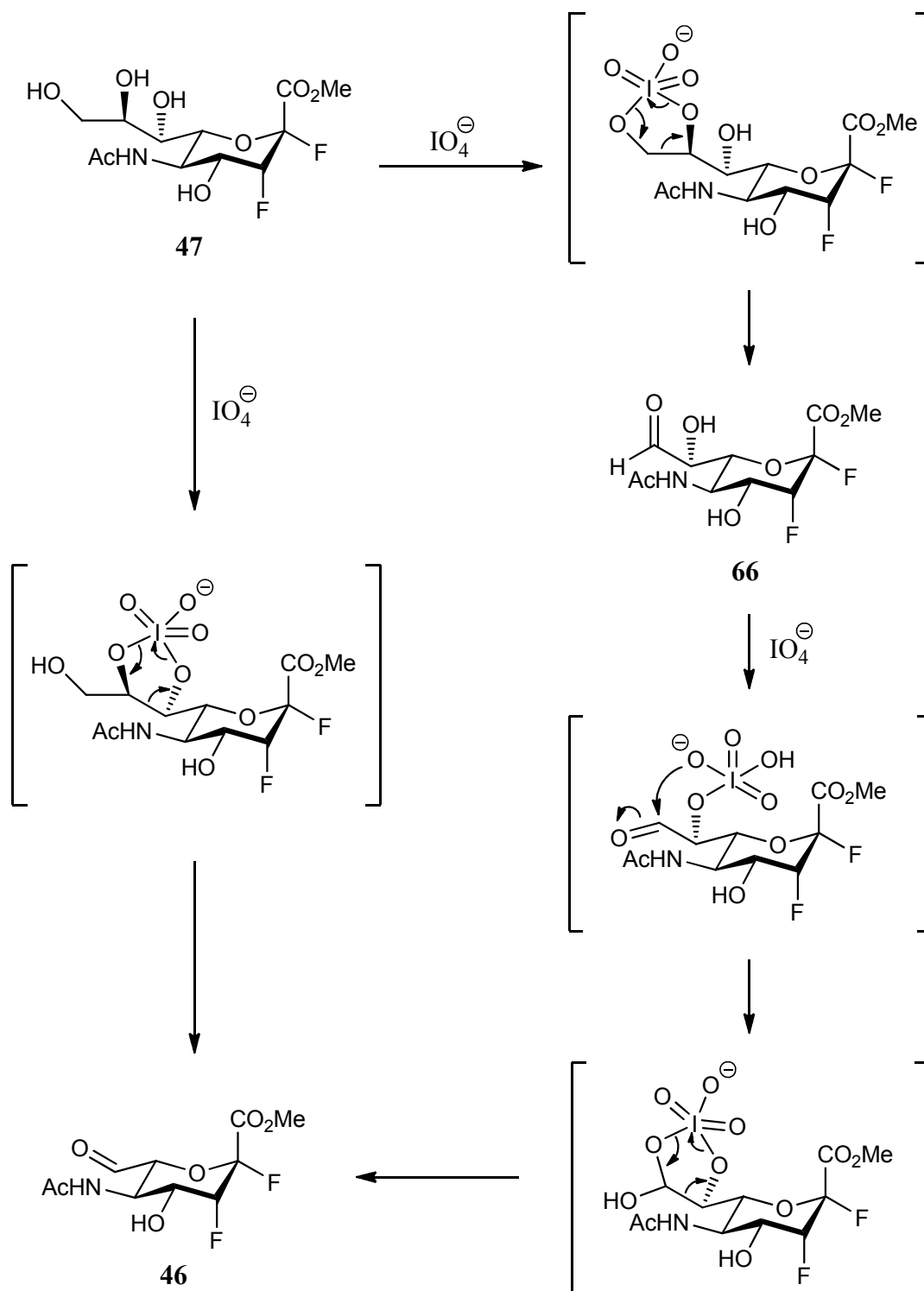


It was envisaged that the formation of the 7-aldehyde (**46**) could be achieved in a single transformation from the 2,3-difluorosialic acid methyl ester (**47**) by performing an oxidative cleavage of the glycerol side chain. An aqueous solution of the 2,3-difluorosialic acid methyl ester (**47**) was treated with a 0.4 M solution of sodium periodate at room temperature for 90 min followed by passage of the reaction mixture through a plug of silica gel in order to remove periodate salts, with no product being isolated (Scheme 17).



Scheme 17 Oxidative cleavage of 2,3-difluorosialic acid (**47**). NaIO₄, H₂O, r.t., 1h30 min.

Considering the structure of the 2,3-difluorosialic acid methyl ester (**47**), the oxidative cleavage with sodium periodate has the potential to occur at two positions in the glycerol side chain, between either the C-9 and C-8, or the C-8 and C-7 diols.



Scheme 18 Proposed mechanism for the oxidative cleavage of the glycerol side chain of 2,3-difluorosialic acid methyl ester (**47**) using sodium periodate.

Oxidative cleavage at either of these positions would produce the aldehydes (**46** or **66**), respectively (Scheme 18). The aldehyde formed from the oxidative cleavage of the C-8 - C-9 diol (**66**) has the potential to undergo a further oxidative cleavage reaction between C-8 and C-7 to afford the desired aldehyde (**46**).

In an attempt to determine why the formation of the aldehyde could not be detected upon periodate treatment of the 2,3-difluorosialic acid (**47**) it was decided to repeat the reaction and monitor the progress of the reaction by ^1H NMR using periodic acid as the reagent (due to its higher solubility in D_2O) and the 2,3-difluorosialic acid methyl ester (**47**). After only 15 min of reaction, a signal at δ 8.06 ppm could be observed, which was attributed to the presence of an aldehyde proton (Figure 12).

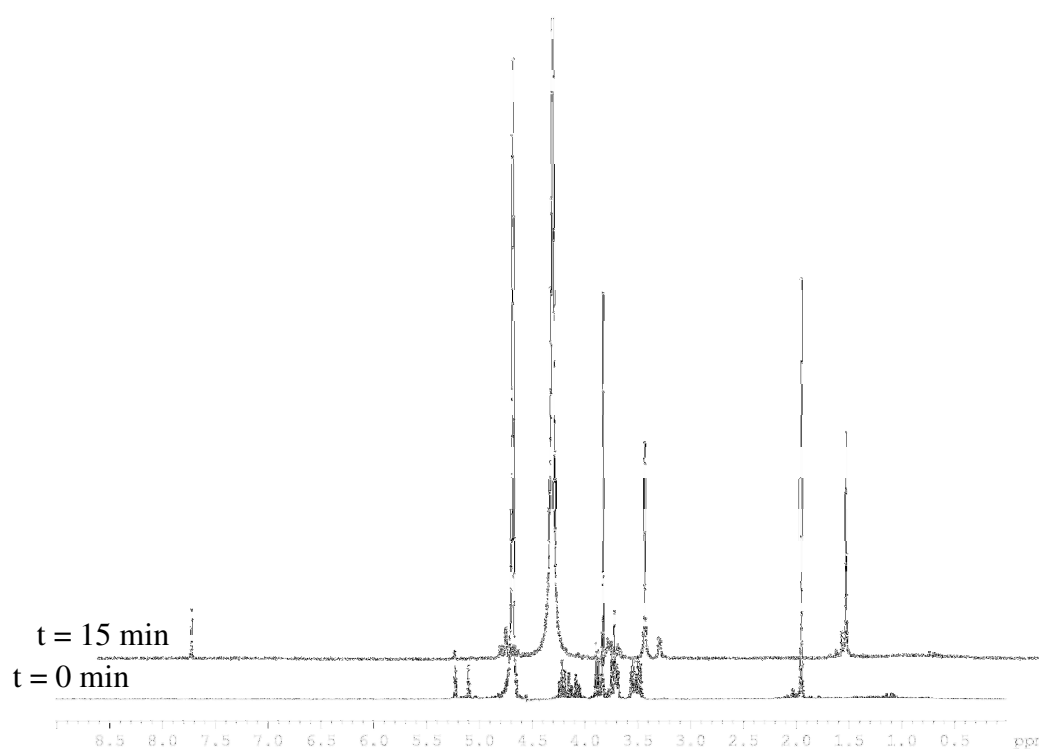


Figure 12 ^1H NMR spectrum of the oxidative cleavage reaction, showing the formation of a signal at δ 8.06 ppm after 15 min.

A second experiment was undertaken, using sodium periodate in water at room temperature (30 min) after which the solvent was removed *in vacuo*, and ^1H NMR again confirmed the presence of a singlet signal at δ 8.06 ppm. These results lead us to propose that the aldehyde may be unstable, decomposing when passing through a silica gel column. Therefore, it was decided to use the product of the periodate reaction crude, only removing the solvent from the reaction (*in vacuo*). Confirmation

of the desired cleavage of the glycerol side chain (between C-7 and C-8) was provided by mass spectrometry (MS). The compound identified was not the aldehyde but the geminal diol (**67**) (322.07 m/z) (Figure 13).

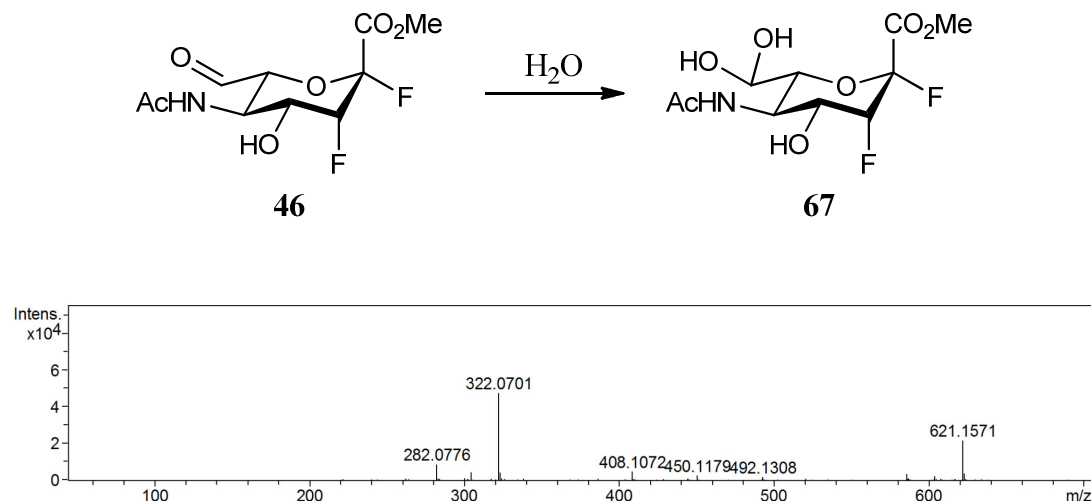
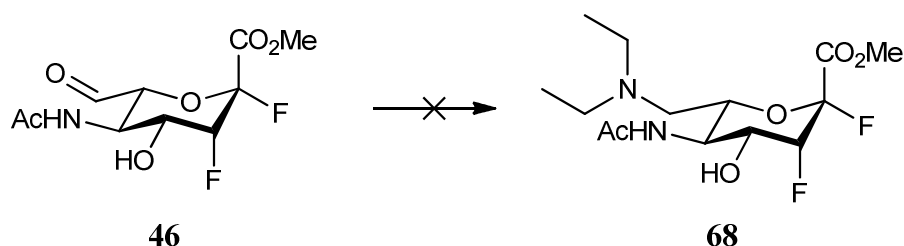


Figure 13 Mass spectrum of the C-7 aldehyde 2,3-difluorosialic acid (**46**).

The next step in the synthesis involved the reductive amination at the aldehyde (**46**) with a series of amines to afford the desired C-7 modified targets. The first derivative synthesised was the 7-*N,N*-diethylamino (**68**). A solution of the aldehyde (**46**) in methanol was treated with diethylamine and sodium cyanoborohydride at room temperature (Scheme 19).



Scheme 19 Reductive amination of the aldehyde (**46**). Diethylamine, NaCNBH₃, AcOH, MeOH, r.t., O/N.

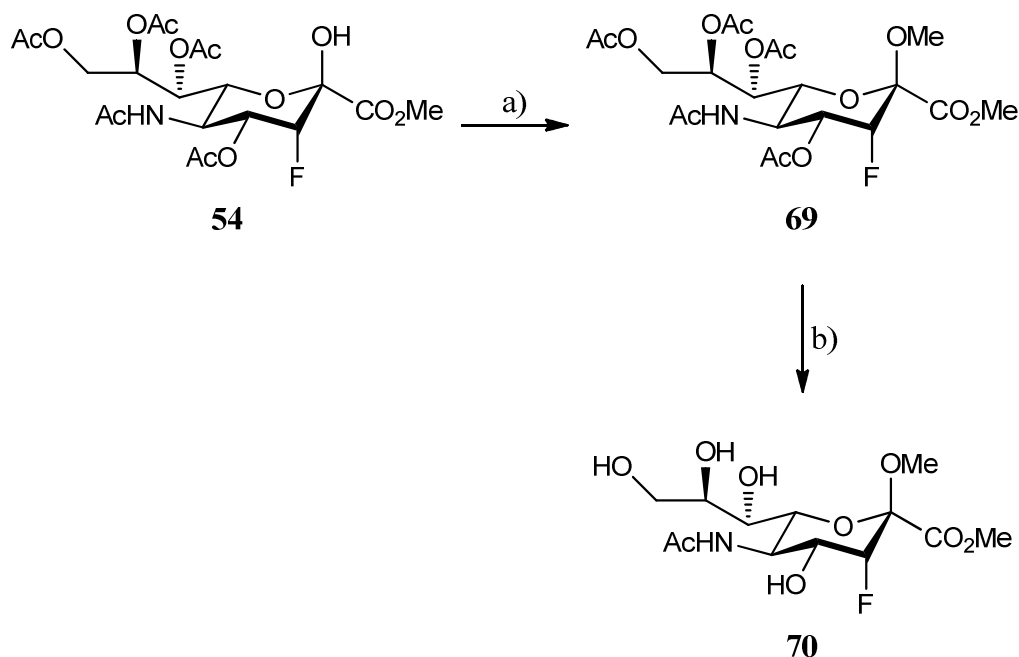
The reaction was monitored using t.l.c. and MS, following the consumption of starting material. Once all starting material was consumed, the mixture was evaporated *in vacuo* and purified by passage through silica gel. Unfortunately, it was not possible to isolate any of the desired 7-*N,N*-diethylamino derivative (**68**).

Several attempts were made to repeat the reaction, varying the temperature and the time of reaction with no positive outcome.

The synthesis of the 2,3-difluorosialic acid (**47**) compound is arduous to obtain, primarily due to the problems associated with the fluorination step. Therefore, it was decided to investigate the oxidative cleavage and reductive amination conditions with a more readily available substrate.

3.5.1 Formation of the methyl sialoside (**70**)

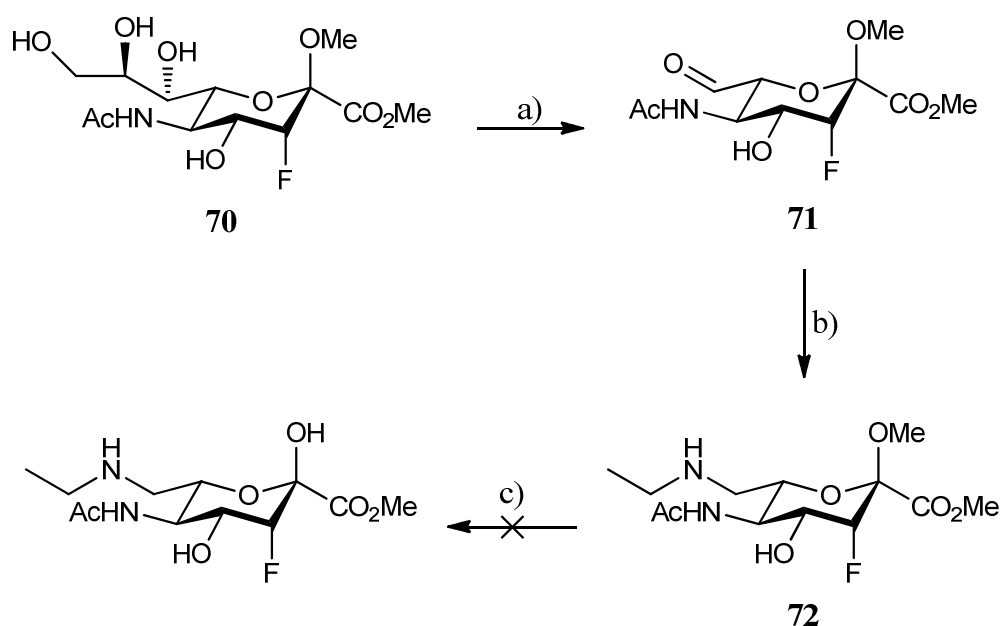
The readily available methyl sialoside (**69**) was selected in order to test the conditions for the oxidative cleavage and reductive amination at C-7. Once the amines are introduced at C-7, the removal of the methyl sialoside could be investigated and the introduction of fluorine attempted. With this intent, the hemiketal (**54**) was methylated by treatment with methyl iodide in DMF, generating the methyl sialoside (**69**) in good yield (68%) (Scheme 20).¹⁵⁰ Deacetylation under Zemplén conditions afford the 3-fluorosialic acid methyl sialoside (**70**) in quantitative yield.



Scheme 20 Formation of 3-fluorosialic acid methyl sialoside (**70**). a) NaH, MeI, DMF, r.t., 2h, 68%; b) NaOMe, MeOH, r.t. O/N, 100%.

The 3-fluorosialic acid methyl sialoside (**70**) was treated with a 0.4 M solution of sodium periodate in water for 30 min, after which the solvent was removed *in vacuo* affording the aldehyde (**71**), which was used without further purification (Scheme

21). The aldehyde was subsequently dissolved in methanol and ethylamine added and the reaction was stirred at room temperature for 2h. The solution was treated with sodium cyanoborohydride at room temperature and left stirring over night. The solvent was then evaporated *in vacuo* and the reaction mixture passed through a plug of silica affording the 7-*N*-ethylamine-3-fluorosialic acid methyl sialoside (**72**).



Scheme 21 Formation of 7-*N*-ethylamine 3 fluorosialic acid. a) 0.4 M NaIO₄, H₂O, r.t., 30 min; b) Ethylamine, NaCNBH₃, AcOH, MeOH, r.t., O/N; c) 1 M HCl, H₂O, r.t.

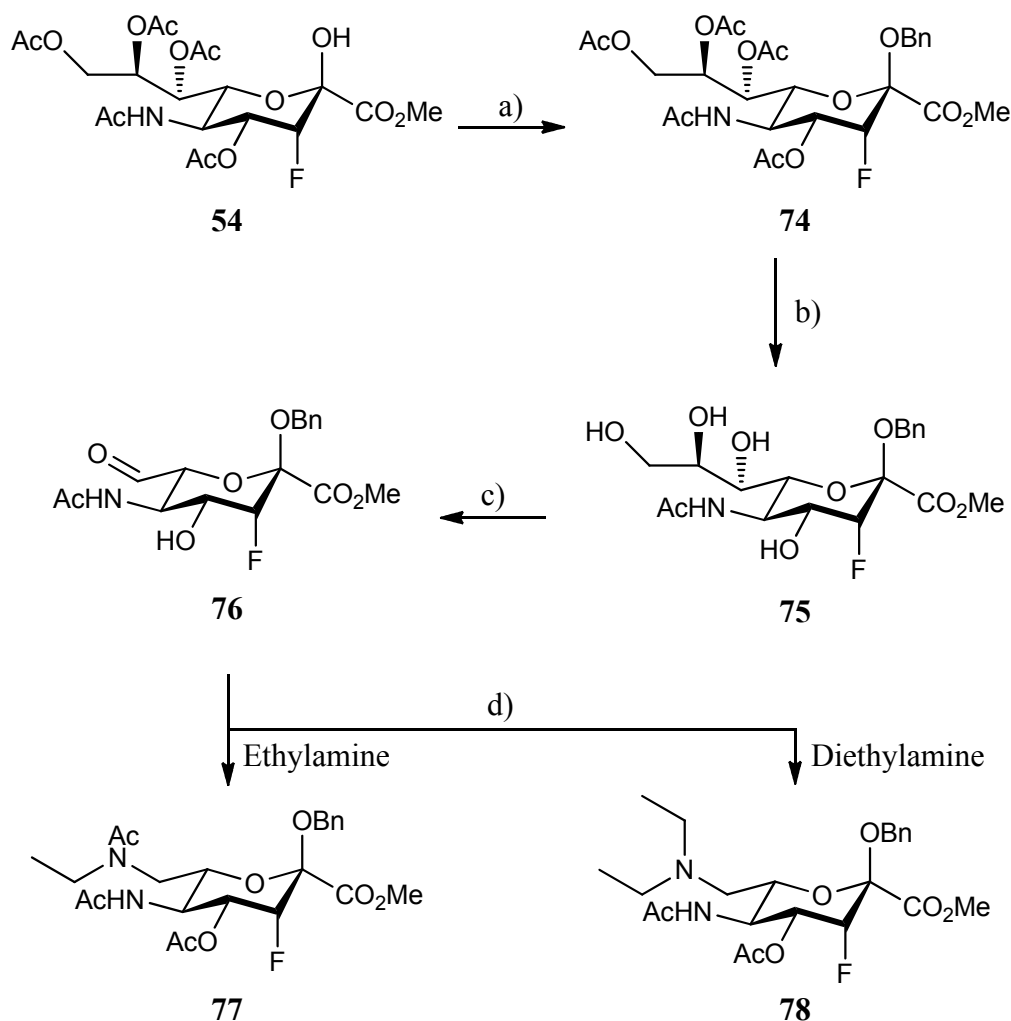
In order to introduce the fluorine at the anomeric position, removal of the methyl substituent of the 7-*N*-ethylamine-3-fluorosialic acid methyl sialoside (**72**) was attempted. The conditions tried, 1 M HCl at room temperature, were ineffective and no reaction was observed. When the concentration of hydrochloric acid was increased to 6 M, and used at room temperature no reaction was observed. At reflux, decomposition of the starting material was observed by t.l.c. and MS. A possible reason as to why the removal of the methyl sialoside was not possible is the fluorine at C-3. The fluorine could be inductively reducing the electron density away from the glycosidic hydroxyl, hampering the deprotection reaction.

With this result, it was clear that this route was not realistic in terms of achieving the desired 7-*N*-alkylamine 2,3-difluorosialic acids, as the removal of the methyl sialoside required conditions that proved to be too extreme for the compound, resulting in decomposition.

3.5.2 Formation of the benzyl sialoside (75)

As the previous route involving the methyl sialoside proved unsuccessful, an alternative protecting group was investigated, this time forming a benzyl sialoside that should be possible to remove via a simple hydrogenation, after the oxidative cleavage and reductive amination reactions were performed. The benzylation of the hemiketal (**54**) was carried out using benzyl bromide in DMF, affording the 3-fluorosialic acid benzyl sialoside (**74**) in excellent yield (95%). Zemplén conditions were used to deacetylate the benzyl sialoside (**74**), affording the 3-fluorosialic acid benzyl sialoside (**75**) in excellent yield (95%). Oxidative cleavage of the 3-fluorosialic acid benzyl sialoside (**75**) was performed under similar conditions to those used successfully to synthesise aldehyde (**71**), *i.e.* a 0.4 M solution of sodium periodate in water, at room temperature for 30 min. The reductive amination was performed in methanol using different amines, ethylamine; diethylamine; and dimethylamine; with sodium cyanoborohydride and acetic acid, at room temperature. In an attempt to simplify the purification procedure and the characterisation process, the synthesised 7-*N*-alkylamines were acetylated (Scheme 22).

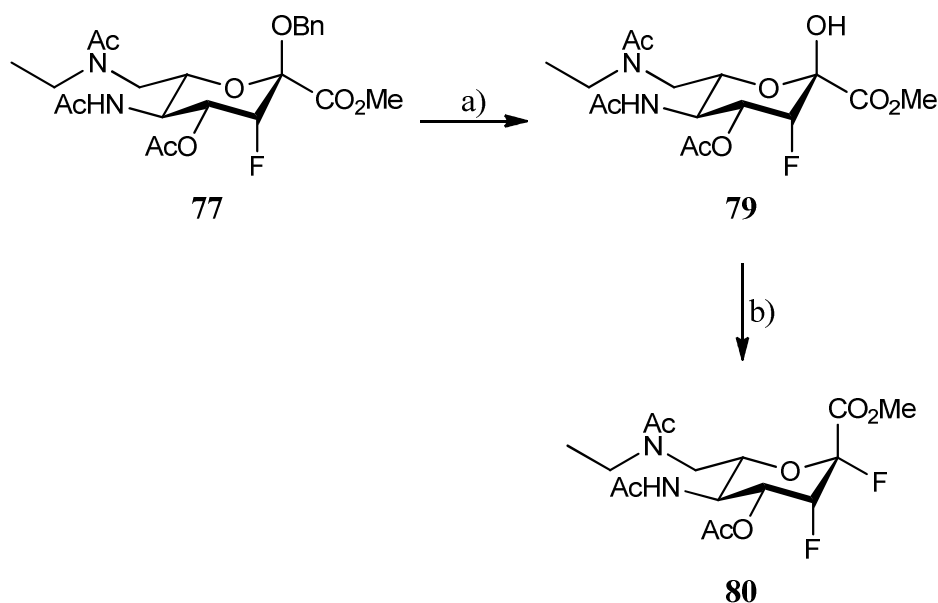
During the reductive amination, the presence of salts could be observed, from unreacted sodium periodate and excess sodium cyanoborohydride. It was considered that the presence of such salts could hamper the reductive amination since the reducing agent could be reacting with the excess periodate, impeding the reductive amination step. In order to address the problems derived from the presence of sodium periodate salts in the reductive amination, the oxidative cleavage reaction products were passed through a reverse phase column, in an attempt to separate the salts from the product, the C-7 aldehyde (**76**). Using this method, the majority of salts could be removed successfully. The next approach attempted was to precipitate the unreacted periodate by the addition of cold THF to the reaction mixture once this was complete. During the reductive amination, a large excess of the reducing agent was used. Once the reaction was complete, this excess of NaCNBH₃ had to be removed; however, this procedure proved to be complicated due to a similarity of polarities between the sodium cyanoborohydride salts and the products, when separating them using silica gel.



Scheme 22 Formation of 7-*N*-ethylacetamido (**70**) and diethylamino (**78**) 3-fluorosialic acid benzyl sialosides. a) NaH, BnBr, DMF, r.t., 1 day, 95%; b) NaOMe, MeOH, r.t., 1h, 95%; c) NaIO₄, H₂O, r.t., 30 min; d) i) Amine, AcOH, NaCNBH₃, MeOH, r.t., O/N; ii) Ac₂O, Pyr, r.t., O/N. 36% for *N*-ethyl-*N*-acetamido (**77**) (over 3 steps); 2% for *N,N*-diethylamine (**78**) (over 3 steps).

A solution was to acetylate the reaction mixture, generating the acetylated final compounds, which at this stage were easier to separate from the reducing agent by work up and chromatography. Therefore, the 7-*N*-ethylamino-3-fluorosialic acid benzyl sialoside was treated with acetic anhydride in pyridine at room temperature (overnight). The solvent was then removed *in vacuo* and the reaction mixture passed through a silica gel column to afford the 4-*O*-acetyl-7-*N*-ethyl-*N*-acetamido-3-fluorosialic acid benzyl sialoside (**77**) in reasonable yield (36%).

Once the 7-*N*-ethyl-*N*-acetamido was purified, the removal of the benzyl group was attempted successfully by using hydrogen with palladium adsorbed on charcoal (10%) in THF acidified to pH 5 with AcOH to give the hemiketal (**79**) in moderate yield (48%) (Scheme 23).



Scheme 23 Formation of 7-*N*-ethylacetamido-2,3-difluorosialic acid (**80**). a) H₂, Pd/C (10%), THF, AcOH, r.t., 10 days, 48%; b) DAST, DCM, -30 °C, 30 min, 50%.

The hydrogenolysis reaction proved to be very slow, taking 10 days to reach completion, and required the addition of fresh catalyst each day. Notwithstanding, the hydrogenation was accomplished after 10 days affording the hemiacetal (**79**) in moderate yield (48%). A variety of conditions were investigated in an attempt to improve the rate of reaction. Tetrahydrofuran and methanol were investigated as alternative solvents, using Pd/C 10%; however, no improvement in rate was observed. An alternative Pd catalyst, Pd(OH)₂, was investigated using either tetrahydrofuran or methanol, again with no improvement in the rate. Finally, the reaction was also attempted at high pressure (4 atmospheres), with again no significant improvement to the rate of reaction.

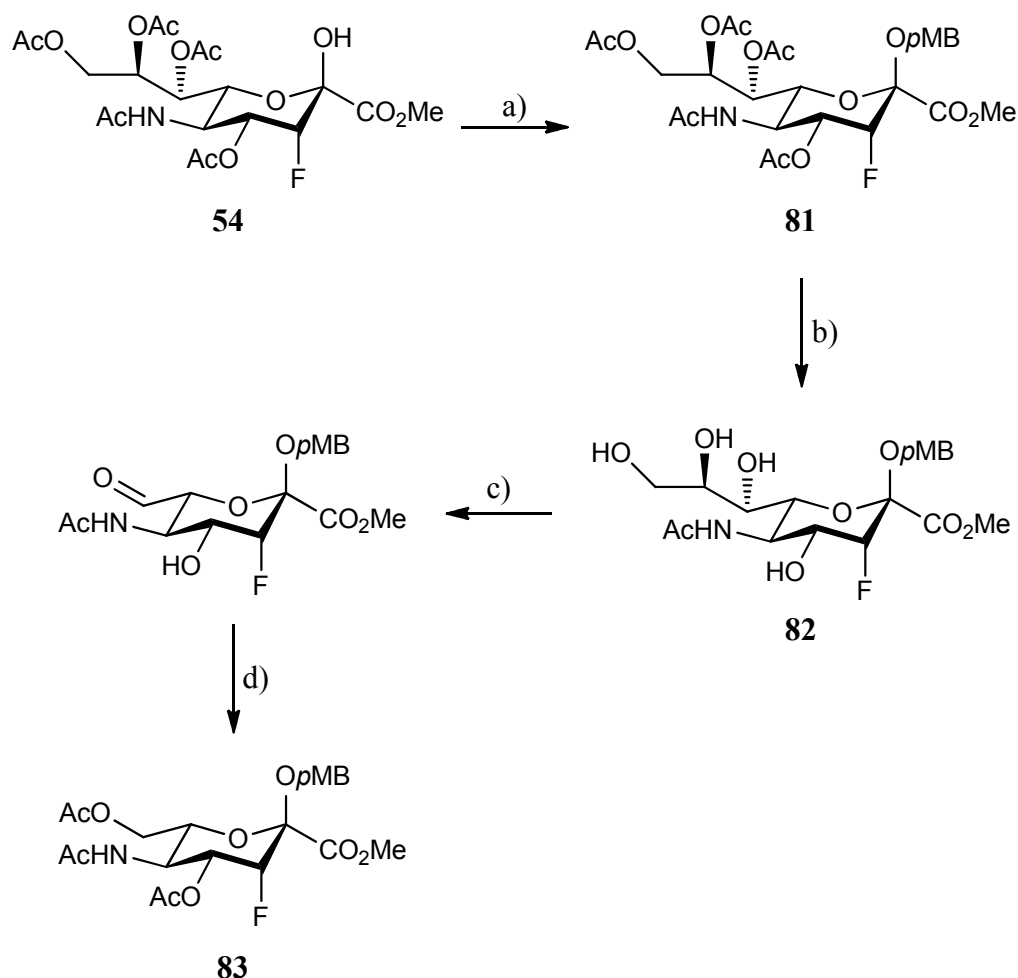
Despite our lack of success at improving the rate of reaction, the removal of the benzyl sialoside could be effected over 10 days, with a reasonable yield (48%).

With the anomeric hydroxyl deprotected (**79**), we then attempted the fluorination of the anomeric position using DAST (**55**). This reaction proceeded smoothly, giving the desired 7-*N*-ethylacetamido-2,3-difluorosialic acid methyl ester (**80**) in moderate yield (50%). Although this synthetic route produced the desired 7-*N*-ethylamido-2,3-difluorosialic acid (**80**), the deprotection step of the benzyl sialoside proved to be less than ideal. It was hypothesised that due to the presence of the fluorine at C-3, the stability of the sialoside present at C-2 is increased. Although the bond that is being cleaved is not the glycosidic one (as with the methyl sialoside), but that between the

glycosidic oxygen and the CH₂, the effect of the electronegativity of the fluorine at C-3 makes the deprotection of the anomeric hydroxyl more complex than it would have been if the fluorine at C-3 were to be absent.

3.5.3 Formation of the *para*-methoxybenzyl sialoside (**82**)

In an attempt to improve the removal of the protecting group of the anomeric hydroxyl, *para*-methoxybenzyl (*p*MB) was used, since the *p*MB is a more labile group than either the methoxy or the benzyl sialosides. The procedure to introduce the *p*MB was similar to the one employed for the introduction of the methoxide and benzyl groups. Therefore, starting from the hemiketal (**54**) the protecting reaction was undertaken generating the 3-fluorosialic acid *p*MB sialoside (**81**) in good yield (86%). The next step was the removal of the acetyl groups, using for that purpose the Zemplén conditions, generating the 3-fluorosialic acid *p*MB sialoside (**82**) in good yield (81%). The conditions employed for the oxidative cleavage of the glycerol side chain and the reductive amination with diethylamine, were similar to the ones used with the benzyl sialoside. The acetylation, once again with conditions similar to those previously used with the benzyl sialoside, afforded, surprisingly, the reduced aldehyde, 4,7-di-*O*-acetyl-3-fluorosialic acid *p*MB sialoside (**83**) rather than the expected 7-*N,N*-diethylamine-3-fluorosialic acid *p*MB sialoside (Scheme 24). With this result in hand, a decision had to be made on whether the strategy of protecting the anomeric hydroxyl should be pursued or if the fluorine at the anomeric position should be introduced prior to the modifications at the glycerol side chain. The main reason for trying more readily available substrates was to develop a robust method for performing the oxidative cleavage and reductive amination steps. This goal was accomplished, since the removal of the salts derived from unreacted sodium periodate and excess sodium cyanoborohydride had been optimized, as well as methods developed for the purification of the 7-*N*-alkylamino products.



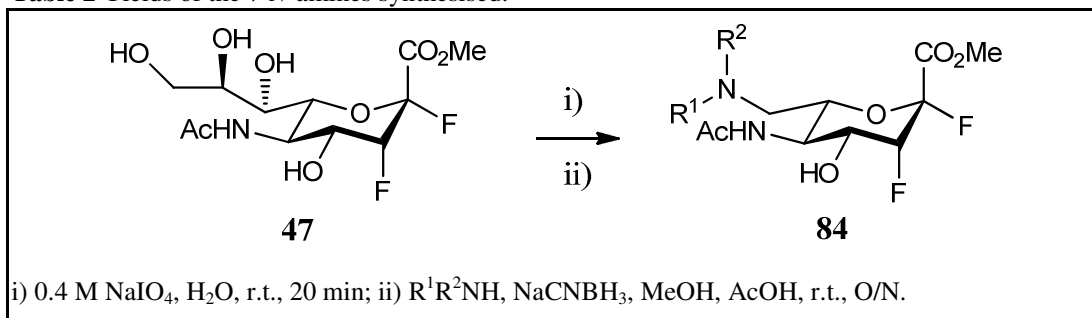
Scheme 24 Formation of 4,7-di-*O*-acetyl-3-fluorosialic acid *p*MB sialoside. a) NaH, *p*MBCl, DMF, r.t., 1 day, 86%; b) NaOMe, MeOH, r.t., O/N, 81%; c) NaIO₄, H₂O, r.t., 30 min; d) i) Diethylamine, AcOH, NaCNBH₃, MeOH, r.t., O/N; ii) Ac₂O, Pyr, r.t., O/N, 10% from the C-7 aldehyde.

Therefore, it was decided at this stage to return to the 2,3-difluorosialic acid methyl ester (**47**) scaffold as a substrate for the oxidative cleavage and reductive amination and employ the knowledge developed on the synthesis of the methyl, benzyl and *para*-methoxybenzyl sialosides.

3.6 Synthesis of a series of 7-*N*-alkylamino 2,3-difluorosialic acids

The aldehyde (**46**) was obtained by treating the 2,3-difluorosialic acid methyl ester (**47**) with a 0.4 M aqueous solution of sodium periodate in water, removal of the sodium periodate salts by precipitation (using cold tetrahydrofuran), evaporation of the solvent *in vacuo* and then used without further purification. During the reductive amination reaction, and due to the use of excess of reducing agent, salts were present, which proved difficult to remove from solution; therefore, a solid supported sodium

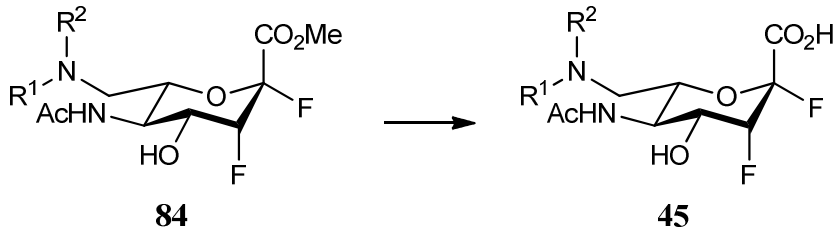
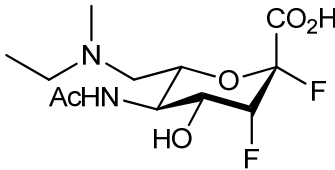
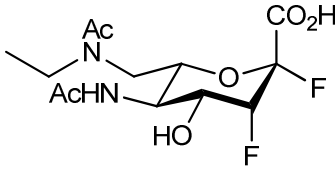
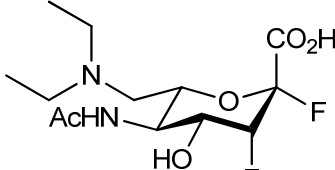
cyanoborohydride was used in an attempt to remove the excess of sodium cyanoborohydride salts from solution by a simple filtration. By this “desalting” procedure, the purification of the desired amines by silica gel column became simpler, since the salts that have the same polarity as the 7-*N*-alkylamines were no longer present. To avoid any possible reduction of the aldehyde to the alcohol, as seen previously for *p*MB-3-fluorosialic acid sialoside (**82**), longer reaction times were allowed for the formation of the iminium ion. With all of these measures in place, the reactions were performed in a two-step fashion, with the reductive amination being performed immediately after the oxidative cleavage, successfully affording the desired *N*-alkylamines in rather moderate/low yields after two steps (Table 2).

Table 2 Yields of the 7-*N*-amines synthesised.

Amine			
Entry	$\begin{array}{c} \text{R}^1 \\ \\ \text{R}^2\text{-NH} \end{array}$	Product	Yield (%)
1	$\begin{array}{l} \text{R}^1 = \text{Methyl} \\ \text{R}^2 = \text{Ethyl} \end{array}$	<p>85</p>	11
2	$\begin{array}{l} \text{R}^1 = \text{Ac} \\ \text{R}^2 = \text{Ethyl} \end{array}$	<p>80</p>	22
3	$\text{R}^1 = \text{R}^2 = \text{Ethyl}$	<p>68</p>	18

Following the successful oxidative cleavage and reductive amination of 2,3-difluorosialic acid (**47**) to produce the series of 7 modified amines (**68**, **80**, and **85**), the final step in order to achieve the desired 7-*N*-amines-2,3-difluorosialic acids was the saponification of the methyl ester. This proceeded smoothly using a 1 M sodium hydroxide solution in water to afford the final targets (**37** - **39**) in good yield (Table 3).

Table 3 Yields for the saponified final compounds, 7-*N*-alkylamine 2,3-difluorosialic acids.

<div style="text-align: center;">  <p>84 45</p> <p>1 M NaOH, H₂O, 4 °C, 1h</p> </div>		
Entry	Product	Yield (%)
1	<div style="text-align: center;">  <p>37</p> </div>	50
2	<div style="text-align: center;">  <p>38</p> </div>	75
3	<div style="text-align: center;">  <p>39</p> </div>	67

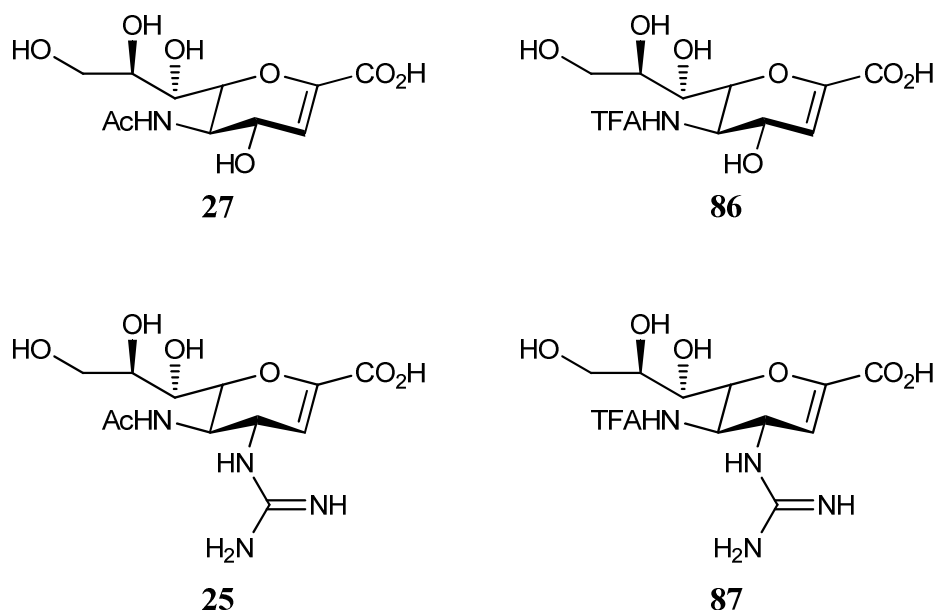
These final compounds (**37** - **39**) were subsequently tested against a series of influenza viruses and the results are shown in Chapter 6.3.

Chapter 4 - Synthesis of 5-*N*-trifluoroacetamido-2,3-difluorosialic acid (94)

4.1 Rationale

Until the end of the 1980's, 5-*N*-trifluoroacetamido-Neu5Ac2ene (**86**) was the most potent inhibitor known towards the influenza A virus, having an IC₅₀ of 5 µM against influenza neuraminidase N1, whilst Neu5Ac2ene (**27**) showed inhibition of 30 µM against the same strain of influenza virus.^{77,140,151}

Smith *et al* synthesised derivatives of zanamivir (**25**), and amongst other C-5 modifications, the 5-*N*-trifluoroacetemido analogue (**87**). The compounds were tested against influenza neuraminidase N2 and 5-*N*-trifluoroacetamido (**87**) had an IC₅₀ of 21 nM whilst zanamivir (**25**) had an IC₅₀ of 5 nM.¹⁵²



The *N*-acetamido group present at C-5 interacts with three amino acid residues, with the methyl group appearing to have hydrophobic interactions with Trp178 and Ile222, while the oxygen appears to form hydrogen bond interactions with Arg152 (Figure 14).

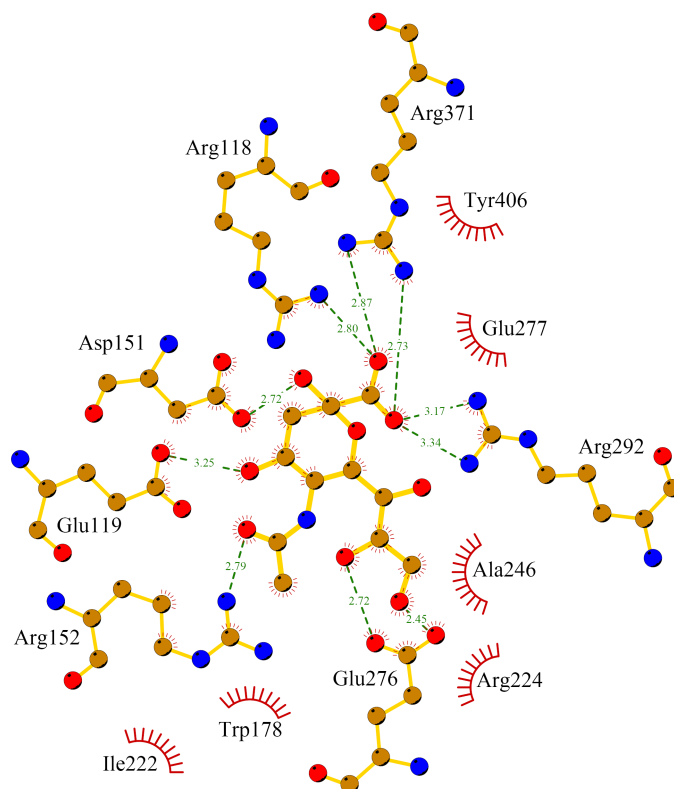


Figure 14 Interactions of the *N*-acetyl group with Arg152, Ile222 and Trp178. Generated with LigPlot⁺ (PDB 2C4A).

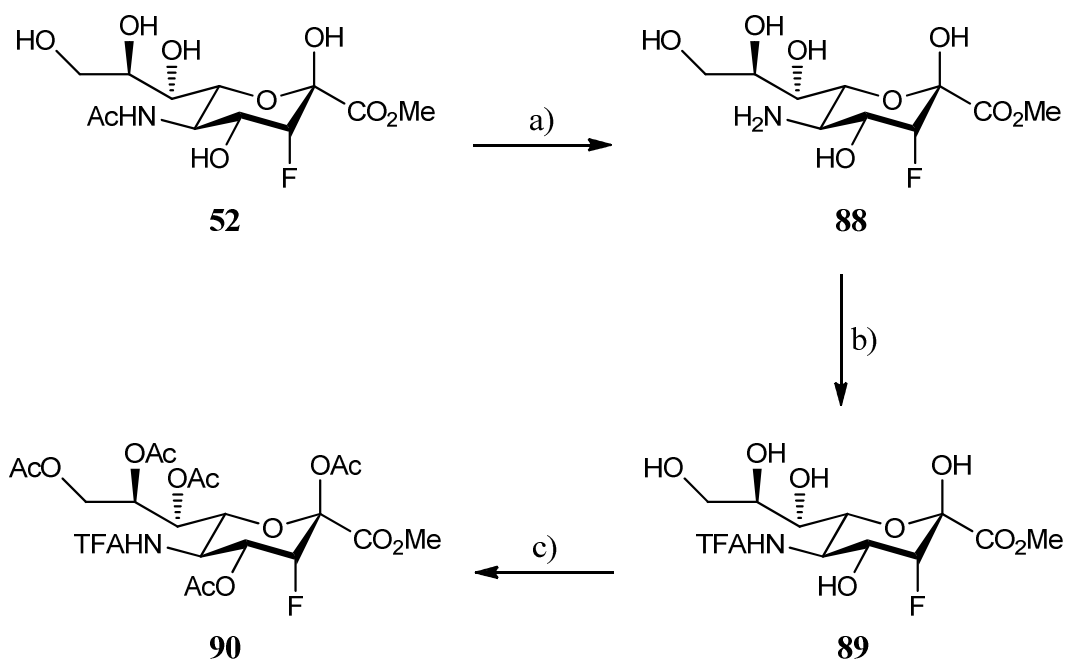
It was our aim to exchange the 5-*N*-acetamido group present in the inhibitor 2,3-difluorosialic acid (**19**) with a 5-*N*-trifluoroacetamido in order to assess the impact of this modification on mechanism-based inhibition towards a series of influenza neuraminidases. By combining the presence of the 2,3-difluoro substituents, targeting the covalent intermediate formed during the catalytic mechanism of influenza neuraminidase, with the 5-*N*-trifluoroacetamido group, which interacts with active site arginine and glutamate residues, a synergistic effect could occur to improve the binding of this class of compound towards influenza neuraminidases.

4.2 Synthesis of the 5-*N*-trifluoroacetamido-2,3-difluorosialic acid (**94**)

For the synthesis of the 5-*N*-trifluoroacetamido-2,3-difluorosialic acid (**94**), it was envisaged that we could utilise an intermediate compound produced previously during the synthesis of 2,3-difluorosialic acid (**19**) and simply exchange the *N*-acetamido for a *N*-trifluoroacetamido at a late stage in the synthetic sequence. It

has been shown by Schroyen *et al* that the NHAc group can be converted to the primary amine, which should then be readily convertible to the desired NHTFA derivative.¹⁵³

As such, the 3-fluorosialic acid methyl ester (**52**) was treated with methanesulfonic acid in methanol at room temperature, to produce the primary amine at C-5 (**88**) (Scheme 25).¹⁵³ Acetylation using trifluoroacetic anhydride in methanol at room temperature, generated the 5-*N*-trifluoroacetamido-3-fluorosialic acid (**89**).¹⁵³ Global acetylation of the hydroxyl groups of 5-*N*-trifluoroacetamido-3-fluorosialic acid methyl ester (**89**) was achieved using acetic anhydride in pyridine; this proceeded slowly over 5 days to afford the per-*O*-acetylated-5-*N*-trifluoroacetamido-3-fluorosialic acid (**90**) in low yield (20% over three steps).

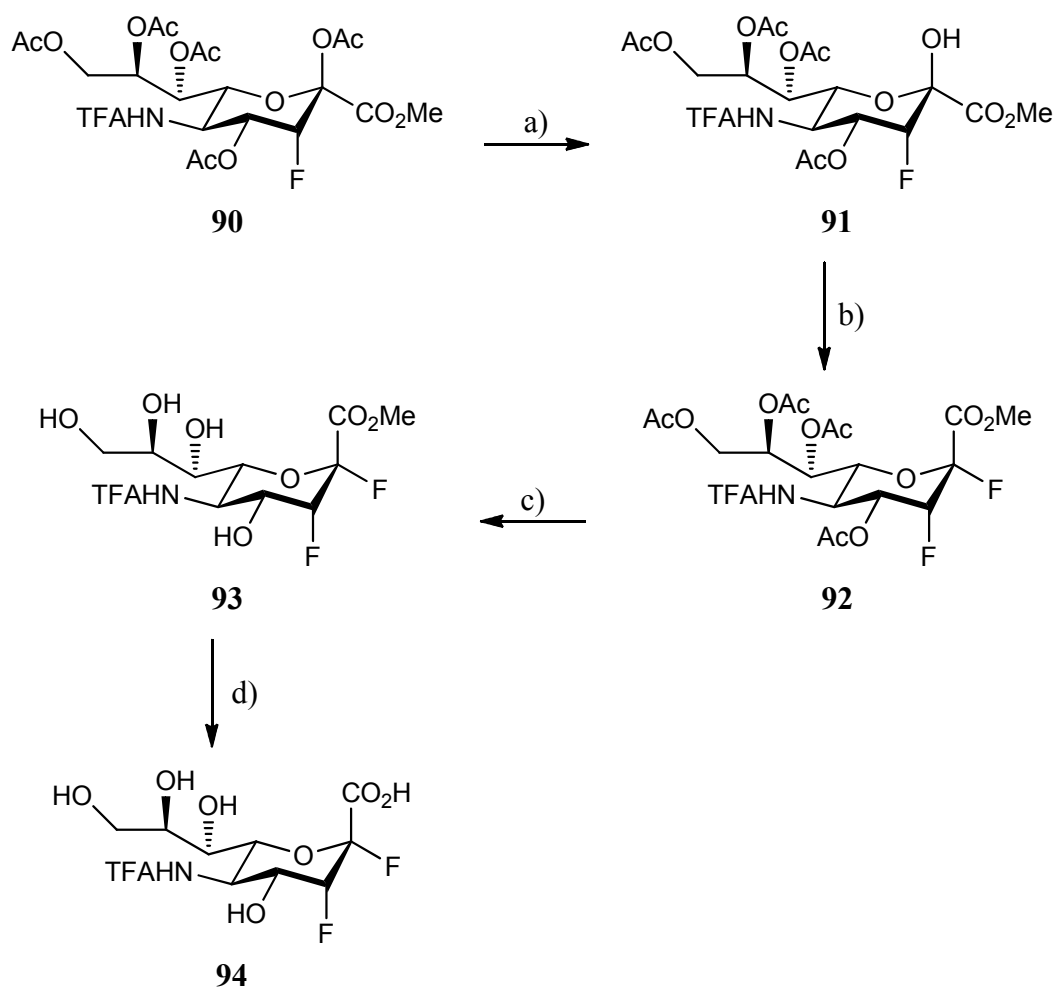


Scheme 25 Formation of 5-*N*-trifluoroacetamido-3-fluorosialic acid (**90**). a) MsOH, MeOH, reflux, 1 day; b) TFA₂O, Et₃N, MeOH, 4 °C, 1h; c) Ac₂O, Pyr, r.t., 5 days, 20 % (over 3 steps).

One possible reason for the low yield in the reaction sequence could be due to the deprotection and subsequent acylation of the amine not being optimized. One other plausible reason was the choice of solvent in which the acylation of the primary amine was performed, methanol. Methanol could have reacted with the trifluoroacetic anhydride to reduce the effectiveness of the acylation of the primary amine. Unfortunately, owing to the high polarity of the free amine (**88**), it was

difficult to follow the progress of the reaction and determine when the acylation was complete.

The next step in the synthetic pathway was to deprotect selectively the anomeric position. A solution of the per-*O*-acetylated-5-*N*-trifluoroacetamido-3-fluorosialic acid (**90**) was treated with hydrazine acetate to afford the 5-*N*-trifluoroacetamido-3-fluorosialic acid (**91**) in good yield (67%) (Scheme 26). The hemiketal (**91**) was treated with DAST, in DCM, at -30 °C, resulting in fluorination at C-2 to produce the desired 2,3-difluorosialic acid derivative (**92**) which was isolated in moderate yield (44%) (Scheme 26).¹³⁷ Subsequent deacetylation of the per-*O*-acetylated-5-*N*-acetamido-2,3-difluorosialic acid (**92**) was performed following Zemplén conditions by treatment with a solution of sodium methoxide in methanol at 4 °C, to yield the 5-*N*-trifluoroacetamido-2,3-difluorosialic acid (**93**) in quantitative yield (Scheme 26).



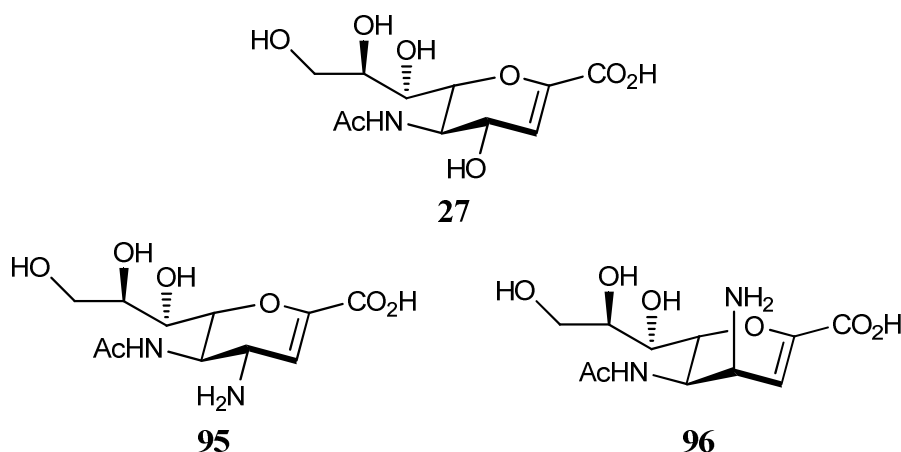
Scheme 26 Formation of 5-*N*-trifluoroacetamido-2,3-difluorosialic acid (**94**). a) Hydrazine acetate, DCM/MeOH 4:1, 4 °C, 3h, 67%; b) DAST, DCM, -30 °C, 30 min, 44%; c) NaOMe, MeOH, 4 °C → r.t., 1h, 100%; d) NaOH, H_2O , 4 °C, 1h, 100%.

Finally, saponification of the methyl ester (**93**) was performed with a 1M sodium hydroxide solution in water, generating the desired target 5-*N*-trifluoroacetamido-2,3-difluorosialic acid (**94**) in quantitative yield. The 5-*N*-trifluoroacetamido-2,3-difluorosialic acid (**94**) will be tested *in vitro* against a series of influenza viruses (CSIRO, Australia).

Chapter 5 - Synthesis of C-4 *N*-alkylamino Neu5Ac2ene derivatives

5.1 Prelude

Work performed by the group of von Itzstein originally showed that the introduction of an equatorial amino group at the C-4 position of Neu5Ac2ene (**95**) resulted in improved inhibitory activity against influenza neuraminidase N2, when compared with the “parent” compound Neu5Ac2ene (**27**), improving the K_i from 4 μM to 0.04 μM .^{97,104,154} This seminal finding was one of the early results that ultimately led to the development of both zanamivir (**25**) and oseltamivir (**6**), as potential inhibitors of influenza neuraminidase. Alongside this modification, von Itzstein’s group also synthesised the 4-epi-amino Neu5Ac2ene derivative (**96**), where the C-4 amino group is now in a axial orientation. Interestingly, the 4-epi-amino Neu5Ac2ene (**96**) also showed superior inhibitory activity ($K_i = 0.3 \mu\text{M}$) when compared to the parent compound Neu5Ac2ene (**27**), but was never developed further as the equatorial amino derivative (**95**) showed the most potent inhibitory activity.⁹⁷



Within the active site of influenza neuraminidase there are several acidic amino acids capable of interacting with basic substituents in either an equatorial, or axial, conformation at C-4 of sialic acid (Figure 15). Examining the X-Ray crystal structure of sialic acid bound to the active site of influenza neuraminidase N2, it is clear that there is potential for an axial amino substituent at C-4 to interact with the residues

Glu119 and Glu227. Alternatively, an amino group in the equatorial orientation can interact with Asp151, which is the case observed with zanamivir (**25**) and oseltamivir (**6**).

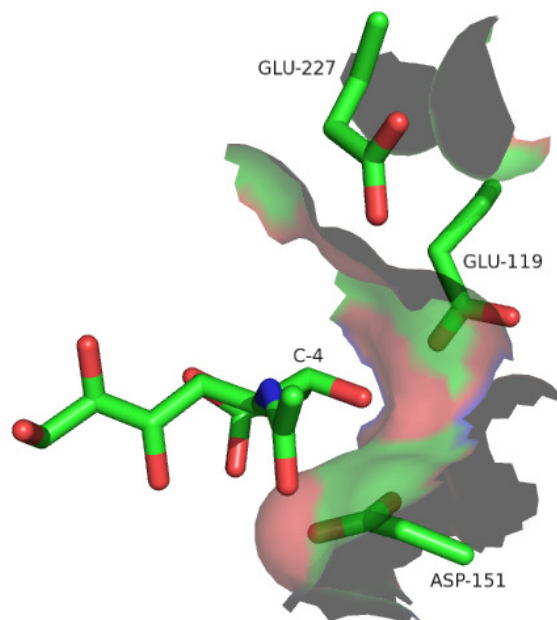
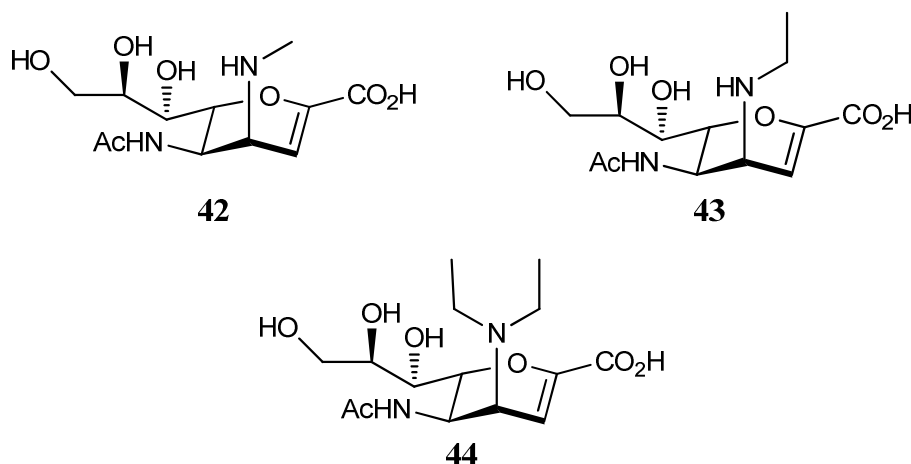


Figure 15 Possible interactions with glutamate or aspartate residues around C-4 position of sialic acid bound in the active site of influenza neuraminidase N2 with an axial or equatorial amino substituent at this position, respectively. Generated with PyMOL (PDB 2BAT).

5.2 Rationale

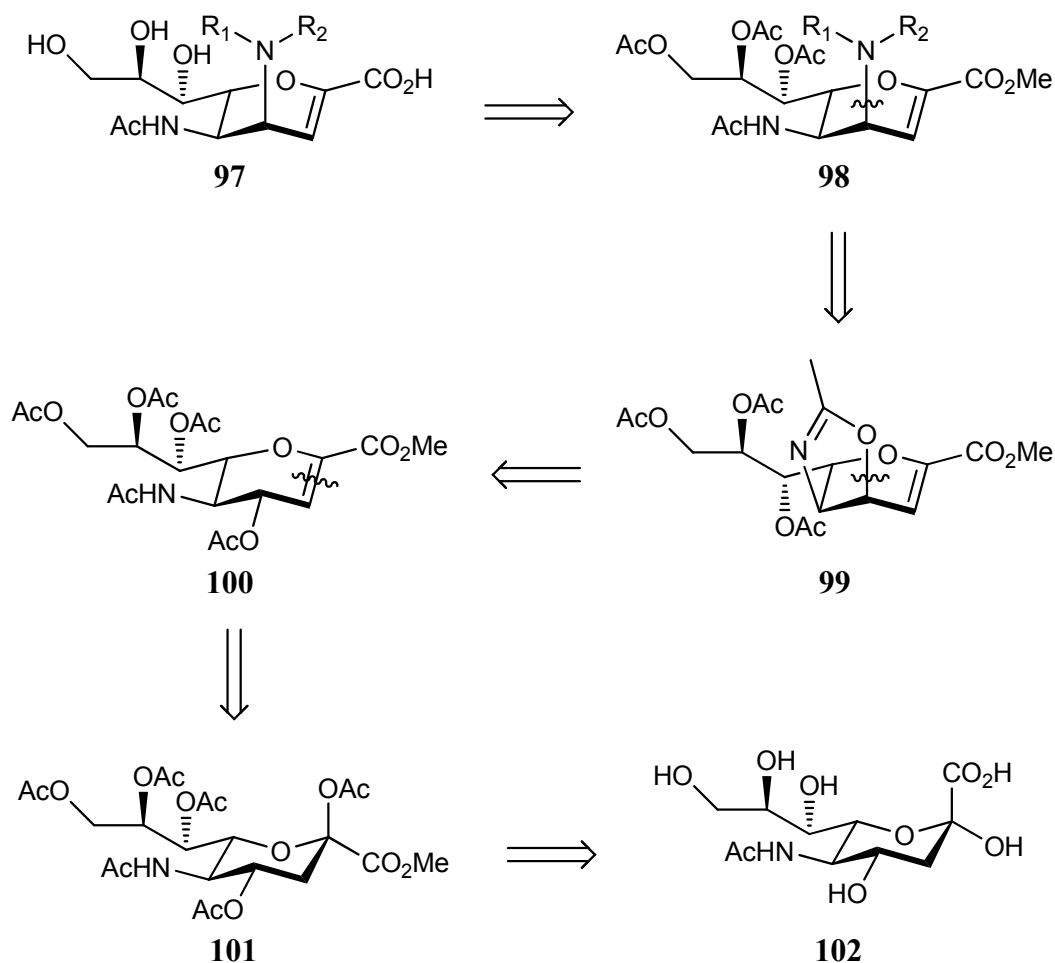
We were interested in investigating the effect of an axial C-4 amino group on the inhibitor activity of 2,3-difluorosialic acids towards influenza neuraminidase. As a first course of action, we set out to investigate the size of modifications that could be accepted axially at C-4. Owing to the difficult synthesis of the 2,3-difluorosialic acids, we first investigate the C-4 amine substituents on Neu5Ac2ene and the information gained would be implemented into the synthesis of the 2,3-difluorosialic acid derivatives. Furthermore, the presence of an axial group at C-4 could allow some steric control over the introduction of a fluorine at C-3 to afford an improved yield of the desired stereochemistry (axial fluorine). In order to study the binding between the glutamate residue and the C-4 amines, in addition to the study of the available physical space around this position, it was decided to undertake the synthesis of a series of 4-epi-*N*-alkylamines, namely 4-epi-*N*-methylamino-

Neu5Ac2ene (**42**); 4-*epi-N*-ethylamino-Neu5Ac2ene (**43**); and 4-*epi-N,N*-diethylamino-Neu5Ac2ene (**44**).



5.3 Retrosynthetic analysis of the formation of the series of 4-*epi-N*-alkylamines (**97**)

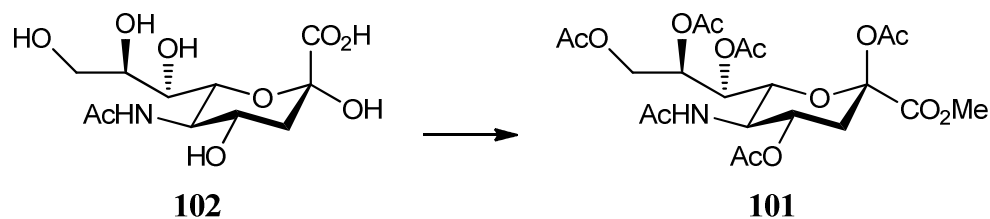
The general strategy for the construction of a series of 4-*epi-N*-alkylamino Neu5Ac2ene (**97**) is based on the retrosynthetic analysis shown (Scheme 27). Through a straightforward sequence of deprotections, the desired 4-*epi-N,N*-alkylamino Neu5Ac2ene (**97**) could be derived from the per-*O*-acetylated compound (**98**). Retrosynthetic cleavage of the bond indicated in the 4-*epi-N,N*-alkylamino Neu5Ac2ene (**97**) furnishes the oxazoline (**99**) as a viable precursor. The oxazoline (**99**) is readily available from sialic acid (**102**) via literature procedures.^{155,156}



Scheme 27 Retrosynthetic pathway for the formation of a series of 4-epi-*N,N*-alkylamino Neu5Ac2ene (**97**).

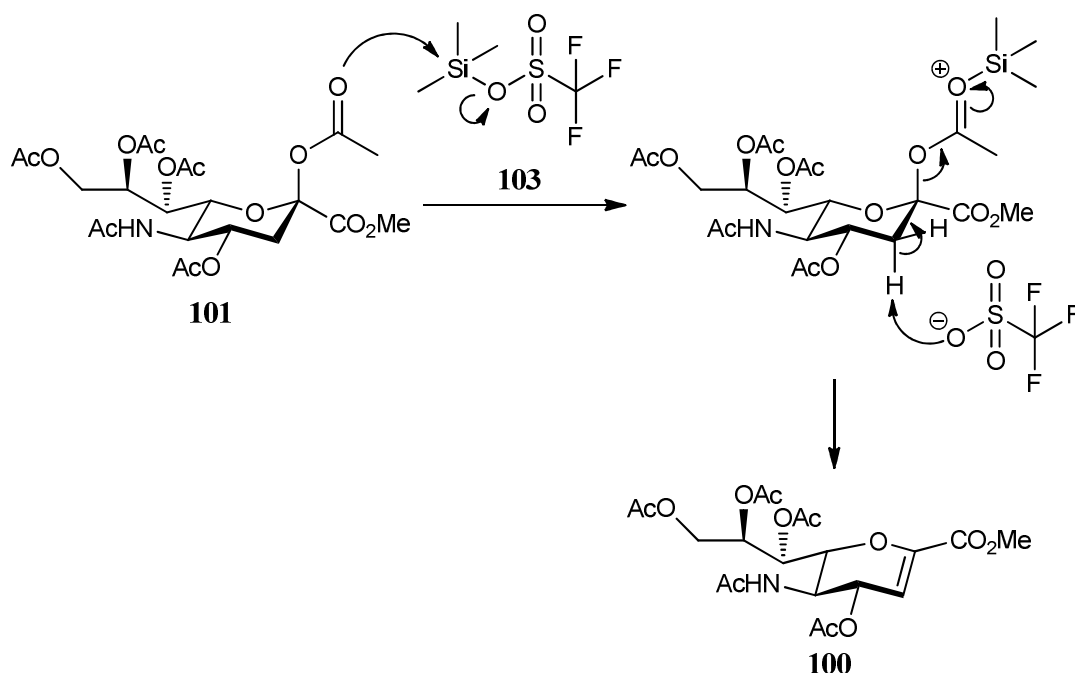
5.4 Synthesis of the common precursor, oxazoline (**99**)

In order to synthesise oxazoline (**99**), esterification of sialic acid (**102**), using TFA in MeOH at room temperature and subsequent acetylation with acetic anhydride in pyridine, was conducted affording the per-*O*-acetylated sialic acid (**101**) in good overall yield (81% over two steps) (Scheme 28).



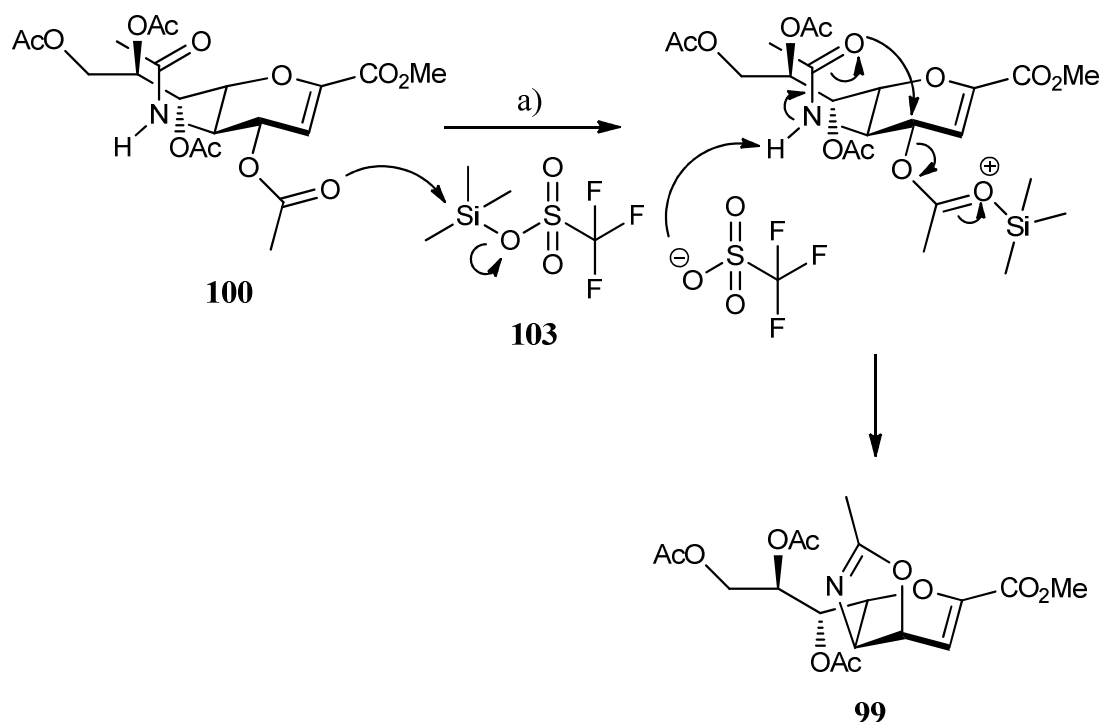
Scheme 28 Acetylation of sialic acid (**102**). i) TFA, MeOH, r.t., O/N; ii) Ac₂O, Pyr, r.t., 4 days, 81% (over 2 steps).

Elimination of the anomeric acetyl group was then achieved by following a literature procedure.¹⁵⁵ The per-*O*-acetylated sialic acid (**101**) was dissolved in acetonitrile and trimethylsilyl trifluoromethanesulfonate (TMSOTf) was added. The reaction was stirred at room temperature overnight, affording the per-*O*-acetylated Neu5Ac2ene (**100**) in good yield (75%) (Scheme 29). The elimination of the anomeric acetyl group occurs due to the activation of the anomeric acetyl of the per-*O*-acetyl sialic acid (**101**), which triggers a *trans*-diaxial elimination, forming the per-*O*-acetylated Neu5Ac2ene (**100**) (Scheme 29).



Scheme 29 Mechanism of formation of the per-*O*-acetylated Neu5Ac2ene (**100**). TMSOTf, MeCN, r.t., O/N, 75%.

The formation of the oxazoline (**99**) was also achieved following a literature procedure, where the per-*O*-acetylated Neu5Ac2ene (**100**) was dissolved in acetonitrile, TMSOTf was added and the reaction heated to 50 °C overnight generating the oxazoline (**99**) in good yield (76%) (Scheme 30).¹⁵⁶ In this transformation TMSOTf (**103**) activates the C-4 acetyl group, which can be displaced by a nucleophilic attack from the oxygen of the *N*-acetamido present at C-5. Oxazoline (**99**) is then the product of such a nucleophilic attack (Scheme 30).



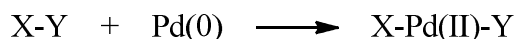
Scheme 30 Mechanism for the formation of oxazoline (**99**). TMSOTf, MeCN, 50 °C, O/N, 76%.

5.5 Overview of the use of palladium for the formation of C-C bonds

The oxazoline (**99**) is an excellent starting point towards the introduction of alkyl amines at C-4, since this position is susceptible to nucleophilic attack and, furthermore, the orientation of the 5 member ring dictates the pattern of substitution. If a direct nucleophilic attack from an amine at C-4 of oxazoline (**99**) were to occur, the product would yield an equatorial amine at C-4, as opposed to our desired C-4 axial derivatives. Therefore, methodology was developed that would enable the introduction of the desired amines with an axial stereochemistry at C-4.

Palladium is widely used in organic chemistry to form carbon-carbon bonds, due to its versatility, stability and low toxicity. Two forms of palladium (Pd) are commonly used in synthesis, Pd (0) complexes and Pd (II) salts.¹⁵⁷ The Pd (II) salts can be used as stoichiometric reagents or catalysts, and as a general example we have Pd(OAc)₂; whilst Pd (0) complexes are solely used as catalysts, for instance Pd(PPh₃)₄.¹⁵⁷

The Pd complexes can promote the formation of the carbon-carbon bond in different ways such as oxidative addition; insertion; transmetallation; reductive elimination; β -H elimination; and elimination of β -heteroatom groups and β -carbon.¹⁵⁷ We shall focus our attention on oxidative addition. The reaction between a molecule of general structure X-Y and Pd (0) leads to the cleavage of the chemical bond between X and Y and the formation of two new bonds, between X, Pd and Y, to form X-Pd-Y.¹⁵⁷



Two non-bonding electrons of Pd are now involved in the coordination with X and Y; therefore, the formal oxidation state of Pd is raised by two, passing from Pd (0) to Pd (II).¹⁵⁷ Taking $\text{Pd(PPh}_3)_4$ as an example of a Pd (0) complex, this undergoes a reversible dissociation *in situ* losing two molecules of PPh_3 , reducing the four coordination sites to two and from 18 electrons to 14, and it is this species that undertakes the oxidative addition (Figure 16).¹⁵⁷

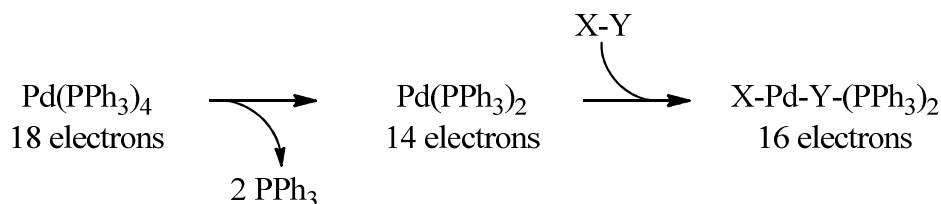
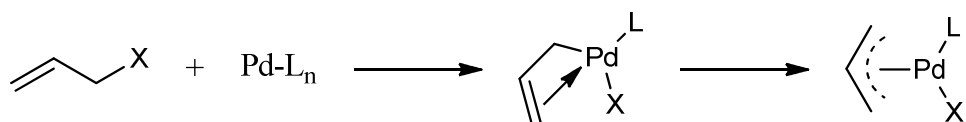


Figure 16 Example of an oxidative addition between $\text{Pd(PPh}_3)_4$ and a general molecule X-Y.

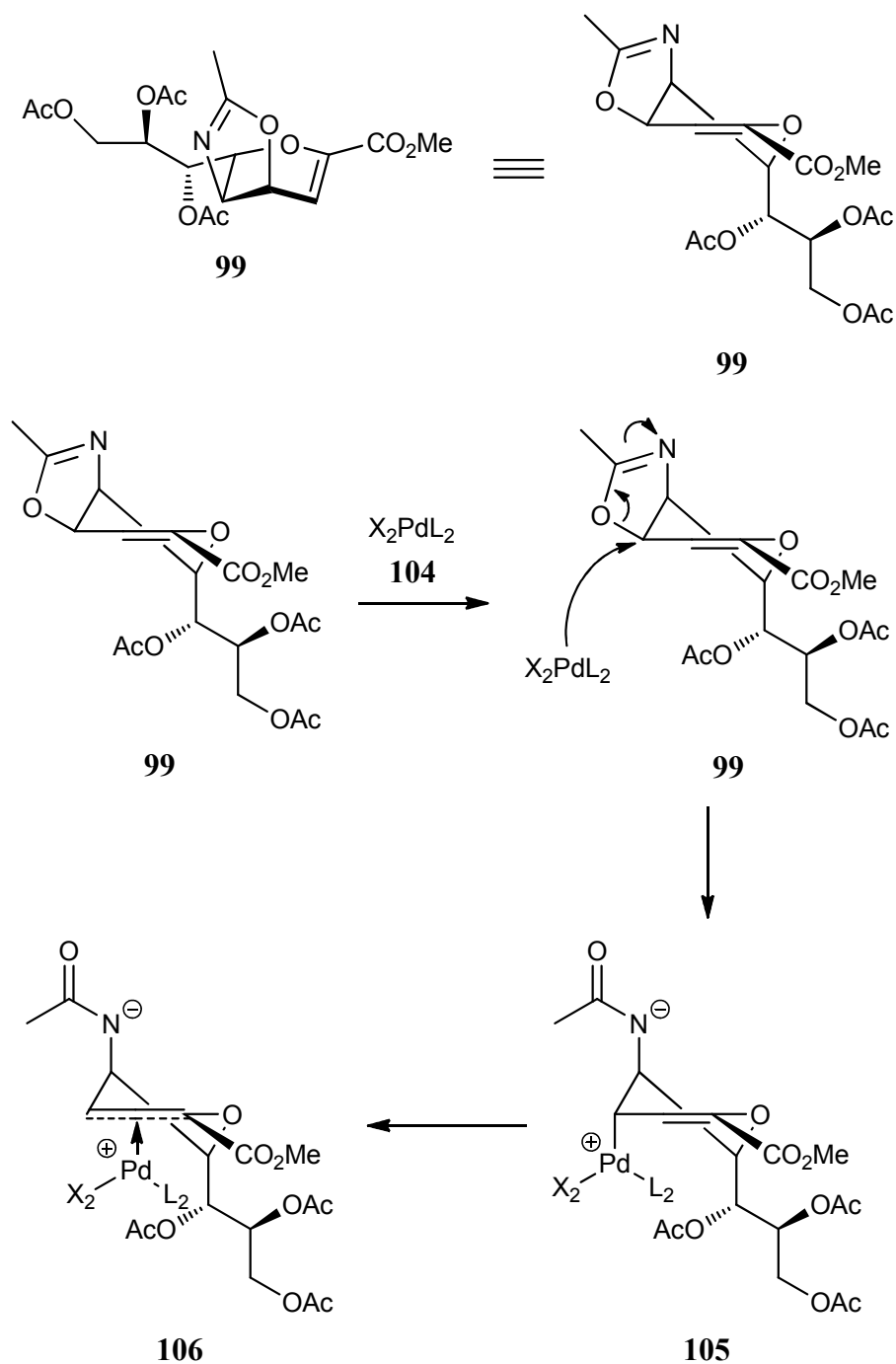
The oxidative addition is aided if the Pd has a high electron density, meaning the more electron donating the ligands are, the faster the oxidative addition will occur.¹⁵⁷ However, the presence of π -acceptor ligands tends to diminish the rate of oxidative addition.¹⁵⁷ Notwithstanding these factors, when one is about to undertake a oxidative addition reaction with a palladium complex, it is necessary to investigate a myriad of ligands as their effects are not fully understood, therefore surprises can be encountered.¹⁵⁷

In general, the formation of a π -allylpalladium complex involves the cleavage of a bond (leaving group) and the delocalization of the double bond (Scheme 31).¹⁵⁷



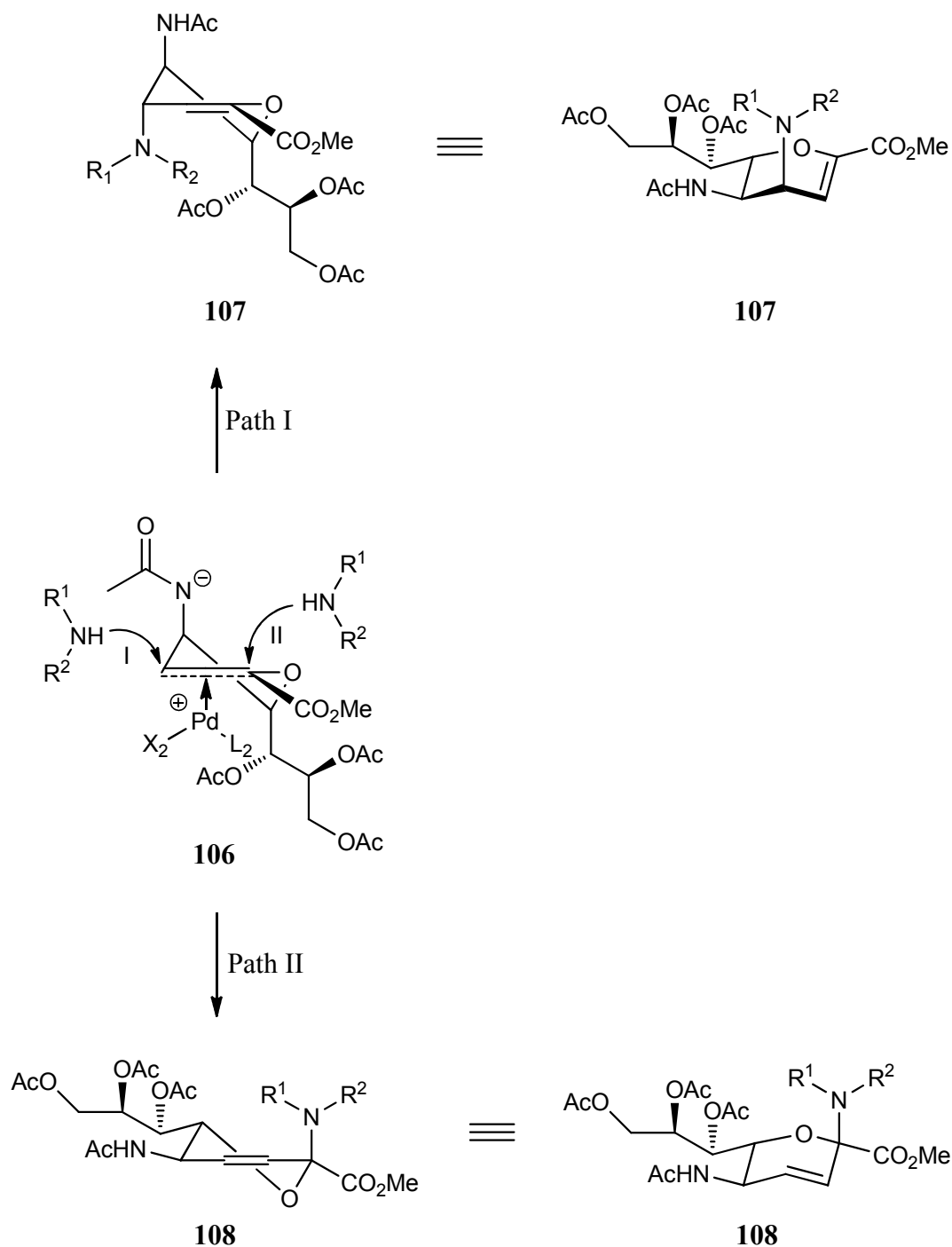
Scheme 31 General method for the formation of π -allylpalladium complexes.

Applying this general example to the structure of the oxazoline (**99**), there is the presence of the double bond between C-2 and C-3 and it is possible to envisage that the “leaving group” is the oxygen of the oxazoline. The addition of palladium to the oxazoline (**99**) enables the formation of an η^3 -allylpalladium complex (**106**) (Scheme 32).



Scheme 32 Opening of the oxazoline with the aid of a palladium (0) complex.

Once the palladium is coordinated to the π system (**106**), the nucleophile, in our case an *N*-alkyl amine, will attack the palladium complex from the opposite face, either at the α position (path I) or at the γ position (path II), forming the axial C-4 *N*-alkylamino (**107**) or the axial C-2 *N*-alkyl amine (**108**) (Scheme 33).



Scheme 33 The two different pathways that the nucleophilic *N*-alkylamine can use to attack the palladium complex, in both cases from the *re*-face.

As can be seen, the palladium orientates the attack of the *N*-alkylamine from the desired face of the ring, the *re*-face, inverting the stereochemistry at C-4. The incoming nucleophile can attack either of two positions, at C-4 to give the α product, or at C-2 to afford the γ product. These two distinct attacks may be controlled by the choice of catalyst employed in the reaction; however, a clear explanation on the reasons why this orientation can be directed with a change in the catalyst used has

not been found. Due to a possible decomposition of the compound, the stereochemistry of 2-*epi-N*-alkylamino (**108**) could not be confirmed; however, it is inferred by observation of the mechanism of the reaction.^{158,159}

5.6 Palladium-catalysed allylic amination for the direct synthesis of *epi-4-N*-alkylamino Neu5Ac2ene derivatives

In order to probe the optimal conditions for the introduction of *N*-alkyl amines into C-4 of the oxazoline (**99**), methylamine (**114**) was used as a model amine whilst the solvent and catalyst were varied. The catalysts investigated were tetrakis(triphenylphosphine)palladium (0) ($\text{Pd}(\text{Ph}_3\text{P})_4$) (**109**); tri(dibenzylideneacetone)dipalladium (0) ($\text{Pd}_2(\text{dba})_3$) (**110**); and allylpalladium (II) chloride dimer ($\text{Pd}_2(\pi\text{-allyl})_2\text{Cl}_2$), exchanged with triethylphosphine (**111**), trimethylphosphine (**112**) or triphenylphosphine (**113**) (Figure 17). Once the optimal conditions were achieved two further *N*-alkylamines were used, ethylamine (**115**) and diethylamine (**116**) (Figure 17).

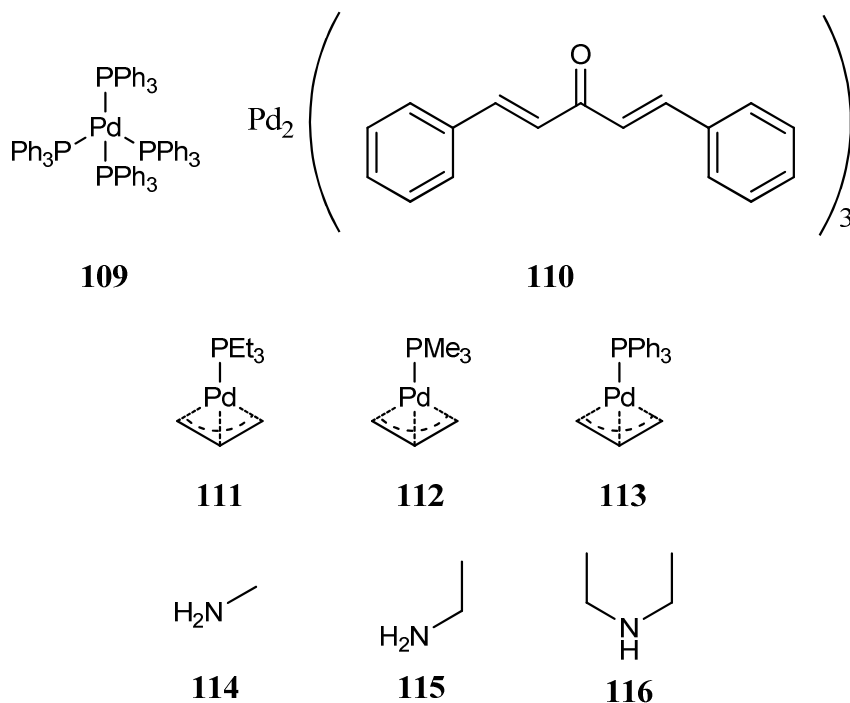
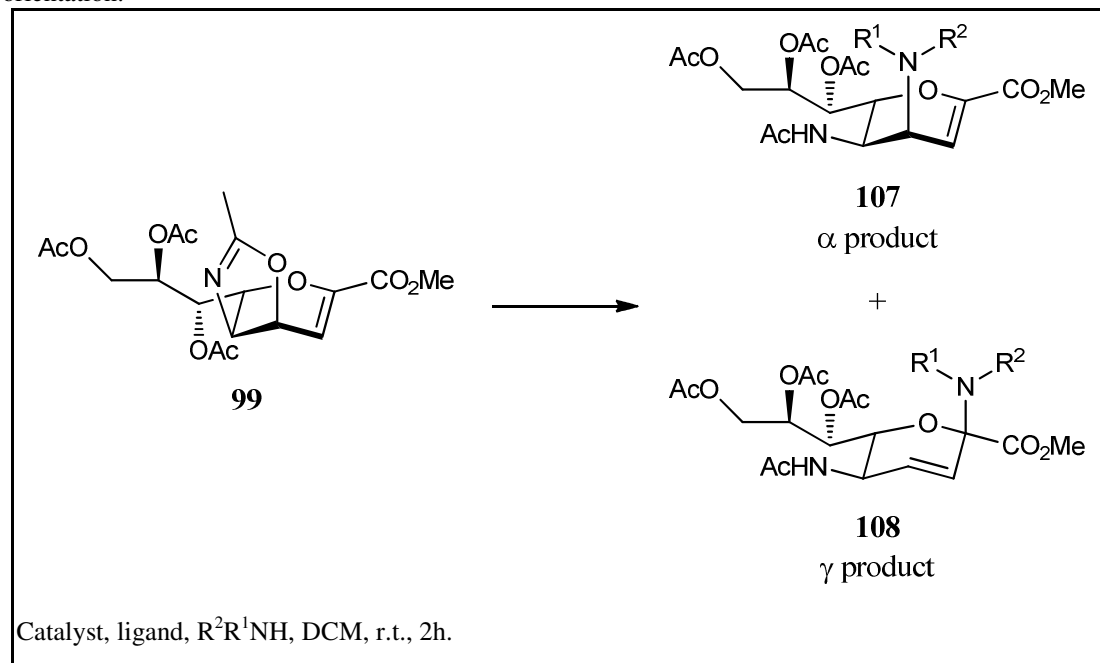


Figure 17 Structures of the different catalyst (**109** - **113**) used for the opening of the oxazoline (**99**) with a series of *N*-alkylamines (**114** - **116**).

The reactions were performed in dichloromethane at room temperature. The first catalyst to be employed was $\text{Pd}(\text{Ph}_3\text{P})_4$ (**109**) which was found to give a mixture of amination products at the α and γ positions in a ratio of 1:5, with a low combined yield (37%) (Table 4). $\text{Pd}_2(\text{dba})_3$ (**110**) was found to produce a α : γ ratio of 1:0; however, the yield of the reaction was found to be poor (16%).

Table 4 Resume of the conditions used to synthesise the series of 4-*N*-alkylamines with an axial orientation.

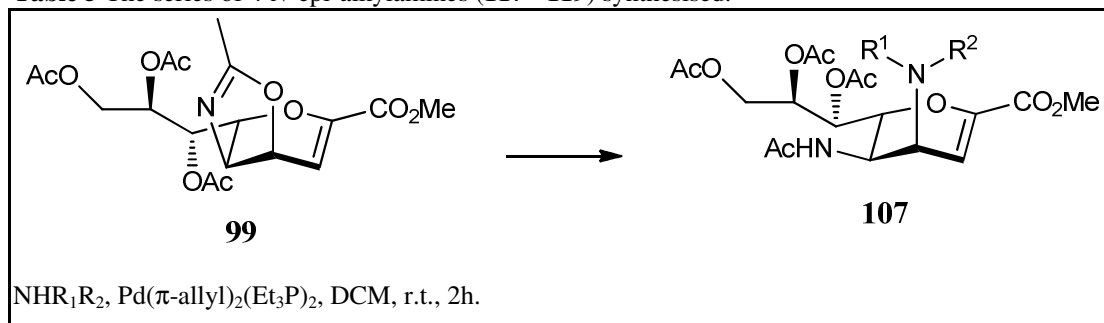


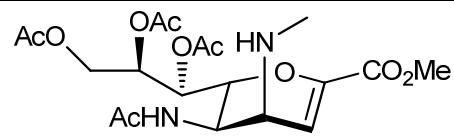
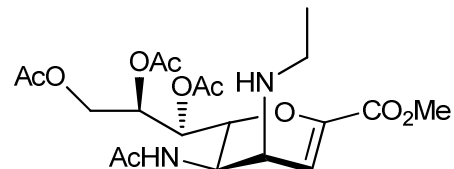
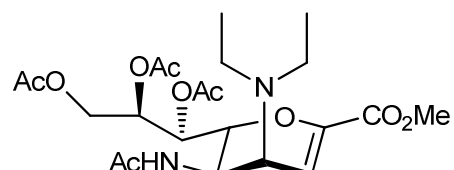
Entry	Amine		Catalyst	Ratio $\alpha : \gamma$	Yield (%) $\alpha + \gamma$
	R^1	R^2			
1	Me	H	$\text{Pd}(\text{Ph}_3\text{P})_4$	1:5	37
2	Me	H	$\text{Pd}_2(\text{dba})_3$	1:0	16
3	Me	H	$\text{Pd}(\pi\text{-allyl})_2(\text{Me}_3\text{P})_2$	1:0	20
4	Me	H	$\text{Pd}(\pi\text{-allyl})_2(\text{Et}_3\text{P})_2$	1:0	46
5	Me	H	$\text{Pd}(\pi\text{-allyl})_2(\text{Ph}_3\text{P})_2$	1:10	61
6	Et	H	$\text{Pd}(\pi\text{-allyl})_2(\text{Et}_3\text{P})_2$	1:0	75
7	Et	Et	$\text{Pd}(\pi\text{-allyl})_2(\text{Et}_3\text{P})_2$	1:0	71

Allylpalladium (II) chloride was then used, with trimethylphosphine as ligand (**112**), producing a slight improvement in the yield (20%); therefore, it was then decided to try a slightly longer alkyl chain in the ligand, triethylphosphine (**111**), with

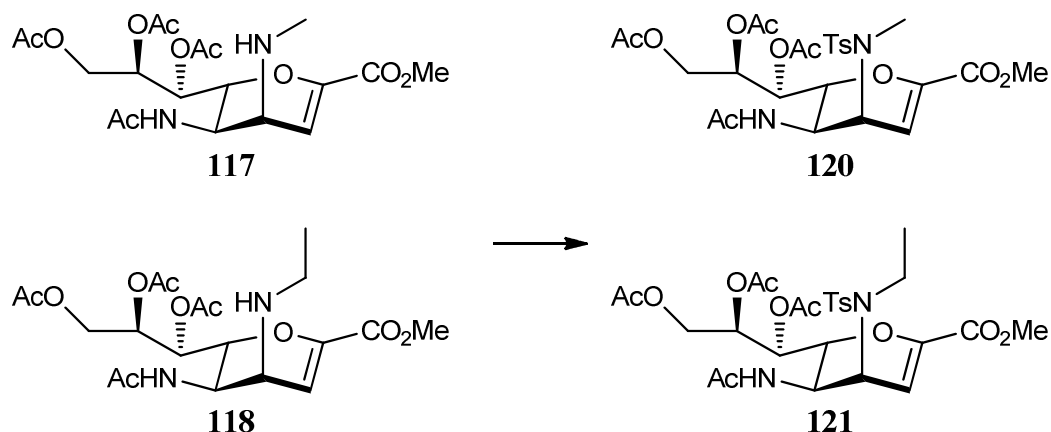
satisfactory results (46%) (Table 4). With these results in hand, only generating the α product and the yields increasing, the replacement of the ligand for triphenylphosphine (**113**) was tried; however, the ratio of substitution changed to a 1:10 of α to γ amination products, albeit with a good overall yield (61%) (Table 4). Analysing the results, it can be concluded that the electronic donating effect of the ligand in the Pd complex is important for increasing the yield of the reaction, since a significant increase in yield was observed when passing from trimethyl to triethylphosphine (20 to 46%) (entries 3 and 4) (Table 4). The replacement of the linear chain of the phosphine with a phenyl group changed the ratio between both α and γ amination reactions, shifting from a 1:0 to 1:10 ratio, respectively (entry 5) (Table 4). It is postulated that this may be due to steric effects arising from the phenyl substituent, since a similar trend was observed when $\text{Pd}(\text{Ph}_3\text{P})_4$ was used, where there was a ratio of 1:5 between α and γ amination products (entry 1) (Table 4). Regarding the alkyl amines employed, the yield of the reaction improved with longer alkyl chain amines, from 46% for the methylamine (**114**) (entry 4) to 75 and 71% when using ethylamine (**115**) and diethylamine (**116**), respectively (entries 6 and 7). It is worth mentioning that when the amination reaction was performed either with no catalyst or with no ligand; or with only the allylpalladium chloride catalyst present, no reaction was observed, proving that the presence of the activated catalyst is essential for the reaction to proceed.¹⁵⁹

It was decided to use the $\text{Pd}(\pi\text{-allyl})_2(\text{Et}_3\text{P})_2$ for the formation of the desired amine products. Therefore, the oxazoline (**99**) was dissolved in dichloromethane and a solution of the catalyst was added at room temperature. The amine was then added and the reaction stirred at room temperature for 2h, affording the desired epi-4-*N*-alkylamines in reasonable to good yields (Table 5).

Table 5 The series of 4-*N*-epi-alkylamines (**117** - **119**) synthesised.

Entry	Amine		Product	Yield (%)
	R ¹	R ²		
1	Me	H	 117	46
2	Et	H	 118	75
3	Et	Et	 119	71

In order to confirm the stereochemistry of the amino substituent at C-4, the 4-*N*-methyl and 4-*N*-ethyl-amines (**117** and **118**) were protected using TsCl (Scheme 34). The *N*-alkylamines (**117** and **118**) were dissolved in dichloromethane at room temperature and TsCl was added, and the reaction left overnight to afford the desired sulfonamide compounds (**120** and **121**) in low yields (38 and 29%).



Scheme 34 Formation of sulfonamides (**120** and **121**). TsCl, DCM, r.t., O/N, 38% for **120** and 29% for **121**.

NOESY was then used to assign the stereochemistry of the *N*-alkylamines at C-4, where an interaction between the methyl group of the *N*-alkylamine and H-6 could be clearly be seen. This interaction can only occur when the amino group is in an axial orientation, since the stereochemistry of position 6 is well established (Figure 18).

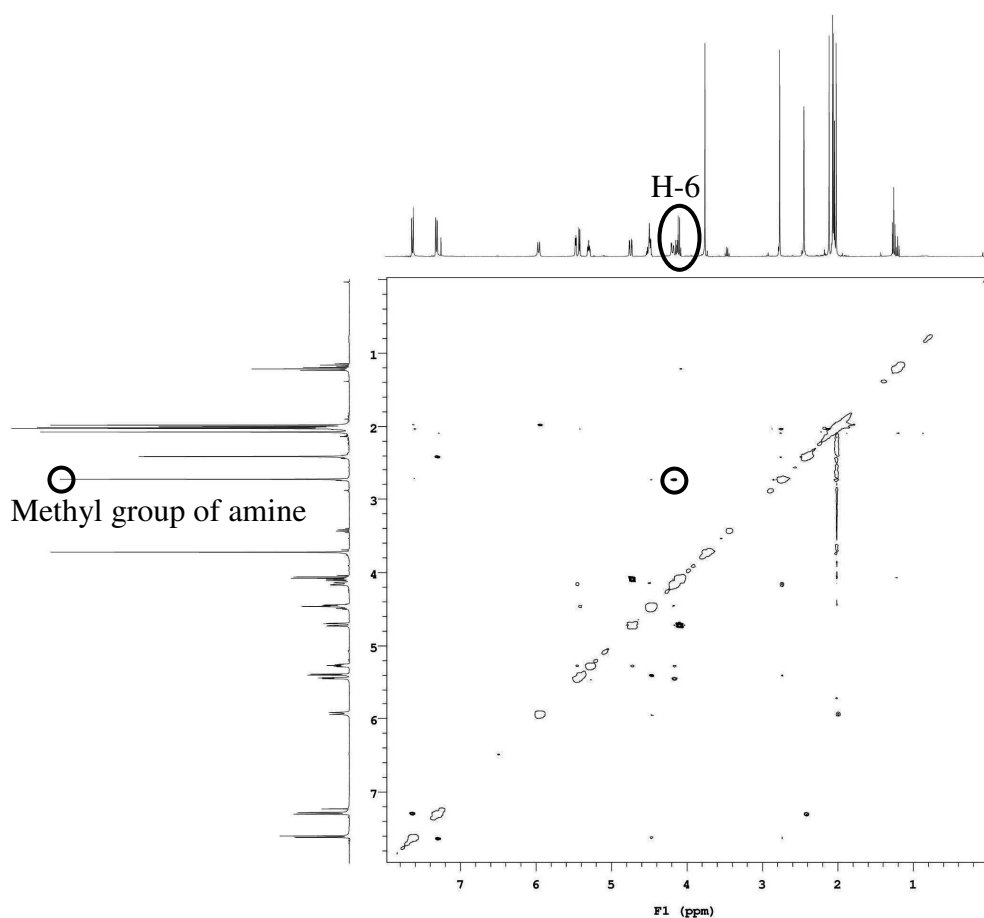


Figure 18 NOESY spectrum of 4-epi-*N*-sulfonamide (**120**) where the interaction between H-6 and the methylamine can be observed (highlighted with a circle).

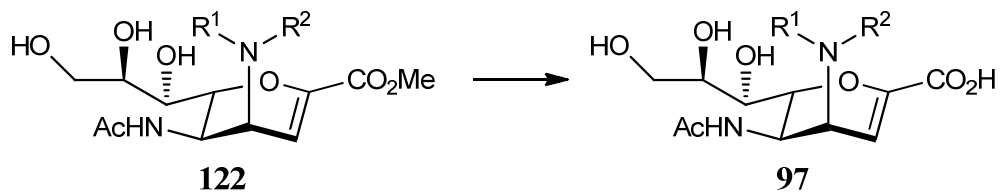
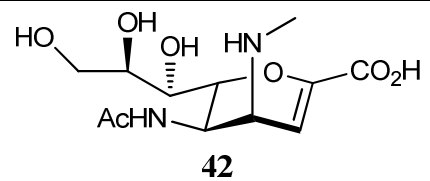
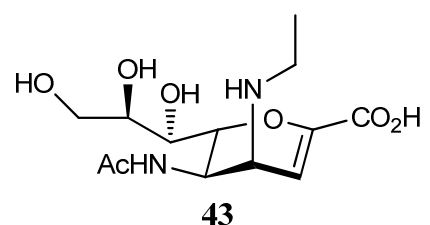
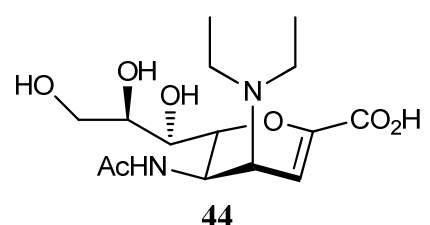
Following the successful introduction of the axial amino groups at C-4, the next step was the global deacetylation of 4-epi-*N*-alkylamines Neu5Ac2ene (**98**) which was performed using classical Zemplén conditions. A solution of sodium methoxide in methanol at 4 °C was added to the 4-epi-*N*-alkylamines Neu5Ac2ene (**98**), affording the deprotected 4-epi-*N*-alkylamines (**122**) in good overall yields (60 – 78%) (Table 6).¹⁴⁸

Table 6 Yields of the different 4-epi-*N*-alkylamines (**123** - **125**) synthesised.

Table 3. Yields of the different 4-epi-7-aminoamines (123 – 125) synthesized.				
NaOMe, MeOH, r.t., 1h.				
Entry	Amine		Product	Yield (%)
	R ¹	R ²		
1	Me	H		80
2	Et	H		70
3	Et	Et		78

The final step of the synthesis was the saponification of the ester functionality present at C-1, which was accomplished with a solution of 1M NaOH to give the desired products (**42** - **44**) in quantitative yields (Table 7).

Table 7 Yields for the saponified final compounds, 4-*epi-N*-alkylamino Neu5Ac2ene (**42** - **44**).

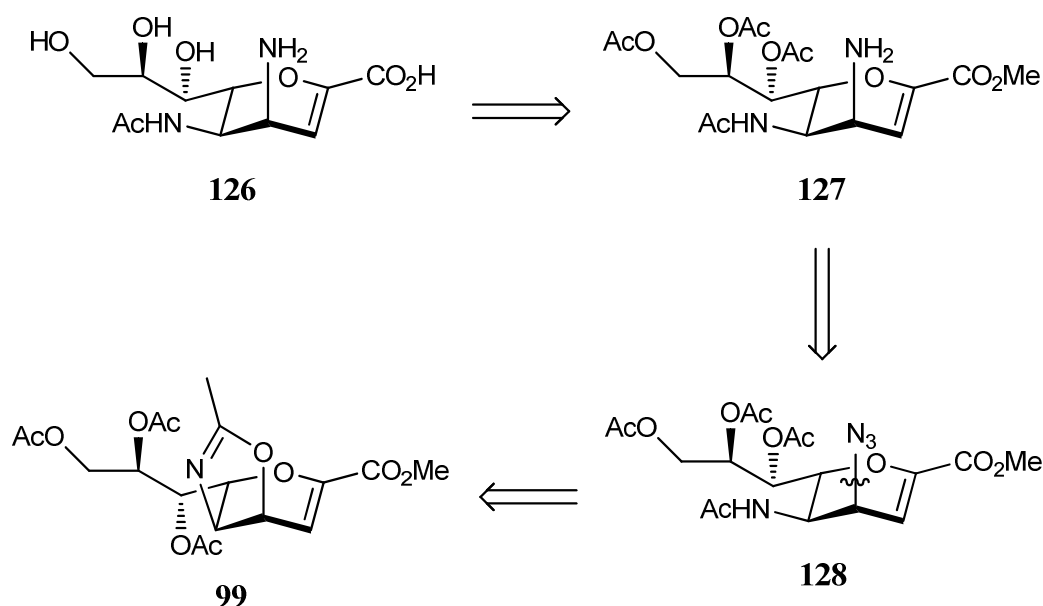
 <p>1M NaOH, H₂O, 4 °C, 1h.</p>				
Entry	Amine		Product	Yield (%)
	R ¹	R ²		
1	Me	H	 <p>42</p>	Quantitative
2	Et	H	 <p>43</p>	Quantitative
3	Et	Et	 <p>44</p>	Quantitative

5.7 Synthesis of 4-*epi*-azido (**131**) and 4-*epi-N*-amino Neu5Ac2ene (**126**)

In addition to the synthesis of the secondary (**42** and **43**) and tertiary amines (**44**), the synthesis of 4-*epi*-azido Neu5Ac2ene (**131**) was carried out in order to investigate the effects of the azide in the active site of influenza neuraminidase. Moreover, the 4-*epi*-azide was a desired scaffold in order to introduce the fluorines at C-2 and C-3 since the group at C-4 could direct the attack of the incoming fluorine. Additionally, reduction of the azide would provide a route to the primary amine (**126**).

The general strategy for the construction of the 4-*epi-N*-amino Neu5Ac2ene (**126**) was based on the retrosynthetic analysis shown (Scheme 35). As a result of a simple

sequence of deprotections, the 4-*epi*-amino Neu5Ac2ene (**126**) could be obtained from the per-*O*-acetylated-4-*epi*-*N*-amino Neu5Ac2ene (**127**). Through a straightforward hydrogenation, the per-*O*-acetylated-4-*epi*-*N*-amino Neu5Ac2ene (**127**) could be obtained from per-*O*-acetylated-4-*epi*-azido Neu5Ac2ene (**128**). Retrosynthetic cleavage of the bond indicated in the per-*O*-acetylated-4-*epi*-azido Neu5Ac2ene (**128**) furnishes the oxazoline (**99**) as a viable precursor, to which the retrosynthetic analysis has been explained previously.



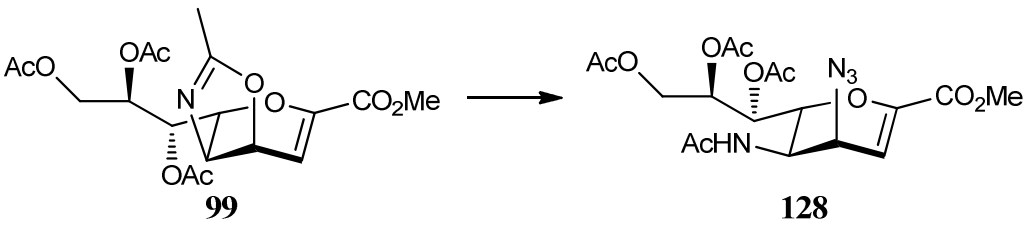
Scheme 35 Retrosynthetic analysis towards 4-*epi*-*N*-amino Neu5Ac2ene (**126**).

5.7.1 Studies towards the introduction of an azide at C-4 of oxazoline (**99**)

The first set of conditions employed for the introduction of an azide group axially at C-4, were the ones that proved successful for the introduction of the *N*-alkylamines. Therefore, to a solution of oxazoline (**99**) in dichloromethane at room temperature, was added a solution of $\text{Pd}(\pi\text{-allyl})_2(\text{Et}_3\text{P})_2$ (**111**) in dichloromethane, using as a source of azide, TMSN_3 (entry 1) (Table 8). Unfortunately, these conditions proved to be unsuccessful, with no desired product being observed. As a result, a variety of solvents were investigated, as well as the source of azide.

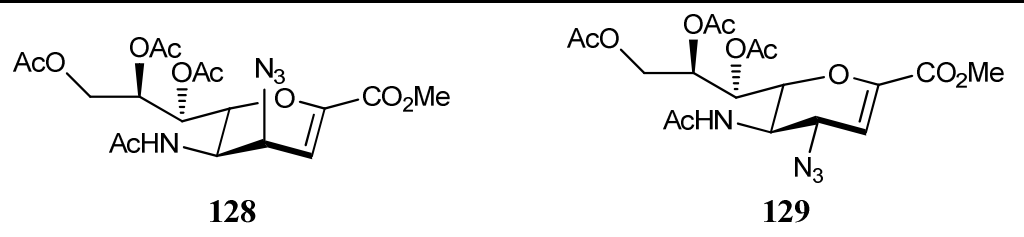
Using $\text{Pd}_2(\text{dba})_3$ (**110**) with triphenylphosphine in THF at 50 °C overnight, the per-*O*-acetyl-4-*epi*-azido Neu5Ac2ene (**128**) was prepared in moderate yield, (30%) (entry 5) (Table 8).

Table 8 Different conditions used in order to introduce the azide in an equatorial orientation.
^a Stereochemistry of the OH group is undetermined; ^b Microwave reaction set at 100 °C.

					
Entry	Azide	Catalyst	Solvent	Temp (°C)	Yield (%)
1	TMSN ₃	Pd(π -allyl) ₂ (Et ₃ P) ₂ (111)	DCM	r.t.	No rx.
2	TMSN ₃	Pd(π -allyl) ₂ (Et ₃ P) ₂ (111)	MeCN	reflux	No rx.
3	TMSN ₃	Pd(π -allyl) ₂ (Et ₃ P) ₂ (111)	MeCN + ^t BuOH	reflux	No rx.
4	TMSN ₃	Pd(π -allyl) ₂ (Et ₃ P) ₂ (111)	DCM + ^t BuOH	r.t.	No rx.
5	TMSN ₃	Pd ₂ (dba)(PPh ₃) ₂ (110)	THF	50	30
6	NaN ₃	Pd(Ph ₃ P) ₄ (109)	THF + H ₂ O	50	No rx.
7	NaN ₃	Pd(Ph ₃ P) ₄ (109)	THF + H ₂ O	60	Hydrolysis ^a
8	NaN ₃	Pd(Ph ₃ P) ₄ (109)	DMF	100 ^b	No rx.

The assignment of the stereochemistry of the azide at C-4 was achieved by comparing the ¹³C NMR chemical shifts of the per-*O*-acetyl-4-epi-azido Neu5Ac2ene (**128**) with the per-*O*-acetyl-4-azido Neu5Ac2ene (**129**), reported in the literature (Table 9).¹⁶⁰

Table 9 Comparison of the ¹³C NMR chemical shifts for the 4-epi-azido and 4-azido Neu5Ac2ene derivatives (**128** and **129**)

									
	C-1	C-2	C-3	C-4	C-5	C-6	C-7	C-8	C-9
(128)	161.5	146.3	104.5	54.8	44.8	73.6	67.6	71.3	62.1
(129)	161.5	145.1	107.6	57.8	48.3	75.9	67.7	70.9	62.1

In addition, a mass spectrum of the per-*O*-acetylated-4-epi-azido Neu5Ac2ene (**128**) was conducted, showing a peak referring to the sodium salt of the compound (479.1379), confirming the presence of the azide (Figure 19).

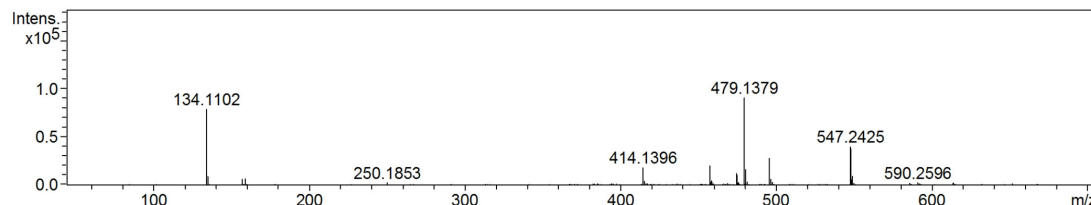
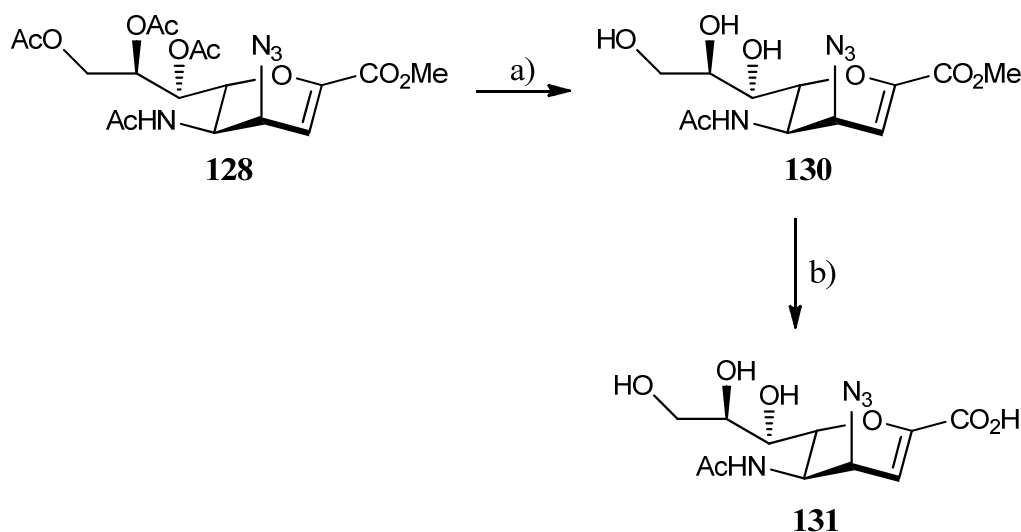


Figure 19 Mass spectrum showing the sodium peak (479.1379 m/z) of the per-*O*-acetylated-4-epi-azido Neu5Ac2ene (**128**).

5.7.2 Synthesis of the 4-epi-azido Neu5Ac2ene (**131**)

After the insertion of the azide at C-4, the next steps comprised the deacetylation and saponification in order to achieve the desired compound, 4-epi-azido Neu5Ac2ene (**131**) (Scheme 36).

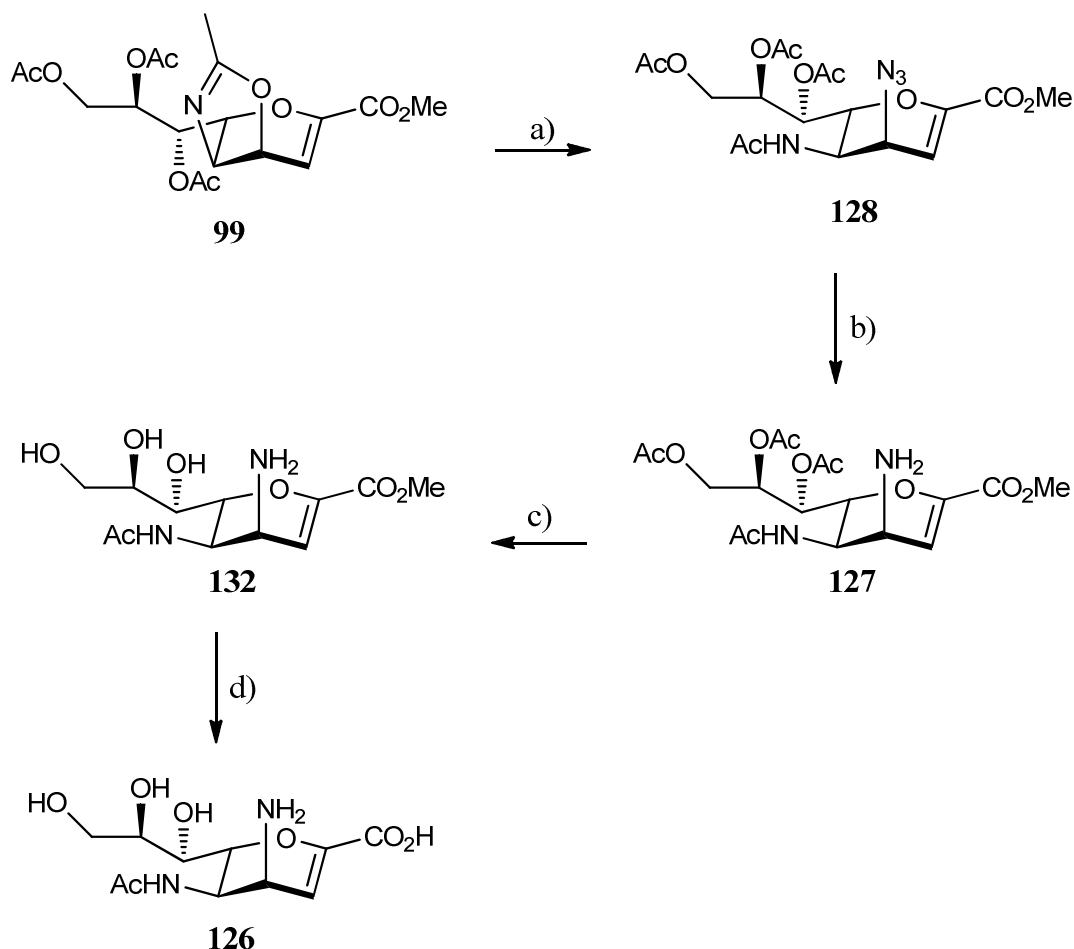


Scheme 36 Formation of 4-azido Neu5Ac2ene (**131**). a) NaOMe, MeOH, 4 °C, 2h, 92%; b) 1M NaOH, H₂O, 4 °C, 1h, 100%.

Zemplén conditions, aqueous sodium methoxide in water at 4 °C, were used to remove the acetyl groups, affording the 4-epi-azido methyl ester (**130**) in excellent yield (92%). The saponification reaction was performed in water using a 1M sodium hydroxide solution to remove the methyl ester and afford 4-epi-azido Neu5Ac2ene (**131**) in quantitative yield.

5.7.3 Synthesis of the 4-*epi*-*N*-amino Neu5Ac2ene (**126**)

Once the azide was inserted with the correct stereochemistry at C-4, it could then be reduced; after which the removal of the acetyl groups would take place, with the last reaction being the saponification, to afford the free acid (**126**) (Scheme 37).



Scheme 37 Formation of 4-aminoNeu5Ac2ene (**126**). a) $\text{Pd}_2(\text{dba})(\text{PPh}_3)_2$, TMSN_3 , THF, 50 °C, O/N, 30%; b) 1,3-propanedithiol, Et_3N , MeOH, 4 °C \rightarrow r.t., 2h, 63%; c) NaOMe, MeOH, 4 °C, 2h, 54%; d) 1M NaOH, H_2O , 4 °C, 1h, 100%.

The reduction of the azide to the amino group was first attempted using H_2 with Pd/C 10%; however, the reduction of the double bond was observed. Reduction of the azide was subsequently attempted in the presence of 1,3-propanedithiol and triethylamine in methanol, following a literature procedure.¹⁶¹ The reaction proceeded smoothly, affording the per-*O*-acetylated-4-*epi*-*N*-amino Neu5Ac2ene (**127**) in good yield (63%). The next step was the deacetylation of the compound, and once again, this was accomplished by using Zemplén conditions, with a solution of

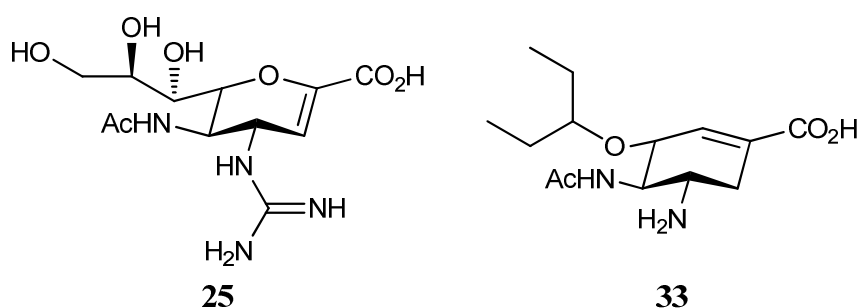
sodium methoxide in methanol at 4 °C for 2h, giving the 4-epi-*N*-amino (**132**) in average yield (54%). The reaction produced more than one compound, thus necessitating a flash chromatography step where due to the polar nature of the compound, material was lost, affecting the yield.

The final step in the synthetic pathway was the saponification of the methyl ester, accomplished in water using a 1M sodium hydroxide solution. The reaction proceeded smoothly, affording the 4-epi-*N*-amino (**126**) in quantitative yield.

Chapter 6 - Inhibitory activity of a series of 7-*N*-alkylamino 2,3-difluorosialic acids against a panel of influenza viruses

As discussed previously (Chapter 2), the influenza virus has a high propensity to generate point mutations (antigenic drift and shift). In addition, during the treatment of the influenza virus with specific inhibitors, the virus will suffer pressure to mutate certain amino acid residues in order to reduce (or eliminate) the inhibitory activity of such compounds. As a result, when developing any new inhibitors it is necessary to investigate the performance of such inhibitors against both the wild type virus and prevalent mutants of the virus.

This chapter will begin by discussing a crystal structure obtained with the 7-*N,N*-diethylamino-2,3-difluorosialic acid (**39**) and influenza neuraminidase N9 followed by a brief explanation of the different neuraminidase mutations observed clinically as a result of the treatment of influenza with the currently approved drugs, zanamivir (**25**) and GS4071 (**33**). A brief explanation will be given as to how each point mutation influences the inhibitory activity of each inhibitor. Finally, the inhibitory profile of each of the inhibitors developed in this thesis will be described against a panel of wild type and drug resistant influenza viruses.



6.1 Crystal structure obtained with 7-*N,N*-diethylamino-2,3-difluorosialic acid (**39**) and influenza neuraminidase N9

The inhibitor 7-*N,N*-diethylamino-2,3-difluorosialic acid (**39**) was co-crystallised with influenza neuraminidase N9 and the crystal structure obtained is shown in Figure 20.

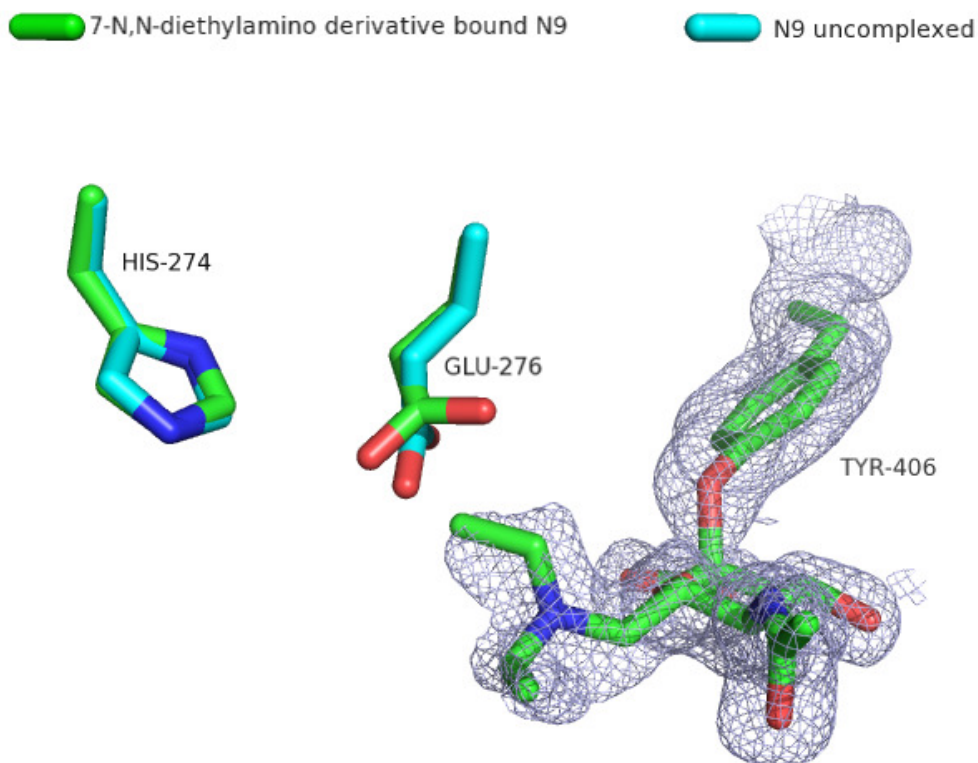


Figure 20 Superimposition of the view of 7-*N,N*-diethylamino-2,3-difluorosialic acid (**39**) covalently bound in the active site of influenza neuraminidase N9 (green) with the uncomplexed influenza neuraminidase N9 (blue). Only the residues interacting with the diethylamino side chain are shown. Generated with PyMOL (PDB unpublished, green, and 2C4A, blue).

This crystal structure (Figure 20) is the first one to prove the formation of the covalent intermediate with influenza neuraminidase (A. Watts, unpublished results), which confirms our inhibitor design strategy based on an alternative catalytic mechanism for influenza neuraminidase. There are two important aspects observed in the crystal structure, firstly the presence of the covalent intermediate between Tyr406 and the 7-*N,N*-diethylamino derivative (**39**), which proves that during the catalytic cycle of influenza neuraminidase there is the formation of a covalent enzyme-sialoside intermediate. The other important aspect is that there is a rotation of the

Glu276 to accommodate the diethyl side chain, akin to the rotation observed with GS4071 (**33**).

6.2 Point mutations conferring resistance towards influenza neuraminidase inhibitors

The mutations so far observed clinically, and *in vivo*, have been Glu119, Arg292, His274, Arg152 and Gln136. Their relative position in the active site, and the position of the sialic acid moiety with which they interact is summarised in Figure 21.

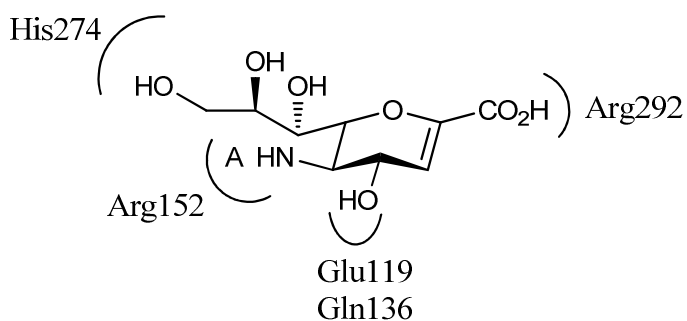


Figure 21 Mutants of influenza neuraminidase known to confer resistance to the currently approved drugs and their interactions with C-4, 5 and glycerol side chain of Neu5Ac2ene.

One of the major problems affecting oseltamivir (**6**), and to a lesser extent zanamivir (**25**), is the development of resistant strains where the efficacy of the inhibitor is diminished or abolished. A brief overview at the important mutations identified so far from clinical isolates, and their effect on the efficacy of the inhibitors towards them is given here.

Glu119

Glu119 interacts strongly with the basic nitrogen groups present at C-4 of both zanamivir (**25**) and GS4071 (**33**).¹²⁵ Therefore, mutation of this residue will alter the binding affinity between the inhibitors and the active site, making them less effective. The Glu119Val mutation was identified in a patient infected with H3N2 and being treated with oseltamivir (**6**).¹²⁵ Replacement of Glu119 with a smaller amino acid residue, allows space for a water molecule. Val119 has the effect of

pushing the water molecule into the space required by the basic moiety present at C-4 in the inhibitors (zanamivir (**25**) and GS4071 (**33**)).¹²⁵ As no crystal structure of the Glu119Val mutation exists, the Glu119Gly mutation is shown instead, in order to illustrate the difference in size (Figure 22).¹⁶²

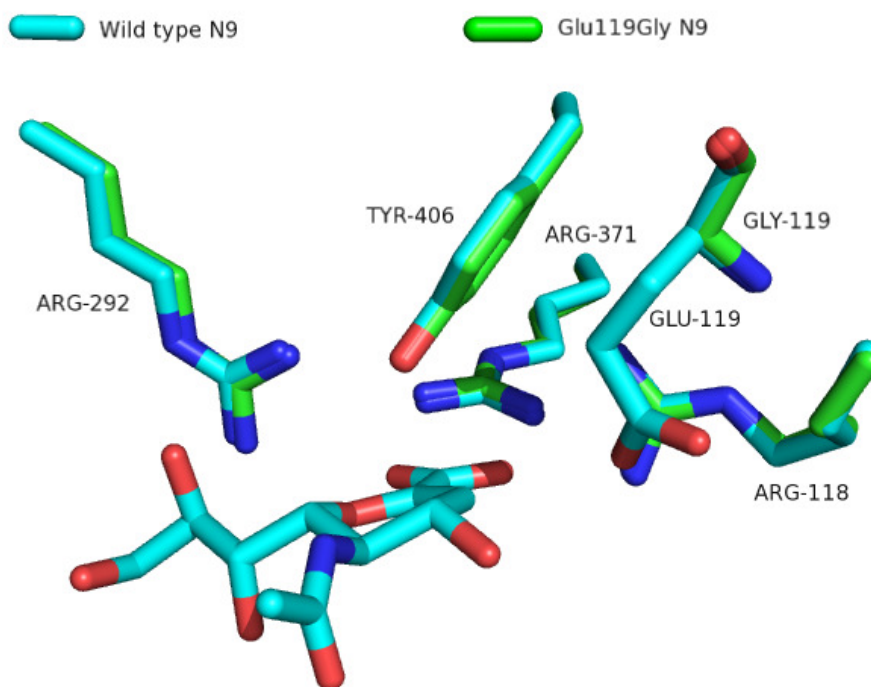


Figure 22 Superimposition of the active site of wild type N9 (blue) with Neu5Ac2ene (**27**) present in the active site and Glu119Gly N9 (green). Generated with PyMOL (PDB 1F8B, blue, and 1L7G, green).

Arg292

Arg292 is part of the three highly conserved arginine amino acid residues that form the catalytic triad of the active site binding to the carboxylic acid present in the natural substrate and inhibitors. The Arg292Lys mutation occurred in patients being treated with oseltamivir (**6**). This new strain of influenza virus is highly resistant to oseltamivir (**6**) whilst with zanamivir (**25**) it shows low levels of resistance.¹²⁵ This difference in resistance can be explained by a secondary cause of this mutation. For GS4071 (**33**) to bind in the active site of influenza neuraminidase a reorientation of Glu276 towards Arg224 is needed, so that a salt bridge can be formed between them.¹²⁴ With this reorientation, a hydrophobic pocket is created to accommodate the hydrophilic side chain of GS4071 (**33**) (Figure 23). However, due to the Arg292Lys mutation, the lysine will stabilize the Glu276, preventing this from moving and

forming a salt bridge with Arg224. As a result, the space necessary to accommodate the hydrophobic side chain is not created and the binding action of GS4071 (**33**) in the active site is heavily diminished.¹²⁵

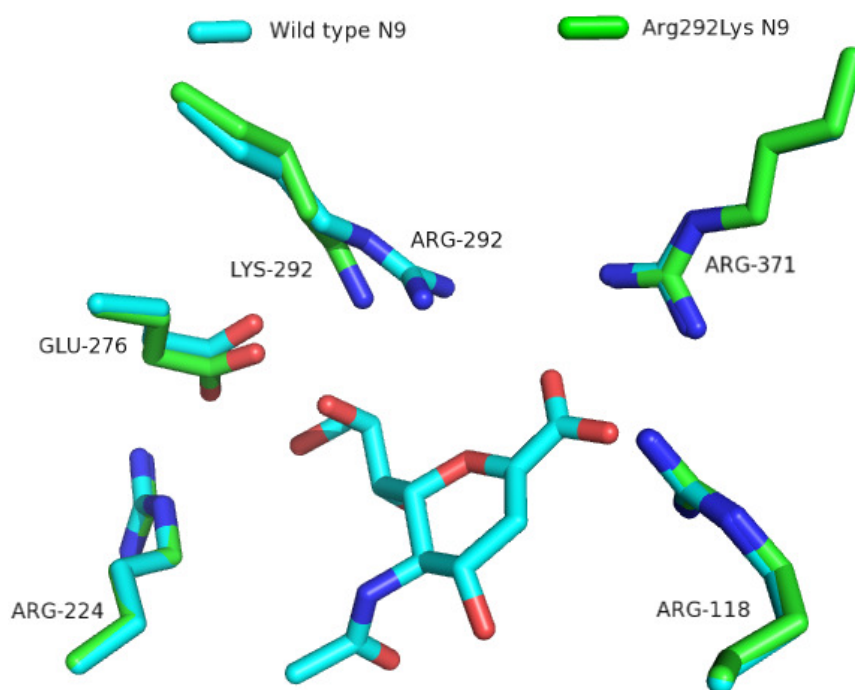


Figure 23 Superimposition of the active site of wild type N9 (blue) with Neu5Ac2ene (**27**) bound in the active site, and the active site of N9, with the Arg292Lys mutation (green). Generated with PyMOL (PDB 1F8B, blue, and 2QWB, green).

His274

One other mutation that stabilizes the Glu276 residue, halting its reorientation is the His274Tyr (Figure 24).¹²⁴ This mutation was identified in seasonal H1N1 in the 2008-2009 flu season in the United States and Japan. 99% of the circulating virus had this mutation, with cases also reported concerning the pandemic strain of H1N1.^{70,163,164}

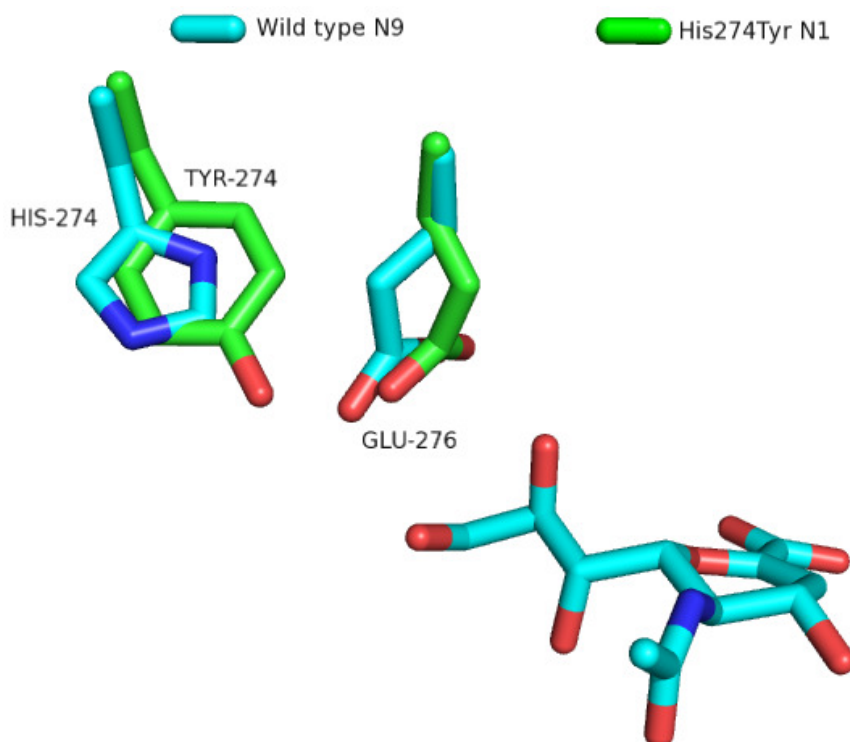


Figure 24 Superimposition of the active sites of the wild type N9 (blue) and the His274Tyr N1 (green) with Neu5Ac2ene bound in the active site. Generated with PyMOL (PDB 1F8B, blue, and 3CKZ, green).

Arg152

An immunocompromised child infected with influenza B that was being treated with zanamivir (**25**) developed a mutation on the Arg152 residue.¹¹⁰ This residue is conserved in all influenza A and B viruses, forming a hydrogen bond with the *N*-acetamido group present at C-5.¹²⁴ The enzyme shows a lower activity when compared with the wild type and is less sensitive to zanamivir (**25**) and oseltamivir (**6**).¹²⁴

Gln136

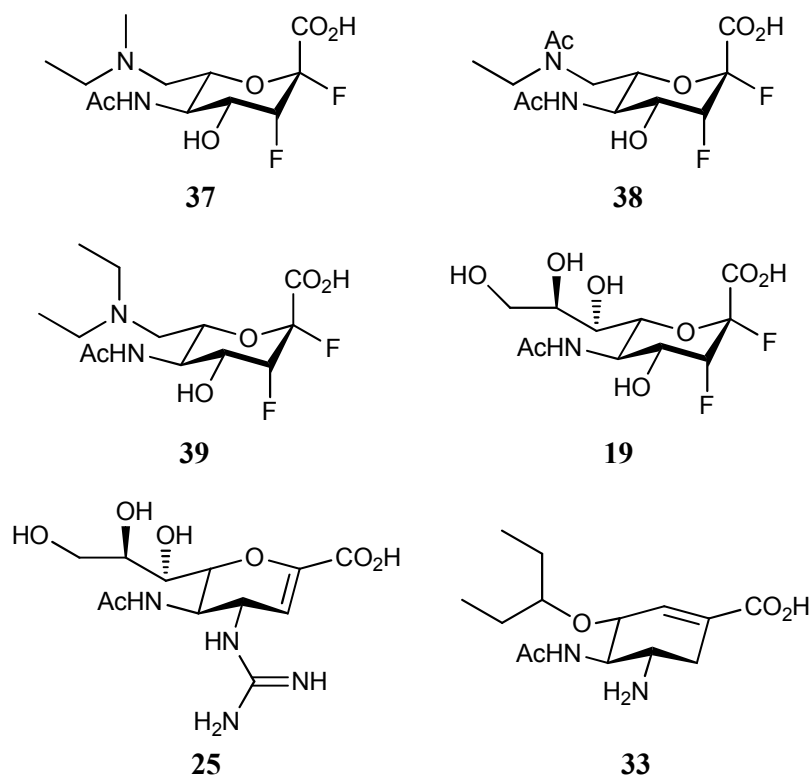
This mutation, Gln136Lys, was identified during a study on almost 400 cases of influenza virus H1N1 between 2006 and 2008.¹¹² The mutated virus showed a reduced susceptibility towards zanamivir (**25**), and no effect with oseltamivir (**6**).¹¹² A possible explanation to this selected susceptibility is due to a complex hydrogen bond network.¹¹² Gln136 interacts with Arg156 side chain, which in turn interacts with Asp151. All of these interactions imply that the residues are in a stable

conformation so any mutation will disrupt these interactions. This mutation is highly prejudicial to zanamivir (**25**) since it possesses a guanidine moiety at C-4, which forms two hydrogen bonds with Asp151. Furthermore, Arg156 forms van der Waals interactions with the same moiety. Therefore, a mutation in Gln136 disrupts the intricate network of hydrogen bonds, leaving the residues with increased mobility, greatly disturbing the interactions between the residues and the inhibitor.¹¹² GS4071 (**33**) only interacts with the backbone of Asp151, which should be unaltered in the mutant.¹⁶⁵

6.3 Inhibition of a panel of influenza viruses with 7-*N*-alkylamine 2,3-difluorosialic acids

6.3.1 IC₅₀ results obtained against a panel of influenza viruses (CSIRO)

In order to evaluate the inhibitory activity of the synthesised C-7 modified compounds, 7-*N*-ethyl-*N*-methlamino (**37**); 7-*N*-ethyl-*N*-acetamido (**38**); and 7-*N,N*-diethylamino (**39**) -2,3-difluorosialic acids were tested against a series of influenza viruses (CSIRO). The influenza viruses used were the H1N1 wild type and His274Tyr mutant; H3N2 wild type and Glu119Val mutant; H1N9 wild type and Glu119Gly mutant. Inhibitory results are given in comparison to the currently approved drugs for the treatment of influenza virus, zanamivir (**25**), the active moiety of oseltamivir (**33**), as well as to the parent 2,3-difluorosialic acid (**19**).



The compounds tested by our collaborators were the 7-*N*-ethyl-*N*-methylamino (**37**), 7-*N*-ethyl-*N*-acetamido (**38**) and the 7-*N,N*-diethylamino (**39**) -2,3-difluorosialic acid. Two different experimental conditions were used, one with no pre-incubation, with the inhibitor and substrate being added simultaneous to the influenza virus; and with pre-incubation, where the inhibitor and the influenza virus are incubated for 30 min prior to addition of the substrate.¹⁶⁶

The first experiment (no pre-incubation) allowed the examination of the rate of association of the inhibitor with the influenza neuraminidase over a 60 min period. The rate of reaction is measured by the cleavage of a fluorescent tag present at the anomeric position of the substrate (sialic acid). If there is a reduction in the fluorescence it implies that there is a slow association of the inhibitor to the enzyme, slowing down the rate at which the enzyme can process the substrate, releasing the fluorescent tag. All of the inhibitors tested showed a slow association with influenza neuraminidase (results not shown).

Subsequently, the IC₅₀'s were measured at 60 min with the data shown in Table 10.

Table 10 IC₅₀ values obtained for the inhibitors given in μ M. wt – wild type.

No pre-incubation						
Compound	H1N1		H3N2		H1N9	
	wt	His274Tyr	wt	Glu119Val	wt	Glu119Val
Zanamivir (25)	0.008	0.006	0.03	0.05	0.006	0.816
GS4071 (33)	0.007	2.4	0.005	0.208	0.004	0.005
(19)	0.1	0.1	1.7	0.5	1.1	1.2
(39)	30.1	57.1	333.6	84.1	152.5	219.4

The 7-*N,N*-diethylamino (**39**) derivative showed poor IC₅₀ results, either when tested against the wild type or the mutants of the several strains of influenza virus. When tested against H3N2, there was an improvement of the IC₅₀ with the mutant Glu119Val when compared with the wild type. The same occurrence happened with the parent inhibitor, the 2,3-difluorosialic acid (**19**). This could be due to the fact that neither inhibitor possesses a bulky group at C-4 (the position targeted by this mutation), therefore they are not affected by it. The reason why there is an improvement of the inhibition with the mutation, at the present time eludes us. Analysing the inhibition results obtained for the 7-*N,N*-diethylamino derivative (**39**) against H1N9, it can be seen that there is less inhibition with the mutant than when tested against the wild type, which is the opposite of what was observed with the H3N2 viral strain. More assays are required in order to establish an explanation of these observations.

The second experiment (pre-incubation) enabled the examination of whether any further association or dissociation of the influenza neuraminidase-inhibitor complex occurred upon addition of substrate. By measuring the rate of reaction during a set time period it can be seen if there is an increase in the rate of reaction, which indicates that there is slow dissociation of the inhibitor. All of the inhibitors tested showed a slow dissociation with influenza neuraminidase (results not shown).

Subsequently, the IC₅₀'s were measured at 60 min with the data shown in Table 11.

Table 11 IC₅₀ values obtained for the inhibitors are given in μM . wt – wild type, ^a No data available.

Pre-incubation						
Compound	H1N1		H3N2		H1N9	
	wt	His274Tyr	wt	Glu119Val	wt	Glu119Val
Zanamivir (25)	0.002	0.002	0.004	0.003	0.003	0.678
GS4071 (33)	0.003	2.4	0.002	0.260	0.003	0.003
(19)	0.08	0.1	1.4	0.2	1.2	1.2
(39)	28.1	43.2	150.5	25.8	68.4	77.2
(37)	41.9	48.5	467.7	76.2	326.1	319.6
(38)	119.4	--- ^a	159.0	--- ^a	--- ^a	--- ^a

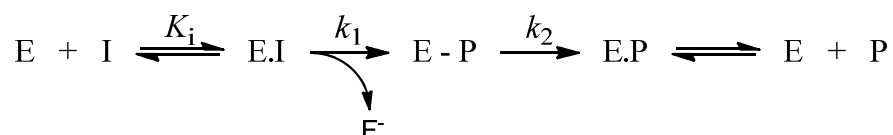
The inhibition results obtained with the 7-*N,N*-diethylamino derivative (**39**), although better than the ones observed with no pre-incubation (Table 10), still showed poor inhibition against all of the influenza viruses tested. The same behaviour, akin to the non pre-incubation experiment, was observed with the H3N2 and H1N9 influenza virus strains. When tested against H1N1, the inhibition of the wild type and mutant (His274Tyr) was comparable. This mutation affects the alkylamino substituent; however, there was a minimal loss of inhibition. The 7-*N,N*-diethylamino derivative (**39**) was designed as an isostere of the pentyloxy ester side chain of GS4071 (**33**) and when comparing the inhibition results between these two inhibitors, it can be seen that the loss of inhibition is much greater with GS4071 (**33**).

The inhibition results obtained with the 7-*N*-ethyl-*N*-methylethylamino derivative (**37**) were similar to the ones obtained with the 7-*N,N*-diethylamino derivative (**39**), with an improvement of inhibition between the wild type and mutant of H3N2. Contrary to the 7-*N,N*-diethylamino derivative (**39**), there is a decline of the IC₅₀ between the wild type and mutant of H1N9. More experiments have to be carried in order to explain the inhibition results obtained by these two inhibitors.

The inhibition results obtained with the 7-*N*-ethyl-*N*-acetamido derivative (**38**) are limited since the inhibitor was only tested against the wild type of H1N1 and H3N2.

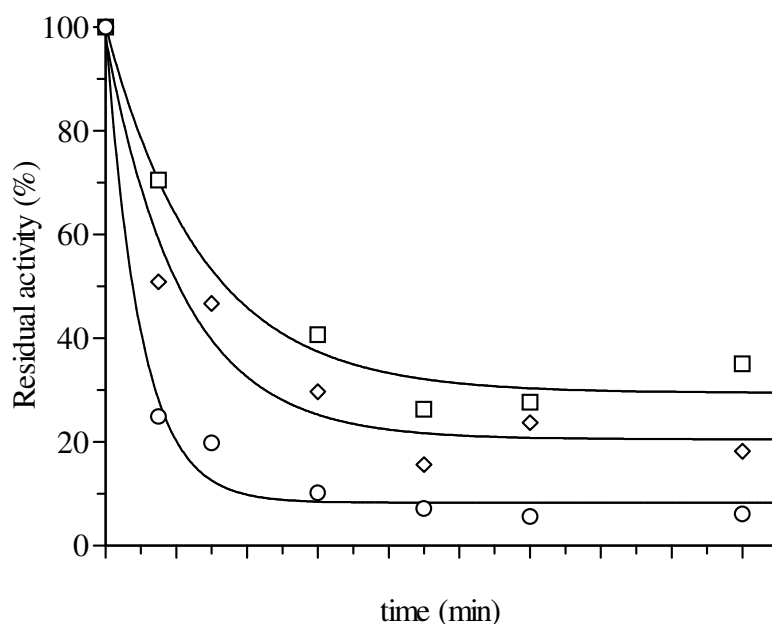
6.3.2 Determination of the K_i for the 7-*N,N*-diethylamino-2,3-difluorosialic acid (**39**)

The influenza virus H1N9 showed a time-dependent inactivation by the 7-*N,N*-diethylamino derivative (**39**), which is expressed by the following equation.



The species E, I and P represent the enzyme, 7-*N,N*-diethylamino-2,3-difluorosialic acid (**39**) and 7-*N,N*-diethylamino-3-fluorosialic acid (**50**), respectively. E – P represents the covalent sialoside intermediate, whilst k_1 and k_2 represent the rate constant for the glycosylation and deglycosylation steps.¹⁶⁷

Kinetic studies were performed at 37 °C in 56 mM Tris.HCl buffer and 4 mM of CaCl₂ at pH 7.2. The time dependence inactivation of influenza neuraminidase by the 7-*N,N*-diethylamino derivative (**39**) was monitored by incubation of the enzyme under the above conditions in the presence of several concentrations (100, 250 µM and 2.5 mM) of the inhibitor. Residual enzyme activity was determined at specific time points by the addition of an aliquot (20 µL) of the inactivation mixture to an assay solution (150 µL) containing 4-nitrophenol-sialic acid (100 µM) (Graph 1). K_i was determined by fitting the residual activity *versus* time to a single exponential equation using GraFit version 5.0.

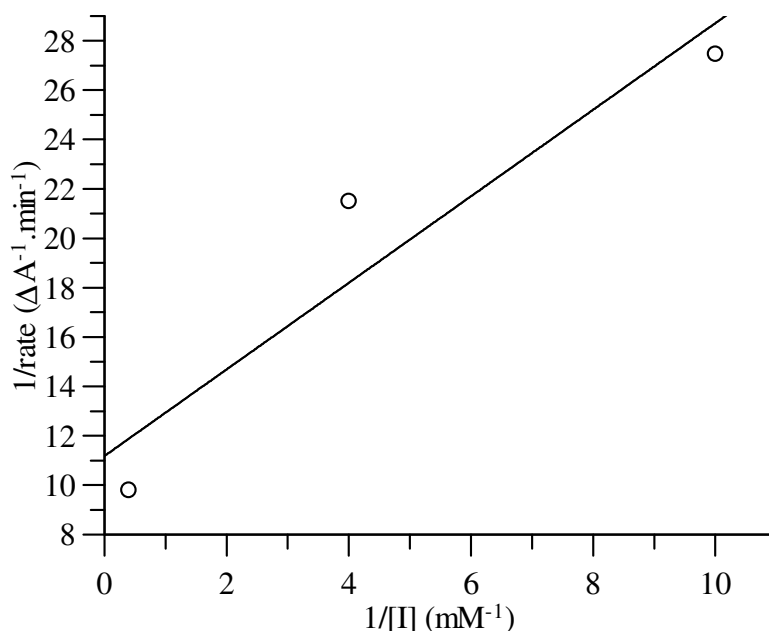


Graph 1 Residual activity *versus* time, giving the initial rate of the reaction and the time at which the inhibitor has inhibited the enzyme (steady-state). □ – 100 μM; ◇ – 250 μM; ○ – 2.5 mM of inhibitor (39).

Increasing the concentration of inhibitor increases the rate at which the enzyme is inactivated, reaching a steady-state more quickly, where the inhibition becomes constant.

By plotting the residual activity *versus* time it was possible to determine the initial rate for each of the concentrations employed. The inverse of the relative rates was then plotted against the inverse of the concentrations, obeying to the Lineweaver-Burk equation (Graph 2).¹⁶⁸

$$\frac{1}{v} = \frac{K_i}{V_{\max} [I]} + \frac{1}{V_{\max}}$$



Graph 2 Lineweaver-Burk plot, where the intercept at y axis gives the inverse of V_{\max} and the gradient gives K_i/V_{\max} .

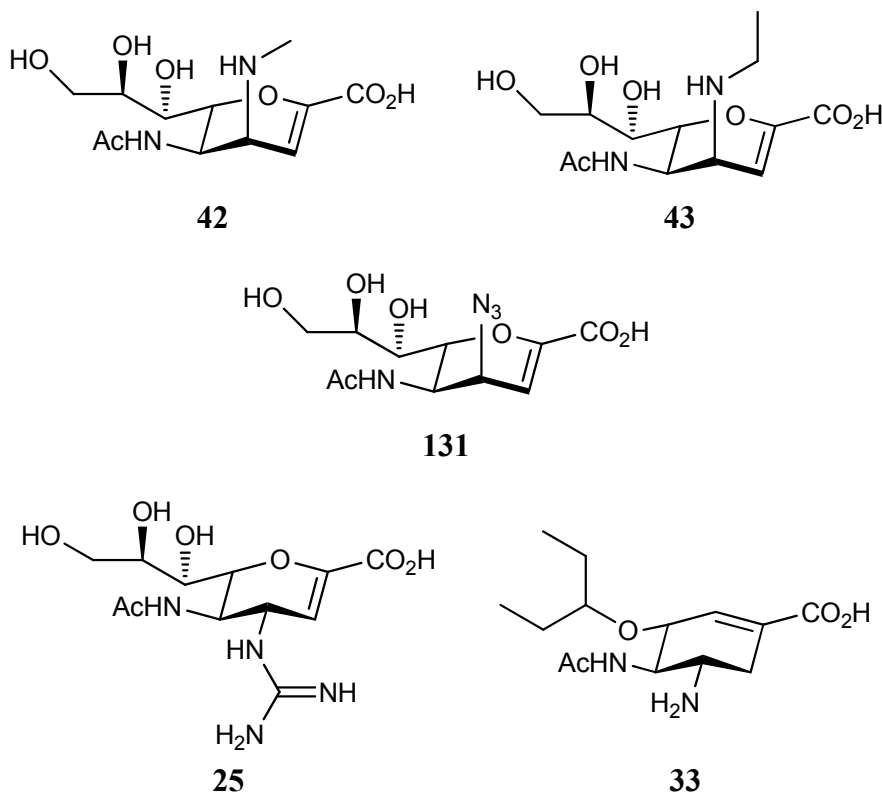
The results obtained with the 7-*N,N*-diethylamino-2,3-difluorosialic acid (**39**) showed a K_i of 157 μM .

6.4 Inhibition results obtained for the 4-*epi-N*-alkylamino Neu5Ac2ene derivatives (**42**), (**43**) and (**131**) against a panel of influenza viruses (CSIRO)

In order to evaluate the inhibitory activity of the synthesised C-4 modified compounds, 4-*epi-N*-methylanino- (**42**), 4-*epi-N*-ethylamino- (**43**) and the 4-*epi*-azido Neu5Ac2ene (**131**) were tested against a series of influenza viruses (CSIRO). The influenza viruses used were the H1N1 wild type and His274Tyr mutant; H3N2 wild type and Glu119Val mutant; H1N9 wild type and Glu119Gly mutant. Inhibitory results are given in comparison to the currently approved drugs for the treatment of influenza virus, zanamivir (**25**), the active moiety of oseltamivir (**33**), as well as to the parent 2,3-difluorosialic acid (**19**).

As with the C-7 modified compounds, two different experimental conditions were used, pre-incubation (30 min) between the inhibitor and the influenza virus prior to

the addition of substrate and no pre-incubation, with the inhibitor and substrate being added simultaneous to the influenza virus.



All of the inhibitors tested showed a slow association with influenza neuraminidase (results not shown). Subsequently, the IC₅₀'s were measured at 60 min with the data shown in Table 12.

The 4-epi-*N*-methylamino Neu5Ac2ene (**42**) generally showed lower IC₅₀ values for the mutants of influenza virus when comparing with the wild types. For H3N2 and H1N9 the reduction in the inhibition was significant, 1 to 2 fold better inhibition with the mutant Glu119Val. This mutant targets the presence of an equatorial substituent at C-4. With the present inhibitor the substituent has an axial orientation, not being affected by this specific mutation.

Table 12 IC₅₀ values obtained for the inhibitors are given in μ M. wt - wild type.

No pre-incubation						
Compound	H1N1		H3N2		H1N9	
	wt	His274Tyr	wt	Glu119Val	wt	Glu119Val
Zanamivir (25)	0.008	0.006	0.032	0.052	0.006	0.816
GS4071 (33)	0.007	2.4	0.005	0.208	0.004	0.005
(42)	77.5	56.7	273.7	70.7	185.5	3.9
(131)	379.7	301.1	60.6	411.4	44.0	47.1

The 4-epi-azido-Neu5Ac2ene (**131**) showed better results for the wild type than the mutants, with the exception of the H1N1 His274Tyr mutant. The reason why the IC₅₀ values are higher for the mutant Glu119Val could be linked to the structure of the azide, a linear and rigid structure.

All of the inhibitors tested showed a slow dissociation with influenza neuraminidase (results not shown). Subsequently, the IC₅₀'s were measured at 60 min with the data shown in Table 11.

Table 13 IC₅₀ values obtained for the inhibitors are given in μ M. wt – wild type.

Pre-incubation						
Compound	H1N1		H3N2		H1N9	
	wt	His274Tyr	Wt	Glu119Val	Wt	Glu119Val
Zanamivir (25)	0.002	0.002	0.004	0.003	0.003	0.678
GS4071 (33)	0.003	2.4	0.002	0.260	0.003	0.003
(42)	69.7	57.7	332.9	133.0	193.0	4.5
(43)	548.3	539.5	3594.5	5469.6	604.2	0.4
(131)	302.4	249.6	64.3	335.8	47.2	50.2

As observed with the no pre-incubation experiment, the 4-epi-*N*-methylamino derivative (**42**) showed better IC₅₀ values for the mutants than the wild type of the influenza viruses.

The 4-epi-*N*-methylamino Neu5Ac2ene (**43**) gave very poor inhibition results, with the only exception the inhibition observed for the H1N1 Glu119Val mutant. The reason why with H3N2 the difference in inhibition between the wild type and the mutant is almost 2 fold poorer and with H1N1 is 3 fold better with the mutant, elude us at the present time.

The inhibition observed for the 4-epi-azido derivative (**131**) was similar to the one observed for the no pre-incubation experiment.

The 4-epi-*N*-amino Neu5Ac2ene (**96**) synthesised by the group of von Itzstein gave a K_i of 0.3 μ M against influenza neuraminidase N2.⁹⁷ The 4-epi-*N*-methylamino Neu5Ac2ene (**42**) gave an IC₅₀ of 332 μ M; the 4-epi-*N*-ethylamino Neu5Ac2ene (**43**) an IC₅₀ of 3595 μ M and the 4-epi-*N*-azido Neu5Ac2ene (**131**) and IC₅₀ of 64 μ M. By comparing the inhibition observed against influenza neuraminidase N2, by employing the synthesised compounds (**42**, **43** and **131**) with the 4-*N*-amino Neu5Ac2ene (**96**) becomes apparent the restrictions on the group with an axial orientation at C-4.

Chapter 7 - Conclusions

Various approaches to the synthesis of novel 7-*N*-alkylamino 2,3-difluorosialic acids, 4-*N*-alkylamino Neu5Ac2ene's and 5-*N*-trifluoroacetamido-2,3-difluorosialic acid were investigated.

Several fluorination conditions were investigated in an attempt to improve the yield during the introduction of a fluorine atom at C-2 of the 3-fluorosialic acid (**54**). Unfortunately, none of the trial conditions improved the initial (and literature) condition that afforded the desired 2,3-difluorosialic acid (**54**) in moderate yield (45%). This compound served as scaffold for the modifications at the glycerol side chain, where through oxidative cleavage and reductive amination the desired 7-*N*-alkylamino 2,3-difluorosialic acids were obtained. Problems encountered during the oxidative cleavage and reductive amination reactions, caused difficulties in achieving the desired aldehyde (**46**) due to the presence of a vast amount of salts once the reductive amination was complete. This hindered the purification of the desired 7-*N*-alkylamino compounds. These problems were addressed and resolved by employing different scaffolds for the oxidative cleavage and reductive amination (methyl, benzyl and *p*MB sialosides) reactions optimising the experimental conditions.

For the introduction of the *N*-alkylamines at C-4 of the Neu5Ac2ene moiety, new methodologies had to be developed in order to introduce the target *N*-alkylamines with an axial stereochemistry. For this, palladium chemistry was employed and with the aid of an oxazoline (which directed the stereochemistry of the target *N*-alkylamines) a series of *N*-alkylamines was prepared. Using the same methodology, the azide was also introduced, allowing the formation of the 4-*epi*-azido (**131**) as well as the 4-*epi*-*N*-amino (**126**) derivatives.

The introduction of the *N*-trifluoroacetamido at C-5 of 3-fluorosialic acid was achieved by removing the 5-*N*-acetamido and introducing the trifluoroacetamido, using a literature procedure. Once the 5-*N*-trifluoroacetamido-3-fluorosialic acid (**89**) was obtained, it was only necessary to introduce the fluorine at C-2 and the target compound was achieved.

In conclusion, different synthetic methodologies were developed to introduce the desired derivatives in the different positions of the 2,3-difluorosialic acid (**19**). A series of C-5 and C-7 2,3-difluorosialic acid derivatives and the C-4 Neu5Ac2ene derivatives were successfully prepared. With the methodology developed it is possible to introduce a variety of alkylamino substituents in the fore-mentioned positions in an attempt to expand the range of compounds to be tested against the influenza virus.

The 7-*N*-alkylamino 2,3-difluorosialic acid modified inhibitors (**37** – **39**), as well as the Neu5Ac2ene C-4 modified inhibitors (**42** – **44**), were tested against a series of influenza viruses (CSIRO). The 7-*N,N*-diethylamino, 7-*N*-ethyl-*N*-methylethylamino and 7-*N*-ethyl-*N*-acetamido-2,3-difluorosialic acid (**37** – **39**) showed a 1000 fold poorer inhibition than the currently approved compounds, zanamivir (**25**) and the active moiety of oseltamivir (**33**). However, the inhibition results obtained showed that the inhibitors do not lose activity when tested against clinically identified mutants of influenza neuraminidase.

The biological behaviour of the inhibitors tested was a surprise since the rationale behind their design was based on the parent compound, 2,3-difluorosialic acid (**19**) as well as GS4071 (**33**). Therefore, it was expected that the IC₅₀ values of the inhibitors would be comparable to the parent compound. The IC₅₀ values of the inhibitors were poor when compared to the parent compound, which might be due to a slow association between the inhibitors and the influenza neuraminidase active site.

For future work, several compounds could be synthesised in an attempt to improve the inhibition of influenza neuraminidase. The introduction of cyclic amines at C-7 could improve the inhibition by reducing the potential rotational freedom of the alkyl chain. The synthesis of a dimeric 2,3-difluorosialic acid at C-7, with a 16 carbon linker could improve the inhibition results by agglomerating the influenza viruses, improving the host defence system.

The crystal structure obtained for the 7-*N,N*-diethylamino-2,3-difluorosialic acid (**39**) with the influenza neuraminidase N9, showed the presence of the covalent bond formed between Tyr406 and the inhibitor, supporting our proposed catalytic mechanism of influenza neuraminidase.

In respect with the C-4 modified Neu5Ac2ene, the next step could be the development of a synthetic strategy to introduce the fluorines at C-2 and C-3 on the amino (**126**) and azido (**131**) derivatives. With the fluorines at C-2 and C-3, the compounds would target the covalent intermediate sialoside-enzyme that is formed during the catalytic mechanism, instead of the transition state.

Chapter 8 - Introduction to Chagas' disease and *Trypanosoma cruzi*

8.1 Historical perspectives, prevalence and modes of infection

The parasite *Trypanosoma cruzi* is the causative agent of Chagas' disease in humans. This disease was first discovered over a century ago by Dr. Carlos Chagas in Brazil.¹⁶⁹ The disease is endemic to Central and South America, where it is estimated that roughly 18 million people are currently infected by the parasite, with a further 100 million people living in conditions which place them at high risk of becoming infected (Figure 25).¹⁷⁰



Figure 25 Geographical distribution of Chagas' disease in Central and South America.¹⁷¹

The natural reservoir for the *T. cruzi* parasite is the reduviid insect, which is endemic to most areas of Central and South America. The parasite is found to be present in the midgut (stomach) and hindgut (rectum) of the insect (Figure 26).¹⁷²



Figure 26 Reduviid insect, the natural reservoir for the *Trypanosoma cruzi* parasite.¹⁷³

The insect is noctivagous, attacking its prey while they are asleep. The insect, whilst taking a blood meal, defecates (with the parasites present in the faeces) near the bite wound and upon awakening the mammal often scratches the area of the bite, which rubs the faeces into the skin, allowing the parasite to penetrate and initiate the infection process.¹⁷⁰ There are three common ways of becoming infected with the parasite: by direct contact with the reduviid bug (accounts for 80 to 90% of cases); through a blood transfusion with infected blood (5 to 20% of infections) or via congenital routes (0.5 to 8% of infections).¹⁷⁴

8.2 Life-cycle of the *Trypanosoma cruzi* parasite and the progression of Chagas' disease

The life-cycle of the parasite encompasses a variety of developmental stages, which occur either in the reduviid insect or in the human host (Figure 27).¹⁷⁵ As mentioned previously, whilst the insect is taking a blood meal it defecates near the bite, depositing the parasites on the skin (step 1). The metacyclic trypomastigotes penetrate the skin near the bite wound, infecting cells (step 2). Once inside the cells, the metacyclic trypomastigotes differentiate into amastigotes, which are responsible for further replication (step 3).¹⁷² Following extensive replication in the cell cytoplasm, the amastigotes differentiate into trypomastigotes prior to cell rupture.¹⁷² The newly formed trypomastigotes can then either infect neighbouring cells directly or enter the bloodstream to infect a variety of cells systematically (step 4). The trypomastigotes are able to pass unharmed past the host defence mechanisms. The exact reason why this occurs is unclear; however, it is thought to be likely owing to

the production of a surface protein, complement regulatory protein (CRP), which is known to interfere with complement activation, one of the early stages in host defence mechanisms.¹⁷⁶

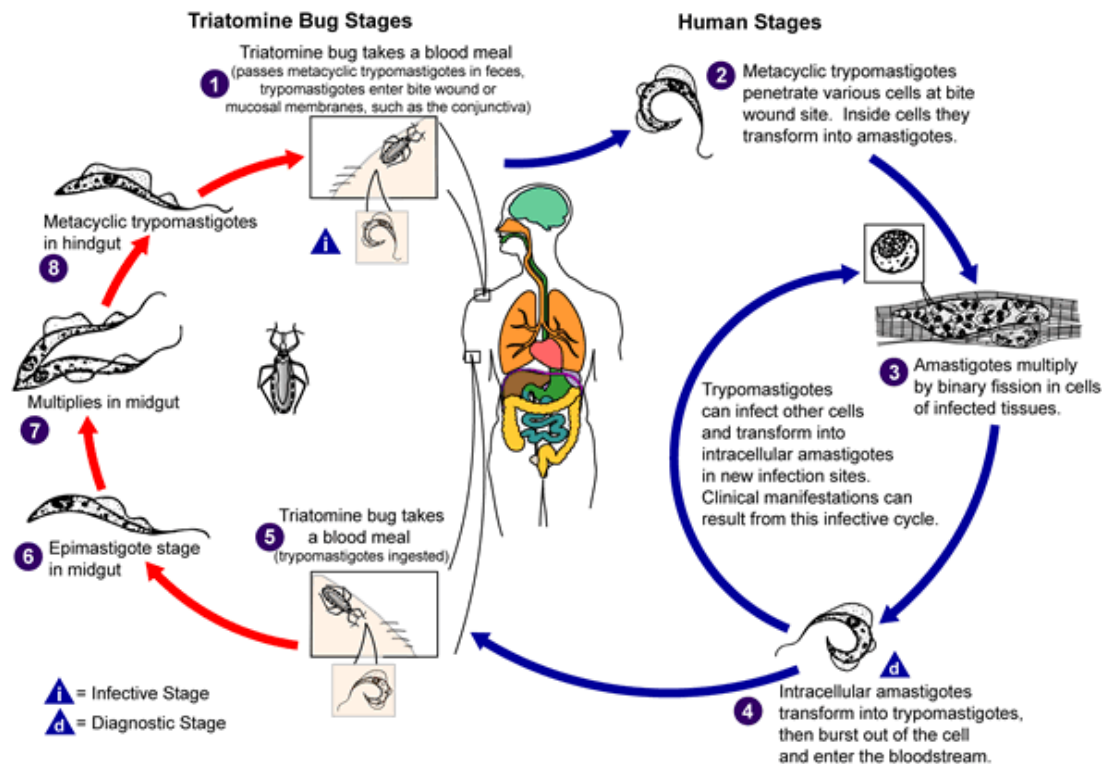


Figure 27 Life-cycle of the *Trypanosoma cruzi* parasite in the reduviid insect (red arrows) and in a human host (blue arrows).¹⁷⁵

The trypomastigotes present in the human bloodstream can then be re-ingested by a reduviid insect, and once in the midgut of the insect the trypomastigotes will differentiate into epimastigotes that replicate by binary fusion (step 5 to 7).¹⁷² The epimastigotes then pass to the hindgut of the insect where they differentiate to metacyclic trypomastigotes, and are now ready to begin another cycle of infection (step 8) (Figure 27).¹⁷²

Chagas' disease has two distinct phases of infection: the acute phase, which starts roughly a week after the host has been infected, lasting usually up to two months; and the chronic phase, which persists for life. The majority of symptoms during the acute phase are usually mild and are often confused with other diseases. One notable exception is a symptom characterised by a sign on the face (the most common site of infection), the Romaña sign (a unilateral swelling of the eyelids) that appears at the

site of the bite (Figure 28).^{169,177} In rare cases, more deadly symptoms such as myocarditis may also occur.

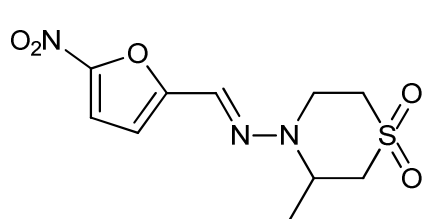
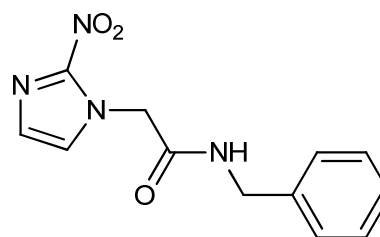


Figure 28 Characteristic sign of a reduviid insect bite, called the Romañas' sign.¹⁷⁷

Roughly two months after infection the chronic phase begins, where it is difficult to detect the trypomastigotes in the bloodstream; however, serological tests are positive. The chronic phase is further subdivided into three separate stages: the indeterminate; the cardiac; and the digestive stages. Up to 70% of all infected patients are part of the indeterminate form, where there are no signs of infection or further complications. In the remaining cases there is the development of either the cardiac form, which is associated with heart conditions (e.g. arrhythmia, cardiac failure) that can be deadly; or the digestive form, where there is the formation of megavisceras, more precisely megaoesophagus and/or megacolon.^{169,171,174,178}

8.3 Current treatments for Chagas' disease

There are currently only two drugs available for the treatment of Chagas' disease, both of which were discovered in the 1970's, Nifurtimox (**133**) produced by Bayer and marketed as Lampit[®]; and Benznidazole (**134**) which is produced by F. Hoffmann-La Roche and marketed as Rochagan[®].¹⁷⁹

**133****134**

Both drugs are administered during the acute phase of the disease as they have proven more effective against trypomastigotes (extracellular), as opposed to the chronic phase where their effectiveness against amastigotes (intracellular) is disputable.^{174,180-187}

8.3.1 Mode of action of currently approved drugs

Nifurtimox (**133**) and Benznidazole (**134**) are active against Chagas' disease due to the presence of the nitro group, which can be reduced to a nitro anion radical *in vivo* to produce either potential alkylating agents or free radicals (Figure 29).¹⁷⁸ Firstly, the action of NADPH-cytochrome P450 reductase produces the nitro anion radical that takes part in redox cycling with molecular oxygen.¹⁷⁸

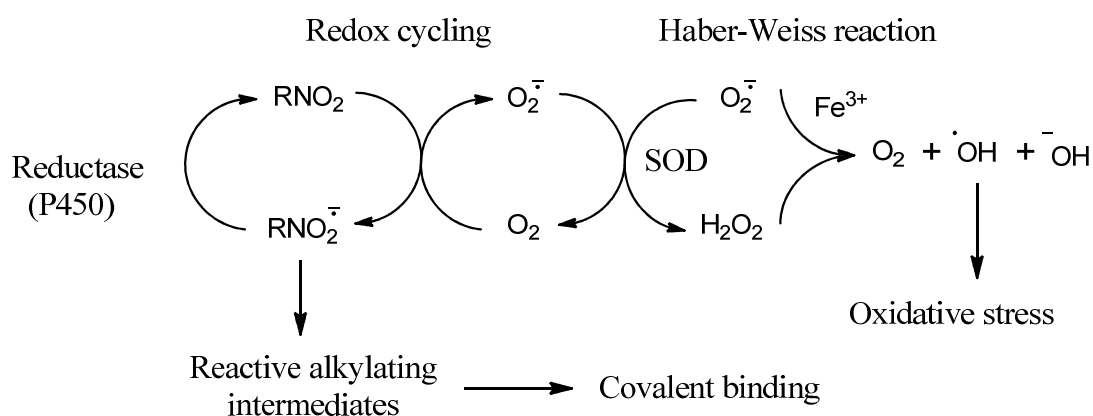


Figure 29 Mode of action of a molecule containing a nitro group.¹⁷⁸

The superoxide anion, $O_2^{\cdot-}$, can generate H_2O_2 through the action of superoxide dismutase (SOD). H_2O_2 and $O_2^{\cdot-}$ in the presence of Fe^{3+} can undergo the Haber-Weiss reaction to produce a hydroxyl radical ($\cdot OH$), which is one of the most

harmful low molecular weight radical species through binding to lipids, proteins and DNA.^{170,178,188,189}

It has been shown that *Trypanosoma cruzi* is more sensitive to oxidative stress than host cells due to the lack of detoxification mechanisms for oxygen metabolites in the parasite, a fact that is exploited by Nifurtimox (**133**).^{190,191} On the other hand, it has been postulated that Benznidazole (**134**) acts by covalently binding one or more of its nitroreduction intermediates, to inhibit RNA synthesis in the parasite.^{174,179} It is also thought that Benznidazole may be acting on several other processes within the parasite, such as interacting with IFN- γ , or inhibiting *Trypanosoma cruzi* NADH-fumarate reductase.^{188,192-194}

8.3.2 Side-effects associated with current therapies

As a consequence of their non-selective mechanisms of action, both of the currently approved drugs have serious side effects. The common side-effects from Nifurtimox (**133**) generally target the central nervous system and can result in anorexia, loss of weight, excitability or sleepiness. It can also cause gastrointestinal problems resulting in nausea, vomiting, and occasional intestinal colic and diarrhoea.^{170,174} Benznidazole (**134**) causes similar side effects to Nifurtimox (**133**), as well as additional effects which are more serious in nature. These can be divided into three groups: hypersensitivity, dermatitis with coetaneous eruptions, articular and muscular pain, fever and lymphadenopathy; depression of bone marrow, thrombocytopenic purpura and agranulocytosis (the most severe complications reported); polyneuropathy, paresthesia and polyneuritis of peripheric nerves. There is also speculation that the prolonged use of both drugs can induce tumorigenic/carcinogenic events in cells.^{170,174}

8.4 Novel therapeutic targets for inhibition of *Trypanosoma cruzi*

Given the serious problems associated with the currently approved drugs, there is a pressing need to develop new and safer drugs able to halt the progression of the disease.

In the 1990's numerous drug candidates were developed, synthesised and tested against Chagas' disease with little success. Recent advances in the understanding of

the biochemistry of the parasite have identified several potential new targets for therapeutic interventions, including the targeting of sterol biosynthesis, trypanothione reductase, and cysteine proteases.^{174,191,195,196} Amongst the several enzymes identified as possible targets for chemotherapeutics, one of significant importance is *Trypanosoma cruzi* trans-sialidase.¹⁹⁷ This enzyme is present on the cell surface of trypomastigotes and is crucial for cell invasion.¹⁹⁸ Although this protein is only valid for targeting the acute phase of the disease, it is still an important target, as halting the infection of host cells by the trypomastigotes will neutralize the disease.¹⁹⁷ *Trypanosoma cruzi* trans-sialidase also plays an important additional role in protection of the parasites by shielding them from detection by the host immune system.¹⁹⁷

8.5 *Trypanosoma cruzi* trans-sialidase

The existence of *Trypanosoma cruzi* trans-sialidase (TcTS) was first postulated by Previato *et al* and latter supported by Zingales *et al*.^{199,200} Zingales *et al* showed that the cell surface of the parasite must possess an enzyme that not only has the capability of cleaving sialic acid from host cell glycoconjugates, but must also have the ability to transfer sialic acid onto the surface of the parasite.²⁰⁰ These observations were latter confirmed by several other researchers.^{172,201-204}

TcTS and the acceptor of sialic acid, a mucin-like protein, are bound to the surface of the parasite by glycosylphosphatidylinositol (GPI) anchors.²⁰⁵ TcTS has two distinct enzymatic activities, namely the cleavage of sialic acid from the host cell surface glycoconjugates and the transfer of the cleaved sialic acid to an acceptor substrate of the parasites mucin like surface proteins (Figure 30).²⁰⁶ TcTS is of the upmost importance for the parasite, as the parasite is unable to synthesise sialic acid *de novo* to coat the surface of the trypomastigotes with sialic acid.

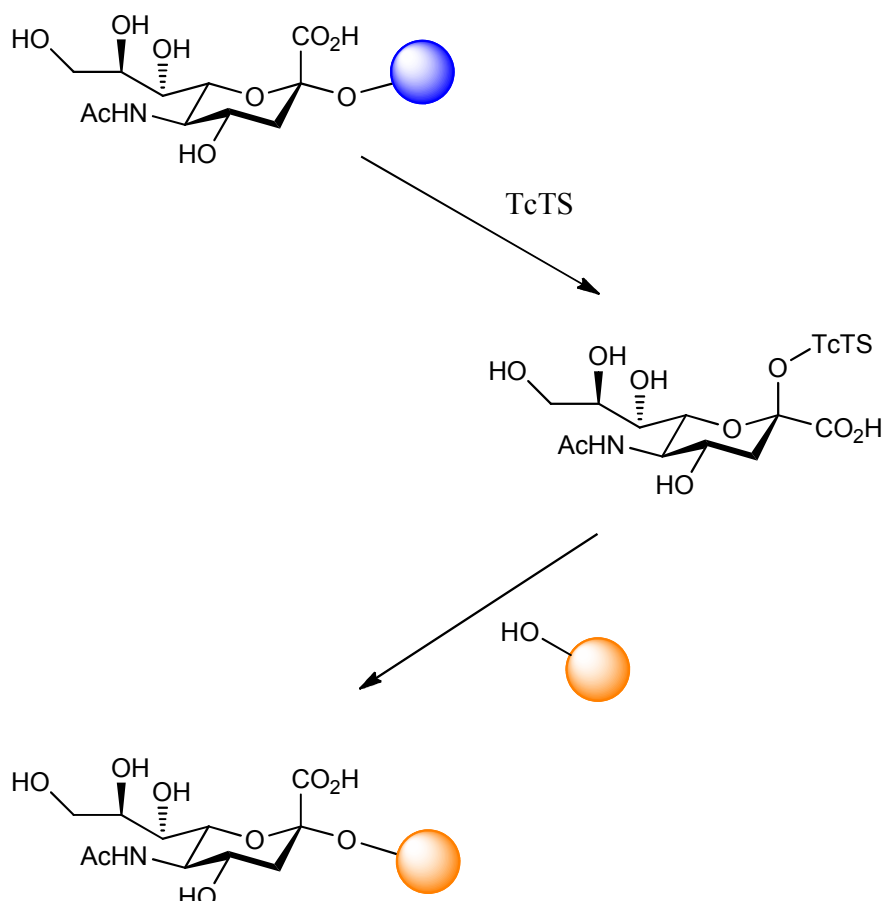


Figure 30 The role of TcTS on the transfer of sialic acid from a host cell glycoconjugate (blue sphere) to a mucin receptor at the surface of the parasite (orange sphere).

Once the parasite's surface is coated with sialic acid it can evade the host defence mechanisms due to the masking of the terminal sugar moiety (a galactose) of the glycoconjugate (Figure 31).^{172,197,205} *Trypanosoma cruzi* trans-sialidase can also be shed into the bloodstream by the action of phosphatidylinositol-phospholipase C (PI-PLC). Once in the blood stream, TcTS is able to interact with different biological processes, such as inducing apoptosis in components of the host immune system; induction of immunopathology; promoting the desialylation of platelets; and, surprisingly, enhancing the regeneration and outgrowth of neurons (Figure 31).²⁰⁷⁻²¹⁰

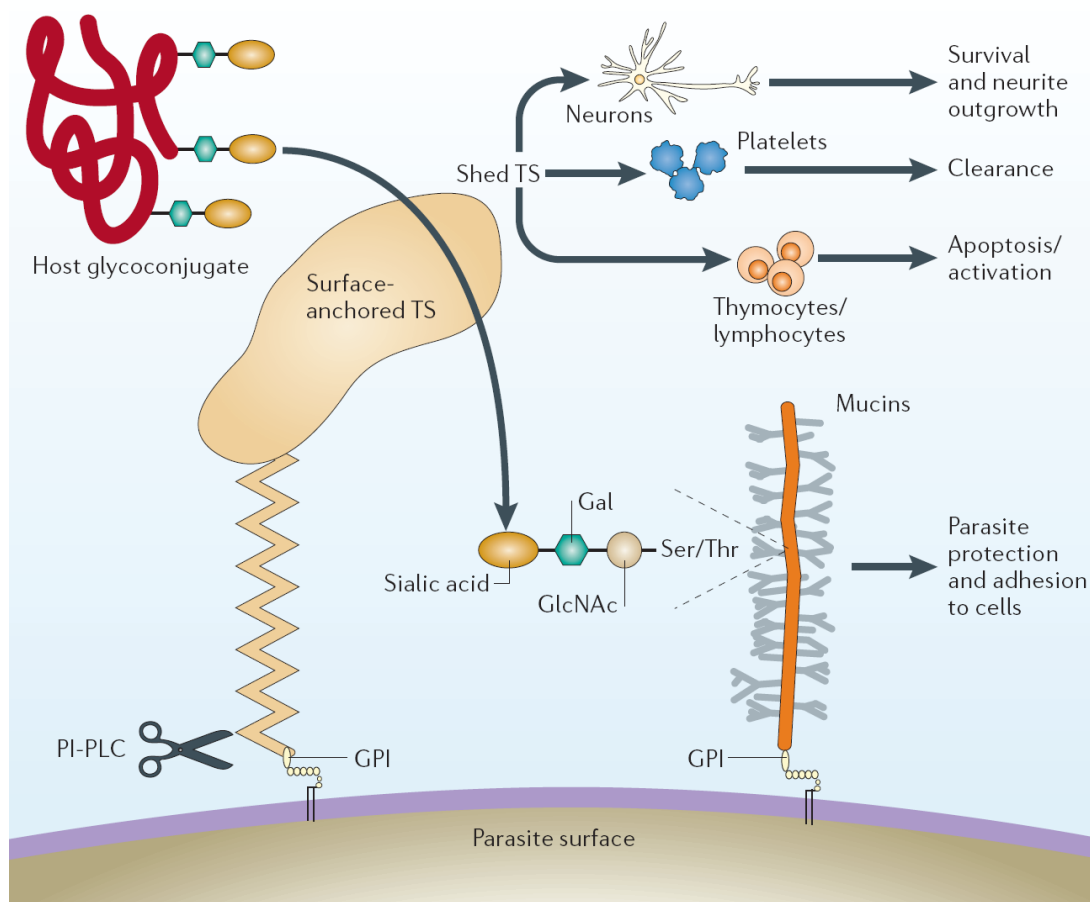
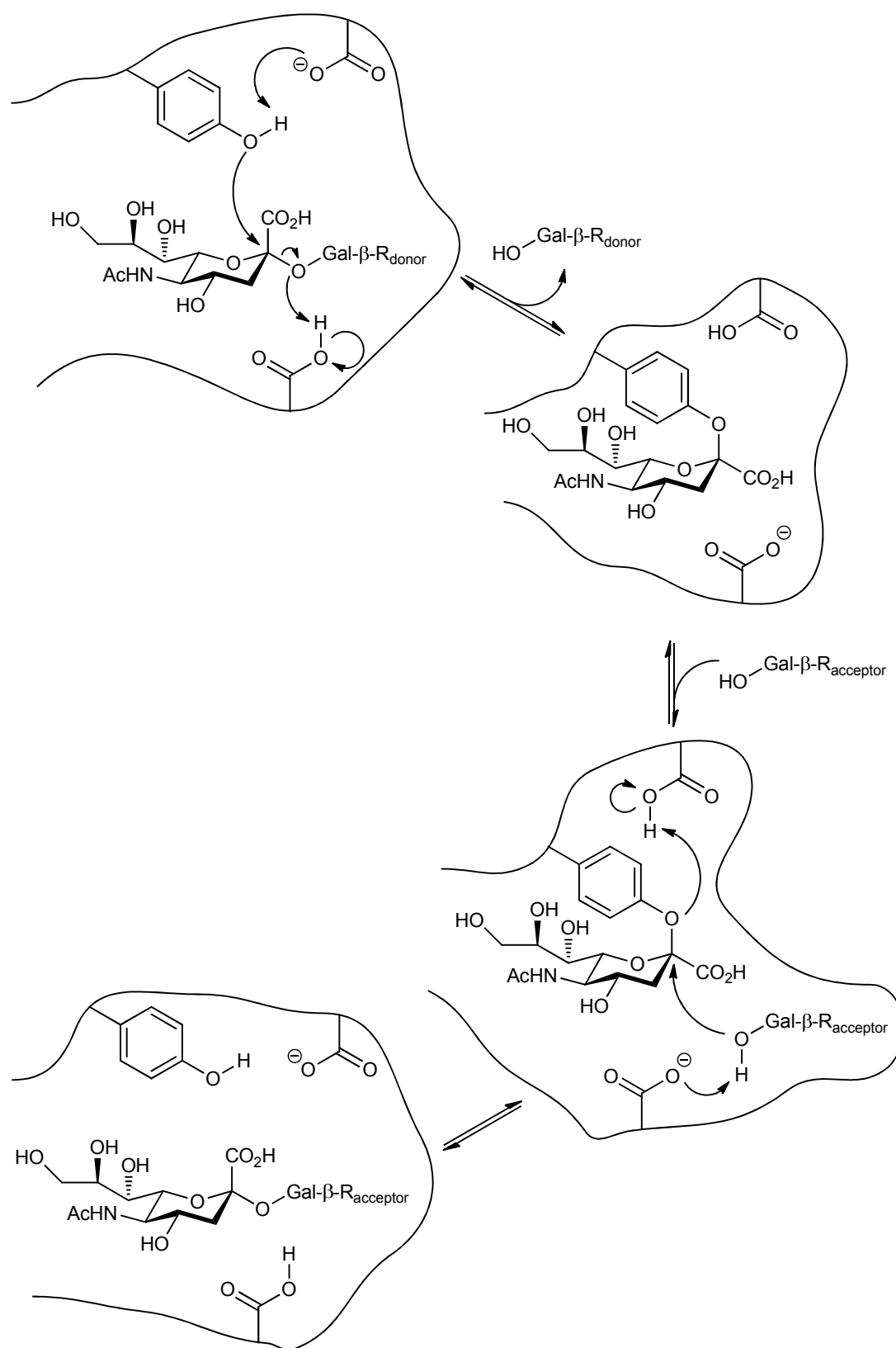


Figure 31 Role of *Trypanosoma cruzi* trans-sialidase on transferring sialic acid from host glycoconjugates and its biological effects when it is free from the parasitic surface.²⁰⁵

8.5.1 Catalytic mechanism

The catalytic mechanism of *Trypanosoma cruzi* trans-sialidase is very similar to that of influenza neuraminidase (Scheme 38).^{211,212} In the first step of the mechanism the glutamate residue, Glu230, acts as a general base catalyst, deprotonating the hydroxyl group of the catalytic tyrosine residue, Tyr342.¹³⁶ The hydroxyl group of the tyrosine residue then acts as a nucleophile, attacking the anomeric position (C-2) of the sialic acid residue, forming a covalent sialyl-enzyme intermediate.¹³⁶ Departure of the aglycone is assisted through protonation of the glycosidic oxygen by an aspartate residue, Asp59.¹³⁶ In the second step of the mechanism the aspartate residue now acts as a general base, deprotonating the C-3 hydroxyl group of an acceptor galactoside which acts as a nucleophile, attacking the anomeric position (C-2) of the sialic acid, turning over the covalent intermediate.¹³⁶ As a result, the

sialic acid is now transferred from the host cell glycoconjugates to a mucin acceptor on the surface of the parasite with an overall retention of anomeric configuration.²¹²



Scheme 38 Catalytic mechanism of *Trypanosoma cruzi* trans-sialidase.²¹²

8.5.2 Active site architecture of TcTS

The crystal structure of *Trypanosoma cruzi trans*-sialidase was solved in 2002 by Buschiazzi *et al* who showed that the enzyme consists of two domains: an *N*-terminus domain of 371 residues which forms a six bladed β propeller that contains the active site; and a *C*-terminus lectin-like domain, containing 260 residues, which is not involved in the enzymatic activity (Figure 32).²¹³ In the majority of *trans*-sialidases the *C*-terminal part possesses a repetitive unit of 12 amino acids called shed acute phase antigen (SAPA) that generates an early antibody response from the human host in the acute and congenital stages of infection.^{172,214}

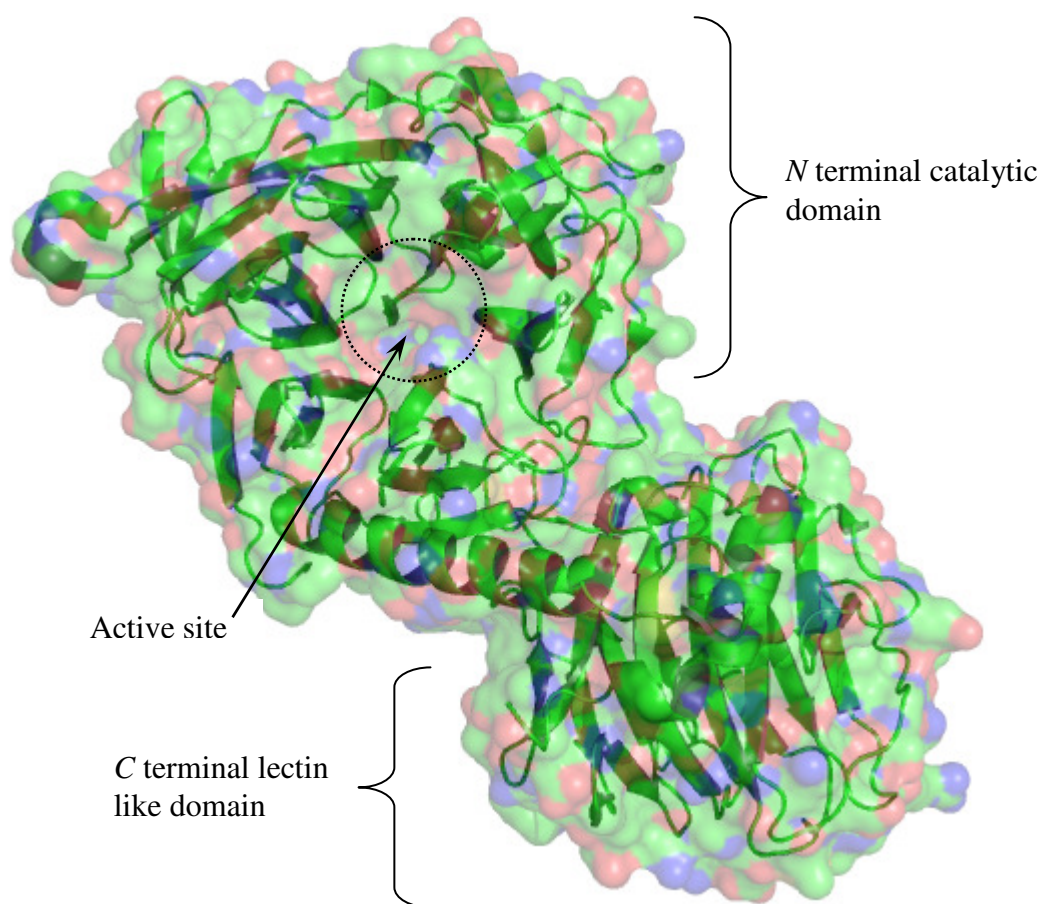


Figure 32 A monomeric subunit of TcTS (in Corey-Pauling-Kolton form). Generated with PyMol (PDB 1MS4).

The active site of *trans*-sialidase contains several highly conserved residues that are common to most sialidases, such as the arginine triad (Arg35, Arg245 and Arg314) which interact with the carboxylate of sialic acid; the catalytic nucleophile residue, Tyr342, and the general acid/base residues Asp59 and Glu230.²¹³ Moreover there are

several residues that, although not involved in the catalytic cycle, are required to interact with the *N*-acetyl group and the glycerol side chain, namely Val95, Asp96, Trp120 and Leu176 (Figure 33).^{136,213}

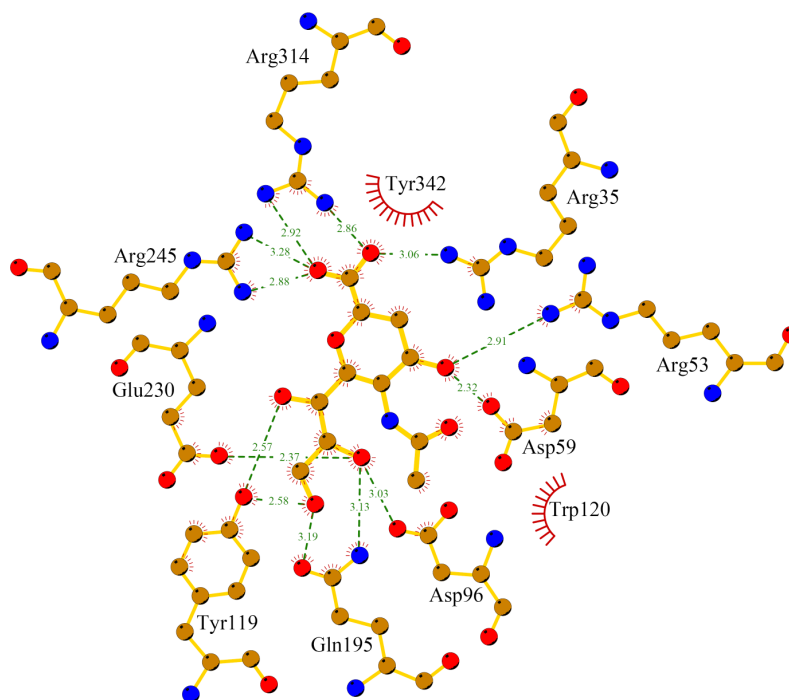


Figure 33 Representation of the catalytic site of *Trypanosoma cruzi* *trans*-sialidase with Neu5Ac2ene (27) binding to the key amino acids. Generated with LigPlot⁺ (PDB 1MS8).

In addition to the sialic acid binding site, there is also a lactose binding site present, which will accommodate the galactose moiety. The key residues responsible for the *trans*-sialidase activity are Tyr119, Trp120, Val203, Tyr248 and Trp312 which have been seen to regulate the accessibility of the acceptor glycoconjugate to the catalytic site.²¹³ Once sialic acid is covalently bound to the enzyme the Tyr119 residue can adopt one of two conformations: inside the active site, close to the glycerol moiety of sialic acid; or outside the catalytic site creating a slot like cavity with the aid of Trp312 residue.^{206,213} Tyr119 plays an important role in the transfer of the sialic acid from the donor to the acceptor substrate, as the mutation Tyr119Ser has been shown to abolish the *trans*-glycosylation activity.²¹⁵ One other residue that seems crucial for effective formation of the acceptor binding site is Pro283, which interacts with Trp312 a residue that modulates the acceptor binding site.^{213,215} A cartoon representation of the mode of action of *trans*-sialidase illustrates how the enzyme,

after accepting the donor substrate, alters the architecture of its active site to promote binding of the acceptor substrate (Figure 34).

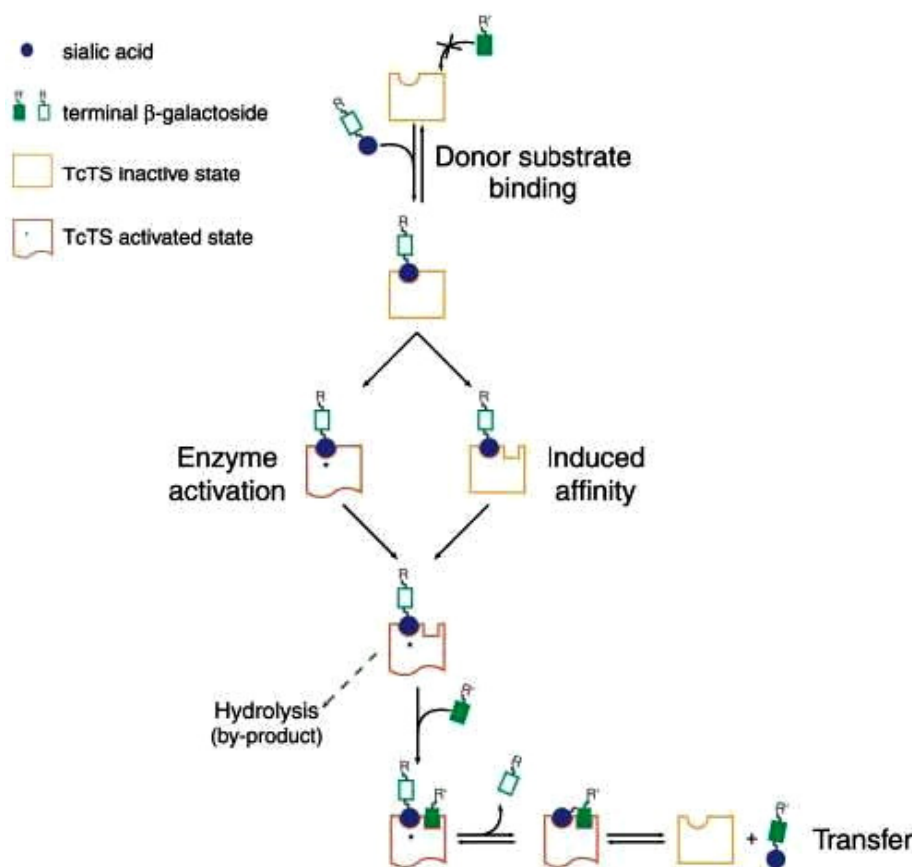


Figure 34 Cartoon representation of *Trypanosoma cruzi* trans-sialidase.²¹³

8.6 The development of novel inhibitors of *Trypanosoma cruzi* trans-sialidase

In order to inhibit *Trypanosoma cruzi* trans-sialidase, one can either target the sialic acid binding site (by mimicking sialic acid) or the lactose binding site.

Regarding mimetics of sialic acid as potential inhibitors of TcTS, inhibitors of a similar enzyme, influenza neuraminidase, have been tested since both enzymes share many of the same active site residues and both process sialic acid as their natural substrate (Figure 35).

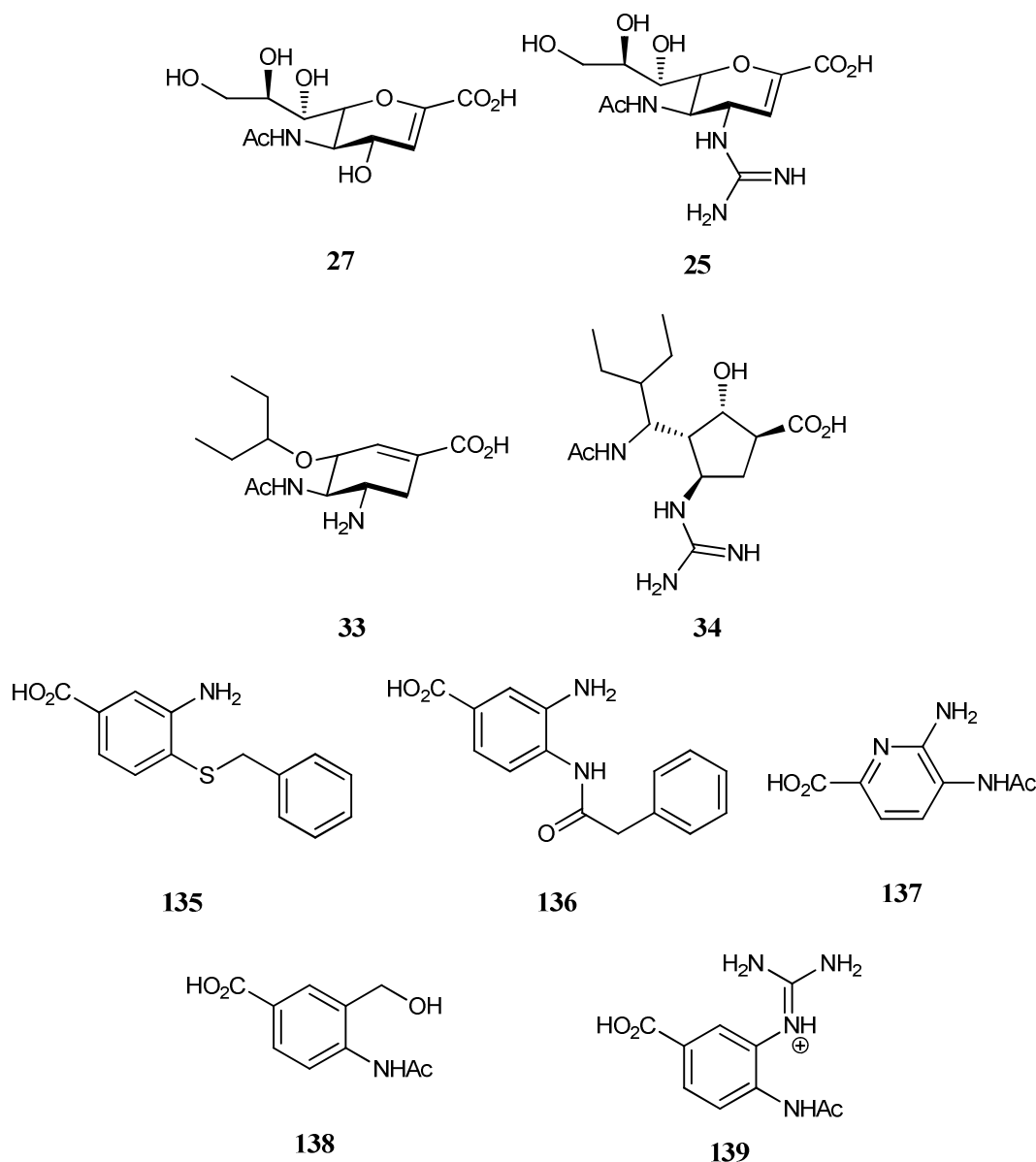


Figure 35 Structures of inhibitors towards the sialic acid binding site.²¹²

Surprisingly Neu5Ac2en (**27**) showed only a weak inhibition towards *Trypanosoma cruzi* *trans*-sialidase with a K_i of 12.3 mM, whilst zanamivir (**25**), GS4071 (**33**) and peramivir (**34**) showed no inhibition (> 10 mM) towards the enzyme.^{212,216,217} Other compounds based on a benzoic acid scaffold (**135** - **139**) showed slightly better levels of inhibition, in the order of 0.1 to 1 mM.^{212,216}

The use of analogues that can occupy both the sialic acid and lactose binding sites (**140** - **142**) have also been studied (Figure 36).²¹²

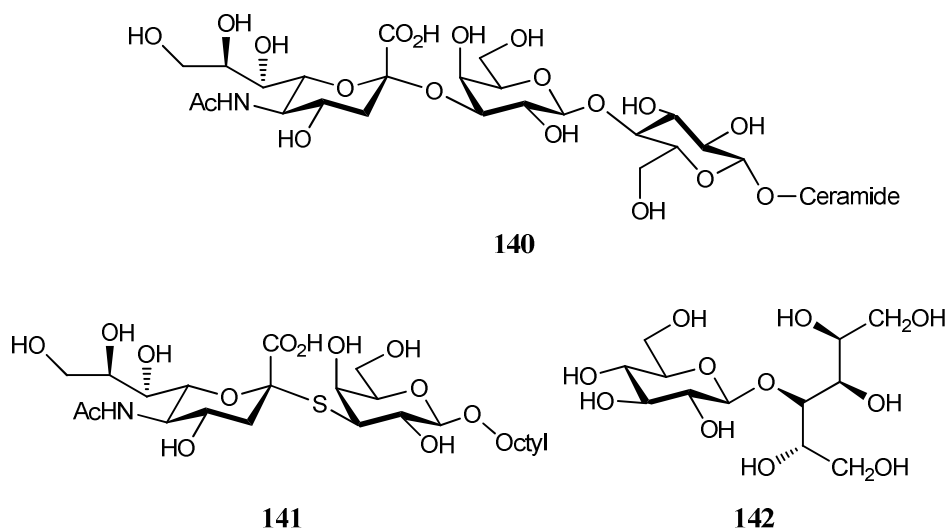


Figure 36 Structures of inhibitors towards the lactose binding site as well as both binding sites.²¹²

The GM3 ganglioside analogue (**140**) showed good inhibition (10 to 100 μM) whilst no inhibition was observed for the α -2,3-sialyl- β -thiogalactoside (**141**).^{218,219} Lactitol (**142**) on the other hand, was found to have an IC_{50} of 0.57mM.^{220,221}

Finally, 2,3-difluorosialic acids have also been investigated as mechanism-based inhibitors of TcTS (Figure 37).^{57,222}

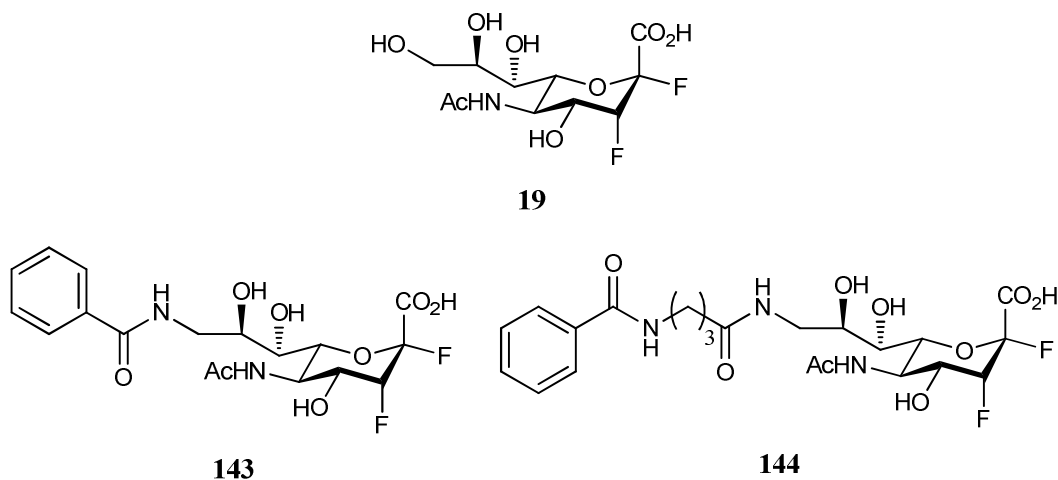


Figure 37 Structures of novel fluorinated inhibitors of *Trypanosoma cruzi* trans-sialidase.²²²

The 2,3-difluorosialic acid (**19**) has been shown to inhibit TcTS in a time dependent manner, forming a covalent bond with Tyr342, although high concentrations are necessary to achieve complete inactivation (K_i of 20 mM).⁵⁷ More recently, Buchini *et al* have shown the C-9 modified 2,3-difluorosialic acids (**143** - **144**) are inhibitors of TcTS, having a K_i/K_d of 2.9 and 3.2 $\text{min}^{-1}\text{mM}^{-1}$ respectively.²²² The compounds were observed to have an interaction between the aryl substituent at C-9 and the

lactose binding site residues (Trp312 and Tyr119), hampering the binding of lactose into the active site (Figure 38).²²²

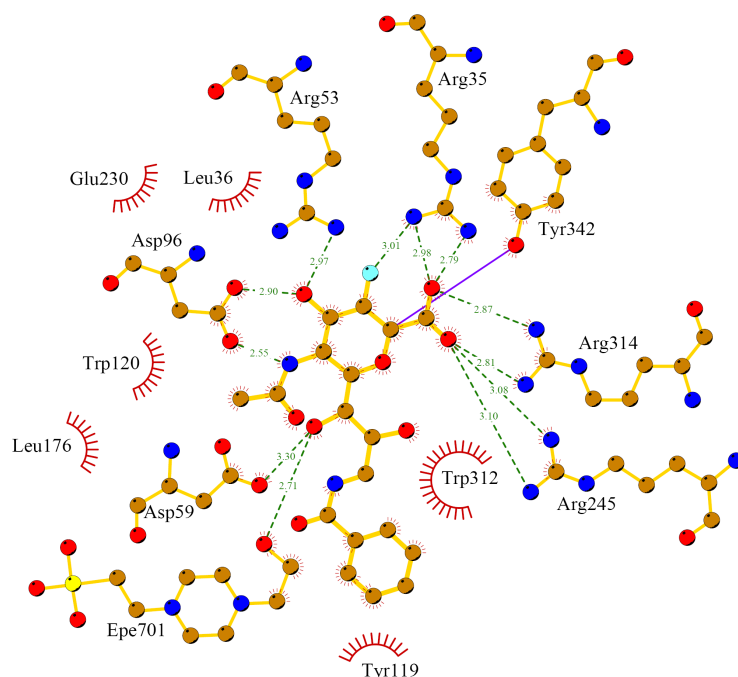
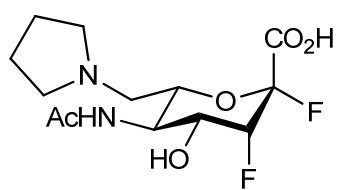


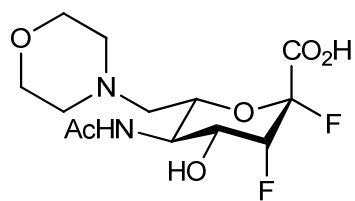
Figure 38 Representation of the interactions within the active site with the C-9 benzoylamide (**143**) and the amino acid residues. Generated with LigPlot⁺ (PDB 3B69).

8.7 Aims of the project

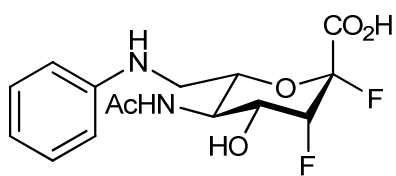
Considering the results observed by Buchini *et al*, where the introduction of a large group at C-9 of the sialic acid was found to inhibit *Trypanosoma cruzi* *trans*-sialidase by restricting the access of lactose to the active site, we set out to further probe this finding by developing a series of modifications at C-7 of 2,3-difluorosialic acid (**19**).²²² Several cyclic amines were introduced at C-7 (**145** - **147**) in order to probe the interaction between the amino acid residues Tyr119 and Trp312 with the cyclic amino substituents. It was anticipated that by introducing cyclic amines we could reduce the degrees of rotational freedom of the bonds, which may improve the binding of the compounds within the active site. In addition, an aromatic C-7 amine was developed (**147**) with the intention of possibly forming π - π interactions between the Tyr119, Trp312 and the aromatic substituent. The introduction of this series of amines was accomplished by employing the methodology developed previously (Chapter 3), and the synthesised compounds were tested against *Trypanosoma cruzi* *trans*-sialidase.



145



146

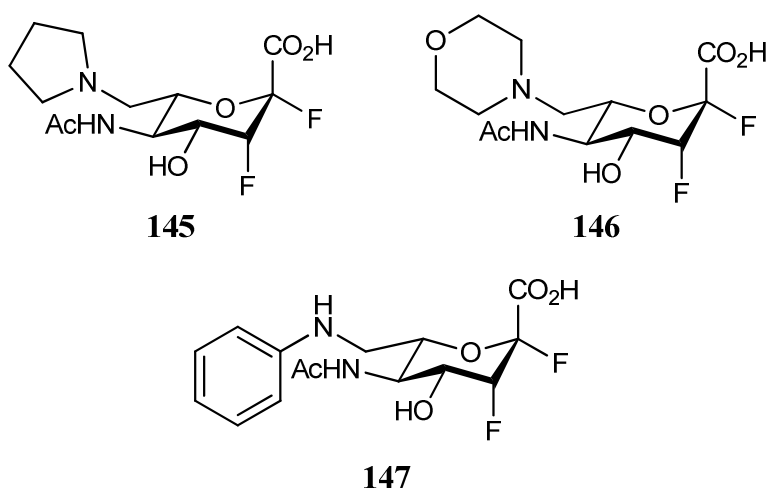


147

Chapter 9 – Synthesis of 7-*N*-alkylamino 2,3-difluorosialic acids and their biological evaluation against TcTS and trypomastigotes

9.1 Prelude

As described previously (Chapter 8) the 7-*N*-pyrrolidino (**145**), 7-*N*-morpholino (**146**) and 7-*N*-anilino-2,3-difluorosialic acid (**147**) were developed as inhibitors of *Trypanosoma cruzi* *trans*-sialidase.




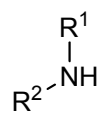
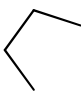
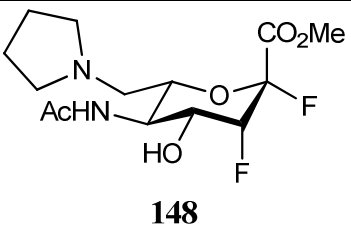
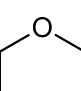
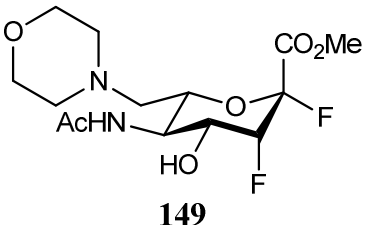
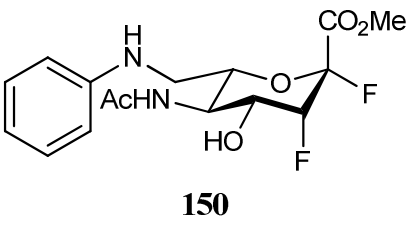
The 7-*N*-morpholino derivative (**146**) was developed to investigate the available space in the glycerol side chain binding pocket. In addition, the presence of the oxygen could prove advantageous to the binding of the compound with the potential formation of hydrogen bonds with neighbouring amino acid residues, such as Gly195. For the 7-*N,N*-diethylamino-2,3-difluorosialic acid (**39**) the ethyl groups have high degrees of rotational freedom; therefore, the introduction of a pyrrolidine group (**145**) would reduce the rotational freedom of the ethyl groups and the difference in binding affinity may be determined. Finally, the 7-*N*-anilino-2,3-difluorosialic acid (**147**) was developed in order to interact with the amino acid residues Tyr119 and Trp312 present at the lactose binding site. Buchini *et al* showed that the aromatic substituents at C-9 of 2,3-difluorosialic acid interact with the amino

acid residues present in the lactose binding site, preventing efficient binding in this case.²²²

The 7-*N*-pyrrolidino (**145**), 7-*N*-morpholino (**146**) and 7-*N*-anilino-2,3-difluorosialic acid (**147**) were all synthesised using the strategy developed (Chapter 3), by performing a oxidative cleavage followed by reductive amination on the 2,3-difluorosialic acid (**48**).

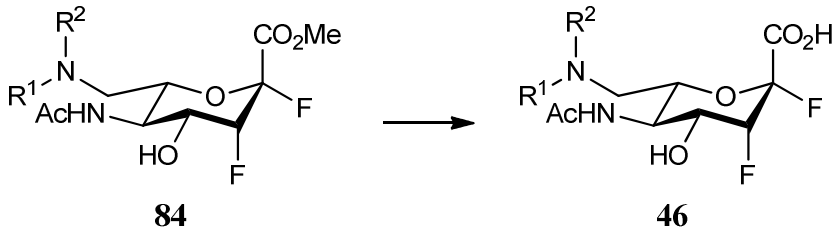
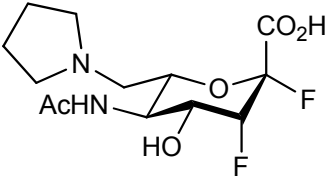
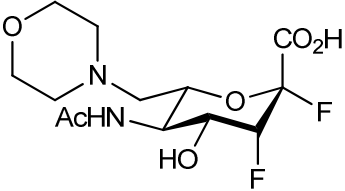
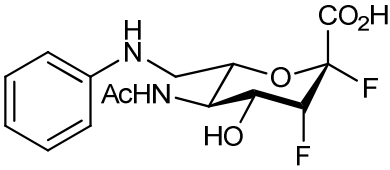
The 2,3-difluorosialic acid (**48**) was treated with an aqueous solution of sodium periodate (0.4 M) in water, and upon the completion of the reaction the solvent was removed *in vacuo* and the C-7 aldehyde (**47**) was used without further purification. The C-7 aldehyde (**47**) was then treated with the desired alkylamine in methanol, to afford a series of 7-*N*-alkylamine 2,3-difluorosialic acid (**84**) (Table 14).

Table 14 Yields of the different 7-*N*-alkylamines synthesised (**148** – **150**).

<div style="text-align: center;">  <p>48 84</p> <p>i) 0.4M NaIO₄, H₂O, r.t., 20 min; ii) R₁R₂NH, NaCNBH₃, MeOH, AcOH, r.t., O/N.</p> </div>			
Entry	Amine 	Product	Yield (%)
1	$R^1 = R^2 =$ 	 148	42
2	$R^1 = R^2 =$ 	 149	21
3	$R^1 = \text{Ph}$ $R^2 = \text{H}$	 150	22

The final step in order to achieve the desired 7-*N*-alkylamines 2,3-difluorosialic acids was the saponification of each of the methyl esters. This conversion proceeded smoothly by using a 1M sodium hydroxide solution in water to afford the final targets (**145** – **147**) in good yield (Table 15).

Table 15 Yields for the saponified final compounds (**145** - **147**).

<div style="text-align: center;">  <p>84 46</p> <p>1M NaOH, H₂O, 4 °C, 1h</p> </div>		
Entry	Product	Yield (%)
1	<div style="text-align: center;">  <p>145</p> </div>	Quantitative
2	<div style="text-align: center;">  <p>146</p> </div>	84
3	<div style="text-align: center;">  <p>147</p> </div>	60

9.2 IC₅₀ determination of the inhibitors (**145** – **147**)

The determination of the IC₅₀ of 7-*N*-pyrrolidino (**145**), 7-*N*-morpholino (**146**) and 7-*N*-anilino (**147**) derivatives was carried out using a ¹⁴C radiolabelled lactose. The enzyme activity was determined using purified TcTS and it was measured by the transfer of sialic acid from 1 mM sialyl- α -(2 \rightarrow 3)-lactose to 12 μ M [D-glucose-1-¹⁴C]lactose (55 mCi/mmol), in 30 μ L containing 0.5 ng of TcTS, 20 mM Hepes-Na (pH 7.5), 0.2% BSA and 30 mM NaCl. After 30 min at 25 °C the reaction was stopped by dilution with 1mL of water, QAE-Sephadex was added, and the resin washed twice with water. Negatively charged compounds were eluted with 0.8 mL of 1M NaCl and quantified in a WinSpectral 1414 liquid scintillation counter (Figure

39).²²³ The inhibition of the TcTS implies a lower transfer of sialic acid to the ^{14}C radio labelled lactose. The amount of ^{14}C radio labelled lactose was measured with a scintillation counter.

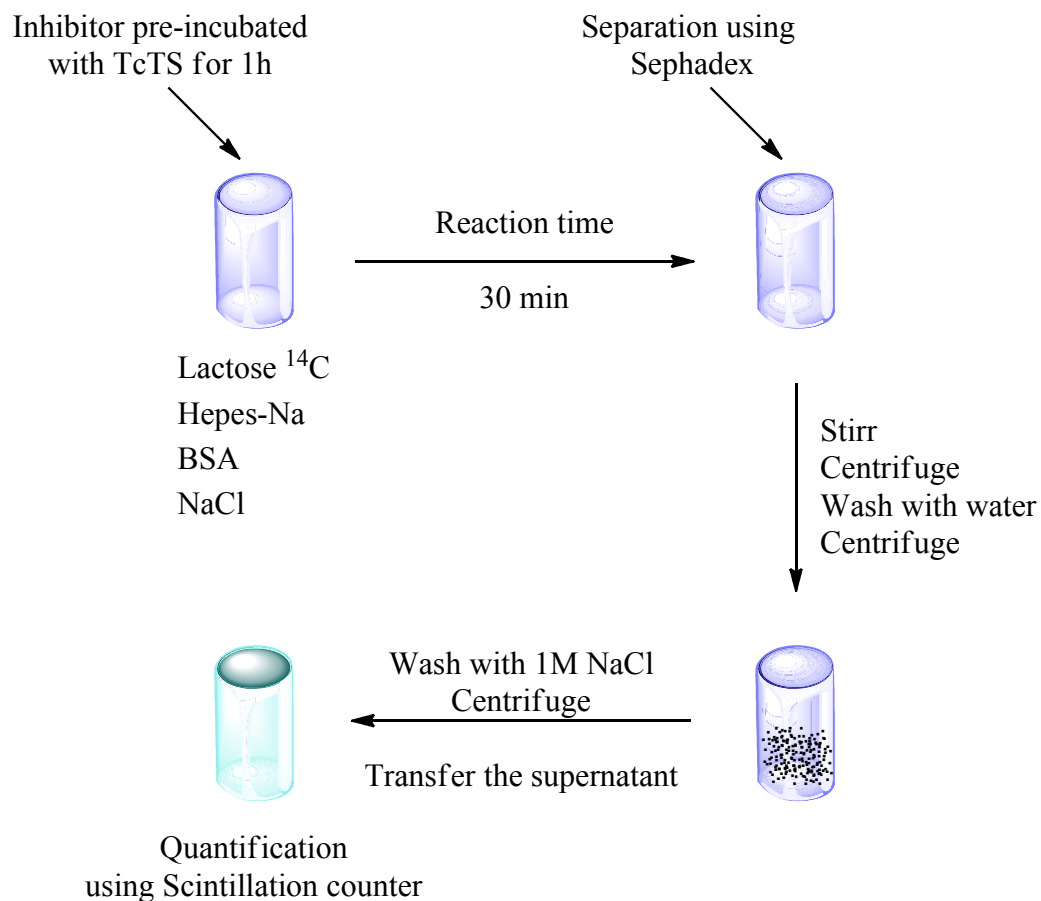
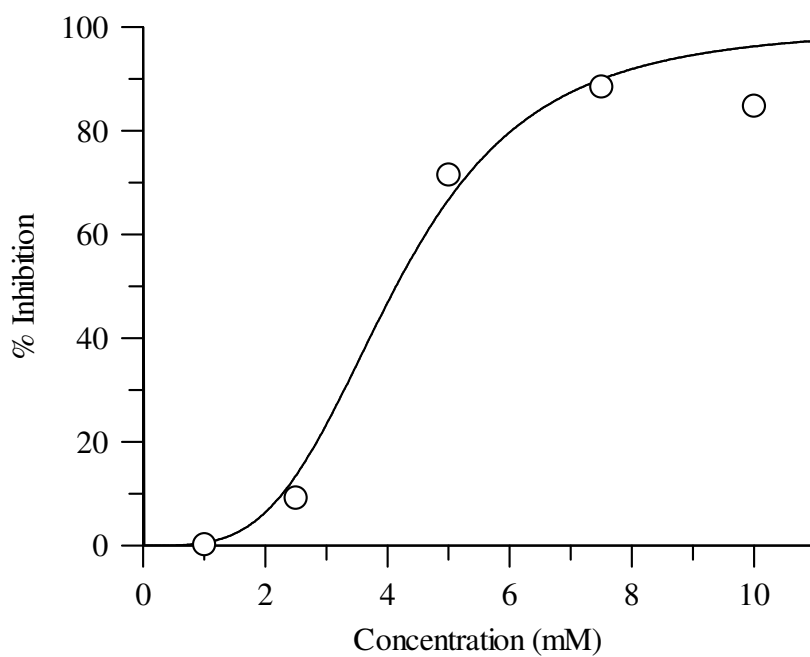
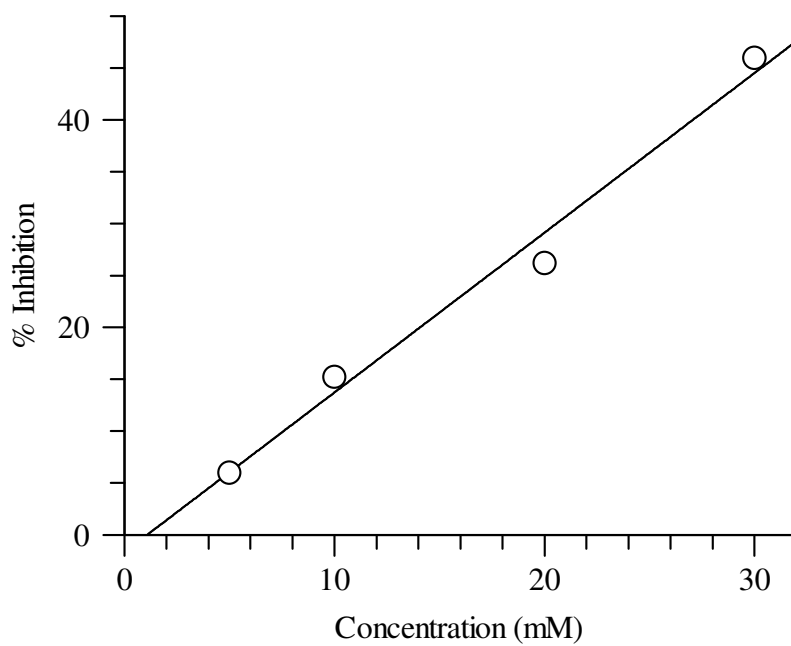


Figure 39 Illustration of the procedure for the determination of the IC_{50} .

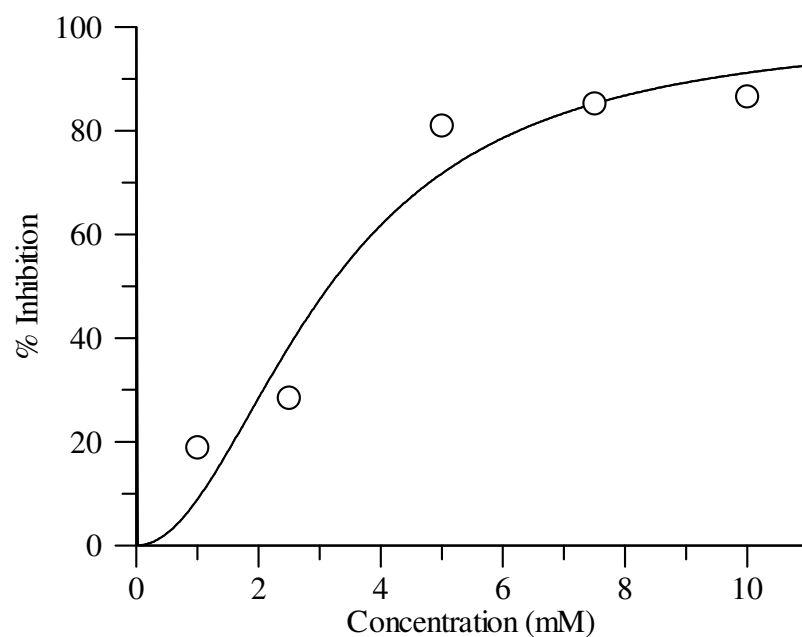
The reason for pre-incubation of the inhibitors with TcTS for 1h is to take into account the potential for slow binding behaviour of the inhibitors (akin to the behaviour observed with influenza neuraminidase). The inhibition data obtained for the 7-*N*-pyrrolidino- (**145**), 7-*N*-morpholino- (**146**) and 7-*N*-anilino-2,3-difluorosialic acid (**147**) is presented in the following graphs (Graph 3 - Graph 5).



Graph 3 IC₅₀ determination for inhibitor 7-*N*-pyrrolidino-2,3-difluorosialic acid (**145**).



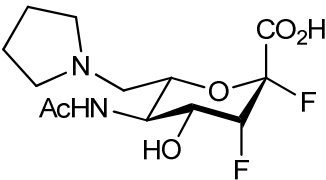
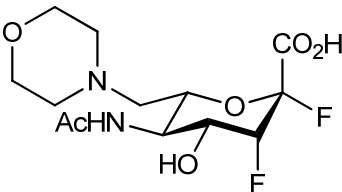
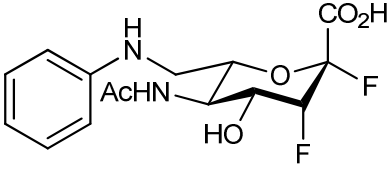
Graph 4 IC₅₀ determination for inhibitor 7-*N*-morpholino-2,3-difluorosialic acid (**146**).



Graph 5 IC_{50} determination for inhibitor 7-*N*-anilino-2,3-difluorosialic acid (**147**).

The IC_{50} values are present in Table 16.

Table 16 IC_{50} values for the inhibitors (**145** – **146**).

Compound	IC_{50} (mM)
 <p>145</p>	4.1
 <p>146</p>	35.5
 <p>147</p>	3.2

The IC_{50} obtained for the 7-*N*-pyrrolidino (**145**) and 7-*N*-anilino derivatives (**147**) are similar, 4.1 and 3.2 mM respectively. These two compounds could be interacting with the amino acid residues present in the lactose binding site, Tyr119 and Trp312, akin to the compounds synthesised by Buchini *et al.*²²² The 7-*N*-anilino derivative (**147**) could be involved in π - π interactions with the above mentioned amino acid residues, leading to a lower IC_{50} than the 7-*N*-pyrrolidino derivative (**145**).

The 7-*N*-morpholino derivative (**146**) showed an IC_{50} of 35.5 mM, which could be due to the fact that the inhibitor has a lower rate of association with the enzyme, requiring longer pre-incubation periods with TcTS.

The technique employed is prone to experimental errors, since a suspended resin with the labelled lactose is used, and when adding the resin it is difficult to ensure that the same amount of resin is being added. In addition, during the washing of the resin it is probable that some of the resin is lost. These types of errors will reduce the amount of ^{14}C radio labelled lactose present in solution.

9.3 Evaluation of the ability of the inhibitors to prevent the infection of cells by trypomastigotes

The *in vitro* inhibition of infectivity assay is based on the principle that if the inhibitors are effective they will halt the infection of host cells by the trypomastigotes.

Vero cells were inserted in a 24-well plate (10^4 cells/well) fitted with a sterile 12-mm-diameter glass cover slip in 500 μ L 10% FBS-MEM and used after 24h of growth (Stage I, Figure 40). Before infection, the medium was removed and the cells washed twice with PBS. Different concentrations of inhibitor were added followed by 0.2% BSA-MEM. Prior to incubation, trypomastigotes (100 parasites/cell) were added and the plate was examined under microscope to ensure that both cells and parasites were well, and that the introduction of the inhibitor did not produce secondary effects, such as death of the cells and/or parasites (Stage II, Figure 40). Once the inspection was complete, the plate was incubated for 20h, at a constant temperature of 37 °C under 5% CO_2 . The plate was re-examined before changing the

medium to ensure that both cells and parasites were alive after the incubation period and that the inhibitor was not cytotoxic.

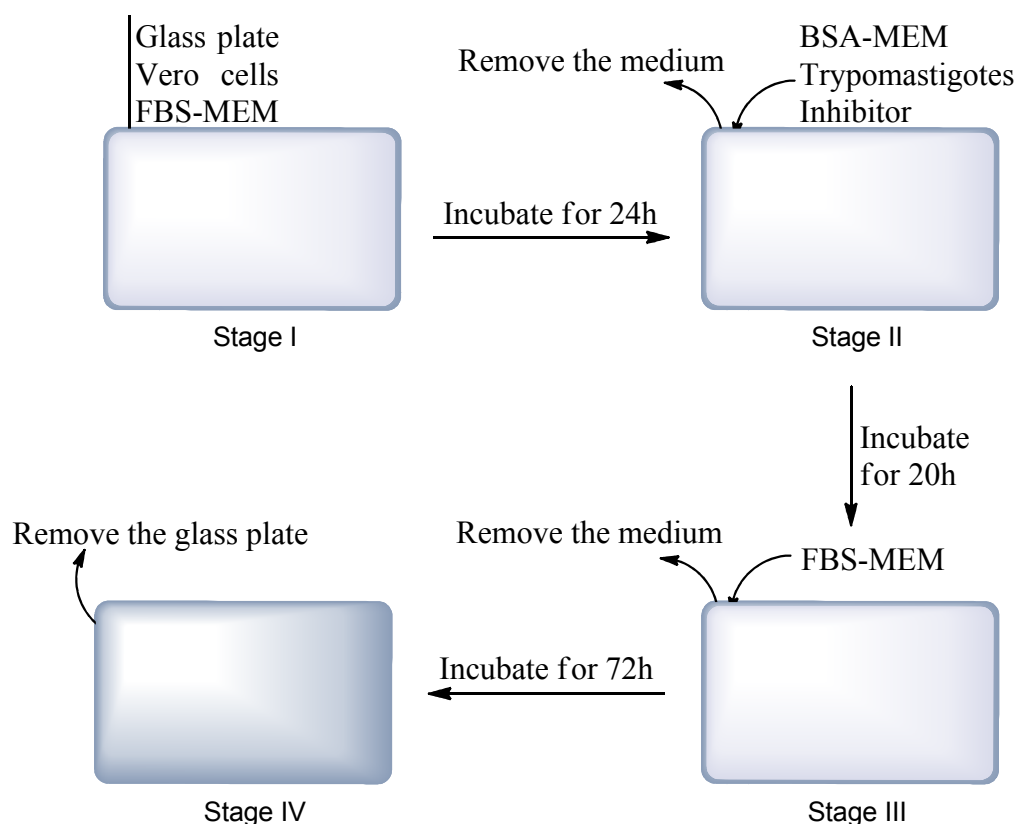


Figure 40 Illustration of the assay for the inhibition of trypanomastigotes assay, with the key steps shown.

After removing the parasites, the wells were washed with PBS and maintained with 3% FBS-MEM (Stage III, Figure 40). After the changing of the medium, the plate was examined again at the microscope to certify that the cells were not removed during the procedure. The plate was introduced again in the incubator for a final 72h incubation period. The cells should stick to the glass plate during the initial 20h; however, if any anomaly occurs during this period (*e.g.* the inhibitor proved toxic) the cells and parasite will die, hence not adhering to the glass plate. After 72h incubation, the medium was removed and the wells washed with PBS to remove any free particles (*e.g.* dead cells, some parasites that survived the previous wash) several times (Stage IV, Figure 40). After the washings, the glass plates were conditioned for visualisation by the addition of dyes, firstly may-Grünwald (250 μ L). It was left to stand for 5 min, after which water (250 μ L) was added and left to stand for a further 1 min. After removal of the liquid another dye, Giemsa (1/4 dilution with water,

600 μL) was added and left to stand for 5 min. The role of the dyes is to stain and fix the cells and amastigotes (present in the cytoplasm), and ultimately to close the cell membrane, making it impermeable. After this time the glass support was carefully removed, dipped in water to remove the excess of dye and dried (Stage IV, Figure 40). The plate supports were mounted with DPX mountant onto a glass support plate. The number of infected cells was counted (by eye) and the results expressed as the average of the percentage of infected cells in respect with the healthy ones.

When comparing both assays it is possible to see some deviation in the results, which could be related to experimental errors. A possible experimental error can occur during the processing of the data, since the data is obtained by visually counting the healthy cells *versus* the infected ones (Figure 41).

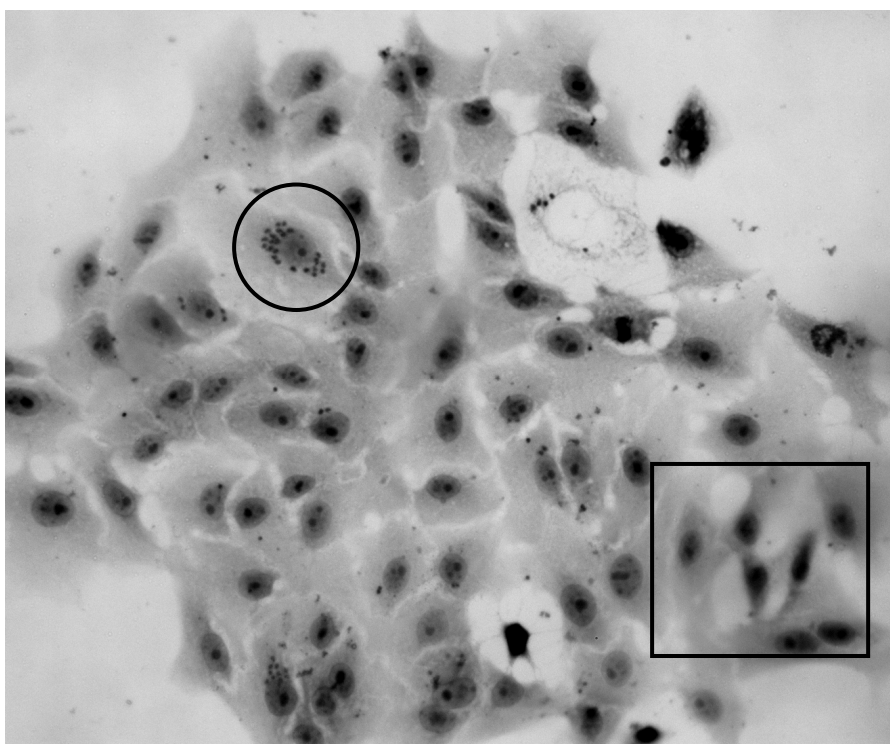
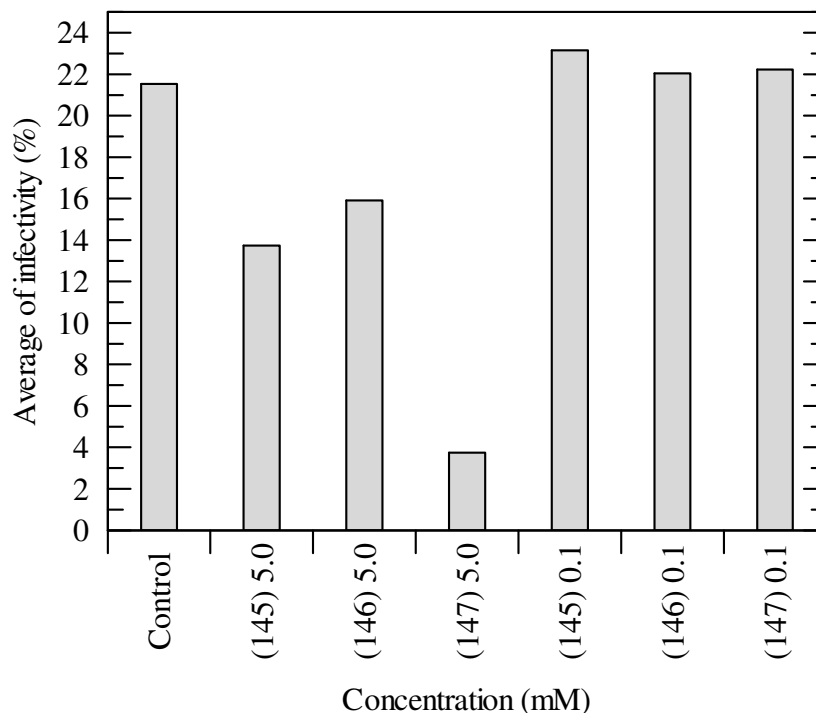


Figure 41 Example of an image from one of the experiments. The presence of infected cells (circle) and healthy cells (square) is evident. The dots inside the cells are amastigotes.

Sometimes the distinction of the cell membrane is complicated due to the high number of cells present; this can cause complications in establishing the correct number of cells present. One other problem could be the presence of impurities on the glass support arising from the washings of the dyes.

The infectivity assay was performed twice and the results for both assays are presented (Graph 6). The values presented are an average of the duplicates performed for each assays.



Graph 6 Rate of infection at different concentrations of the inhibitors (**145**) – (**147**). Infectivity is the ratio between infected and healthy cells.

At 0.1 mM the values of infection were similar to the ones observed in the control; therefore, none of the inhibitors showed any inhibitory activity (Graph 6). At 5 mM the 7-*N*-anilino derivative (**147**) showed a big reduction in the infection of cells by the trypomastigotes, unfortunately the cause for such reduction is linked with a possible toxicity of the compound, which could be seen by the reduced number of cells (and parasites) present in the wells when compared with the control. Although the small rate of infection is clearly very promising, it is important to consider the possible toxicity of the inhibitor when analysing the results. The 7-*N*-pyrrolidino (**145**) and 7-*N*-morpholino (**146**) derivatives at 5 mM showed a reduction in the total number of cells infected, although the number of cells observed was lower than the ones present in the control (Graph 6). At this concentration both compounds show a potentially inhibitory behaviour, with the levels of infection decreasing when compared with the control.

Chapter 10 - Conclusions

In Part Two of this thesis, the synthesis of several C-7 cyclic *N*-alkylamines (**145** - **147**) was achieved and the compounds tested against trypomastigotes and *Trypanosoma cruzi* *trans*-sialidase.

The 7-*N*-pyrrolidino and 7-*N*-anilino derivatives (**145** and **147**) showed IC₅₀ values of 4.1 and 3.5 mM whilst the 7-*N*-morpholino derivative (**146**) showed an IC₅₀ of 36 mM against TcTS. The 7-*N*-anilino derivative (**147**) appears to interact with the amino acid residues Tyr119 and Trp312 present in the lactose binding site. Unfortunately, upon testing *in vitro* the 7-*N*-anilino derivative (**147**) appeared to be cytotoxic at the concentration used (5 mM), killing the cells and parasites present. The 7-*N*-pyrrolidino (**145**) and the 7-*N*-morpholino (**146**) derivative showed poor levels of inhibition when used at a concentration of 5 mM.

The next step would be to develop a longer and bulkier aromatic side chain, in order to improve the interactions with the Tyr119 and Trp312. It might be also possible to develop a 7-*N*-anilino derivative that could be linked through a sialosidic bond to a modified lactose (*e.g.* removal of the C-3 hydroxyl of galactose). This compound may show increased binding affinity between the inhibitor and the *Trypanosoma cruzi* *trans*-sialidase with the advantage that the cleaved lactose could not be the acceptor for the sialic acid, but might interfere with the amino acids present at the lactose binding site.

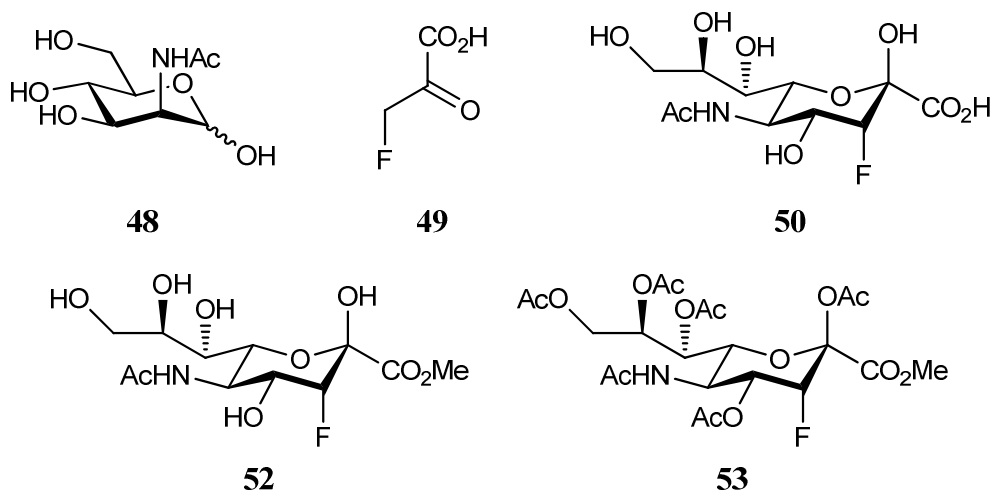
Chapter 11 - Experimental

11.1 General

Chemical reagents were purchased from Sigma-Aldrich unless otherwise stated. Anhydrous dichloromethane and tetrahydrofuran were obtained by distillation over calcium hydride or sodium/benzophenone, respectively. All other solvents were purchased from Fisher Scientific and used without further purification. Analytical thin layer chromatography (t.l.c.) was performed using silica gel 60 F₂₅₄ pre-coated on aluminium sheets (0.25 mm thickness) and reverse phase analytical tlc was performed with RP-18 F_{254s} pre-coated on aluminium sheets (0.27 mm thickness) purchased from Merck. Column chromatography was performed on silica gel 60 (35-70 micron) from Fisher Scientific. Melting points were recorded on a Reichert-Jung Kofler block apparatus and are uncorrected. Specific rotations were determined on an Optical Activity Ltd.: AA-10 automatic polarimeter. ¹H, ¹³C and ¹⁹F NMR were recorded using a Jeol Delta (270 MHz), Varian Mercury (400 MHz) or Bruker Avance III (400 and 500 MHz) spectrometers, with acquisition frequencies of 270, 400 or 500 for ¹H; 100 or 125 for ¹³C; and 376 or 470 for ¹⁹F. *J* values are given in Hz and δ in parts per million (ppm). All ¹H and ¹³C NMR assignments are corroborated by gCOSY, gHMBC, gHMQC, and DEPT experiments. Abbreviations for splitting patterns are as follows: br, broad; s, singlet; d, doublet; q, quartet; t, triplet; and m, multiplet.

High resolution mass spectrometry was performed using a Bruker MicrOTOFTM electrospray ionisation mass spectrometer. Standard work up means diluting the reaction residue in the appropriate organic solvent (mentioned), and washing with an aqueous saturated sodium bicarbonate solution followed by brine. The organic phases were then combined and dried over anhydrous sodium sulfate.

11.2 Synthesis



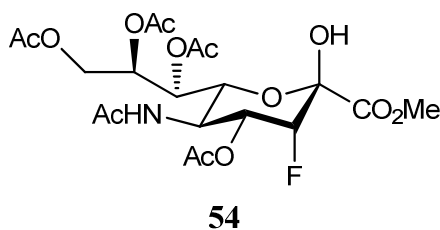
Methyl 5-*N*-acetamido-2,4,7,8,9-penta-*O*-acetyl-3,5-dideoxy-3-fluoro-D-erythro- α -L-manno-non-2-ulopyranosonate (**53**)

i) Neu5Ac aldolase (90.0 mg, 8 U/mg) was added to a solution of 3-fluoropyruvic acid (**49**) (1.50 g, 11.7 mmol) and *N*-acetyl-D-mannosamine monohydrate (**48**) (5.18 g, 23.4 mmol) in water (120 mL) and the mixture was left to stand at room temperature for 5 days. The reaction was followed using ^{19}F NMR by monitoring the disappearance of the signal from β -fluoropyruvic acid (**49**) at δ -233.3 ppm, and the formation of a signal corresponding to the 3-fluorosialic acid (**50**) at δ -208.3 ppm. The reaction mixture was purified by ion exchange chromatography (Dowex 1x2 200 ion exchange resin, formate form) eluting with 0 \rightarrow 1 M formic acid. Lyophilisation of the eluent gave 3-fluorosialic acid (**50**) as a colourless, hygroscopic solid which was used without further purification.

ii) Trifluoroacetic acid (2.20 mL, 28.7 mmol) was added to a solution of 3-fluorosialic acid (**50**) (3.15 g, 10.2 mmol) in methanol (110 mL) at 4 $^{\circ}\text{C}$ and the solution was left to warm to room temperature over night. The mixture was then concentrated *in vacuo* affording the 3-fluorosialic acid methyl ester (**52**) as a white solid (3.36 g) which was used without further purification.

iii) Acetic anhydride (24.6 mL, 260 mmol) was added to a solution of the crude methyl ester (**52**) (3.36 g, 10.4 mmol) in pyridine (90 mL) at 4 $^{\circ}\text{C}$ and the solution was stirred at room temperature for 4 days. The solution was then concentrated *in vacuo* and residual pyridine removed by azeotropic evaporation with toluene to give

a brown oil. The oil was subjected to a standard work up (EtOAc) and purified by flash chromatography (EtOAc:Hexane 9:1 \rightarrow EtOAc) to give the per-*O*-acetylated-3-fluorosialic acid (**53**) as a white solid (4.12 g, 72% over 3 steps). m.p. 193-196 °C (Lit. 194 °C)²²⁴. ¹H NMR (270 MHz, CDCl₃): δ 1.91 (s, 3H, NHC(O)CH₃); 2.03, 2.10, 2.16, 2.17 (4s, 12H, C(O)CH₃); 3.83 (s, 3H, OCH₃); 4.08 - 4.25 (m, 3H, H-5, H-6, 9); 4.55 (dd, 1H, $J_{8,9'} = 2.5$, $J_{9,9'} = 12.4$ Hz, H-9'); 4.92 (br dd, 1H, $J_{3,4} = 2.5$, $J_{3,F3} = 49.0$ Hz, H-3); 4.91 - 5.14 (m, 1H, H-8); 5.32 - 5.34 (m, 1H, H-7); 5.54 (ddd, 1H, $J_{4,F3} = 28.1$, $J_{4,5} = 11.0$ Hz, H-4). HRMS (ESI +ve) m/z 574.1509 [M+Na]⁺ (C₂₂H₃₀NFO₁₄Na requires 574.1548). Spectroscopic data were analogous to those reported in the literature.²²⁴

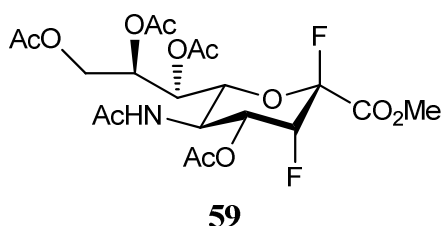
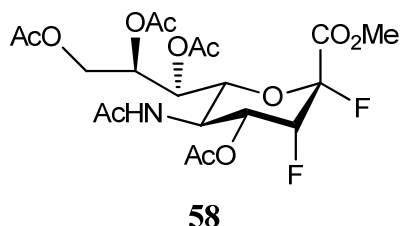


Methyl 5-*N*-acetamido-4,7,8,9-tetra-*O*-acetyl-3,5-dideoxy-3-fluoro-D-erythro- α -L-manno-non-2-ulopyranosonate (**54**)

A solution of hydrazine acetate (0.936 g, 10.4 mmol) in methanol (10 mL) was added to a solution of the per-acetylated 3-fluorosialic acid (**53**) (1.91 g, 3.46 mmol) in dichloromethane (40 mL) at 4 °C and the solution left to stand at this temperature (4h). The solution was then subjected to a standard work up (DCM) and the residue purified by flash chromatography (EtOAc:Hexane 9:1 \rightarrow EtOAc) to yield the hemiketal (**54**) as a white solid (1.43 g, 81%). ¹H NMR (270 MHz, CDCl₃): δ 1.90 (s, 3H, NHC(O)CH₃); 2.02, 2.07, 2.09, 2.15 (4s, 12H, C(O)CH₃); 3.84 (s, 3H, OCH₃); 4.08 (br dd, 1H, $J_{8,9} = 8.3$, $J_{9,9'} = 12.4$ Hz, H-9); 4.28 - 4.40 (m, 2H, H-5, H-6); 4.82 (t, 1H, $J_{8,9'} = 2.5$ Hz, H-9'); 4.94 (br dd, 1H, $J_{3,4} = 2.5$, $J_{3,F3} = 34.4$ Hz, H-3); 5.23 - 5.39 (m, 2H, H-7, H-8); 5.41 (br dd, 1H, $J_{4,F3} = 28.0$ Hz, H-4); 5.52 (br s, 1H, OH); 5.97 (d, 1H, $J_{5,NHAc} = 9.1$ Hz, NH). HRMS (ESI +ve) m/z 510.1612 [M+H]⁺ (C₂₀H₂₉NFO₁₃ requires 510.1623); 532.1435 [M+Na]⁺ (C₂₀H₂₈NFO₁₃Na requires 532.1442). Spectroscopic data were analogous to those reported in the literature.²²⁵

Methyl 5-*N*-acetamido-4,7,8,9-tetra-*O*-acetyl-2,3,5-trideoxy-2,3-difluoro-D-erythro- β -L-manno-non-2-ulopyranosonate (**58**)

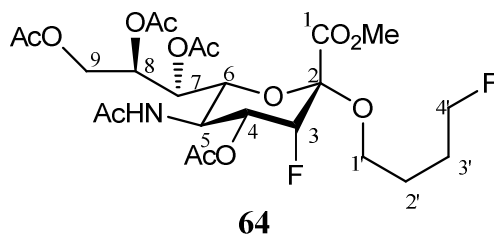
(Diethylamino)sulphur trifluoride (0.19 mL, 1.47 mmol) was added drop-wise to a stirred solution of the hemiketal (**54**) (500 mg, 0.98 mmol) in dichloromethane (20 mL) at -30 °C and the mixture held at this temperature (30 min). The reaction was quenched by the addition of methanol (0.5 mL) then subjected to a standard work up (DCM) and the residue purified by flash chromatography (EtOAc:Pet Ether 7:3 with 3 drops of TFA) to give the per-*O*-acetylated-2,3-difluorosialic acid (**58**) as a white solid (248 mg, 44%) plus the per-*O*-acetylated-2,3-difluorosialic acid (**59**) as a colourless oil (175 mg, 35%). Data for (**58**): ^1H NMR (400 MHz, CDCl_3): δ 1.91 (s, 3H, NHC(O)CH_3); 2.02, 2.09, 2.09, 2.14 (4s, 12H, C(O)CH_3); 3.88 (s, 3H, OCH_3); 4.06 - 4.18 (m, 2H, H-5, H-9); 4.29 - 4.34 (m, 2H, H-6, H-9'); 5.10 (br dt, 1H, $J_{3,4} = 2.7$, $J_{3,\text{F}2} = 5.1$, $J_{3,\text{F}3} = 53.2$ Hz, H-3); 5.28 (br d, 1H, $J_{7,8} = 8.2$ Hz, H-7); 5.35 (ddd, 1H, $J_{8,9} = 2.7$, $J_{8,9'} = 5.5$ Hz, H-8); 5.43 (br dd, 1H, $J_{4,5} = 10.6$, $J_{4,\text{F}3} = 25.0$ Hz, H-4); 5.61 (br d, 1H, $J_{5,\text{NHAc}} = 9.0$ Hz, NH); ^{19}F NMR (376 MHz, CDCl_3): δ -123.31 (br d, 1F, $J_{\text{F}2,\text{F}3} = 12.0$ Hz, F-2); -216.66 (ddd, 1F, $J_{\text{F}3,4} = 26.3$, $J_{\text{F}3,3} = 51.3$ Hz, F-3). HRMS (ESI +ve) m/z 512.1559 $[\text{M}+\text{H}]^+$ ($\text{C}_{20}\text{H}_{28}\text{NF}_2\text{O}_{12}$ requires 512.1580); 534.1375 $[\text{M}+\text{Na}]^+$ ($\text{C}_{20}\text{H}_{27}\text{NF}_2\text{O}_{12}\text{Na}$ requires 534.1375). Spectroscopic data were analogous to those reported in the literature.¹³⁷



Methyl 5-*N*-acetamido-4,7,8,9-tetra-*O*-acetyl-2,3,5-trideoxy-2,3-difluoro-D-erythro- α -L-manno-non-2-ulopyranosonate (**59**)

Deoxofluor[®] (0.2 mL, 0.5 mmol) was added drop-wise to a stirred solution of the hemiketal (**54**) (50.0 mg, 0.1 mmol) in dichloromethane (3 mL) at -30 °C and the mixture held at this temperature (30 min). The reaction was quenched by the addition of methanol (0.5 mL) then subjected to a standard work up (DCM) and the residue purified by flash chromatography (EtOAc:Hexane 9:1 \rightarrow EtOAc) to give the per-*O*-

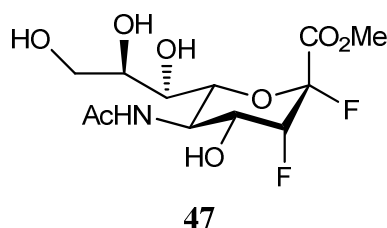
acetylated-2,3-difluorosialic acid (**59**) as a colourless oil (17.2 mg, 30%). ^1H NMR (400 MHz, CDCl_3): δ 1.90 (s, 3H, NHC(O)CH_3); 2.04, 2.06, 2.10, 2.14 (4s, 12H, C(O)CH_3); 3.87 (s, 3H, OCH_3); 4.11 (dd, 1H, $J_{8,9} = 6.3$, $J_{9,9'} = 12.5$ Hz, H-9); 4.31 (br d, 1H, $J_{5,6} = 11.3$ Hz, H-5); 4.44 (q, 1H, H-6); 4.50 (br dd, 1H, $J_{8,9'} = 2.7$ Hz, H-9'); 5.11 (br dd, 1H, $J_{3,4} = 2.0$, $J_{3,\text{F}3} = 50.5$ Hz, H-3); 5.26 (br dt, 1H, H-8); 5.32 - 5.42 (m, 1H, H-4); 5.40 (br dd, 1H, $J_{6,7} = 2.0$, $J_{7,8} = 6.5$ Hz, H-7); 5.47 (d, 1H, $J_{5,\text{NHAc}} = 9.8$ Hz, NH). ^{19}F NMR (376 MHz, CDCl_3): δ -122.19 (d, 1F, $J_{\text{F}2,\text{F}3} = 17.1$ Hz, F-2); -206.67 (ddd, 1F, $J_{\text{F}3,4} = 27.6$, $J_{\text{F}3,3} = 47.4$ Hz, F-3). HRMS (ESI +ve) m/z 512.1559 $[\text{M}+\text{H}]^+$ ($\text{C}_{20}\text{H}_{28}\text{NF}_2\text{O}_{12}$ requires 512.1580); 534.1375 $[\text{M}+\text{Na}]^+$ ($\text{C}_{20}\text{H}_{27}\text{NF}_2\text{O}_{12}\text{Na}$ requires 534.1375).



Methyl (4-fluorobutyl-5-*N*-acetamido-4,7,8,9-tetra-*O*-acetyl-3,5-dideoxy-3-fluoro-*D*-erythro- β -*L*-manno-non-2-ulopyranosid)onate (**64**)

(Diethylamino)sulphur trifluoride (20.0 μL , 0.15 mmol) was added drop-wise to a stirred solution of the hemiketal (**54**) (50 mg, 0.10 mmol) in tetrahydrofuran (2 mL) at -30°C and the mixture was held at this temperature (1h). The reaction was quenched by the addition of methanol (0.5 mL) and solvent removed *in vacuo*. The residue was then subjected to a standard work up (EtOAc) and purified by flash chromatography (EtOAc:Hexane 9:1 \rightarrow EtOAc) to afford the title sialoside (**64**) as a colourless oil (15.0 mg, 26%). ^1H NMR (400 MHz, CDCl_3): δ 1.60 – 1.68 (m, 2H, H-3', 3''); 1.89 (s, 3H, NHC(O)CH_3); 2.03, 2.08, 2.14, 2.15 (4s, 12H, C(O)CH_3); 3.30 - 3.44 (m, 4H, H-1', 1'', 2', 2''); 3.82 (s, 3H, OCH_3); 4.13 - 4.15 (m, 1H, H-9); 4.20 (br d, 1H, $J_{6,7} = 10.6$ Hz, H-6); 4.28 (br dd, 1H, $J_{8,9'} = 2.3$, $J_{9,9'} = 12.5$ Hz, H-9'); 4.39 (br t, 1H, $J_{4',4''} = 5.5$, $J_{4',\text{F}4'} = 11.7$ Hz, H-4'); 4.51 (br t, 1H, $J_{4'',\text{F}4'} = 12.1$ Hz, H-4''); 4.99 (br d, 1H, $J_{3,\text{F}3} = 51.3$ Hz, H-3); 5.08 – 5.17 (m, 1H, H-4); 5.26 – 5.31 (m, 2H, H-5, H-7); 5.43 (ddd, 1H, $J_{8,9} = 5.1$, $J_{7,8} = 8.2$ Hz, H-8). ^{13}C NMR (100 MHz, CDCl_3): δ 20.67, 20.74, 20.83, 21.08 (C(O)CH_3); 23.31 (NHC(O)CH_3); 45.30 (d, $J_{5,\text{F}3} = 3.8$ Hz, C-5); 53.00 (OCH_3); 62.20 (C-9); 65.44 (d, $J_{3',\text{F}4'} = 3.8$ Hz, C-3');

67.21 (C-7); 68.00 (C-8); 69.46 (d, $J_{4,F3} = 17.6$ Hz, C-4); 70.20 (d, $J_{2',F4'} = 23.8$ Hz, C-2'); 70.58 (d, $J_{1',F4'} = 7.7$ Hz, C-1'); 71.21 (C-6); 83.88 (dd, $J_{4',F3} = 25.3$, $J_{4',F4'} = 164.1$ Hz, C-4'); 87.47 (d, $J_{3,F3} = 194.0$ Hz, C-3); 97.95 (dd, $J_{2,F4'} = 8.4$, $J_{2,F3} = 16.9$ Hz, C-2); 166.07 (d, $J_{1,F3} = 3.1$ Hz, C-1); 169.92 (NHC(O)CH₃); 170.17, 170.57, 170.61 (C(O)CH₃). ¹⁹F NMR (376 MHz, CDCl₃): δ -215.85 (dt, 1F, $J_{F3,4} = 28.9$, $J_{F3,3} = 52.6$ Hz, F-3); -218.58 to -217.92 (m, 1F, F-4'). HRMS (ESI +ve) m/z 584.2196 [M+H]⁺ (C₂₄H₃₆NF₂O₁₃ requires 584.2155); 606.2022 [M+Na]⁺ (C₂₄H₃₅NF₂O₁₃Na requires 606.1974).

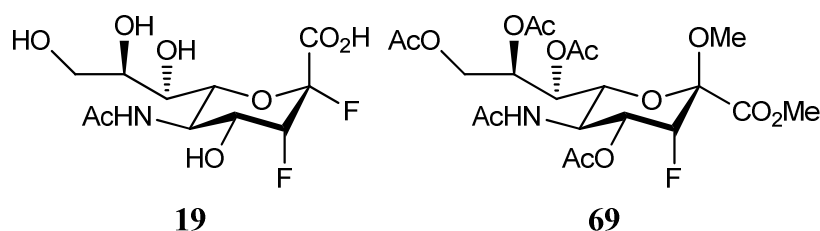


Methyl 5-*N*-acetamido-2,3,5-trideoxy-2,3-difluoro-D-erythro- β -L-manno-non-2-ulopyranosonate (**47**)

A solution of sodium methoxide in methanol (10.0 μ L, 0.5M) was added to a solution of the per-*O*-acetylated-2,3-difluorosialic acid (**58**) (355 mg, 0.69 mmol) in methanol (10 mL) at 4 °C and the solution left to stand overnight at room temperature. The solution was then neutralized (Dowex 50WX8, H⁺ form), filtered, then the filtrate concentrated *in vacuo* to afford the 2,3-difluorosialic acid (**47**) as a off-white solid (236 mg, quantitative). ¹H NMR (400 MHz, CDCl₃): δ 1.84 (s, 3H, NHC(O)CH₃); 3.21 (s, 3H, OCH₃); 3.32 (br d, 1H, $J_{7,8} = 9.0$ Hz, H-7); 3.46 – 3.52 (m, 2H, H-4, H-9); 3.62 – 3.68 (m, 3H, H-6, H-8, H-9'); 4.03 (br t, 1H, $J_{4,5} = 10.6$ Hz, H-5); 4.91 (d, 1H, $J_{3,F3} = 50.5$ Hz, H-3); 7.69 (d, 1H, $J_{5,NHAc} = 8.2$ Hz, NH). ¹³C NMR (100 MHz, CDCl₃): δ 21.97 (NHC(O)CH₃); 47.06 (d, $J_{5,F3} = 3.1$ Hz, C-5); 49.31 (OCH₃); 53.12 (C-6); 63.49 (C-9); 68.10 (C-7); 69.61 (C-8); 73.51 (d, $J_{4,F3} = 3.0$ Hz, C-4); 87.39 (dd, $J_{3,F2} = 17.6$, $J_{3,F3} = 188.6$ Hz, C-3); 104.97 (dd, $J_{2,F3} = 17.6$, $J_{2,F2} = 221.6$ Hz, C-2); 165.16 (dd, $J_{1,F3} = 4.6$, $J_{1,F2} = 34.5$ Hz, C-1); 173.90 (NHC(O)CH₃). ¹⁹F NMR (376 MHz, CDCl₃): δ -122.80 (d, 1F, $J_{F2,F3} = 11.5$ Hz, F-2); -219.76 (ddd, 1F, $J_{F3,4} = 27.4$, $J_{F3,3} = 50.4$ Hz, F-3). HRMS (ESI +ve) m/z 344.1151 [M+H]⁺ (C₁₂H₂₀F₂N₁O₈ requires 344.1157); 366.1809 [M+Na]⁺ (C₁₂H₁₉NF₂O₈ requires 366.0976).

5-*N*-Acetamido-2,3,5-trideoxy-2,3-difluoro-D-erythro- β -L-manno-non-2-ulopyranosonic acid (**19**)

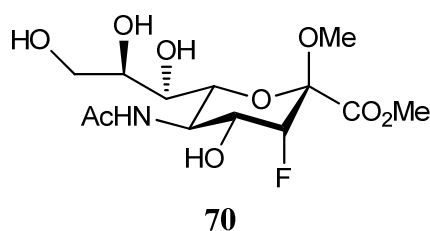
A 0.5 M aqueous solution of sodium hydroxide (4 drops) was added to a solution of 2,3-difluorosialic acid (**47**) (173 mg, 0.50 mmol) in water (3 mL) at 4 °C and the solution left to warm to room temperature (1h). The solution was then neutralized (Dowex 50WX8, H⁺ form), filtered, then the filtrate concentrated *in vacuo* to afford 2,3-difluorosialic acid (**19**) as a white solid (187 mg, quantitative). m.p. 21 - 25 °C. $[\alpha]_D -17$ (c 0.005 H₂O). ¹H NMR (400 MHz, D₂O): δ 1.85 (s, 3H, NHC(O)CH₃); 3.37 (br d, 1H, $J_{7,8} = 9.0$ Hz, H-7); 3.44 (br dd, 1H, $J_{8,9} = 6.7$, $J_{9,9'} = 12.5$ Hz, H-9); 3.60 (br d, 1H, $J_{5,6} = 10.6$ Hz, H-6); 3.65 – 3.71 (m, 2H, H-8, H-9'); 3.97 (br dd, 1H, $J_{4,5} = 10.9$, $J_{4,F3} = 26.0$ Hz, H-4); 4.09 (t, 1H, $J_{4,5} = 10.8$ Hz, H-5); 5.02 (br dt, 1H, $J_{3,4} = 2.7$, $J_{3,F3} = 51.6$ Hz, H-3). ¹³C NMR (100 MHz, CDCl₃): δ 21.14 (NHC(O)CH₃); 46.96 (d, $J_{5,F3} = 3.1$ Hz, C-5); 63.03 (C-9); 67.96 (C-7); 69.31 (br dd, $J_{4,F2} = 6.1$, $J_{4,F3} = 17.6$ Hz, C-4); 70.62 (C-8); 72.73 (d, $J_{6,F2} = 4.6$ Hz, C-6); 89.06 (dd, $J_{3,F2} = 18.4$, $J_{3,F3} = 184.0$ Hz, C-3); 106.77 (dd, $J_{2,F3} = 14.6$, $J_{2,F2} = 229.3$ Hz, C-2); 169.72 (d, $J_{1,F2} = 23.0$ Hz, C-1); 175.15 (NHC(O)CH₃). ¹⁹F NMR (376 MHz, CDCl₃): δ -121.38 (d, 1F, $J_{F2,F3} = 11.5$ Hz, F-2); -218.03 (ddd, 1F, $J_{F3,4} = 27.4$, $J_{F3,3} = 50.4$ Hz, F-3). $[\alpha]_D^{20} = -17.4$ (c 0.09, H₂O). HRMS (ESI -ve) m/z 328.1123 [M-H]⁻ (C₁₁H₁₆NF₂O₈ requires 328.0844). Spectroscopic data were analogous to those reported in the literature.¹³⁷



Methyl (methyl 5-*N*-acetamido-4,7,8,9-tetra-*O*-acetyl-3,5-dideoxy-3-fluoro-D-erythro- α -L-manno-non-2-ulopyranosid)onate (**69**)

Sodium hydride (25.0 mg, 1.03 mmol) was added to a solution of the hemiketal (**54**) (500.0 mg, 0.98 mmol) in dimethylformamide (10.0 mL) and the resulting solution was stirred for 15 min, after which methyl iodide (91.0 μ L, 1.47 mmol) was added

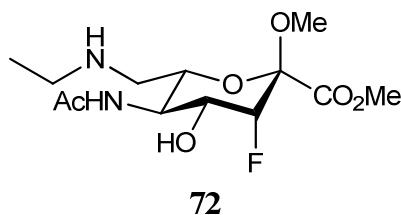
and the solution stirred for 2h at room temperature. The solution was concentrated *in vacuo* and subjected to a standard work up (EtOAc). The resultant residue was then loaded to a flash column (EtOAc:Pet Ether 9:1) affording the per-*O*-acetylated-3-fluorosialic acid methyl sialoside (**69**) as an off white solid (353 mg, 68%). ¹H NMR (400 MHz, CDCl₃): δ 1.88 (s, 3H, NHC(O)CH₃); 2.02, 2.07, 2.08, 2.15 (4s, 12H, C(O)CH₃); 3.29 (s, 3H, OCH₃); 3.85 (s, 3H, CO₂CH₃); 4.03 (dd, 1H, $J_{6,7} = 1.4$, $J_{5,6} = 10.3$ Hz, H-6); 4.15 (dd, 1H, $J_{8,9} = 7.5$, $J_{9,9'} = 12.2$ Hz, H-9); 4.35 (q, 1H, H-5); 4.84 – 5.01 (m, 2H, H-3, H-9'); 5.25 – 5.41 (m, 3H, H-4, H-7, H-8). ¹³C NMR (100 MHz, CDCl₃): δ 15.26, 20.67, 20.78, 21.00 (C(O)CH₃); 23.21 (NHC(O)CH₃); 45.25 (C-5); 51.56 (OCH₃); 53.07 (CO₂CH₃); 62.33 (C-9); 68.16 (C-7); 69.15 (d, $J_{4,F3} = 16.9$ Hz, C-4); 71.34 (C-6); 71.77 (C-8); 87.32 (d, $J_{3,F3} = 183.3$ Hz, C-3); 98.73 (d, $J_{2,F3} = 27.6$ Hz, C-2); 165.23 (C-1); 170.03 (NHC(O)CH₃); 170.39, 170.60, 170.68, 170.77 (C(O)CH₃). ¹⁹F NMR (376 MHz, CDCl₃): δ -205.99 (dd, 1F, $J_{F3,4} = 29.0$, $J_{F3,3} = 48.8$ Hz, F-3). HRMS (ESI +ve) m/z 524.1755 [M+H]⁺ (C₂₁H₃₁NFO₁₃ requires 524.1779); 546.1578 [M+Na]⁺ (C₂₁H₃₀NFO₁₃Na requires 546.1599).



Methyl (methyl 5-*N*-acetamido-3,5-dideoxy-3-fluoro-*D*-erythro- α -*L*-manno-non-2-ulopyranosid)onate (**70**)

A solution of sodium methoxide in methanol (10.0 μ L, 0.5M) was added to a solution of per-*O*-acetylated-3-fluorosialic acid methyl sialoside (**69**) (46.0 mg, 0.09 mmol) in methanol (1 mL) at 4 °C and the solution stirred overnight at room temperature. The solution was then neutralized (Dowex 50WX8, H⁺ form), filtered and the filtrate concentrated *in vacuo* to afford the 3-fluorosialic acid methyl sialoside (**70**) as a off-white solid (31.0 mg, quantitative). ¹H NMR (400 MHz, D₂O): δ 1.96 (s, 3H, NHC(O)CH₃); 3.23 (s, 3H, OCH₃); 3.52 (d, 1H, $J_{7,8} = 9.8$ Hz, H-7); 3.60 (dd, 1H, $J_{8,9} = 5.7$, $J_{9,9'} = 12.1$ Hz, H-9); 3.75 – 3.82 (m, 2H, H-8, 9'); 3.83 (s, 3H, CO₂CH₃); 3.87 (d, 1H, $J_{5,6} = 10.6$ Hz, H-6); 4.03 (br ddd, 1H, $J_{3,4} = 2.7$, $J_{4,5} = 11.0$, $J_{4,F3} = 30.5$ Hz, H-4); 4.17 (t, 1H, H-5); 4.89 (br dd, 1H, $J_{3,F3} = 48.9$ Hz, H-3).

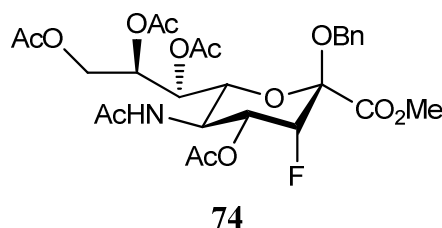
^{13}C NMR (100 MHz, D_2O): δ 22.04 (NHC(O)CH_3); 47.03 (C-5); 51.19 (OCH_3); 53.84 (CO_2CH_3); 63.30 (C-9); 67.67 (d, $J_{4,\text{F}3} = 17.6$ Hz, C-4); 67.81 (C-7); 69.84 (C-8); 70.51 (C-6); 89.48 (d, $J_{3,\text{F}3} = 177.1$ Hz, C-3); 98.78 (d, $J_{2,\text{F}3} = 26.8$ Hz, C-2); 168.37 (C-1); 174.88 (NHC(O)CH_3). ^{19}F NMR (376 MHz, D_2O): δ -208.86 (dd, 1F, $J_{\text{F}3,4} = 30.5$, $J_{\text{F}3,3} = 48.8$ Hz, F-3). HRMS (ESI +ve) m/z 356.1320 $[\text{M}+\text{H}]^+$ ($\text{C}_{27}\text{H}_{35}\text{NFO}_{13}$ requires 356.1357).



Methyl (methyl-5-*N*-acetamido-3,5,7-trideoxy-7-*N*-ethylamine-3-fluoro- α -L-mannohept-2-ulopyranosid)onate (**72**)

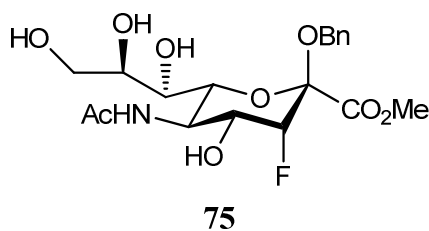
i) A 0.4 M aqueous solution of sodium periodate (0.5 mL) was added to a solution of 3-fluorosialic acid methyl sialoside (**70**) (31 mg, 0.09 mmol) in water (0.5 mL) at room temperature and the resulting solution was stirred for 30 min. The mixture was then evaporated *in vacuo* and the aldehyde (**71**) formed was used without further purification.

ii) A solution of aqueous ethylamine 70% (0.11 mL, 2.0 mmol) in methanol (0.5 mL) was acidified to pH 5 with glacial acetic acid, and this solution then added to a solution of the crude mixture (above) in methanol (0.5 mL). The mixture was left to equilibrate for 1h at room temperature and then sodium cyanoborohydride (57 mg, 0.9 mmol) dissolved in methanol (0.5 mL) was added to the reaction. The mixture was stirred overnight. The reaction mixture was then adsorbed in silica, concentrated *in vacuo* and the residue purified by flash chromatography (EtOAc \rightarrow EtOAc:MeOH 9:1) to give the 3-fluorosialic acid methyl sialoside (**72**) as a colourless oil (3 mg, 10% over two steps). ^1H NMR (270 MHz, CD_3OD): δ 1.29 (t, 3H, $J = 7.4$ Hz, NHCH_2CH_3); 1.97 (s, 3H, NHC(O)CH_3); 3.25 – 3.66 (m, 7H, H-4, H-5, H-6, H-7, H-7', NHCH_2CH_3); 3.59 (s, 3H, OCH_3); 3.86 (s, 3H, CO_2CH_3); 4.87 (br dd, 1H, $J_{3,4} = 2.2$, $J_{3,\text{F}3} = 49.0$ Hz, H-3). HRMS (ESI +ve) m/z 323.1618 $[\text{M}+\text{H}]^+$ ($\text{C}_{13}\text{H}_{24}\text{N}_2\text{FO}_6$ requires 323.1618).



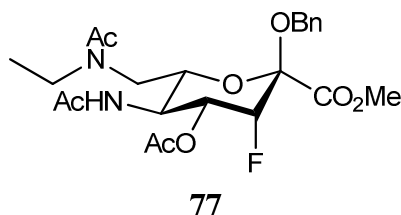
Methyl (benzyl-5-*N*-acetamido-4,7,8,9-tetra-*O*-acetyl-3,5-dideoxy-3-fluoro-D-erythro- α -L-manno-non-2-ulopyranosid)onate (**74**)

Sodium hydride (113 mg, 4.71 mmol) was added to a solution of the of the hemiketal (**54**) (2.00 g, 3.93 mmol) in dimethylformamide (10.0 mL) and the resulting solution was stirred for 15 min, after which benzyl bromide (0.56 mL, 4.71 mmol) was added and the solution stirred for 2h at room temperature. The reaction was then quenched with methanol (5 mL), concentrated *in vacuo* and subjected to a standard work up (EtOAc). The resultant residue was then purified by flash chromatography (EtOAc:Pet ether 9:1 \rightarrow EtOAc) affording the benzyl sialoside (**74**) as an off-white solid (2.08 g, 95%). ^1H NMR (400 MHz, CDCl_3): δ 1.88 (s, 3H, $\text{NH}(\text{O})\text{CH}_3$); 1.96, 2.04, 2.08, 2.16 (4s, 12 H, $\text{C}(\text{O})\text{CH}_3$); 3.73 (s, 3H, OCH_3); 4.10 (br dd, 1H, $J_{6,7} = 1.6$, $J_{5,6} = 10.9$ Hz, H-6); 4.15 (dd, 1H, $J_{8,9} = 7.8$, $J_{9,9'} = 10.9$ Hz, H-9); 4.37 (q, 1H, $J_{5,\text{NHAc}} = 10.6$ Hz, H-5); 4.46 (d, 1H, $J = 11.7$ Hz, OCH_2Ph); 4.65 (d, 1H, OCH_2Ph); 4.91 (dd, 1H, $J_{8,9'} = 2.7$ Hz, H-9'); 5.05 (dd, 1H, $J_{3,4} = 2.3$, $J_{3,\text{F}3} = 49.3$ Hz, H-3); 5.22 (d, 1H, NH); 5.31 – 5.46 (m, 3H, H-4, H-7, H-8); 7.26 – 7.39 (m, 5H, Ph). ^{13}C NMR (100 MHz, CDCl_3): δ 20.68, 20.79, 20.81, 20.87 ($\text{C}(\text{O})\text{CH}_3$); 23.21 ($\text{NHC}(\text{O})\text{CH}_3$); 45.34 (d, $J_{5,\text{F}3} = 2.3$ Hz, C-5); 52.98 (OCH_3); 62.36 (C-9); 66.17 (OCH_2Ph); 68.19 (C-7); 69.21 (d, $J_{4,\text{F}3} = 17.6$ Hz, C-4); 71.53 (C-6); 71.60 (C-8); 87.40 (d, $J_{3,\text{F}3} = 184.0$ Hz, C-3); 98.22 (d, $J_{2,\text{F}3} = 26.8$ Hz, C-2); 127.67 (C Ph); 128.28 (C Ph); 128.59 (C Ph); 135.63 (Cq Ph); 165.27 (C-1); 170.00 ($\text{NHC}(\text{O})\text{CH}_3$); 170.38, 170.59, 170.66, 170.73 ($\text{C}(\text{O})\text{CH}_3$). ^{19}F NMR (376 MHz, CDCl_3): δ -205.84 (dd, 1F, $J_{\text{F}3,4} = 29.0$, $J_{\text{F}3,3} = 48.8$ Hz, F-3). HRMS (ESI +ve) m/z 600.2061 $[\text{M}+\text{H}]^+$ ($\text{C}_{27}\text{H}_{35}\text{NFO}_{13}$ requires 600.2092); 622.1869 $[\text{M}+\text{Na}]^+$ ($\text{C}_{27}\text{H}_{34}\text{NFO}_{13}\text{Na}$ requires 622.1912).



Methyl (benzyl-5-*N*-acetamido-3,5-dideoxy-3-fluoro-*D*-erythro- α -*L*-manno-non-2-ulopyranosid)onate (**75**)

Sodium methoxide (180 μ L) was added to a solution of the per-*O*-acetylated-3-fluorosialic acid benzyl sialoside (**74**) (787 mg, 1.31 mmol) in methanol (18 mL) at 4 °C and the mixture left to warm to room temperature (1h). The mixture was then neutralized (Dowex 50 WX8 H⁺ form), filtered and concentrated *in vacuo*. The resultant oil was then dissolved in warm methanol to give 3-fluorosialic acid benzyl sialoside (**75**) as white crystals (533 mg, 95%). ¹H NMR (400 MHz, D₂O): δ 1.96 (s, 3H, NHC(O)CH₃); 3.58 (d, 1H, $J_{7,8}$ = 9.8 Hz, H-7); 3.62 (dd, 1H, $J_{8,9}$ = 5.5, $J_{9,9'}$ = 12.1 Hz, H-9); 3.74 (s, 3H, OCH₃); 3.77 – 3.81 (m, 1H, H-9'); 3.89 – 3.92 (m, 1H, H-8); 4.00 – 4.11 (m, 2H, H-4, H-6); 4.19 (t, 1H, $J_{4,5}$ = 10.6 Hz, H-5); 4.30 (dd, 1H, J = 11.0 Hz, OCH₂Ph); 4.71 (d, 1H, OCH₂Ph); 4.91 (dd, 1H, $J_{3,4}$ = 2.3, $J_{3,F3}$ = 50.5 Hz, H-3); 7.32 – 7.36 (m, 5H, CH Ph). ¹³C NMR (100 MHz, CDCl₃): δ 22.06 (NHC(O)CH₃); 47.11 (d, $J_{5,F3}$ = 1.5 Hz, C-5); 53.77 (OCH₃); 63.32 (C-9); 65.99 (OCH₂Ph); 67.49 (C-7); 67.68 (d, $J_{4,F3}$ = 2.3 Hz, C-4); 69.88 (C-8); 70.75 (C-6); 89.60 (d, $J_{3,F3}$ = 177.9 Hz, C-3); 98.10 (d, $J_{2,F3}$ = 27.6 Hz, C-2); 128.80 (*m*-, *o*-, *p*-C Ph); 135.42 (Cq Ph); 168.41 (C-1); 174.93 (NHC(O)CH₃). ¹⁹F NMR (376 MHz, CDCl₃): δ -209.06 (dd, 1F, $J_{F3,4}$ = 30.5, $J_{F3,3}$ = 48.8 Hz, F-3). HRMS (ESI +ve) *m/z* 432.1644 [M+H]⁺ (C₁₉H₂₇NFO₉ requires 432.1670); 454.1458 [M+Na]⁺ (C₁₉H₂₆NFO₉Na requires 454.1489).



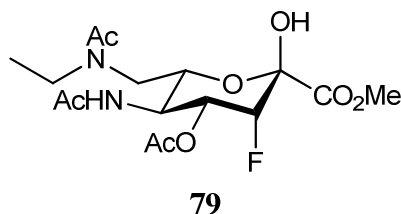
Methyl (benzyl-5-*N*-acetamido-4-*O*-acetyl-3,5,7-trideoxy-7-*N*-ethylacetamido-3-fluoro- α -*L*-manno-hept-2-ulopyranosid)onate (**77**)

i) A 0.4 M aqueous solution of sodium periodate (6.50 mL) was added to a solution of 3-fluorosialic acid benzyl sialoside (**75**) (533 mg, 1.24 mmol) in water (6.5 mL) at room temperature and the resulting solution was stirred for 30 min. The mixture was then evaporated *in vacuo* and the aldehyde (**76**) formed was used without further purification.

ii) A solution of aqueous ethylamine 70% (1.50 mL, 26.5 mmol) in methanol (4 mL) was acidified to pH 5 with glacial acetic acid, and this solution then added to a solution of the crude mixture (above) in methanol (4 mL). The mixture was left to equilibrate for 1h at room temperature and then sodium cyanoborohydride (777 mg, 12.36 mmol) dissolved in methanol (4 mL) was added to the reaction. The mixture was stirred overnight. The reaction mixture was then adsorbed in silica, concentrated *in vacuo* and the residue purified by flash chromatography (EtOAc → EtOAc/MeOH 9:1).

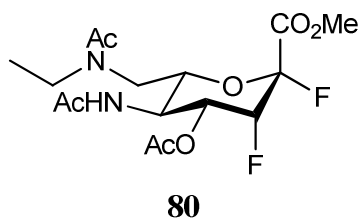
iii) Acetic anhydride (1.27 mL, 13.4 mmol) was added to the purified residue in pyridine (11 mL) at room temperature and the solution was left stirring overnight at room temperature. The solution was then concentrated *in vacuo*, and residual pyridine removed by azeotropic evaporation with toluene to give a yellow oil. The oil was subjected to a standard work up (EtOAc) and purified by flash chromatography (EtOAc:Hexane 9:1 → EtOAc) to give the acetylated-3-fluorosialic acid benzyl sialoside (**77**) as a white solid (215 mg, 36% over three steps). ¹H NMR (400 MHz, CDCl₃): δ 1.24 (t, 3H, *J* = 7.4 Hz, CH₃(O)CNCH₂CH₃); 1.95 (s, 3H, NHC(O)CH₃); 2.07 (s, 3H, CH₃(O)CNCH₂CH₃); 2.09 (s, 3H, C(O)CH₃); 3.14 (dd, 1H, *J* = 7.4, *J* = 14.1 Hz, CH₃(O)CNCH₂CH₃); 3.44 – 3.67 (m, 2H, H-7, H-7'); 3.74 (s, 3H, OCH₃); 3.95 (d, 1H, *J* = 14.1 Hz, CH₃(O)CNCH₂CH₃); 4.07 – 4.13 (m, 1H, H-6); 4.18 – 4.23 (m, 1H, H-5); 4.25 (d, 1H, *J* = 11.0 Hz, OCH₂Ph); 4.42 (d, 1H, OCH₂Ph); 4.98 (br dd, 1H, *J*_{3,4} = 2.3, *J*_{3,F3} = 49.5 Hz, H-3); 5.33 (ddd, 1H, *J*_{4,5} = 10.6, *J*_{4,F3} = 29.0 Hz, H-4); 6.06 (d, 1H, *J*_{5,NHAc} = 9.0 Hz, NH); 7.28 – 7.36 (m, 5H, CH Ph). ¹³C NMR (100 MHz, CDCl₃): δ 13.92 (CH₃(O)CNCH₂CH₃); 20.74 (C(O)CH₃); 21.23 (CH₃(O)CNCH₂CH₃); 23.31 (NHC(O)CH₃); 45.79 (C-7); 47.60 (CH₃(O)CNCH₂CH₃); 47.69 (C-5); 52.86 (OCH₃); 65.96 (OCH₂Ph); 69.30 (d, *J*_{4,F3} = 17.3 Hz, C-4); 72.21 (C-6); 87.60 (d, *J*_{3,F3} = 181.7 Hz, C-3); 97.83 (d, *J*_{2,F3} = 27.6 Hz, C-2); 128.28 (C Ph); 128.42 (C Ph); 128.58 (C Ph); 135.38 (Cq Ph); 165.87 (C-1); 170.74 (NHC(O)CH₃); 170.77 (CH₃(O)CNCH₂CH₃); 170.84

(C(O)CH₃). ¹⁹F NMR (376 MHz, CDCl₃): δ -205.98 (dd, 1F, $J_{F3,4} = 29.0$, $J_{F3,3} = 48.8$ Hz, F-3). HRMS (ESI +ve) m/z 483.2134 [M+H]⁺ (C₂₃H₃₂N₂FO₈ requires 483.2143); 505.1954 [M+Na]⁺ (C₂₃H₃₁N₂FO₈Na requires 505.1962).



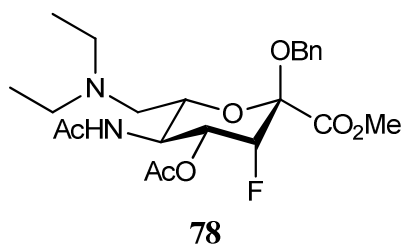
Methyl 5-*N*-acetamido-4-*O*-acetyl-3,5,7-trideoxy-7-*N*-ethylacetamido-3-fluoro- α -L-manno-hepta-2-pyranosonate (**79**)

Glacial acetic acid was added to a solution of acetylated-3-fluorosialic acid benzyl sialoside (**77**) (100 mg, 0.21 mmol) in tetrahydrofuran (10 mL) until pH 4 and then palladium on charcoal (30.0 mg, 10 wt. %) was added to the reaction and the reaction was put under a hydrogen gas atmosphere (10 days). The mixture was filtered through Celite[®], washed with methanol and the filtrate concentrated *in vacuo*. The residue was purified by flash chromatography (EtOAc → EtOAc:MeOH 9:1) to afford the hemiketal (**79**) as a white solid (39.4 mg, 48%). ¹H NMR (400 MHz, CDCl₃): δ 1.18 (t, 3H, $J = 7.4$ Hz, CH₃(O)CNCH₂CH₃); 1.99 (s, 3H, NHC(O)CH₃); 2.06 (s, 3H, CH₃(O)CNCH₂CH₃); 2.10 (s, 3H, C(O)CH₃); 3.08 (dd, 1H, $J = 7.4$, $J = 14.1$ Hz, CH₃(O)CNCH₂CH₃); 3.35 – 3.65 (m, 3H, H-5, H-7, H-7'); 3.83 (s, 3H, OCH₃); 3.90 (d, 1H, $J = 14.1$ Hz, CH₃(O)CNCH₂CH₃); 4.22 – 4.28 (m, 1H, H-6); 4.94 (br dd, 1H, $J_{3,4} = 2.3$, $J_{3,F3} = 50.1$ Hz, H-3); 5.35 – 5.44 (m, 1H, H-4); 6.50 (d, 1H, $J_{5,NHAc} = 8.6$ Hz, NH). ¹³C NMR (100 MHz, CDCl₃): δ 13.64 (CH₃(O)CNCH₂CH₃); 20.79 (NHC(O)CH₃); 21.04 (CH₃(O)CNCH₂CH₃); 23.18 (C(O)CH₃); 46.18 (C-7); 47.61 (C-5); 48.25 (CH₃(O)CNCH₂CH₃); 53.10 (OCH₃); 69.53 (d, $J_{4,F3} = 17.6$ Hz, C-4); 71.24 (C-6); 87.32 (d, $J_{3,F3} = 184.8$ Hz, C-3); 94.21 (d, $J_{2,F3} = 25.3$ Hz, C-2); 167.62 (C-1); 171.07 (NHC(O)CH₃); 171.12 (CH₃(O)CNCH₂CH₃); 171.29 (C(O)CH₃). ¹⁹F NMR (376 MHz, CDCl₃): δ -205.09 (dd, 1F, $J_{F3,4} = 29.0$, $J_{F3,3} = 50.3$ Hz, F-3). HRMS (ESI +ve) m/z 393.1674 [M+H]⁺ (C₁₆H₂₆N₂FO₈ requires 393.1673); 415.1484 [M+Na]⁺ (C₁₆H₂₅N₂FO₈Na requires 415.1493).

**80**

Methyl 5-*N*-acetamido-4-*O*-acetyl-2,3,5,7-tetrafluoro-7-*N*-ethylacetamido-2,3-difluoro- β -L-manno-hept-2-pyranosonate (**80**)

(Diethylamino)sulphur trifluoride (20.0 μ L, 0.15 mmol) was added drop-wise to a stirred solution of the hemiketal (**79**) (39.4 mg, 0.10 mmol) in dichloromethane (2 mL) at -30 °C and the mixture held at this temperature (30 min). The reaction was quenched by the addition of methanol (40.0 μ L) and then subjected to a standard work up (DCM) and the residue purified by flash chromatography (EtOAc:Hexane 9:1 \rightarrow EtOAc) to give the 2,3-difluorosialic acid benzyl sialoside (**80**) as a white solid (19.00 mg, 50%). ^1H NMR (400 MHz, CDCl_3): δ 1.18 (t, 3H, $J = 7.0$ Hz, $\text{CH}_3(\text{O})\text{CNCH}_2\text{CH}_3$); 1.96 (s, 3H, $\text{NHC}(\text{O})\text{CH}_3$); 2.11 (s, 3H, $\text{CH}_3(\text{O})\text{CNCH}_2\text{CH}_3$); 2.11 (s, 3H, $\text{C}(\text{O})\text{CH}_3$); 3.30 (dd, 1H, $J_{6,7} = 6.3$, $J_{7,7'} = 14.5$ Hz, H-7); 3.48 (q, 2H, $J = 5.4$ Hz, $\text{CH}_3\text{OCNCH}_2\text{CH}_3$); 3.81 (d, 1H, $J_{7,7'} = 14.5$ Hz, H-7'); 3.88 (s, 3H, OCH_3); 4.04 – 4.08 (m, 2H, H-5, H-6); 5.13 (ddt, 1H, $J_{3,4} = 2.3$, $J_{3,\text{F}2} = 3.9$, $J_{3,\text{F}3} = 50.5$ Hz, H-3); 5.43 (dd, 1H, $J_{4,\text{F}2} = 6.7$, $J_{4,\text{F}3} = 26.2$ Hz, H-4); 6.33 (d, 1H, $J_{5,\text{NHAc}} = 7.4$ Hz, NH). ^{13}C NMR (100 MHz, CDCl_3): δ 14.18 ($\text{CH}_3(\text{O})\text{CNCH}_2\text{CH}_3$); 20.68 ($\text{NHC}(\text{O})\text{CH}_3$); 21.24 ($\text{CH}_3(\text{O})\text{CNCH}_2\text{CH}_3$); 23.36 ($\text{C}(\text{O})\text{CH}_3$); 45.82 (C-7); 47.44 (d, $J_{5,\text{F}3} = 3.1$ Hz, C-5); 47.50 ($\text{CH}_3(\text{O})\text{CNCH}_2\text{CH}_3$); 53.63 (OCH_3); 68.71 (dd, $J_{4,\text{F}2} = 6.1$, $J_{4,\text{F}3} = 16.9$ Hz, C-4); 74.16 (d, $J_{6,\text{F}2} = 3.1$ Hz, C-6); 85.52 (dd, $J_{3,\text{F}2} = 19.9$, $J_{3,\text{F}3} = 192.5$ Hz, C-3); 104.73 (dd, $J_{2,\text{F}3} = 17.6$, $J_{2,\text{F}2} = 223.1$ Hz, C-2); 164.58 (dd, $J_{1,\text{F}3} = 3.8$, $J_{1,\text{F}2} = 30.7$ Hz, C-1); 170.33 ($\text{NHC}(\text{O})\text{CH}_3$); 171.00 ($\text{CH}_3(\text{O})\text{CNCH}_2\text{CH}_3$); 171.54 ($\text{C}(\text{O})\text{CH}_3$). ^{19}F NMR (376 MHz, CDCl_3): δ -122.37 (d, 1F, $J_{\text{F}2,\text{F}3} = 12.2$ Hz, F2); -217.11 (ddd, 1F, $J_{\text{F}3,4} = 25.9$, $J_{\text{F}3,3} = 50.4$ Hz, F-3). HRMS (ESI +ve) m/z 395.1620 $[\text{M}+\text{H}]^+$ ($\text{C}_{16}\text{H}_{24}\text{N}_2\text{F}_2\text{O}_7$ requires 395.1630); 417.1437 $[\text{M}+\text{Na}]^+$ ($\text{C}_{16}\text{H}_{23}\text{N}_2\text{F}_2\text{O}_7\text{Na}$ requires 417.1449).



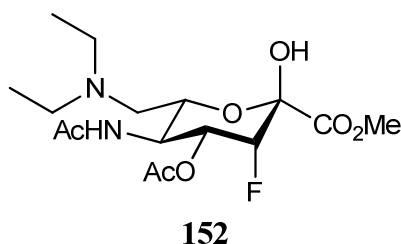
Methyl (benzyl-5-*N*-acetamido-4-*O*-acetyl-3,5,7-trideoxy-7-*N,N*-diethylamine-3-fluoro- α -L-manno-hept-2-pyranosid)onate (**78**)

i) A 0.4 M aqueous solution of sodium periodate (4.9 mL) was added to a solution of 3-fluorosialic acid benzyl sialoside (**75**) (500 mg, 1.16 mmol) in water (4.9 mL) at room temperature and the solution was stirred for 30 min. The solution was concentrated *in vacuo* and the crude residue was used without further purification.

ii) A solution of diethylamine (1.81 mL, 17.4 mmol) in methanol (5 mL) was acidified to pH 5 with glacial acetic acid, and this solution was then added to a solution of the crude mixture (above) in methanol (5 mL). The solution was stirred for 4h at room temperature, then sodium cyanoborohydride (364 mg, 5.79 mmol) was added and the mixture was left stirring overnight. Water (5 mL) and methanol (5 mL) were added, the volume of solution reduced to 5 mL and applied to a reverse phase column (Water \rightarrow Water:MeOH 1:1).

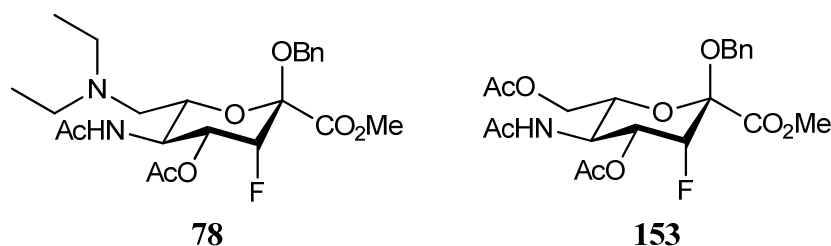
iii) Acetic anhydride (0.53 mL, 5.63 mmol) was added to a solution of the residue (200 mg, 0.47 mmol) in pyridine (4 mL) and the reaction was stirred overnight at room temperature. The solution was then concentrated *in vacuo* and residual pyridine removed by azeotropic evaporation with toluene (3 times) to afford a yellow oil. The oil was then subjected to a standard work up (EtOAc) and then purified by flash chromatography (EtOAc:Pet Ether 8:2 \rightarrow EtOAc:MeOH 9:1) to afford the 7-*N,N*-diethylamino-3-fluorosialic acid benzyl sialoside (**78**) as an off-white solid (11.0 mg, 2% over three steps). ^1H NMR (400 MHz, CD_3OD): δ 1.10 (t, 6H, $J = 7.0$ Hz, $\text{N}(\text{CH}_2\text{CH}_3)_2$); 1.92 (s, 3H, $\text{NHC}(\text{O})\text{CH}_3$); 2.06 (s, 3H, $\text{C}(\text{O})\text{CH}_3$); 2.74 (q, 4H, $J = 14.4$ Hz, $\text{N}(\text{CH}_2\text{CH}_3)_2$); 2.81 – 2.89 (m, 2H, H-7, H-7'); 3.78 (s, 3H, OCH_3); 3.98 – 4.02 (m, 1H, H-6); 4.12 (t, 1H, $J_{4,5} = 10.5$ Hz, H-5); 4.42 (d, 1H, $J = 11.1$ Hz, OCH_2Ph); 4.75 (d, 1H, OCH_2Ph); 5.04 (br dd, $J_{3,4} = 2.6$, $J_{3,\text{F}3} = 49.8$ Hz, H-3); 5.32 (br ddd, 1H, $J_{4,\text{F}3} = 28.7$ Hz, H-4); 7.31 – 7.40 (m, 5H, Ph). ^{13}C NMR (100 MHz, CD_3OD): δ 11.75 ($\text{N}(\text{CH}_2\text{CH}_3)_2$); 20.54 ($\text{C}(\text{O})\text{CH}_3$); 22.67 ($\text{NHC}(\text{O})\text{CH}_3$); 48.32 (d, $J_{5,\text{F}3} = 1.5$ Hz, C-5); 48.93 ($\text{N}(\text{CH}_2\text{CH}_3)_2$); 53.42 (OCH_3); 54.31 (C-7); 67.41

(OCH₂Ph); 70.71 (d, $J_{4,F3} = 17.7$ Hz, C-4); 73.12 (C-6); 88.65 (d, $J_{3,F3} = 180.6$ Hz, C-3); 99.42 (d, $J_{2,F3} = 26.5$ Hz, C-2); 129.02 (C Ph); 129.23 (C Ph); 129.53 (C Ph); 137.57 (Cq Ph); 167.49 (C-1); 171.68 (NHC(O)CH₃); 173.72 (C(O)CH₃). ¹⁹F NMR (376 MHz, CD₃OD): δ -208.80 (dd, 1F, $J_{F3,4} = 29.0$, $J_{F3,3} = 50.4$ Hz, F-3). HRMS (ESI +ve) m/z 469.2359 [M+H]⁺ (C₂₃H₃₄N₂FO₇ requires 469.2350); 491.2173 [M+Na]⁺ (C₂₃H₃₃N₂FO₇Na requires 491.2169).



Methyl 5-*N*-acetamido-4-*O*-acetyl-3,5,7-trideoxy-7-*N,N*-diethylamine-3-fluoro- α -L-manno-hept-2-pyranosonate (**152**)

Glacial acetic acid was added to a solution of 7-*N*-diethylamine-3-fluorosialic acid benzyl sialoside (**78**) (150 mg, 0.32 mmol) in tetrahydrofuran (15 mL) until pH 4, and then palladium on charcoal (40.0 mg, 10 wt. %) was added to the reaction and the reaction was put under a hydrogen gas atmosphere (10 days). The mixture was filtered through Celite[®], washed with methanol and the filtrate concentrated *in vacuo*. The residue was purified by flash chromatography (EtOAc \rightarrow EtOAc:MeOH 9:1) to afford the 7-*N*-diethylamine-3-fluorosialic acid (**152**) as an off-white solid (39.6 mg, 31%). ¹H NMR (400 MHz, CD₃OD): δ 1.17 (t, 6H, $J = 7.2$ Hz, N(CH₂CH₃)₂); 1.95 (s, 3H, NHC(O)CH₃); 2.08 (s, 3H, C(O)CH₃); 2.92 – 3.06 (m, 4H, N(CH₂CH₃)₂); 3.15 – 3.23 (m, 2H, H-7, 7'); 3.35 (s, 3H, OCH₃); 4.08 – 4.13 (m, 1H, H-5); 4.23 – 4.38 (m, 1H, H-6); 5.03 (br dd, $J_{3,4} = 2.4$, $J_{3,F3} = 49.6$ Hz, H-3); 5.40 (br ddd, 1H, $J_{4,5} = 10.8$, $J_{4,F3} = 28.0$ Hz, H-4). ¹³C NMR (400 MHz, CD₃OD): δ 10.56 (N(CH₂CH₃)₂); 20.65 (C(O)CH₃); 22.82 (NHC(O)CH₃); 48.02 (N(CH₂CH₃)₂); 48.14 (C-5); 53.93 (OCH₃); 54.17 (C-7); 66.82 (C-6); 70.38 (d, $J_{4,F3} = 17.1$ Hz, C-4); 89.60 (d, $J_{3,F3} = 179.5$ Hz, C-3); 96.74 (d, $J_{2,F3} = 27.5$ Hz, C-2); 169.56 (C-1); 171.84 (NHC(O)CH₃); 174.07 (C(O)CH₃). ¹⁹F NMR (470 MHz, CD₃OD): δ -209.00 (dd, 1F, $J_{F3,4} = 29.6$, $J_{F3,3} = 49.4$ Hz, F-3). HRMS (ESI +ve) m/z 379.1884 [M+H]⁺ (C₁₆H₂₈N₂FO₇ requires 379.1881); 401.1696 [M+Na]⁺ (C₁₆H₂₇N₂FO₇Na requires 401.1700).



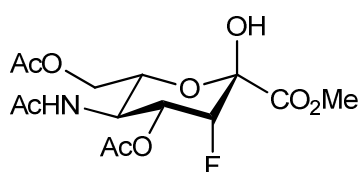
Attempted synthesis of methyl (benzyl-5-*N*-acetamido-4-*O*-acetyl-7-*N,N*-diethylamine-3,5,7-trideoxy-3-fluoro- α -L-manno-hept-2-pyranosid)onate (**78**) where the product obtained was methyl (benzyl-5-*N*-acetamido-4,7-di-*O*-acetyl-3,5-dideoxy-3-fluoro- α -L-manno-hept-2-pyranosid)onate (**153**)

i) A 0.4 M aqueous solution of sodium periodate (4.9 mL) was added to a solution of 3-fluorosialic acid benzyl sialoside (**75**) (500 mg, 1.16 mmol) in water (4.9 mL) at room temperature and the solution was stirred for 30 min. The solution was concentrated *in vacuo* and the crude residue was used without further purification.

ii) A solution of diethylamine (1.81 mL, 17.4 mmol) in methanol (5 mL) was acidified to pH 5 with glacial acetic acid, and this solution was added to a solution of the crude mixture (above) in methanol (5 mL). The solution was stirred for 4h at room temperature, then sodium cyanoborohydride (364 mg, 5.79 mmol) was added and the mixture was left stirring overnight. Water (5 mL) and methanol (5 mL) were added, the volume of solution reduced to 5 mL. This solution was applied to a reverse phase column and eluted with Water \rightarrow Water:MeOH 1:1.

iii) Acetic anhydride (0.53 mL, 5.63 mmol) was added to a solution of the residue obtained (200 mg, 0.47 mmol) in pyridine (4 mL) and the reaction was stirred overnight at room temperature. The solution was then concentrated *in vacuo* and residual pyridine removed by azeotropic evaporation with toluene (3 times) to afford a yellow oil. The oil was subjected to a standard work up (EtOAc) and then purified by flash chromatography (EtOAc:Pet Ether 8:2) to afford the 7-*O*-acetyl-3-fluorosialic acid benzyl sialoside (**153**) as an off-white solid (170 mg, 21% over three steps). ^1H NMR (400 MHz, CDCl_3): δ 1.92 (s, 3H, NHC(O)CH_3); 2.10 (s, 6H, C(O)CH_3); 3.78 (s, 3H, OCH_3); 3.79 - 3.83 (m, 1H, H-6); 4.24 - 4.33 (m, 2H, H-7, H-7'); 4.37 - 4.45 (m, 2H, OCH_2Ph , H-5); 4.57 (d, 1H, $J = 11.4$ Hz, OCH_2Ph); 5.00 (br dd, $J_{3,4} = 2.6$, $J_{3,\text{F}3} = 49.2$ Hz, H-3); 5.28 (ddd, 1H, $J_{4,5} = 11.1$, $J_{4,\text{F}3} = 28.4$ Hz, H-4); 5.42 (d, 1H, $J_{5,\text{NHAc}} = 9.4$ Hz, NH); 7.25 - 7.39 (m, 5H, Ph). ^{13}C NMR (100

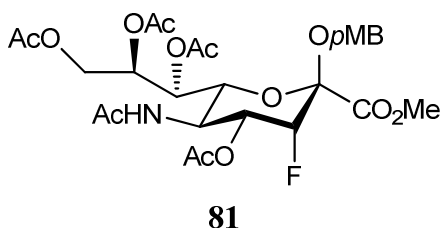
MHz, CDCl₃): δ 20.75, 20.89 (C(O)CH₃); 23.20 (NHC(O)CH₃); 46.56 (d, $J_{5,F3}$ = 2.2 Hz, C-5); 53.07 (OCH₃); 63.22 (C-7); 66.27 (OCH₂Ph); 69.21 (d, $J_{4,F3}$ = 17.0 Hz, C-4); 72.15 (C-6); 87.52 (d, $J_{3,F3}$ = 182.8 Hz, C-3); 98.17 (d, $J_{2,F3}$ = 27.3 Hz, C-2); 128.13 (C Ph); 128.45 (C Ph); 128.62 (C Ph); 135.62 (Cq Ph); 165.65 (C-1); 170.21 (NHC(O)CH₃); 170.89, 171.23 (C(O)CH₃). ¹⁹F NMR (376 MHz, CDCl₃): δ -205.65 (dd, 1F, $J_{F3,4}$ = 28.9, $J_{F3,3}$ = 50.0 Hz, F-3). m/z found (ESI): 456.1660 [M+H]⁺, C₂₁H₂₇F₁N₁O₉ requires 456.1670; 478.1477 [M+Na]⁺, C₂₁H₂₆F₁N₁O₉Na requires 478.1489. HRMS (ESI +ve) m/z 456.1651 [M+H]⁺ (C₂₁H₂₇NFO₉ requires 456.1670); 478.1467 [M+Na]⁺ (C₂₁H₂₆NFO₉Na requires 478.1489).

**154**

Methyl 5-*N*-acetamido-4,7-di-*O*-acetyl-3,5-dideoxy-3-fluoro- α -L-manno-hept-2-pyranosonate (**154**)

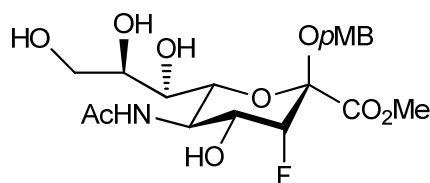
Glacial acetic acid was added to a solution of 4,7-di-*O*-acetyl-3-fluorosialic acid benzyl sialoside (**153**) (170 mg, 0.37 mmol) in tetrahydrofuran (20 mL) until pH 4 and then palladium on carbon (60 mg, 10 wt. %) was added. An atmosphere of hydrogen gas was created with the use of a balloon and the reaction was left stirring for 6 days. The mixture was filtered through Celite[®], washed with ethyl acetate and the filtrate concentrated *in vacuo*. The residue was applied to a chromatographic column (EtOAc) affording 4,7-di-*O*-acetyl-3-fluorosialic acid (**154**) as an off-white solid (92.3 mg, 68%). ¹H NMR (400 MHz, CDCl₃): δ 1.91 (s, 3H, NHC(O)CH₃); 2.06, 2.07 (2s, 6H, C(O)CH₃); 3.81 (s, 3H, OCH₃); 4.14 – 4.19 (m, 2H, H-6, H-7); 4.25 – 4.35 (m, 2H, H-5, H-7'); 4.94 (br dd, 1H, $J_{3,4}$ = 2.3, $J_{3,F3}$ = 50.1 Hz, H-3); 5.35 (br ddd, 1H, $J_{4,5}$ = 10.8, $J_{4,F3}$ = 28.4 Hz, H-4). ¹³C NMR (100 MHz, CDCl₃): δ 20.57, 20.73 (C(O)CH₃); 22.66 (NHC(O)CH₃); 46.72 (d, $J_{5,F3}$ = 2.2 Hz, C-5); 53.31 (OCH₃); 64.20 (C-7); 70.99 (d, $J_{4,F3}$ = 17.0 Hz, C-4); 71.61 (C-6); 88.81 (d, $J_{3,F3}$ = 182.1 Hz, C-3); 95.71 (d, $J_{2,F3}$ = 25.8 Hz, C-2); 169.39 (C-1); 171.77, 172.62 (C(O)CH₃); 173.58 (NHC(O)CH₃). ¹⁹F NMR (376 MHz, CDCl₃): δ -208.41 (dd, 1F, $J_{F3,4}$ = 27.7, $J_{F3,3}$ = 49.2 Hz, F-3). HRMS (ESI +ve) m/z 366.1208 [M+H]⁺

($C_{14}H_{21}F_1N_1O_9$ requires 366.1200); 388.1022 $[M+Na]^+$ ($C_{21}H_{26}F_1N_1O_9Na$ requires 388.1020).



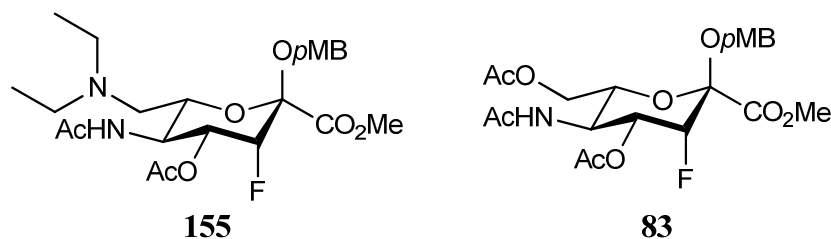
Methyl (*p*-methoxybenzyl-5-*N*-acetamido-4,7,8,9-tetra-*O*-acetyl-3,5-dideoxy-3-fluoro-D-erythro- α -L-manno-non-2-ulopyranosid)onate (**81**)

Sodium hydride (14.0 mg, 0.59 mmol) was added to a solution of hemiketal (**54**) (250 mg, 0.49 mmol) in dimethylformamide (7 mL) and the reaction was stirred for 15 min, after which *para*-methoxybenzyl chloride (0.14 mL, 0.98 mmol) was added and the solution stirred for 2h at room temperature. The solution was quenched with methanol (1 mL) and then concentrated *in vacuo* and subjected to a standard work up (EtOAc). The residue was purified by flash chromatography (EtOAc:Pet ether 2:8 \rightarrow EtOAc) to give the per-*O*-acetylated-3-fluorosialic acid *para*-methoxybenzyl sialoside (**81**) as an off-white solid (266 mg, 86%). 1H NMR (400 MHz, $CDCl_3$): δ 1.87 (s, 3H, $NHC(O)CH_3$); 2.00, 2.04, 2.06, 2.16 (4s, 12H, $C(O)CH_3$); 3.75 (s, 3H, OCH_3); 3.80 (s, 3H, OCH_2PhOCH_3); 4.08 – 4.18 (m, 2H, H-6, H-9); 4.35 – 4.43 (m, 2H, OCH_2PhOCH_3 , H-5); 4.58 (d, 1H, $J = 11.4$ Hz, OCH_2PhOCH_3); 4.92 – 4.94 (m, 1H, H-9'); 5.00 (br dd, $J_{3,4} = 2.1$, $J_{3,F3} = 41.3$ Hz, H-3); 5.31 – 5.41 (m, 4H, NH, H-4, H-7, H-8); 6.89 (d, 2H, $J = 8.8$ Hz, H Ph); 7.26 (d, 2H, H Ph). ^{13}C NMR (100 MHz, $CDCl_3$): δ 20.66, 20.77, 20.79, 20.93 ($C(O)CH_3$); 23.16 ($NHC(O)CH_3$); 45.20 (C-5); 52.96 (CO_2CH_3); 55.29 (OCH_2PhOCH_3); 62.42 (C-9); 66.03 (OCH_2PhOCH_3); 68.31 (C-7); 69.27 (d, $J_{4,F3} = 17.0$ Hz, C-4); 71.61 (C-6); 71.87 (C-8); 87.40 (d, $J_{3,F3} = 183.5$ Hz, C-3); 98.16 (d, $J_{2,F3} = 27.3$ Hz, C-2); 113.98 (C Ph); 127.67 (Cq Ph); 129.51 (C Ph); 159.66 (Cq Ph); 165.40 (C-1); 170.01 ($NHC(O)CH_3$); 170.35, 170.59, 170.74 ($C(O)CH_3$). ^{19}F NMR (376 MHz, $CDCl_3$): δ -206.26 (dd, $J_{F3,4} = 28.9$, $J_{F3,3} = 50.0$ Hz, F-3). HRMS (ESI +ve) m/z 630.2179 $[M+H]^+$ ($C_{28}H_{37}NFO_{14}$ requires 630.2198); 652.2009 $[M+Na]^+$ ($C_{28}H_{36}NFO_{14}Na$ requires 652.2018).

**82**

Methyl (p-methoxybenzyl-5-N-acetamido-3,5-dideoxy-3-fluoro-D-erythro- α -L-manno-non-2-ulopyranosid)onate (**82**)

A 0.5 M solution of sodium methoxide in methanol (0.06 mL) was added to a solution of per-*O*-acetylated-3-fluorosialic acid *para*-methoxybenzyl sialoside (**81**) (266 mg, 0.42 mmol) in methanol (6 mL) at 4 °C and the solution stirred overnight at room temperature. The solution was then neutralized (Dowex 50WX8, H⁺ form), filtered and the filtrate concentrated *in vacuo* to afford the 3-fluorosialic acid *para*-methoxybenzyl sialoside (**82**) as an off-white solid (156.3 mg, 81%). ¹H NMR (400 MHz, CDCl₃): δ 1.99 (s, 3H, NHC(O)CH₃); 3.58 (br dd, 1H, $J_{6,7} = 1.2$, $J_{7,8} = 9.7$ Hz, H-7); 3.71 (br dd, 1H, $J_{8,9} = 5.0$, $J_{9,9'} = 11.4$ Hz, H-9); 3.78 (s, 3H, OCH₂PhOCH₃); 3.81 (s, 3H, OCH₃); 3.85 (br dd, 1H, $J_{8,9'} = 2.9$ Hz, H-9); 3.93 – 3.99 (m, 1H, H-8); 4.01 – 4.09 (m, 2H, H-4, H-6); 4.18 (d, 1H, $J = 10.0$ Hz, OCH₂PhOCH₃); 4.24 (t, 1H, $J_{5,\text{NHAc}} = 10.5$ Hz, H-5); 4.79 – 4.92 (m, 2H, OCH₂PhOCH₃, H-3); 6.85 (d, 2H, $J = 8.8$ Hz, H Ph); 7.31 (d, 2H, H Ph). ¹³C NMR (100 MHz, CDCl₃): δ 22.68 (NHC(O)CH₃); 48.37 (C-5); 53.40 (CO₂CH₃); 55.70 (OCH₂PhOCH₃); 65.24 (C-9); 66.62 (OCH₂PhOCH₃); 69.17 (d, $J_{4,\text{F3}} = 18.4$ Hz, C-4); 69.93 (C-7); 71.44 (C-8); 72.57 (C-6); 91.30 (d, $J_{3,\text{F3}} = 179.1$ Hz, C-3); 99.63 (d, $J_{2,\text{F3}} = 27.3$ Hz, C-2); 114.67 (C Ph); 129.93 (Cq Ph); 131.39 (C Ph); 161.14 (Cq Ph); 168.91 (C-1); 174.87 (NHC(O)CH₃). ¹⁹F NMR (376 MHz, CDCl₃): δ -210.36 (dd, $J_{\text{F3},4} = 30.3$, $J_{\text{F3},3} = 50.0$ Hz, F-3). HRMS (ESI +ve) m/z 462.1768 [M+H]⁺ (C₂₀H₂₉NFO₁₀ requires 462.1775); 484.1577 [M+Na]⁺ (C₂₀H₂₈NFO₁₀Na requires 484.1595).



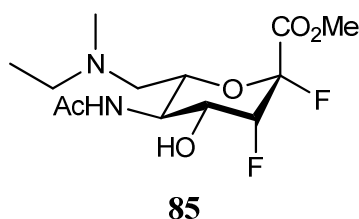
Attempted synthesis of methyl (*p*-methoxybenzyl-5-*N*-acetamido-4-*O*-acetyl-7-*N,N*-diethylamino-3-fluoro-3,5,7-trideoxy- α -L-manno-oct-2-ulopyranosid)onate (**155**) where the product obtained was methyl (*p*-methoxybenzyl-5-*N*-acetamido-4,7-di-*O*-acetyl-3,5-dideoxy-3-fluoro- α -L-manno-hept-2-pyranosid)onate (**83**)

i) A 0.4 M aqueous solution of sodium periodate (8.5 mL) was added to a solution of 3-fluorosialic acid *para*-methoxybenzyl sialoside (**82**) (750 mg, 1.63 mmol) in water (8.5 mL) at room temperature and the solution was stirred for 30 min. The solution was concentrated *in vacuo* and the crude residue was used without further purification.

ii) A solution of diethylamine (3.38 mL, 32.51 mmol) in methanol (5 mL) was acidified to pH 5 with glacial acetic acid, and this solution then added to a solution of the crude mixture (above) in methanol (10 mL). The solution was stirred for 4h at room temperature, then sodium cyanoborohydride (511 mg, 8.13 mmol) was added and the mixture was left stirring overnight. The solution was then concentrated *in vacuo* and the crude residue was used without further purification.

iii) Acetic anhydride (1.55 mL, 16.43 mmol) was added to a solution of the crude mixture (above) in pyridine (14 mL) and stirred overnight at room temperature. The solution was then concentrated *in vacuo* and residual pyridine removed by azeotropic evaporation with toluene (3 times) to afford a yellow oil. The oil was then subjected to a standard work up (EtOAc) and then purified by flash chromatography (EtOAc \rightarrow EtOAc:MeOH 9:2) to afford the 7-*O*-acetyl-3-fluorosialic acid *para*-methoxybenzyl sialoside (**83**) as a off-white solid (76 mg, 10% over three steps). Mp 87 – 92 °C. ^1H NMR (400 MHz, CDCl_3): δ 1.92 (s, 3H, NHC(O)CH_3); 2.10, 2.11 (2s, 6H, C(O)CH_3); 3.80 (s, 3H, $\text{OCH}_2\text{PhOCH}_3$); 3.81 (s, 3H, OCH_3); 3.79 - 3.83 (m, 1H, H-6); 4.25 – 4.51 (m, 5H, $\text{OCH}_2\text{PhOCH}_3$, H-5, H-7, H-7'); 4.98 (br dd, $J_{3,4} = 2.6$, $J_{3,\text{F}3} = 49.2$ Hz, H-3); 5.26 (br ddd, 1H, $J_{4,5} = 11.1$, $J_{4,\text{F}3} = 28.7$ Hz, H-4); 5.47 (d, 1H, $J_{5,\text{NHAc}} = 9.4$ Hz, NH); 6.89 (d, 2H, $J = 8.8$ Hz, H Ph); 7.22 (d, 2H, H Ph). ^{13}C NMR (100 MHz, CDCl_3): δ 20.74, 20.90 (C(O)CH_3); 23.19

(NHC(O)CH₃); 46.58 (d, $J_{5,F3} = 2.2$ Hz, C-5); 53.07 (CO₂CH₃); 55.32 (OCH₂PhOCH₃); 63.27 (C-7); 66.08 (OCH₂PhOCH₃); 69.21 (d, $J_{4,F3} = 17.0$ Hz, C-4); 72.05 (C-6); 87.56 (d, $J_{3,F3} = 182.8$ Hz, C-3); 98.11 (d, $J_{2,F3} = 27.3$ Hz, C-2); 113.99 (C Ph); 127.71 (Cq Ph); 129.94 (C Ph); 159.77 (Cq Ph); 165.79 (C-1); 170.24 (NHC(O)CH₃); 170.93, 171.23 (C(O)CH₃). ¹⁹F NMR (376 MHz, CDCl₃): δ -205.67 (dd, 1F, $J_{F3,4} = 29.0$, $J_{F3,3} = 49.2$ Hz, F-3). HRMS (ESI +ve) m/z 486.1783 [M+H]⁺ (C₂₂H₂₉NFO₁₀ requires 486.1775); 508.1607 [M+Na]⁺ (C₂₂H₂₈NFO₁₀Na requires 508.1595).

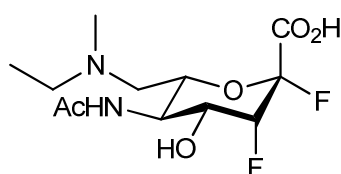


Methyl 5-*N*-acetamido-2,3,5,7-tetra-deoxy-7-*N*-ethyl-*N*-methylamino-2,3-difluoro- β -L-manno-hept-2-pyranosonate (**85**)

i) A 0.4 M aqueous solution of sodium periodate (3.1 mL) was added to a solution of 2,3-difluorosialic acid (**47**) (250 mg, 0.73 mmol) in water (3.1 mL) at room temperature and the solution was stirred for 30 min. Cold tetrahydrofuran (15 mL) was added and the solution was cooled to 4 °C for 15 min, filtered and the filtrate then concentrated *in vacuo* and used without further purification.

ii) A solution of ethylmethylamine (0.94 mL, 10.9 mmol) in methanol (5 mL) was acidified to pH 5 with glacial acetic acid, and this solution then added to a solution of the crude mixture (above) in methanol (5 mL). The solution was stirred for 4h at room temperature, then sodium cyanoborohydride on polymer support (1.13 g, 3.64 mmol) was added and the mixture was stirred overnight. The mixture was filtered and the filtrate evaporated to dryness and then purified using flash chromatography (EtOAc:Pet Ether 7:3) to afford the 7-*N*-ethyl-*N*-methylamino-2,3-difluorosialic acid (**85**) as a colourless oil (25.5 mg, 11% over 2 steps). ¹H NMR (400 MHz, CD₃OD): δ 1.07 (t, 3H, $J = 7.0$ Hz, CH₃NCH₂CH₃); 2.01 (s, 3H, NHC(O)CH₃); 2.33 (d, 3H, $J = 1.2$ Hz, CH₃NCH₂CH₃); 2.53 – 2.61 (m, 3H, H-7, CH₃NCH₂CH₃); 2.70 (dd, 1H, $J_{6,7'} = 7.9$, $J_{7,7'} = 13.7$ Hz, H-7'); 3.87 (s, 2H, exchanging with solvent, OCH₃); 4.21 – 4.26 (m, 2H, H-4, 5); 4.73 – 4.76 (m, 1H, H-6); 5.02 (br ddd, 1H, $J_{3,4} = 3.6$,

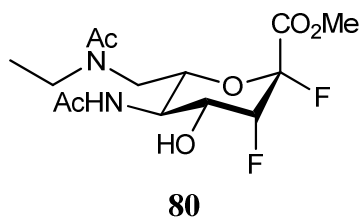
$J_{3,F2} = 23.1$, $J_{3,F3} = 46.9$ Hz, H-3). ^{13}C NMR (100 MHz, CD_3OD): δ 10.35 ($\text{CH}_3\text{NCH}_2\text{CH}_3$); 20.93 (NHC(O)CH_3); 40.78 ($\text{CH}_3\text{NCH}_2\text{CH}_3$); 51.27 ($\text{CH}_3\text{NCH}_2\text{CH}_3$); 52.52 (OCH_3); 52.70 (d, $J_{5,F3} = 5.4$ Hz, C-5); 55.67 (C-7); 66.63 (dd, $J_{4,F2} = 1.2$, $J_{4,F3} = 16.9$ Hz, C-4); 66.81 (d, $J_{6,F2} = 2.3$ Hz, C-6); 84.57 (dd, $J_{3,F2} = 24.5$, $J_{3,F3} = 192.5$ Hz, C-3); 105.92 (dd, $J_{2,F3} = 23.8$, $J_{2,F2} = 249.2$ Hz, C-2); 165.22 (d, $J_{1,F2} = 33.0$ Hz, C-1); 172.33 (NHC(O)CH_3). ^{19}F NMR (376 MHz, CD_3OD): δ -137.46 (t, 1F, $J_{F2,F3} = 22.9$ Hz, F-2); -214.43 (ddt, 1F, $J_{F3,4} = 4.6$, $J_{F3,3} = 42.7$ Hz, F-3). HRMS (ESI +ve) m/z 325.1570 $[\text{M}+\text{H}]^+$ ($\text{C}_{13}\text{H}_{23}\text{N}_2\text{F}_2\text{O}_5$ requires 325.1575); 347.1397 $[\text{M}+\text{Na}]^+$ ($\text{C}_{13}\text{H}_{22}\text{N}_2\text{F}_2\text{O}_5\text{Na}$ requires 347.1394).

**37**

5-*N*-Acetamido-2,3,5,7-tetra-deoxy-7-*N*-ethyl-*N*-methylamino-2,3-difluoro- β -L-manno-hept-2-pyranosonic acid (**37**)

A 0.5 M solution of sodium hydroxide (1 drop) was added to a solution of 7-*N*-ethyl-*N*-methylamino-2,3-difluorosialic acid (**85**) (12.1 mg, 0.04 mmol) in water (0.5 mL) at 4 °C and the solution left to warm to room temperature for 2h. The solution was then neutralized (Dowex 50WX8, H^+ form), filtered and the filtrate concentrated *in vacuo* to afford 7-*N*-ethyl-*N*-methylamino-2,3-difluorosialic acid (**37**) as a yellow solid (7.0 mg, 50%). m.p. 30 °C (hygroscopic). ^1H NMR (400 MHz, CD_3OD): δ 1.33 (t, 3H, $J = 7.4$ Hz, $\text{CH}_3\text{NCH}_2\text{CH}_3$); 2.04 (s, 3H, NHC(O)CH_3); 2.89 (s, 3H, $\text{CH}_3\text{NCH}_2\text{CH}_3$); 3.25 – 3.34 (m, 4H, obscured by solvent peak, $\text{CH}_3\text{NCH}_2\text{CH}_3$, H-7, H-7'); 4.16 – 4.19 (m, 1H, H-4); 4.29 – 4.29 (m, 1H, H-5); 4.85 (s, 1H, obscured by HDO peak, H-6); 4.97 (ddd, 1H, $J_{3,4} = 3.5$, $J_{3,F2} = 22.3$, $J_{3,F3} = 43.0$ Hz, H-3). ^{13}C NMR (100 MHz, CD_3OD): δ 7.77 ($\text{CH}_3\text{NCH}_2\text{CH}_3$); 21.16 (NHC(O)CH_3); 38.19 ($\text{CH}_3\text{NCH}_2\text{CH}_3$); 47.86 ($\text{CH}_3\text{NCH}_2\text{CH}_3$); 51.70 (d, $J_{5,F3} = 6.1$ Hz, C-5); 54.82 (C-7); 63.62 (C-6); 66.98 (d, $J_{4,F3} = 17.7$ Hz, C-4); 84.99 (dd, $J_{3,F2} = 25.3$, $J_{3,F3} = 190.2$ Hz, C-3); 106.32 (dd, $J_{2,F3} = 24.5$, $J_{2,F2} = 173.2$ Hz, C-2); 169.01 (d, $J_{1,F2} = 26.8$ Hz, C-1); 172.27 (NHC(O)CH_3). ^{19}F NMR (376 MHz, CD_3OD): δ -135.36 (t, 1F, $J_{F2,F3} = 21.3$

Hz, F-2); -213.91 (dd, 1F, $J_{F3,3} = 44.3$ Hz, F-3). $[\alpha]_D^{20} = +56.0$ (c 0.05, H₂O). HRMS (ESI -ve) m/z 309.1276 [M-H]⁻ (C₁₂H₂₀N₂F₂O₅ requires 309.1262).



Methyl 5-*N*-acetamido-2,3,5,7-tetradeoxy-7-*N*-ethylacetamido-2,3-difluoro- β -L-manno-hept-2-pyranosonate (**80**)

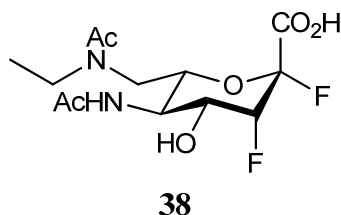
i) A 0.4 M solution of sodium periodate (2.7 mL) was added to a solution of 2,3-difluorosialic acid (**47**) (212 mg, 0.62 mmol) in water (2.7 mL) at room temperature and the solution was stirred for 30 min. Cold tetrahydrofuran (15 mL) was added and the solution was cooled to 4 °C for 15 min, filtered and the filtrate was concentrated *in vacuo* and used without further purification.

ii) A solution of ethylamine (0.61 mL, 9.26 mmol) in methanol (5 mL) was acidified to pH 5 with glacial acetic acid, and this solution then added to a solution of the crude mixture (above) in methanol (5 mL). The solution was stirred for 4h at room temperature, then sodium cyanoborohydride on polymer support (962 mg, 3.09 mmol) was added and the mixture was left stirring overnight. The mixture was filtered and the filtrate evaporate to dryness and then purified by flash chromatography (EtOAc:MeOH 7:3) to afford the 7-*N*-ethylamino-2,3-difluorosialic acid as an oil.

iii) Acetic anhydride (0.59 mL, 6.2 mmol) was added to a solution of the crude mixture (above) in pyridine (3 mL) and stirred overnight at room temperature. The solution was then concentrated *in vacuo* and residual pyridine removed by azeotropic evaporation with toluene (3 times) to afford a yellow oil. The oil was then subjected to a standard work up (EtOAc) and then purified by flash chromatography (EtOAc \rightarrow EtOAc:MeOH 9:2) to afford the 4-*O*-acetyl-7-*N*-ethylacetamido-2,3-difluorosialic acid as a off-white solid.

iv) A 0.5 M solution of sodium methoxide in methanol (0.06 mL) was added to a solution of 4-*O*-acetyl-7-*N*-ethylacetamido-2,3-difluorosialic acid (266 mg, 0.42 mmol) in methanol (6 mL) at 4 °C and the solution stirred overnight at room

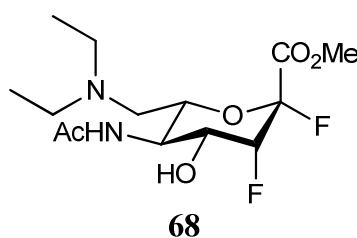
temperature. The solution was then neutralized (Dowex 50WX8, H⁺ form), filtered and the filtrate concentrated *in vacuo* to afford the 7-*N*-ethylacetamido-2,3-difluorosialic acid (**80**) as an off-white solid (11 mg, 22% over 4 steps). m.p. 30 °C (hygroscopic). ¹H NMR (400 MHz, CD₃OD): δ 1.14 (t, 3H, *J* = 7.0 Hz, CH₃C(O)NCH₂CH₃); 2.02 (s, 3H, NHC(O)CH₃); 2.16 (s, 3H, CH₃C(O)NCH₂CH₃); 3.21 (q, 1H, *J* = 7.0, *J* = 14.4 Hz, CH₃C(O)NCH₂CH₃); 3.37 – 4.14 (m, 6H, H-4, H-5, H-6, H-7, H-7', CH₃C(O)NCH₂CH₃); 3.88 (s, 3H, OCH₃); 5.04 – 5.19 (m, 1H, H-3). ¹³C NMR (100 MHz, CD₃OD): δ 10.31 (CH₃C(O)NCH₂CH₃); 22.40 (NHC(O)CH₃); 23.50 (CH₃C(O)NCH₂CH₃); 49.24 (CH₃C(O)NCH₂CH₃); 52.16 (C-7); 51.64 (C-5); 53.99 (OCH₃); 66.99 (d, *J*_{4,F3} = 16.7 Hz, C-4); 67.35 (d, *J*_{6,F2} = 2.4 Hz, C-6); 86.89 (dd, *J*_{3,F2} = 23.7, *J*_{3,F3} = 191.6 Hz, C-3); 107.43 (dd, *J*_{2,F3} = 24.6, *J*_{2,F2} = 250.0 Hz, C-2); 167.89 (d, *J*_{1,F2} = 28.9 Hz, C-1); 173.80 (NHC(O)CH₃); 174.59 (CH₃C(O)NCH₂CH₃). ¹⁹F NMR (376 MHz, CD₃OD): δ -123.80 (d, 1F, *J*_{F2,F3} = 12.2 Hz, F-2); -220.72 (ddd, 1F, *J*_{F3,4} = 27.5, *J*_{F2,F3} = 12.2, *J*_{F3,3} = 50.4 Hz, F-3). HRMS (ESI +ve) *m/z* 375.1338 [M+Na]⁺ (C₁₄H₂₂N₂F₂O₆Na requires 375.1344).



5-*N*-Acetamido-2,3,5,7-tetra-deoxy-7-*N*-ethylacetamido-2,3-difluoro-β-*L*-manno-hept-2-pyranosonic acid (**38**)

A 0.5 M solution of sodium hydroxide (2 drops) was added to a solution of 7-*N*-ethylacetamido-2,3-difluorosialic acid (**80**) (10.0 mg, 0.03 mmol) in water (0.5 mL) at 4 °C and the solution left to warm to room temperature (1h). The solution was then neutralized (Dowex 50WX8, H⁺ form), filtered and the filtrate concentrated *in vacuo* to afford 7-*N*-ethylacetamido-2,3-difluorosialic acid (**38**) as a white solid (7.8 mg, 76%). m.p. 30 °C (hygroscopic). ¹H NMR (400 MHz, D₂O): δ 1.05 (t, 3H, *J* = 7.0 Hz, CH₃C(O)NCH₂CH₃); 1.79 (s, 3H, NHC(O)CH₃); 1.92 (s, 3H, CH₃C(O)NCH₂CH₃); 3.25 – 3.95 (m, 7H, H-4, H-5, H-6, H-7, H-7', CH₃C(O)NCH₂CH₃); 4.98 (br d, 1H, *J*_{3,F3} = 52.4 Hz, H-3). ¹³C NMR (100 MHz, CD₃OD): δ 11.13 (CH₃C(O)NCH₂CH₃); 21.54 (NHC(O)CH₃); 24.56

(CH₃C(O)NCH₂CH₃); 48.76 (CH₃C(O)NCH₂CH₃); 51.34 (C-7); 50.76 (C-5); 67.67 (d, $J_{4,F3}$ = 16.5 Hz, C-4); 66.76 (d, $J_{6,F2}$ = 2.2 Hz, C-6); 87.54 (dd, $J_{3,F2}$ = 23.9, $J_{3,F3}$ = 190.9 Hz, C-3); 108.33 (dd, $J_{2,F3}$ = 24.2, $J_{2,F2}$ = 251.0 Hz, C-2); 168.23 (d, $J_{1,F2}$ = 29.0 Hz, C-1); 174.76 (NHC(O)CH₃); 175.02 (CH₃C(O)NCH₂CH₃). ¹⁹F NMR (376 MHz, CD₃OD): δ -120.13 (d, 1F, $J_{F2,F3}$ = 10.7 Hz, F-2); -217.13 – 216.83 (m, 1F, F-3). $[\alpha]_D^{20}$ = +10.5 (c 0.08, H₂O). HRMS (ESI -ve) m/z 337.1239 [M-H]⁻ (C₁₃H₁₉N₂F₂O₆ requires 337.1211).

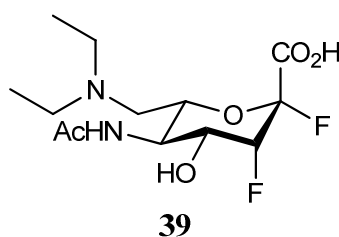


Methyl 5-*N*-acetamido-2,3,5,7-tetra-deoxy-7-*N,N*-diethylamino-2,3-difluoro- β -L-manno-hept-2-pyranosonate (**68**)

i) A 0.4 M solution of sodium periodate (2.7 mL) was added to a solution of 2,3-difluorosialic acid (**47**) (212 mg, 0.62 mmol) in water (2.7 mL) at room temperature and the solution was stirred for 30 min. Cold tetrahydrofuran (15 mL) was added and the solution was cooled to 4 °C for 15 min, filtered and the filtrate was concentrated *in vacuo* and used without further purification.

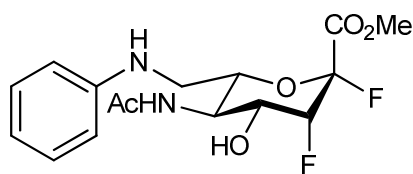
ii) A solution of diethylamine (0.96 mL, 9.26 mmol) in methanol (5 mL) was acidified to pH 5 with glacial acetic acid, and this solution then added to a solution of the crude mixture (above) in methanol (5 mL). The solution was stirred for 4h at room temperature, then sodium cyanoborohydride on polymer support (962 mg, 3.09 mmol) was added and the mixture was left stirring overnight. The mixture was filtered and the filtrate evaporate to dryness and then purified by flash chromatography (EtOAc:Pet Ether 7:3) to afford the 7-*N,N*-diethylamino-2,3-difluorosialic acid (**68**) as an off-white solid (37.9 mg, 18% over 2 steps). m.p. 30 °C (hygroscopic). ¹H NMR (400 MHz, CD₃OD): δ 1.08 (t, 6H, J = 7.0 Hz, N(CH₂CH₃)₂); 2.01 (s, 3H, NHC(O)CH₃); 2.67 – 2.85 (m, 5H, N(CH₂CH₃)₂, H-7); 3.09 – 3.15 (m, 1H, H-7'); 3.87 (s, 3H, OCH₃); 4.25 – 4.26 (m, 2H, H-4, H-5); 4.74 (t, 1H, $J_{6,7}$ = 5.9 Hz, H-6); 5.02 (ddd, $J_{3,4}$ = 2.7, $J_{3,F2}$ = 25.8, $J_{3,F3}$ = 46.1 Hz, H-3). ¹³C NMR (100 MHz, CD₃OD): δ 11.21 (N(CH₂CH₃)₂); 22.40 (NHC(O)CH₃); 50.24

(N(CH₂CH₃)₂) 53.16 (C-7); 53.94 (C-5); 53.99 (OCH₃); 67.99 (d, $J_{4,F3}$ = 16.8 Hz, C-4); 68.25 (d, $J_{6,F2}$ = 2.3 Hz, C-6); 85.90 (dd, $J_{3,F2}$ = 23.8, $J_{3,F3}$ = 191.7 Hz, C-3); 107.32 (dd, $J_{2,F3}$ = 24.5, $J_{2,F2}$ = 249.9 Hz, C-2); 166.60 (d, $J_{1,F2}$ = 29.1 Hz, C-1); 173.80 (NHC(O)CH₃). ¹⁹F NMR (376 MHz, CD₃OD): δ -137.21 to -137.34 (m, 1F, F-2); -214.41 (ddt, 1F, $J_{F3,4}$ = 6.1, $J_{F2,F3}$ = 19.8, $J_{F3,3}$ = 44.2 Hz, F-3). HRMS (ESI +ve) m/z 339.1731 [M+H]⁺ (C₁₄H₂₅N₂F₂O₅ requires 339.1732); 361.1556 [M+Na]⁺ (C₁₄H₂₄N₂F₂O₅Na requires 361.1551).



5-*N*-Acetamido-2,3,5,7-tetra-deoxy-7-*N,N*-diethylamino-2,3-difluoro- β -L-manno-hept-2-pyranosonic acid (**39**)

A 0.5 M solution of sodium hydroxide (2 drops) was added to a solution of 7-*N,N*-diethylamino-2,3-difluorosialic acid (**68**) (20.0 mg, 0.06 mmol) in water (0.5 mL) at 4 °C and the solution left to warm to room temperature (1h). The solution was then neutralized (Dowex 50WX8, H⁺ form), filtered and the filtrate concentrated *in vacuo* to afford 7-*N,N*-diethylamino-2,3-difluorosialic acid (**39**) as a white solid (11.8 mg, 67%). m.p. 30 °C (hygroscopic). ¹H NMR (400 MHz, D₂O): δ 1.16 (q, 6H, J = 7.4, = 13.7 Hz, N(CH₂CH₃)₂); 1.92 (s, 3H, NHC(O)CH₃); 3.09 – 3.28 (m, 6H, N(CH₂CH₃)₂, H-7, H-7'); 4.18 – 4.20 (m, 1H, H-5); 4.21 – 4.25 (m, 1H, H-4); 4.71 – 4.74 (m, 1H, H-6); 4.92 (ddd, 1H, $J_{3,4}$ = 3.9, $J_{3,F2}$ = 23.8, $J_{3,F3}$ = 46.1 Hz, H-3). ¹³C NMR (100 MHz, D₂O): δ 7.71 (N(CH₂CH₃)₂); 7.92 (N(CH₂CH₃)₂); 21.61 (NHC(O)CH₃); 47.33 ((N(CH₂CH₃)₂); 49.06 (N(CH₂CH₃)₂); 51.48 (d, $J_{5,F3}$ = 6.2 Hz, C-5); 51.64 (C-7); 63.78 (d, $J_{6,F2}$ = 3.0 Hz, C-6); 66.27 (d, $J_{4,F3}$ = 16.9 Hz, C-4); 84.45 (dd, $J_{3,F2}$ = 24.6, $J_{3,F3}$ = 189.4 Hz, C-3); 106.44 (dd, $J_{2,F3}$ = 25.3, $J_{2,F2}$ = 246.9 Hz, C-2); 169.78 (d, $J_{1,F2}$ = 28.3 Hz, C-1); 174.46 (NHC(O)CH₃). ¹⁹F NMR (376 MHz, D₂O): δ -134.29 (t, 1F, $J_{F2,F3}$ = 21.4 Hz, F-2); -213.02 (ddt, 1F, $J_{F3,4}$ = 4.6, $J_{F3,3}$ = 42.7 Hz, F-3). $[\alpha]_D^{20}$ = +20.9 (c 0.07, H₂O). HRMS (ESI -ve) m/z 323.1429 [M-H]⁻ (C₁₃H₂₁N₂F₂O₅ requires 323.1419).

**150**

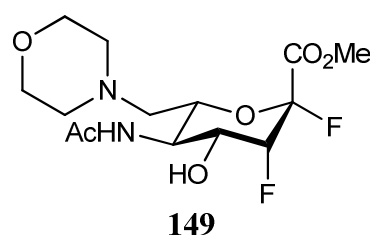
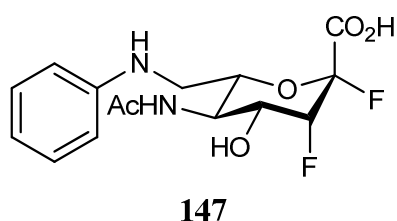
Methyl 5-*N*-acetamido-7-*N*-anilino-2,3,5,7-tetra-deoxy-2,3-difluoro- β -L-manno-hept-2-pyranosonate (**150**)

i) A 0.4 M aqueous solution of sodium periodate (2.7 mL) was added to a solution of 2,3-difluorosialic acid (**47**) (220 mg, 0.64 mmol) in water (2.7 mL) at room temperature and the solution was stirred for 30 min. Cold tetrahydrofuran (10 mL) was added and the solution cooled to 4 °C for 15 min, filtered and the filtrate then concentrated *in vacuo* and used without further purification.

ii) A solution of aniline (0.88 mL, 9.61 mmol) in methanol (5.0 mL) was acidified to pH 5 with glacial acetic acid, and this solution then added to a solution of the crude mixture (above) in methanol (5.0 mL). The mixture was stirred for 4h at room temperature, then sodium cyanoborohydride on polymer support (1.28 g, 3.20 mmol) was added and the mixture left stirring overnight. The mixture was filtered and the filtrate evaporated to dryness and then purified using flash chromatography (EtOAc:Pet Ether 7:3) to afford the 7-*N*-anilino-2,3-difluorosialic acid (**150**) as a yellow solid (25.5 mg, 27% over 2 steps). m p. 82-86 °C. ^1H NMR (400 MHz, CDCl_3): δ 1.97 (s, 3H, NHC(O)CH_3); 3.29 – 3.39 (m, 2H, H-7); 3.91 (s, 3H, OCH_3); 4.43 - 4.45 (m, 2H, H-4, H-5); 4.79 (t, 1H, $J_{5,6} = 5.8$ Hz, H-6); 5.00 (ddd, 1H, $J_{3,4} = 3.1$, $J_{3,\text{F}2} = 22.0$, $J_{3,\text{F}3} = 43.5$ Hz, H-3); 6.47 (d, 1H, $J_{5,\text{NHAc}} = 7.2$ Hz, NH); 6.62 (d, 2H, $J = 7.6$ Hz, H Ph); 6.75 (t, 1H, $J = 14.8$ Hz, H Ph); 7.17 (t, 2H, H Ph). ^{13}C NMR (100 MHz, CDCl_3): δ 23.07 (NHC(O)CH_3); 43.94 (C-7); 52.12 (d, $J_{5,\text{F}3} = 5.9$ Hz, C-5); 53.84 (OCH_3); 66.74 (d, $J_{4,\text{F}3} = 16.2$ Hz, C-4); 67.81 (C-6); 84.58 (dd, $J_{3,\text{F}2} = 24.3$, $J_{3,\text{F}3} = 192.4$ Hz, C-3); 105.91 (dd, $J_{2,\text{F}3} = 24.3$, $J_{2,\text{F}2} = 252.1$ Hz, C-2); 113.37 (C Ph); 118.50 (C Ph); 129.38 (C Ph); 147.14 (Cq Ph); 165.32 (d, $J_{1,\text{F}2} = 30.2$ Hz, C-1); 171.15 (NHC(O)CH_3). ^{19}F NMR (376 MHz, CDCl_3): δ -136.69 (t, 1F, $J_{\text{F}2,\text{F}3} = 20.2$ Hz, F-2); -213.75 (ddt, 1F, $J_{\text{F}3,4} = 5.0$, $J_{\text{F}3,3} = 44.1$ Hz, F-3). HRMS (ESI +ve) m/z 359.1409 $[\text{M}+\text{H}]^+$ ($\text{C}_{16}\text{H}_{21}\text{N}_2\text{F}_2\text{O}_5$ requires 359.1419); 381.1233 $[\text{M}+\text{Na}]^+$ ($\text{C}_{16}\text{H}_{20}\text{N}_2\text{F}_2\text{O}_5\text{Na}$ requires 381.1238).

5-*N*-Acetamido-7-*N*-anilino-2,3,5,7-tetra-deoxy-2,3-difluoro- β -L-manno-hept-2-pyranosonic acid (**147**)

A 0.5 M aqueous solution of sodium hydroxide (4 drops) was added to a solution of 7-*N*-anilino-2,3-difluorosialic acid (**150**) (17.4 mg, 0.05 mmol) in water (0.5 mL) at 4 °C and the solution left to warm to room temperature (1h). The solution was then neutralized (Dowex 50WX8, H⁺ form), filtered and the filtrate concentrated *in vacuo* to afford 7-*N*-anilino-2,3-difluorosialic acid (**147**) as a light brown solid (10.0 mg, 60%). m.p. 36-40 °C. ¹H NMR (400 MHz, CD₃OD): δ 2.03 (s, 3H, NHC(O)CH₃); 3.24 – 3.26 (m, 2H, H-7, H-7'); 4.18 – 4.20 (m, 1H, H-4); 4.31 – 4.33 (m, 1H, H-5); 4.65 (dt, $J_{6,7} = 1.2$, $J_{5,6} = 6.3$ Hz, H-6); 4.91 (ddd, 1H, $J_{3,4} = 3.9$, $J_{3,F2} = 23.0$, $J_{3,F3} = 43.3$ Hz, H-3); 6.62 (d, 2H, $J = 7.8$ Hz, H Ph); 7.09 (t, 3H, H Ph). ¹³C NMR (100 MHz, CD₃OD): δ 22.58 (NHC(O)CH₃); 44.86 (C-7); 53.36 (d, $J_{5,F3} = 3.9$ Hz, C-5); 68.22 (C-6); 68.74 (d, $J_{4,F3} = 16.9$ Hz, C-4); 87.55 (dd, $J_{3,F2} = 26.8$, $J_{3,F3} = 187.8$ Hz, C-3); 107.36 (dd, $J_{2,F3} = 25.1$, $J_{2,F2} = 247.5$ Hz, C-2); 114.05 (C Ph); 118.28 (C Ph); 130.08 (C Ph); 149.58 (Cq Ph); 171.76 (d, $J_{1,F2} = 27.6$ Hz, C-1); 173.53 (NHC(O)CH₃). ¹⁹F NMR (376 MHz, CD₃OD): δ -135.38 (t, 1F, $J_{F2,F3} = 21.4$ Hz, F-2); -213.89 (dd, 1F, $J_{F3,3} = 42.7$ Hz, F-3). $[\alpha]_D^{20} = +72.7$ (c 0.04, H₂O). HRMS (ESI -ve) m/z 343.1121 [M-H]⁻ (C₁₅H₁₇N₂F₂O₅ requires 343.1106).

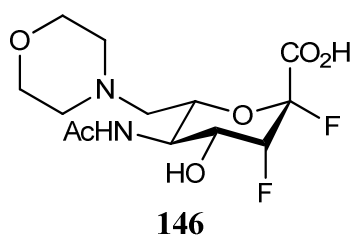


Methyl 5-*N*-acetamido-2,3,5,7-tetra-deoxy-2,3-difluoro-7-*N*-morphonlino- β -L-manno-hept-2-pyranosonate (**149**)

i) A 0.4 M aqueous solution of sodium periodate (3.1 mL) was added to a solution of 2,3-difluorosialic acid (**47**) (250 mg, 0.73 mmol) in water (3.1 mL) at room temperature and the solution was stirred for 30 min. Cold tetrahydrofuran (15 mL)

was added and the solution cooled to 4 °C for 15 min, filtered and the filtrate then concentrated *in vacuo* and used without further purification.

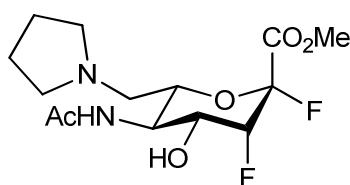
ii) A solution of morpholine (0.96 mL, 10.9 mmol) in methanol (5 mL) was acidified to pH 5 with glacial acetic acid, and this solution then added to a solution of the crude mixture (above) in methanol (5 mL). The mixture was stirred for 4h at room temperature, then sodium cyanoborohydride on polymer support (1.13 g, 3.64 mmol) was added and the mixture was left stirring overnight. The mixture was filtered and the filtrate evaporated to dryness and then purified using flash chromatography (EtOAc:Pet Ether 7:3) to afford the 7-*N*-morpholino-2,3-difluorosialic acid (**149**) as a light yellow solid (53.4 mg, 21% over 2 steps). m.p. 30 °C (hygroscopic). ¹H NMR (400 MHz, CD₃OD): δ 2.01 (s, 3H, NHC(O)CH₃); 2.44 – 2.67 (m, 6H, N(CH₂)₂, H-7, H-7'); 3.67 (t, 4H, *J* = 4.6 Hz, O(CH₂)₂); 3.87 (s, 3H, OCH₃); 4.24 – 4.26 (m, 2H, H-4, H-5); 4.72 – 4.75 (m, 1H, H-6); 5.01 (br ddd, *J*_{3,4} = 2.8, *J*_{3,F2} = 22.7, *J*_{3,F3} = 43.0 Hz, H-3). ¹³C NMR (100 MHz, CD₃OD): δ 22.37 (NHC(O)CH₃); 53.96 (OCH₃); 54.01 (C-5); 55.03 (N(CH₂)₂); 59.05 (C-7); 67.70 (O(CH₂)₂); 68.03 (d, *J*_{4,F3} = 15.4 Hz, C-4); 68.18 (d, *J*_{6,F2} = 3.1 Hz, C-6); 86.02 (dd, *J*_{3,F2} = 23.8, *J*_{3,F3} = 191.7 Hz, C-3); 107.35 (dd, *J*_{2,F3} = 24.5, *J*_{2,F2} = 249.2 Hz, C-2); 166.63 (d, *J*_{1,F2} = 32.2 Hz, C-1); 173.67 (NHC(O)CH₃). ¹⁹F NMR (376 MHz, CD₃OD): δ -137.92 (t, 1F, *J*_{F2,F3} = 21.4 Hz, F-2); -214.98 (m, 1F, F-3). HRMS (ESI +ve) *m/z* 353.1541 [M+H]⁺ (C₁₄H₂₃N₂F₂O₆ requires 353.1524); 375.1368 [M+Na]⁺ (C₁₄H₂₂N₂F₂O₆Na requires 375.1344).



5-*N*-Acetamido-2,3,5,7-tetra-deoxy-2,3-difluoro-7-*N*-morpholino- β -L-manno-hept-2-pyranosonic acid (**146**)

A 0.5 M aqueous solution of sodium hydroxide (4 drops) was added to a solution of 7-*N*-morpholino-2,3-difluorosialic acid (**149**) (112 mg, 0.32 mmol) in water (2 mL) at 4 °C and the solution was left to warm to room temperature (1h). The solution was then neutralized (Dowex 50WX8, H⁺ form), filtered and the filtrate concentrated *in*

vacuo to afford 7-*N*-morpholino-2,3-difluorosialic acid (**146**) as a light brown solid (90.1 mg, 84%). m.p. 30 °C (hygroscopic). ¹H NMR (400 MHz, CD₃OD): δ 20.3 (s, 3H, NHC(O)CH₃); 2.80 – 2.94 (m, 6H, N(CH₂)₂, H-7, H-7'); 3.77 – 3.78 (m, 4H, O(CH₂)₂); 4.16 – 4.17 (m, 1H, H-4); 4.28 (br s, 1H, H-5); 4.81 – 4.89 (m, 1H, H-6); 4.90 – 5.01 (m, 1H, H-3). ¹³C NMR (100 MHz, CD₃OD): δ 22.58 (NHC(O)CH₃); 53.72 (d, *J*_{5,F3} = 5.4 Hz, C-5); 54.47 (N(CH₂)₂); 59.17 (C-7); 66.02 (C-6); 66.37 (O(CH₂)₂); 68.42 (d, *J*_{4,F3} = 16.9 Hz, C-4); 86.91 (dd, *J*_{3,F2} = 26.0, *J*_{3,F3} = 189.3 Hz, C-3); 108.40 (dd, *J*_{2,F3} = 25.4, *J*_{2,F2} = 246.2 Hz, C-2); 171.00 (d, *J*_{1,F2} = 26.9 Hz, C-1); 173.42 (NHC(O)CH₃). ¹⁹F NMR (376 MHz, CD₃OD): δ -135.13 (s, 1F, F-2); -213.62 (dd, 1F, *J*_{F2,F3} = 19.9, *J*_{F3,3} = 42.8 Hz, F-3). [α]_D²⁰ = +66.7 (c 0.09, H₂O). HRMS (ESI -ve) *m/z* 337.1217 [M-H]⁻ (C₁₃H₁₉N₂F₂O₆ requires 337.1211).

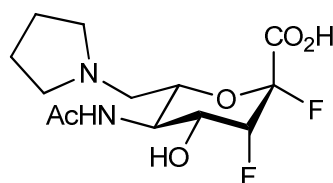
**148**

Methyl 5-*N*-acetamido-2,3,5,7-tetra-deoxy-7-*N*-pyrrolidino-2,3-difluoro-β-*L*-mannohept-2-pyranosonate (**148**)

i) A 0.4 M aqueous solution of sodium periodate (3.1 mL) was added to a solution of 2,3-difluorosialic acid (**47**) (250 mg, 0.73 mmol) in water (3.1 mL) at room temperature and the solution was stirred for 30 min. Cold tetrahydrofuran (15 mL) was added and the solution was cooled to 4 °C for 15 min, filtered and the filtrate then concentrated *in vacuo* and used without further purification.

ii) A solution of diethylamine (0.9 mL, 10.92 mmol) in methanol (5 mL) was acidified to pH 5 with glacial acetic acid, and this solution added to a solution of the crude mixture (above) in methanol (5 mL). The mixture was stirred for 4h at room temperature, then sodium cyanoborohydride on polymer support (1.133 g, 3.64 mmol) was added and the mixture was left stirring overnight. The mixture was filtered and the filtrate evaporated to dryness and then purified by flash chromatography (EtOAc:MeOH 1:0 → EtOAc:MeOH 8:2) to afford the 7-*N*-pyrrolidino-2,3-difluorosialic acid (**148**) as an off-white solid (104.6 mg, 42% over 2 steps). m.p. 30 °C (hygroscopic). ¹H NMR (400 MHz, CD₃OD): δ 2.04 (s, 3H,

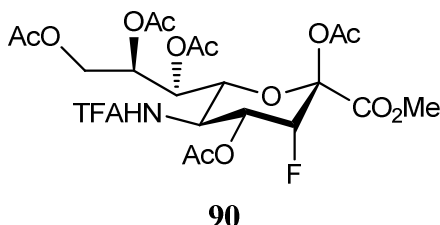
NHC(O)CH₃); 2.06 (s, 4H, N(C₂H₄)(C₂H₄)); 3.28 – 3.39 (m, 6H, N(C₂H₄)(C₂H₄), H-7, 7'); 3.89 (s, 1H exchanging with the solvent, OCH₃); 4.25 – 4.28 (m, 1H, H-5); 4.30 – 4.31 (m, 1H, H-4); 4.92 (dt, 1H, $J_{6,7} = 2.4$, $J_{5,6} = 9.0$ Hz, H-6); 5.04 – 5.22 (ddd, obscured by the HDO peak, $J_{3,4} = 3.5$, $J_{3,F2} = 22.7$ Hz, H-3). ¹³C NMR (100 MHz, CD₃OD): δ 22.47 (NHC(O)CH₃); 23.90 (N(C₂H₄)(C₂H₄)); 53.51 (d, $J_{4,F3} = 6.2$ Hz, C-4); 55.55 (C-7); 67.83 (d, $J_{6,F2} = 3.8$ Hz, C-6); 67.92 (d, $J_{5,F3} = 10.0$ Hz, C-5); 85.47 (dd, $J_{3,F2} = 23.0$, $J_{3,F3} = 191.7$ Hz, C-3); 106.85 (dd, $J_{2,F3} = 24.6$, $J_{2,F2} = 250.0$ Hz, C-2); 165.90 (d, $J_{1,F2} = 31.4$ Hz, C-1); 173.90 (NHC(O)CH₃). ¹⁹F NMR (376 MHz, CD₃OD): δ -136.63 (m, 1F, F-2); -214.15 (ddt, $J_{F3,4} = 6.1$, $J_{F2,F3} = 18.3$, $J_{F3,3} = 42.7$ Hz, 1F, F-3). HRMS (ESI +ve) m/z 337.1565 [M+H]⁺ (C₁₄H₂₃N₂F₂O₅ requires 337.1575); 359.1376 [M+Na]⁺ (C₁₄H₂₂N₂F₂O₅Na requires 359.1394).

**145**

5-*N*-Acetamido-2,3,5,7-tetra-deoxy-7-*N*-pyrrolidino-2,3-difluoro- β -L-manno-hept-2-pyranosonic acid (**145**)

A 0.5 M aqueous solution of sodium hydroxide (5 drops) was added to a solution of 7-*N*-pyrrolidino-2,3-difluorosialic acid (**148**) (105 mg, 0.31 mmol) in water (2 mL) at 4 °C and the solution was left to warm to room temperature (1h). The solution was then neutralized (Dowex 50WX8, H⁺ form), filtered and the filtrate concentrated *in vacuo* to afford 7-*N*-pyrrolidino-2,3-difluorosialic acid (**145**) as a light brown solid (103 mg, quantitative). m.p. 30 °C (hygroscopic). ¹H NMR (400 MHz, CD₃OD): δ 1.88 – 2.00 (m, 4H, N(C₂H₄)(C₂H₄)); 2.03 (s, 3H, NHC(O)CH₃); 2.79 – 2.98 (m, 6H, N(C₂H₄)(C₂H₄), H-7, H-7'); 4.17 – 4.19 (m, 1H, H-4); 4.26 – 4.30 (m, 1H, H-5); 4.70 – 4.73 (m, 1H, H-6); 4.82 – 5.00 (m, 1H, obscured by HDO peak, H-3). ¹³C NMR (100 MHz, CD₃OD): δ 22.56 (NHC(O)CH₃); 24.06 (N(C₂H₄)(C₂H₄)); 53.78 (d, $J_{5,F3} = 5.4$ Hz, C-5); 55.43 (N(C₂H₄)(C₂H₄)); 56.77 (C-7); 67.77 (C-6); 68.39 (d, $J_{4,F3} = 16.9$ Hz, C-4); 86.97 (dd, $J_{3,F2} = 26.1$, $J_{3,F3} = 198.2$ Hz, C-3); 108.48 (dd, $J_{2,F3} = 25.4$, $J_{2,F2} = 245.4$ Hz, C-2); 171.19 (d, $J_{1,F2} = 26.9$ Hz, C-1); 173.42

(NHC(O)CH₃). ¹⁹F NMR (376 MHz, CD₃OD): δ -135.74 (t, 1F, $J_{F2,F3} = 21.4$ Hz, F-2); 213.90 (ddt, 1F, $J_{F3,4} = 4.5$, $J_{F3,3} = 42.7$ Hz, F-3). $[\alpha]_D^{20} = +57.1$ (c 0.07, H₂O). HRMS (ESI -ve) m/z 321.1336 [M-H]⁻ (C₁₃H₁₉N₂F₂O₅ requires 321.1262).



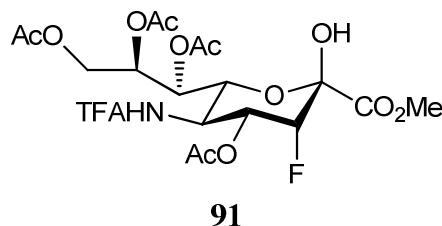
Methyl 2,4,7,8,9-penta-*O*-acetyl-3,5-dideoxy-3-fluoro-5-*N*-trifluoroacetamido-D-erythro- α -L-manno-non-2-ulopyranosonate (**90**)

i) Methanesulfonic acid (3.1 mL, 47.8 mmol) was added to a solution of 3-fluorosialic acid methyl ester (**52**) (3.1 g, 9.08 mmol) in methanol (31.0 mL) and the reaction mixture was stirred at reflux for 24h. After this time triethylamine was added until pH was neutral and the solution was used without further purification.

ii) Triethylamine (3.1 mL, 22.2 mmol) was added, the solution was cooled to 4 °C and trifluoroacetic anhydride (2.53 mL, 18.2 mmol) was added and the reaction was stirred at this temperature for 1h. The solution was evaporated to dryness and the crude mixture used without further purification.

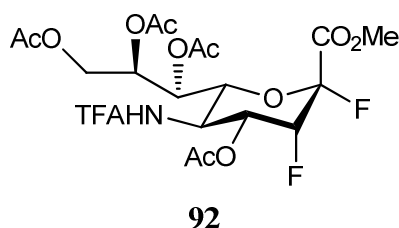
iii) The crude mixture was dissolved in acetic anhydride (21.5 mL, 227 mmol), cooled to 4 °C and pyridine (75.0 mL) was slowly added. The reaction was stirred at room temperature for 24h. The solution was then concentrated *in vacuo* and residual pyridine removed by azeotropic evaporation with toluene to give a dark brown oil. The oil was subjected to a standard work up (EtOAc) and purified by flash chromatography (EtOAc:Pet Ether 9:1 \rightarrow EtOAc) to give per-*O*-acetylated-5-*N*-trifluoroacetamido-3-fluorosialic acid (**90**) as a white solid (1.08 g, 20% over 3 steps). m. p. 75-81 °C. ¹H NMR (400 MHz, CDCl₃): δ 2.03, 2.05, 2.11, 2.16 (4s, 15H, C(O)CH₃); 3.84 (s, 3H, OCH₃); 4.19 – 4.26 (m, 2H, H-5, H-9); 4.32 (dd, 1H, $J_{6,7} = 2.0$, $J_{5,6} = 10.6$ Hz, H-6); 4.59 (br dd, 1H, $J_{8,9'} = 2.4$, $J_{9,9'} = 12.5$ Hz, H-9'); 4.95 (br dd, 1H, $J_{3,4} = 2.3$, $J_{3,F3} = 48.8$ Hz, H-3); 5.08 – 5.11 (m, 1H, H-8); 5.32 (dd, 1H, $J_{7,8} = 5.1$ Hz, H-7); 5.60 (ddd, 1H, $J_{4,5} = 10.6$, $J_{4,F3} = 27.4$ Hz, H-4); 6.90 (d, 1H, $J_{5,NHTFA} = 9.0$ Hz, NH). ¹³C NMR (100 MHz, CDCl₃): δ 20.34, 20.39, 20.62, 20.64, 20.82 (C(O)CH₃); 46.24 (C-5); 53.62 (OCH₃); 61.89 (C-9); 67.56 (C-7); 67.77

(d, $J_{4,F3} = 16.9$ Hz, C-4); 70.94 (C-6); 71.31 (C-8); 86.71 (d, $J_{3,F3} = 185.6$ Hz, C-3); 95.03 (d, $J_{2,F3} = 28.4$ Hz, C-2); 115.33 (q, $J_{C,F} = 288.3$ Hz, NHC(O)CF_3); 157.43 (q, $J_{C(O),F} = 37.5$ Hz, NHC(O)CF_3); 164.72 (C-1); 167.00, 170.52, 170.56, 170.60, 170.76 (C(O)CH_3). ^{19}F NMR (376 MHz, CDCl_3): δ -76.27 (s, 3F, NHC(O)CF_3); -209.06 (dd, 1F, $J_{F3,4} = 27.4$, $J_{F3,3} = 48.8$ Hz, F-3). HRMS (ESI +ve) m/z 628.1275 $[\text{M}+\text{Na}]^+$ ($\text{C}_{22}\text{H}_{27}\text{NF}_4\text{O}_{14}\text{Na}$ requires 628.1265).



Methyl 4,7,8,9-tetra-*O*-acetyl-3,5-dideoxy-3-fluoro-5-*N*-trifluoroacetamido-D-erythro- α -L-manno-non-2-ulopyranosonate (**91**)

A solution of hydrazine acetate (402 mg, 4.46 mmol) in methanol (10.0 mL) was added to a solution of per-*O*-acetylated-5-*N*-trifluoroacetamido-3-fluorosialic acid (**90**) (900 mg, 1.49 mmol) in dichloromethane (30.0 mL) at 4 °C and the solution left to stand at this temperature (3h). The solution was then concentrated *in vacuo*, subjected to a standard work up (EtOAc) to afford the hemiketal (**91**) as a white solid (570 mg, 68%). m. p. 85-90 °C. ^1H NMR (400 MHz, CDCl_3): δ 2.03, 2.05, 2.11, 2.17 (4s, 12H, C(O)CH_3); 3.85 (OCH_3); 4.11 – 4.15 (m, 1H, H-5); 4.47 – 4.51 (m, 2H, H-6, 9); 4.87 – 5.00 (m, 2H, H-3, H-9'); 5.25 – 5.38 (m, 3H, H-4, H-7, H-8); 5.92 (br s, 1H, OH); 7.74 (d, 1H, $J_{5,\text{NHTFA}} = 8.6$ Hz, NH). ^{13}C NMR (100 MHz, CDCl_3): δ 20.27, 20.55, 20.84, 20.88 (C(O)CH_3); 45.35 (C-5); 53.46 (OCH_3); 62.50 (C-9); 68.41 (d, $J_{4,F3} = 16.9$ Hz, C-4); 68.84 (C-7); 71.38 (C-6); 72.67 (C-8); 86.41 (d, $J_{3,F3} = 187.1$ Hz, C-3); 94.37 (d, $J_{2,F3} = 25.3$ Hz, C-2); 115.53 (q, $J_{C,F} = 287.6$ Hz, NHC(O)CF_3); 157.66 (q, $J_{C(O),F} = 37.6$ Hz, NHC(O)CF_3); 166.87 (C-1); 169.97, 170.16, 171.93, 173.44 (C(O)CH_3). ^{19}F NMR (376 MHz, CDCl_3): δ -76.16 (s, 3F, NHC(O)CF_3); -205.34 (dd, 1F, $J_{F3,4} = 27.5$, $J_{F3,3} = 48.9$ Hz, F-3). HRMS (ESI +ve) m/z 586.1091 $[\text{M}+\text{Na}]^+$ ($\text{C}_{20}\text{H}_{25}\text{NF}_4\text{O}_{13}\text{Na}$ requires 586.1160).

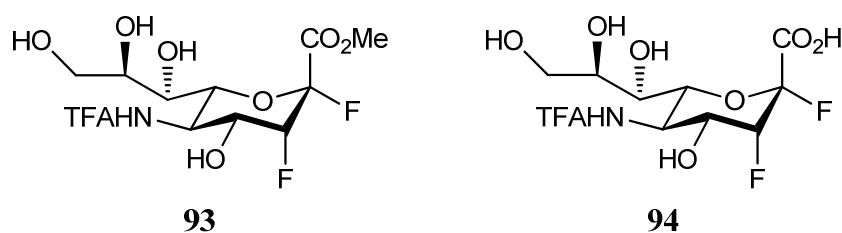


Methyl 4,7,8,9-tetra-*O*-acetyl-2,3,5-trideoxy-2,3-difluoro-5-*N*-trifluoroacetamido-D-erythro- β -L-manno-non-2-ulopyranosonate (**92**)

(Diethylamino)sulphur trifluoride (0.2 mL, 1.49 mmol) was added drop-wise to a solution of hemiketal (**91**) (560 mg, 0.99 mmol) in dichloromethane (18.0 mL) at -30 °C and the solution held at this temperature (30 min). The solution was quenched by the addition of methanol (0.5 mL) and then subjected to a standard work up (DCM) and the residue purified by flash chromatography (EtOAc:Pet Ether 4:6 \rightarrow EtOAc:Pet Ether 7:3) to give the per-*O*-acetylated-5-*N*-trifluoroacetamido-2,3-difluorosialic acid (**92**) as a white solid (270 mg, 48%). m. p. 137 – 141 °C. ^1H NMR (400 MHz, CDCl_3): δ 2.03, 2.10, 2.11, 2.16 (4s, 12H, $\text{C}(\text{O})\text{CH}_3$); 3.90 (s, 3H, OCH_3); 4.17 – 4.25 (m, 2H, H-5, H-9); 4.35 – 4.42 (m, 2H, H-6, H-9'); 5.11 (br dt, 1H, $J_{3,4} = 2.3$, $J_{3,\text{F}3} = 52.7$ Hz, H-3); 5.26 (d, 1H, $J_{7,8} = 7.4$ Hz, H-7); 5.32 – 5.35 (m, 1H, H-8); 5.52 (dd, 1H, $J_{4,5} = 10.9$, $J_{4,\text{F}3} = 26.2$ Hz, H-4); 6.95 (d, 1H, $J_{5,\text{NHTFA}} = 9.0$ Hz, NH). ^{13}C NMR (100 MHz, CDCl_3): δ 20.32, 20.53, 20.58, 20.82 ($\text{C}(\text{O})\text{CH}_3$); 45.81 (d, $J_{5,\text{F}3} = 3.8$ Hz, C-5); 53.88 (OCH_3); 61.70 (C-9); 66.87 (C-7); 68.22 (d, $J_{4,\text{F}2} = 6.1$, $J_{4,\text{F}3} = 17.6$ Hz, C-4); 69.25 (C-8); 71.50 (d, $J_{6,\text{F}2} = 4.6$ Hz, C-6); 85.29 (dd, $J_{3,\text{F}2} = 19.2$, $J_{3,\text{F}3} = 195.6$ Hz, C-3); 104.45 (dd, $J_{2,\text{F}3} = 17.7$, $J_{2,\text{F}2} = 227.8$ Hz, C-2); 115.32 (q, $J_{\text{C},\text{F}} = 288.3$ Hz, $\text{NHC}(\text{O})\text{CF}_3$); 157.45 (q, $J_{\text{C}(\text{O}),\text{F}} = 38.3$ Hz, $\text{NHC}(\text{O})\text{CF}_3$); 164.23 (dd, $J_{1,\text{F}3} = 4.6$, $J_{1,\text{F}2} = 29.9$ Hz, C-1); 170.17, 170.43, 170.52, 170.63 ($\text{C}(\text{O})\text{CH}_3$). ^{19}F NMR (376 MHz, CDCl_3): δ -76.29 (s, 3F, $\text{NHC}(\text{O})\text{CF}_3$); -123.85 (d, 1F, $J_{\text{F}2,3} = 12.2$ Hz, F-2); -216.97 (ddd, 1F, $J_{\text{F}3,4} = 26.0$, $J_{\text{F}3,3} = 51.9$ Hz, F-3). HRMS (ESI +ve) m/z 588.1115 $[\text{M}+\text{Na}]^+$ ($\text{C}_{20}\text{H}_{24}\text{NF}_5\text{O}_{12}\text{Na}$ requires 588.1116).

Methyl 2,3,5-trideoxy-2,3-difluoro-5-*N*-trifluoroacetamido-D-erythro- β -L-manno-non-2-ulopyranosonate (**93**)

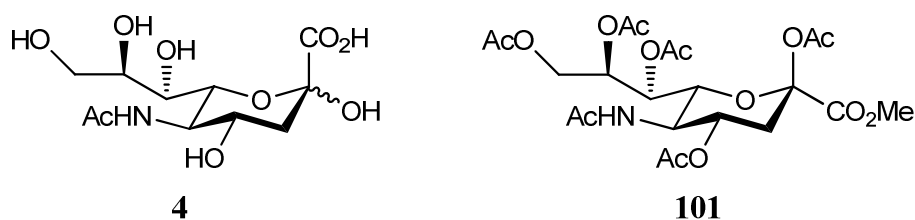
A 0.5 M solution of sodium methoxide in methanol (0.05 mL) was added to a solution of the per-*O*-acetylated-5-*N*-trifluoroacetamido-2,3-difluorosialic acid (**92**) (208 mg, 0.37 mmol) in methanol (5.0 mL) at 4 °C and the solution was left to warm to room temperature overnight. The solution was then neutralized (Dowex 50WX8, H⁺ form), filtered and the filtrate concentrated *in vacuo* to afford the 5-*N*-trifluoroacetamido-2,3-difluorosialic acid (**93**) as a light yellow solid (88.8 mg, 54%). m.p. 30 °C (hygroscopic) ¹H NMR (400 MHz, CD₃OD): δ 3.63 (dd, 1H, $J_{8,9} = 5.9$, $J_{9,9'} = 12.1$ Hz, H-9); 3.76 – 3.87 (m, 2H, H-8, H-9'); 3.88 (OCH₃); 4.01 (d, 1H, $J_{5,6} = 10.5$ Hz, H-6); 4.14 (br dd, 1H, $J_{4,5} = 11.0$, $J_{4,F3} = 28.5$ Hz, H-4); 4.38 - 4.44 (m, 1H, H-5); 5.08 (br dt, 1H, $J_{3,4} = 2.4$, $J_{3,F2} = 4.7$, $J_{3,F3} = 51.2$ Hz, H-3). ¹³C NMR (100 MHz, CD₃OD): δ 48.07 (C-5); 52.50 (OCH₃); 63.37 (C-9); 68.13 (dd, $J_{4,F2} = 5.3$, $J_{4,F3} = 18.4$ Hz, C-4); 68.13 (C-7); 70.07 (C-8); 72.60 (d, $J_{6,F2} = 4.6$ Hz, C-6); 87.91 (dd, $J_{3,F2} = 17.7$, $J_{3,F3} = 187.9$ Hz, C-3); 106.80 (dd, $J_{2,F3} = 17.0$, $J_{2,F2} = 220.80$ Hz, C-2); 117.43 (dd, $J_{C,F} = 287.5$ Hz, NHC(O)CF₃); 159.74 (q, $J_{C(O),F} = 36.8$ Hz, NHC(O)CF₃); 165.32 (d, $J_{1,F2} = 30.0$ Hz, C-1). ¹⁹F NMR (376 MHz, CD₃OD): δ -77.15 (s, 3F, NHC(O)CF₃); -123.97 (d, 1F, $J_{F2,F3} = 12.2$ Hz, F-2); -221.54 to -221.30 (m, 1F, F-3). HRMS (ESI +ve) m/z 398.0881 [M+H]⁺ (C₁₄H₁₉NF₅O₉ requires 398.0874); 420.0696 [M+Na]⁺ (C₁₄H₁₈NF₅O₉Na requires 420.0694).



2,3,5-Trideoxy-2,3-difluoro-5-*N*-trifluoroacetamido-D-erythro- β -L-manno-non-2-ulopyranosonic acid (**94**)

A 0.5 M aqueous sodium hydroxide solution (4 drops) was added to a solution of 5-*N*-trifluoroacetamido-2,3-difluorosialic acid (**93**) (71.2 mg, 0.16 mmol) in water (1.0 mL) at 4 °C and the solution left to warm to room temperature (1h). The solution

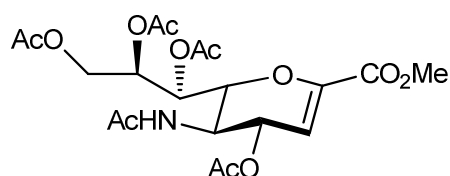
was then neutralized (Dowex 50WX8, H⁺ form), filtered and the filtrate concentrated *in vacuo* to afford 5-*N*-trifluoroacetamido-2,3-difluorosialic acid (**94**) as a white solid (66.0 mg, quantitative). m.p. 30 °C (hygroscopic). ¹H NMR (400 MHz, CD₃OD): δ 3.51 (t, 1H, *J*_{4,5} = 10.6 Hz, H-5); 3.70 – 3.76 (m, 2H, H-7, 9); 3.83 (dd, 1H, *J*_{8,9'} = 2.7, *J*_{9,9'} = 11.3 Hz, H-9'); 3.88 - 3.92 (m, 1H, H-8); 3.98 (d, 1H, *J*_{5,6} = 10.5 Hz, H-6); 4.12 (br dd, *J*_{4,F3} = 27.4 Hz, H-4); 5.16 (d, 1H, *J*_{3,F3} = 52.4 Hz, H-3). ¹³C NMR (100 MHz, CD₃OD): δ 49.29 (C-5); 64.05 (C-9); 69.28 (C-7); 69.58 (dd, *J*_{4,F2} = 6.1, *J*_{4,F3} = 18.4 Hz, C-4), 72.94 (C-8); 73.08 (d, *J*_{6,F2} = 5.4 Hz, C-6); 90.19 (dd, *J*_{3,F2} = 18.4, *J*_{3,F3} = 187.1 Hz, C-3); 107.97 (dd, *J*_{2,F3} = 14.6, *J*_{2,F2} = 222.4 Hz, C-2); 122.97 (q, *J*_{C,F} = 212.4 Hz, NHC(O)CF₃); 170.01 (d, *J*_{1,F2} = 25.3 Hz, C-1). ¹⁹F NMR (376 MHz, CD₃OD): δ -76.98 (s, 3F, NHC(O)CF₃); -124.95 (d, 1F, *J*_{F2,F3} = 10.7 Hz, F-2); -221.26 (ddd, 1F, *J*_{F3,4} = 27.5, *J*_{F3,3} = 51.9 Hz, F-3). [α]_D²⁰ = +8.7 (c 0.05, H₂O). HRMS (ESI -ve) *m/z* 286.0732 [M-TFA-H]⁻ (C₉H₁₄NF₂O₇ requires 286.0738).



Methyl 5-*N*-acetamido-2,4,7,8,9-penta-*O*-acetyl-3,5-dideoxy-D-erythro-β-L-mannono-2-ulopyranosonate (**101**)

Trifluoroacetic acid (10.0 mL, 129 mmol) was added to a solution of sialic acid (**4**) (10.0 g, 32.3 mmol) in methanol (500 mL) at 4 °C and the mixture was left to warm to room temperature overnight. The solution was then concentrated *in vacuo* to give a white solid (11.5 g). Acetic anhydride (55.6 mL, 588 mmol) was slowly added to a solution of the crude mixture (9.5 g, 29.4 mmol) in pyridine (258 mL) at 4 °C and the solution left to warm to room temperature (4 days). The solution was then concentrated *in vacuo* and residual pyridine removed by azeotropic evaporation with toluene to give a yellow oil. The oil was subjected to a standard work up (EtOAc) and purified by flash chromatography (EtOAc:Pet Ether 8:2 → EtOAc) to give the per-*O*-acetylated sialic acid (**101**) as a white solid (14.0 g, 81%). ¹H NMR (270 MHz, CDCl₃): δ 1.88 (s, 3H, NHC(O)CH₃); 2.02, 2.04, 2.13, 2.13 (4s, 15H,

C(O)CH₃); 2.07 – 2.08 (m, 1H, H-3); 2.53 (br dd, 1H, $J_{3',4} = 5.0$, $J_{3',3} = 13.5$ Hz, H-3'); 3.77 (s, 3H, OCH₃); 4.05 – 4.15 (m, 3H, H-5, H-6, H-9); 4.47 (br dd, 1H, $J_{8,9'} = 2.8$, $J_{9,9'} = 12.7$ Hz, H-9'); 5.05 (ddd, 1H, $J_{8,9} = 6.9$ Hz, H-8); 5.18 – 5.26 (m, 1H, H-4); 5.36 (dd, 1H, $J_{7,8} = 5.2$ Hz, H-7). Spectroscopic data are analogous to those reported in the literature.²²⁶

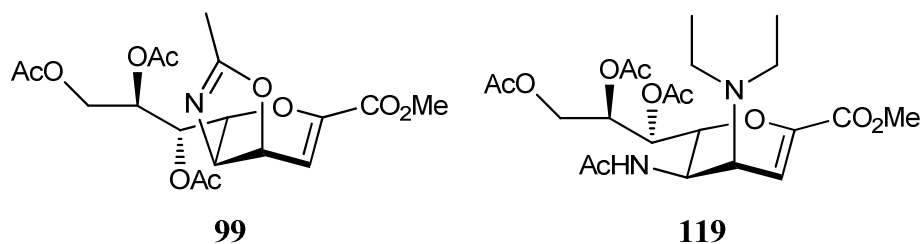
**100**

Methyl 5-*N*-acetamido-4,7,8,9-tetra-*O*-acetyl-2,3,5-trideoxy-D-glycero-D-galactonon-2-enopyranosonate (**100**)

Trimethylsilyl trifluoromethanesulfonate (1.0 mL, 5.6 mmol) was added drop-wise to a solution of the per-*O*-acetylated sialic acid (**101**) (3.0 g, 5.6 mmol) in dry acetonitrile (100 mL) at 4 °C, and the solution left to warm to room temperature overnight. The temperature was then lowered to 4 °C and potassium carbonate (1.2 g, 8.4 mmol) was added. The mixture was left at this temperature for 5 min, filtered, the filtrate evaporated *in vacuo* and the residue purified by flash chromatography (EtOAc:Hexane 9:1 → EtOAc) to afford the per-*O*-acetylated-Neu5Ac2ene (**100**) as a white solid (2.0 g, 75%). ¹H NMR (400 MHz, CDCl₃): δ 1.91 (s, 3H, NHC(O)CH₃); 2.03, 2.04, 2.06, 2.10 (4s, 12H, C(O)CH₃); 3.78 (s, 3H, OCH₃); 4.17 (dd, 1H, $J_{8,9} = 7.0$, $J_{9,9'} = 12.5$ Hz, H-9); 4.34 - 4.42 (m, 2H, H-5, H-6); 4.59 (dd, 1H, $J_{8,9'} = 3.1$ Hz, H-9'); 5.32 – 5.35 (m, 1H, H-8); 5.45 – 5.50 (m, 2H, H-4, H-7); 5.68 (d, 1H, $J_{5,NHAc} = 8.6$ Hz, NH); 5.97 (d, 1H, $J_{3,4} = 3.1$ Hz, H-3). ¹³C NMR (100 MHz, CDCl₃): δ 20.71, 20.84 (C(O)CH₃); 23.15 (NHC(O)CH₃); 46.52 (C-5); 52.58 (OCH₃); 61.85 (C-9); 67.55 (C-4); 67.71 (C-7); 70.53 (C-8); 76.54 (C-6); 107.82 (C-3); 144.99 (C-2); 161.57 (C-1); 170.02, 170.06, 170.13, 170.57 (C(O)CH₃); 170.72 (NHC(O)CH₃). Spectroscopic data are analogous to those reported in the literature.²²⁷

Methyl 7,8,9-tri-*O*-acetyl-2,3-didehydro-2,3,5-trideoxy-4',5'-dihydro-2'-methyloxazolo[5,4d]-D-glycero-D-talo-non-2-ulopyranosidonate (**99**)

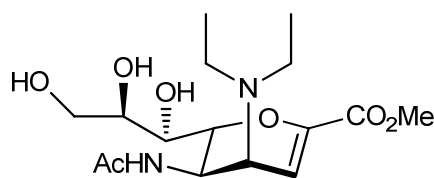
Trimethylsilyl trifluoromethanesulfonate (1.05 mL, 5.62 mmol) was added to a solution of per-*O*-acetylated-Neu5Ac2ene (**100**) (1.0 g, 1.87 mmol) in acetonitrile (20.0 mL) at 4 °C and the solution was heated to 50 °C overnight. The solution was then cooled to 4 °C and potassium carbonate (1.55 g, 11.3 mmol) was added and stirred for 5 min. The mixture was filtered over Celite[®] and the filtrate evaporated to dryness. The crude mixture was purified by flash chromatography (EtOAc:Pet Ether 6:4 → EtOAc:Pet Ether 9:1) affording the oxazoline (**99**) as a light yellow solid (587 mg, 76%). ¹H NMR (400 MHz, CDCl₃): δ 2.01, 2.05, 2.06 (3s, 9H, C(O)CH₃); 2.15 (s, 3H, CCH₃); 3.43 (dd, 1H, *J*_{6,7} = 2.7, *J*_{5,6} = 9.8 Hz, H-6); 3.81 (s, 3H, OCH₃); 3.95 (t, 1H, H-5); 4.23 (dd, 1H, *J*_{8,9} = 6.3, *J*_{9,9'} = 12.5 Hz, H-9); 4.60 (br dd, 1H, *J*_{8,9'} = 2.7 Hz, H-9'); 4.82 (dd, 1H, *J*_{3,4} = 4.0, *J*_{4,5} = 8.5 Hz, H-4); 5.44 (dt, 1H, *J*_{7,8} = 6.3 Hz, H-8); 5.63 (dd, 1H, H-7); 6.38 (d, 1H, H-3). ¹³C NMR (100 MHz, CDCl₃): δ 14.18 (CCH₃); 20.65, 20.81, 20.88 (C(O)CH₃); 52.57 (OCH₃); 62.02 (C-9); 62.10 (C-5); 68.89 (C-7); 70.32 (C-8); 72.27 (C-4); 76.78 (C-6); 107.59 (C-3); 147.19 (C-2); 161.90 (C-1); 167.20 (CCH₃); 169.60, 169.83, 170.68 (C(O)CH₃). HRMS (ESI +ve) *m/z* 414.1396 [M+H]⁺ (C₁₈H₂₄NO₁₀ requires 414.1400). Spectroscopic data are analogous to those reported in the literature.¹⁵⁶



Methyl 5-*N*-acetamido-7,8,9-tri-*O*-acetyl-2,3-didehydro-2,3,4,5-tetradeoxy-4-*N,N*-diethylamino-D-glycero-D-talo-non-2-ulopyranosidonate (**119**)

Triethylphosphine (0.12 mL, 20 mol%) was added to palladium allyl chloride dimer (11.0 mg, 5 mol%) in deoxygenated dichloromethane (1.5 mL) and the mixture was stirred at room temperature for 30 min. The diethylamine (0.05 mL, 0.73 mmol) and the catalyst solution were then added to a solution of the oxazoline (**99**) (250 mg, 0.61 mmol) in dichloromethane (1.5 mL) and the solution was stirred for a further

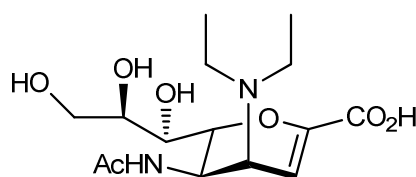
2h. The solution was then filtered over Celite[®] and the filtrate washed with EtOAc. The volume of the solution was reduced *in vacuo* and applied to a flash column (EtOAc \rightarrow EtOAc:MeOH 8:2) to afford the per-*O*-acetylated-4-*epi-N,N*-diethylamino Neu5Ac2ene (**119**) as a pale yellow solid (143 mg, 48%). ¹H NMR (400 MHz, CD₃OD): δ 1.04 (t, 6H, J = 7.4 Hz, N(CH₂CH₃)₂); 1.94 (s, 3H, NHC(O)CH₃); 2.03, 2.03, 2.06 (3s, 9H, C(O)CH₃); 2.70 (q, 4H, N(CH₂CH₃)₂); 3.51 – 3.54 (m, 1H, H-4); 3.78 (s, 3H, OCH₃); 4.16 – 4.20 (m, 3H, H-5, H-6, H-9); 4.60 (br dd, 1H, $J_{8,9'} = 2.9$, $J_{9,9'} = 12.4$ Hz, H-9'); 5.34 (ddd, 1H, $J_{8,9} = 6.5$, $J_{7,8} = 12.1$ Hz, H-8); 5.46 (dd, 1H, $J_{6,7} = 2.9$ Hz, H-7); 6.11 (d, 1H, $J_{3,4} = 5.2$ Hz, H-3). ¹³C NMR (100 MHz, CD₃OD): δ 13.68 (N(CH₂CH₃)₂); 20.64, 20.70, 20.73 (C(O)CH₃); 22.73 (NHC(O)CH₃); 46.96 (N(CH₂CH₃)₂); 47.82 (C-5); 52.76 (OCH₃); 54.65 (C-4); 63.20 (C-9); 69.63 (C-7); 71.79 (C-8); 75.16 (C-6); 110.85 (C-3); 145.14 (C-2); 163.66 (C-1); 171.58, 171.63, 172.42 (C(O)CH₃); 173.06 (NHC(O)CH₃). HRMS (ESI +ve) m/z 487.2285 [M+H]⁺ (C₂₂H₃₅N₂O₁₀ requires 487.2292); 509.2107 [M+Na]⁺ (C₂₂H₃₄N₂O₁₀Na requires 509.2111). Spectroscopic data are analogous to those reported in the literature.¹⁵⁹

**125**

Methyl 5-*N*-acetamido-2,3-didehydro-2,3,4,5-tetradeoxy-4-*N,N*-diethylamino-D-glycero-D-talo-non-2-ulopyranosidonate (**125**)

A 0.5 M solution of sodium methoxide in methanol (0.05 mL) was added to a solution of the per-*O*-acetylated-4-*epi-N,N*-diethylamino Neu5Ac2ene (**119**) (193 mg, 0.4 mmol) in methanol (5.0 mL) at 4 °C and the solution was stirred for 2h at room temperature. The solution was then neutralized (Dowex 50WX8, H⁺ form), filtered and the filtrate concentrated *in vacuo*. Flash chromatography (EtOAc \rightarrow EtOAc:MeOH 9:1) afford the 4-*epi-N,N*-diethylamino Neu5Ac2ene (**125**) as a light yellow solid (111 mg, 78%). m.p. 30 °C (hygroscopic). ¹H NMR (400 MHz, CD₃OD): δ 1.07 (t, 6H, J = 7.0 Hz, N(CH₂CH₃)₂); 2.05 (s, 3H, NHC(O)CH₃); 2.66 - 2.77 (m, 4H, N(CH₂CH₃)₂); 3.53 (dd, 1H, $J_{6,7} = 1.2$, $J_{7,8} = 9.4$ Hz, H-7); 3.60

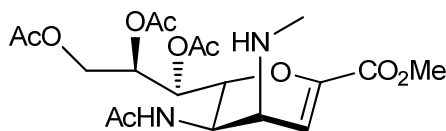
(t, 1H, $J_{4,5} = 5.4$ Hz, H-4); 3.65 (dd, 1H, $J_{8,9} = 5.5$, $J_{9,9'} = 11.8$ Hz, H-9); 3.79 (s, 3H, OCH₃); 3.82 (dd, 1H, $J_{8,9'} = 2.7$ Hz, H-9'); 3.88 – 3.92 (m, 1H, H-8); 4.07 (d, 1H, $J_{5,6} = 10.5$ Hz, H-6); 4.14 (dd, 1H, H-5); 6.10 (d, 1H, $J_{3,4} = 5.5$ Hz, H-3). ¹³C NMR (100 MHz, CD₃OD): δ 12.40 (N(CH₂CH₃)₂); 21.41 (NHC(O)CH₃); 45.83 (N(CH₂CH₃)₂); 46.63 (C-5); 51.34 (OCH₃); 53.34 (C-4); 63.56 (C-9); 69.06 (C-7); 69.87 (C-8); 73.92 (C-6); 108.13 (C-3); 144.85 (C-2); 162.92 (C-1); 172.70 (NHC(O)CH₃). HRMS (ESI +ve) m/z 361.1993 [M+H]⁺ (C₁₆H₂₉N₂O₇ requires 361.1975); 383.1814 [M+Na]⁺ (C₁₆H₂₈N₂O₇Na requires 383.1794).



44

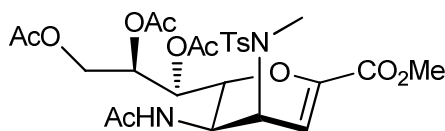
5-*N*-Acetamido-2,3-didehydro-2,3,4,5-tetrahydro-4-*N,N*-diethylamino-D-glycero-D-talo-non-2-ulopyranosonic acid (**44**)

A 0.5 M aqueous solution of sodium hydroxide (2 drops) was added to a solution of 4-*epi-N,N*-diethylamino Neu5Ac2ene (**125**) (96.0 mg, 0.27 mmol) in water (2 mL) at 4 °C and the solution left to warm to room temperature (2h). The solution was then neutralized (Dowex 50WX8, H⁺ form), filtered and the filtrate concentrated *in vacuo* to afford 4-*epi-N,N*-diethylamino Neu5Ac2ene (**44**) as a white solid (93 mg, quantitative). m.p. 141 – 143 °C. ¹H NMR (400 MHz, CD₃OD): δ 1.34 (t, 6H, $J = 7.4$ Hz, N(CH₂CH₃)₂); 2.07 (s, 3H, NHC(O)CH₃); 3.33 – 3.44 (m, 4H, N(CH₂CH₃)₂); 3.61 – 3.74 (m, 3H, H-7, H-8, H-9); 3.78 (dd, 1H, $J_{8,9'} = 2.8$, $J_{9,9'} = 11.0$ Hz, H-9'); 4.44 (t, 1H, $J_{6,7} = 3.9$ Hz, H-6); 4.58 (q, 1H, $J_{3,4} = 2.7$, $J_{4,5} = 4.6$ Hz, H-4); 4.93 (t, 1H, H-5); 5.92 (br s, 1H, H-3). ¹³C NMR (100 MHz, CD₃OD): δ 8.24 (N(CH₂CH₃)₂); 21.41 (NHC(O)CH₃); 43.81 (C-5); 45.50 (N(CH₂CH₃)₂); 55.18 (C-4); 63.26 (C-9); 70.74 (C-7); 70.81 (C-8); 79.44 (C-6); 96.43 (C-3); 149.55 (C-2); 164.75 (C-1); 173.03 (NHC(O)CH₃). $[\alpha]_D^{20} = -62.7$ (c 0.05, H₂O). HRMS (ESI -ve) m/z 345.1711 [M-H]⁻ (C₁₅H₂₅N₂O₇ requires 345.1662).

**117**

Methyl 5-*N*-acetamido-7,8,9-tri-*O*-acetyl-2,3-didehydro-2,3,4,5-tetradexoy-4-*N*-methylamino-D-glycero-D-talo-non-2-ulopyranosidonate (**117**)

Triethylphosphine (0.12 mL, 20 mol%) was added to the palladium allyl chloride dimer (11.0 mg, 5 mol%) in deoxygenated dichloromethane (1.5 mL) and the mixture was stirred at room temperature (30 min). A solution of methylamine in tetrahydrofuran (0.37 mL, 2.0 M) and the catalyst solution were then added to a solution of oxazoline (**99**) (250 mg, 0.61 mmol) in dichloromethane (1.5 mL) and the solution was stirred for further 2h. The solution was then filtered over Celite[®] and the filtrate washed with EtOAc. The volume of the solution was reduced *in vacuo* and applied to a flash column (EtOAc:Et₃N 1:0.05 → EtOAc:MeOH:Et₃N 9:1:0.05) to afford per-*O*-acetylated-4-*epi-N*-methylamino Neu5Ac2ene (**117**) as a pale yellow solid (126 mg, 46%). m.p. 35 – 40 °C. ¹H NMR (400 MHz, CD₃OD): δ 1.94 (s, 3H, NHC(O)CH₃); 2.03, 2.04, 2.06 (3s, 9H, C(O)CH₃); 2.45 (s, 3H, NHCH₃); 3.22 (t, 1H, *J*_{4,5} = 4.9 Hz, H-4); 3.77 (s, 3H, OCH₃); 4.18 (dd, 1H, *J*_{8,9} = 6.5, *J*_{9,9'} = 12.6 Hz, H-9); 4.24 (dd, 1H, *J*_{5,6} = 9.7 Hz, H-5); 4.30 (dd, 1H, *J*_{6,7} = 2.9 Hz, H-6); 4.57 (dd, 1H, *J*_{8,9'} = 2.9 Hz, H-9'); 5.35 (ddd, 1H, *J*_{7,8} = 6.5 Hz, H-8); 5.47 (dd, 1H, H-7); 6.17 (d, 1H, *J*_{3,4} = 5.2 Hz, H-3). ¹³C NMR (100 MHz, CD₃OD): δ 20.65, 20.70, 20.75 (C(O)CH₃); 22.71 (NHC(O)CH₃); 35.35 (NHCH₃); 47.46 (C-5); 52.75 (OCH₃); 53.45 (C-4); 63.17 (C-9); 69.49 (C-7); 71.60 (C-8); 74.45 (C-6); 110.77 (C-3); 144.67 (C-2); 163.87 (C-1); 171.58, 172.40 (C(O)CH₃); 173.37 (NHC(O)CH₃). HRMS (ESI +ve) *m/z* 445.1803 [M+H]⁺ (C₁₉H₂₉N₂O₁₀ requires 445.1822); 467.1619 [M+Na]⁺ (C₁₉H₂₈N₂O₁₀Na requires 467.1642). Spectroscopic data are analogous to those reported in the literature.¹⁵⁹

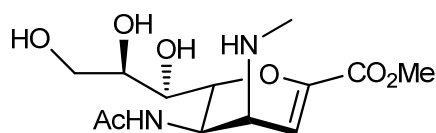
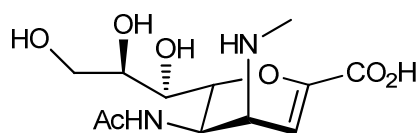
**120**

Methyl 5-*N*-acetamido-7,8,9-tri-*O*-acetyl-2,3-didehydro-2,3,4,5-tetradecoxy-4-(*N*-methyl-*N*-4-methylbenzenesulfonamide)-D-glycero-D-talo-non-2-ulopyranosidonate (**120**)

Triethylamine (0.06 mL, 0.43 mmol) and *p*-toluenesulfonyl chloride (81.7 mg, 0.43 mmol) were added to a solution of per-*O*-acetylated-4-*epi-N*-methylamino Neu5Ac2ene (**117**) (127 mg, 0.29 mmol) in dichloromethane (2 mL) at room temperature and stirred overnight. The solution was then subject to a standard work up (DCM) and the residue purified by flash chromatography (EtOAc:Pet Ether 9:1 → EtOAc:MeOH:Et₃N 7:3:0.5) to afford the tosyl protected compound (**120**) as a light yellow solid (64.2 mg, 38%). ¹H NMR (400 MHz, CDCl₃): δ 2.01 (s, 3H, NHC(O)CH₃); 2.04, 2.06, 2.10 (3s, 9H, C(O)CH₃); 2.44 (s, 3H, CH₃NSO₂PhCH₃); 2.76 (s, 3H, CH₃NSO₂PhCH₃); 3.76 (s, 3H, OCH₃); 4.12 (dd, 1H, *J*_{8,9} = 7.4, *J*_{9,9'} = 12.2 Hz, H-9); 4.17 (br dd, 1H, *J*_{6,7} = 2.2, *J*_{5,6} = 11.3 Hz, H-6); 4.47 – 4.53 (m, 2H, H-4, H-5); 4.74 (dd, 1H, *J*_{8,9'} = 2.6 Hz, H-9'); 5.28 – 5.32 (m, 1H, H-8); 5.43 (d, 1H, *J*_{3,4} = 5.2 Hz, H-3); 4.97 (dd, 1H, *J*_{7,8} = 4.3 Hz, H-7); 5.87 (d, 1H, *J*_{5,NHAc} = 9.6 Hz, NH); 7.33 (d, 2H, *J* = 8.3 Hz, CH Ph); 7.65 (d, 2H, *J* = 8.3 Hz, CH Ph). ¹³C NMR (100 MHz, CDCl₃): δ 20.63, 20.72, 20.85 (C(O)CH₃); 21.51 (CH₃NSO₂PhCH₃); 23.24 (NHC(O)CH₃); 34.67 (CH₃NSO₂PhCH₃); 45.39 (C-4); 51.10 (C-5); 52.56 (OCH₃); 62.18 (C-9); 67.98 (C-7); 71.53 (C-8); 74.06 (C-6); 104.81 (C-3); 127.18 (C Ph); 130.06 (C Ph); 134.80 (Cq Ph); 144.21 (Cq Ph); 146.49 (C-2); 161.55 (C-1); 169.84, 170.32, 170.54 (C(O)CH₃); 170.90 (NHC(O)CH₃). HRMS (ESI +ve) *m/z* 599.1904 [M+H]⁺ (C₂₆H₃₅N₂O₁₂S requires 599.1911); 621.1709 [M+Na]⁺ (C₂₆H₃₄N₂O₁₂SNa requires 621.1730). Spectroscopic data are analogous to those reported in the literature.¹⁵⁹

Methyl 5-*N*-acetamido-2,3-didehydro-2,3,4,5-tetradeoxy-4-*N*-methylamino-D-glycero-D-talo-2-nonulopyranosidonate (**123**)

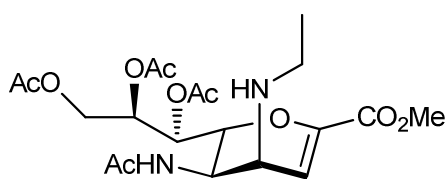
A 0.5 M solution of sodium methoxide in methanol (0.04 mL) was added to a solution of the per-*O*-acetylated-4-*epi-N*-methylamino Neu5Ac2ene (**117**) (74.5 mg, 0.17 mmol) in methanol (2.2 mL) at 4 °C and the solution allowed to warm to room temperature (2h). The solution was then neutralized (Dowex 50WX8, H⁺ form), filtered and the filtrate concentrated *in vacuo*. Flash chromatography (EtOAc → EtOAc:MeOH 8:2) afforded the 4-*epi-N*-methylamino Neu5Ac2ene (**123**) as a light yellow solid (45.0 mg, 83%). m.p. 30 °C (hygroscopic). ¹H NMR (400 MHz, CD₃OD): δ 2.03 (s, 3H, NHC(O)CH₃); 2.48 (s, 3H, NHCH₃); 3.33 (t, 1H, *J*_{4,5} = 4.7 Hz, H-4); 3.60 (d, 1H, *J*_{7,8} = 7.8 Hz, H-7); 3.65 (dd, 1H, *J*_{8,9} = 5.5, *J*_{9,9'} = 11.3 Hz, H-9); 3.78 (s, 3H, OCH₃); 3.80 – 3.90 (m, 2H, H-8, H-9'); 4.17 (dd, 1H, *J*_{6,7} = 1.2, *J*_{5,6} = 9.0 Hz, H-6); 4.28 (dd, 1H, H-5); 6.19 (d, 1H, *J*_{3,4} = 5.1 Hz, H-3). ¹³C NMR (100 MHz, CD₃OD): δ 21.28 (NHC(O)CH₃); 33.51 (NHCH₃); 46.55 (C-5); 51.34 (OCH₃); 51.71 (C-4); 63.49 (C-9); 69.37 (C-7); 70.19 (C-8); 74.17 (C-6); 108.90 (C-3); 143.62 (C-2); 163.24 (C-1); 172.67 (NHC(O)CH₃). HRMS (ESI +ve) *m/z* 319.1497 [M+H]⁺ (C₁₃H₂₃N₂O₇ requires 319.1505); 341.1319 [M+Na]⁺ (C₁₃H₂₂N₂O₇Na requires 341.1325).

**123****42**

5-*N*-Acetamido-2,3-didehydro-2,3,4,5-tetradeoxy-4-*N*-methylamino-D-glycero-D-talo-2-nonulopyranosonic acid (**42**)

A 0.5 M aqueous solution of sodium hydroxide (1 drop) was added to a solution of 4-*epi-N*-methylamino Neu5Ac2ene (**123**) (14.6 mg, 0.05 mmol) in water (0.5 mL) at 4 °C and the solution left to warm to room temperature (2h). The solution was then neutralized (Dowex 50WX8, H⁺ form), filtered and the filtrate concentrated *in vacuo* to afford 4-*epi-N*-methylamino Neu5Ac2ene (**42**) as a white solid (20 mg,

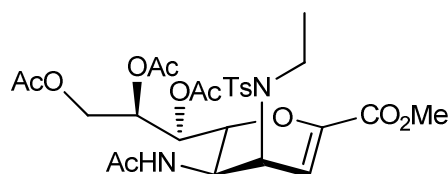
quantitative). m.p. 30 °C (hygroscopic). ^1H NMR (500 MHz, D_2O): δ 2.00 (s, 3H, NHC(O)CH_3); 2.34 (s, 3H, NHCH_3); 3.38 – 3.40 (m, 1H, H-4); 3.58 – 3.89 (m, 4H, H-7, H-8, H-9, H-9'); 4.23 (dd, 1H, $J_{6,7} = 2.0$, $J_{5,6} = 8.5$ Hz, H-6); 4.31 (dd, 1H, $J_{4,5} = 4.5$ Hz, H-5); 5.81 (d, 1H, $J_{3,4} = 4.5$ Hz, H-3). ^{13}C NMR (125 MHz, D_2O): δ 21.68 (NHC(O)CH_3); 32.58 (NHCH_3); 46.23 (C-5); 50.96 (C-4); 62.85 (C-9); 68.94 (C-7); 70.04 (C-8); 73.04 (C-6); 104.06 (C-3); 146.02 (C-2); 165.04 (C-1); 173.07 (NHC(O)CH_3). $[\alpha]_D^{20} = +22.2$ (c 0.03, H_2O). HRMS (ESI -ve) m/z 303.1199 $[\text{M-H}]^-$ ($\text{C}_{12}\text{H}_{19}\text{N}_2\text{O}_7$ requires 303.1192).

**118**

Methyl 5-*N*-acetamido-7,8,9-tri-*O*-acetyl-2,3-didehydro-2,3,4,5-tetradeoxy-4-*N*-ethylamino-D-glycero-D-talo-non-2-ulopyranosidonate (**118**)

Triethylphosphine (0.24 mL, 20 mol%) was added to the palladium allyl chloride dimer (22.0 mg, 5 mol%) in deoxygenated dichloromethane (3 mL) and the mixture was stirred at room temperature (30 min). A solution of ethylamine in tetrahydrofuran (1.45 mL, 2.0 M) and the catalyst solution were then added to a solution of oxazoline (**99**) (500 mg, 1.21 mmol) in dichloromethane (3 mL) and the solution was stirred for further 2h. The solution was then filtered over Celite[®] and this was washed with EtOAc. The volume of the solution was reduced *in vacuo* and applied to a flash column (EtOAc → EtOAc:MeOH:Et₃N 9:1:0.5) to afford per-*O*-acetylated-4-*epi-N*-ethylamino Neu5Ac2ene (**118**) as an off white solid (356 mg, 64%). ^1H NMR (400 MHz, CD_3OD): δ 1.12 (t, 3H, $J = 7.3$ Hz, NHCH_2CH_3); 1.94 (s, 3H, NHC(O)CH_3); 2.03, 2.04, 2.06 (3s, 9H, C(O)CH_3); 2.66–2.82 (m, 2H, NHCH_2CH_3); 3.30–3.34 (m, 1H, H-4); 3.77 (s, 3H, OCH_3); 4.18 (br dd, 1H, $J_{8,9} = 6.6$, $J_{9,9'} = 12.2$ Hz, H-9); 4.22 (dd, 1H, $J_{4,5} = 4.8$, $J_{5,6} = 9.8$ Hz, H-5); 4.29 (dd, 1H, $J_{6,7} = 3.1$ Hz, H-6); 4.59 (br dd, 1H, $J_{8,9'} = 3.1$, H-9'); 5.35 (ddd, 1H, $J_{7,8} = 6.3$ Hz, H-8); 5.47 (dd, 1H, H-7); 6.16 (d, 1H, $J_{3,4} = 5.2$ Hz, H-3). ^{13}C NMR (100 MHz, CD_3OD): δ 15.33 (NHCH_2CH_3); 20.65, 20.73, 20.76, (C(O)CH_3); 22.73

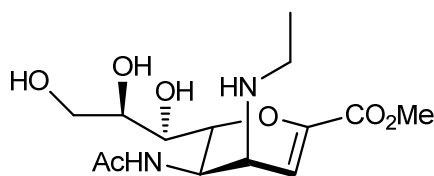
(NHC(O)CH₃); 44.00 (NHCH₂CH₃); 47.42 (C-5); 51.59 (C-4); 52.76 (OCH₃); 63.20 (C-9); 69.52 (C-7); 71.70 (C-8); 74.57 (C-6); 111.08 (C-3); 144.64 (C-2); 163.87 (C-1); 171.58, 171.61, 172.39 (C(O)CH₃); 173.29 (NHC(O)CH₃). HRMS (ESI +ve) m/z 459.1960 [M+H]⁺ (C₂₀H₃₁N₂O₁₀ requires 459.1979); 481.1790 [M+Na]⁺ (C₂₀H₃₀N₂O₁₀Na requires 481.1798). Spectroscopic data are analogous to those reported in the literature.¹⁵⁹

**121**

Methyl 5-*N*-acetamido-7,8,9-tri-*O*-acetyl-2,3-didehydro-2,3,4,5-tetradecoxy-4-(*N*-ethyl-*N*-4-methylbenzenesulfonamide)-D-glycero-D-talo-non-2-ulopyranosidonate (**121**)

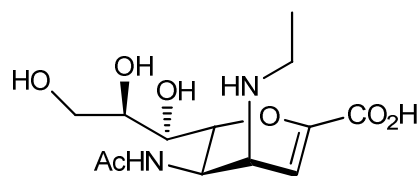
Triethylamine (0.08 mL, 0.64 mmol) and *p*-toluenesulfonyl chloride (122 mg, 0.64 mmol) were added to a solution of per-*O*-acetylated-4-*epi-N*-ethylamino Neu5Ac2ene (**118**) (195mg, 0.42 mmol) in dichloromethane (2 mL) at room temperature and stirred overnight. The solution was then subject to a standard work up (DCM) and the residue purified by flash chromatography (EtOAc:Pet Ether 9:1 → EtOAc:MeOH:Et₃N 7:3:0.5) to give the tosyl protected compound (**121**) as an off white solid (76.1 mg, 29%). ¹H NMR (400 MHz, CDCl₃): δ 1.18 (t, 3H, J = 7.1 Hz, CH₃CH₂NSO₂PhCH₃); 2.02 (s, 3H, NHC(O)CH₃); 2.05, 2.06, 2.09 (3s, 9H, C(O)CH₃); 2.43 (s, 3H, CH₃CH₂NSO₂PhCH₃); 3.21 – 3.28 (m, 2H, CH₃CH₂NSO₂PhCH₃); 3.76 (s, 3H, OCH₃); 4.15 (br dd, 1H, $J_{8,9}$ = 7.1, $J_{9,9'}$ = 12.3 Hz, H-9); 4.28 (br dd, 1H, $J_{6,7}$ = 2.4, $J_{5,6}$ = 10.4 Hz, H-6); 4.34 (t, 1H, $J_{3,4}$ = 5.2 Hz, H-4); 4.50 – 4.57 (m, 1H, H-5); 4.64 (dd, 1H, $J_{8,9'}$ = 2.8 Hz, H-9'); 5.31 – 5.35 (m, 1H, H-8); 5.45 – 5.47 (m, 1H, H-7); 5.51 (d, 1H, H-3); 5.88 (d, 1H, $J_{5,NHAc}$ = 9.9 Hz, NH); 7.30 (d, 2H, J = 8.0 Hz, CH Ph); 7.66 (d, 2H, J = 8.0 Hz, CH Ph). ¹³C NMR (100 MHz, CDCl₃): δ 15.94 (CH₃CH₂NSO₂PhCH₃); 20.64, 20.75, 20.82 (C(O)CH₃); 21.51 (CH₃CH₂NSO₂PhCH₃); 23.30 (NHC(O)CH₃); 43.48 (CH₃CH₂NSO₂PhCH₃); 45.31 (C-5); 52.53 (C-4); 52.54 (OCH₃); 62.04 (C-9); 67.83 (C-7); 70.96 (C-8); 73.73 (C-6); 106.45 (C-3); 127.26 (C Ph), 129.92 (C Ph); 136.73

(Cq Ph), 144.10 (Cq Ph); 145.88 (C-2); 161.66 (C-1); 169.87, 170.14, 170.59 (C(O)CH₃); 170.84 (NHC(O)CH₃). HRMS (ESI +ve) m/z 613.2074 [M+H]⁺ (C₂₇H₃₇N₂O₁₂S requires 613.2067); 635.1897 [M+Na]⁺ (C₂₇H₃₆N₂O₁₂SNa requires 635.1887).

**124**

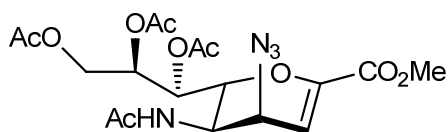
Methyl 5-*N*-acetamido-2,3-didehydro-2,3,4,5-tetradeoxy-4-*N*-ethylamino-D-glycero-D-talo-2-nonulopyranosidonate (**124**)

A 0.5 M solution of sodium methoxide in methanol (0.08 mL) was added to a solution of the per-*O*-acetylated-4-*epi-N*-ethylamino Neu5Ac2ene (**118**) (267 mg, 0.58 mmol) in methanol (8.0 mL) at 4 °C and the solution stirred for 2h at room temperature. The solution was then neutralized (Dowex 50WX8, H⁺ form), filtered and the filtrate concentrated *in vacuo*. The residue was subjected to flash chromatography (EtOAc:MeOH 9:1) to afford the 4-*epi-N*-ethylamino Neu5Ac2ene (**124**) as a white solid (116 mg, 60%). m.p. 30 °C (hygroscopic). ¹H NMR (400 MHz, CD₃OD): δ 1.13 (t, 3H, J = 7.0 Hz, NHCH₂CH₃); 2.04 (s, 3H, NHC(O)CH₃); 2.69 - 2.75 (m, 1H, NHCH₂CH₃); 2.81 - 2.87 (m, 1H, NHCH₂CH₃); 3.43 (t, 1H, $J_{4,5}$ = 5.1 Hz, H-4); 3.58 (d, 1H, $J_{7,8}$ = 9.0 Hz, H-7); 3.65 (dd, 1H, $J_{8,9}$ = 5.5 Hz, $J_{9,9'}$ = 11.3 Hz, H-9); 3.78 (s, 3H, OCH₃); 3.81 - 3.89 (m, 2H, H-8, 9'); 4.15 (d, 1H, $J_{5,6}$ = 9.4 Hz, H-6); 4.24 (dd, $J_{4,5}$ = 4.9, $J_{5,6}$ = 9.5 Hz, 1H, H-5); 6.18 (d, 1H, $J_{3,4}$ = 4.7 Hz, H-3). ¹³C NMR (100 MHz, CD₃OD): δ 14.11 (NHCH₂CH₃); 21.47 (NHC(O)CH₃); 42.21 (NHCH₂CH₃); 46.53 (C-5); 49.90 (C-4); 51.49 (OCH₃); 63.55 (C-9); 69.35 (C-7); 70.18 (C-8); 74.17 (C-6); 109.38 (C-3); 143.56 (C-2); 163.28 (C-1); 172.67 (NHC(O)CH₃). HRMS (ESI +ve) m/z 333.1666 [M+H]⁺ (C₁₄H₂₅N₂O₇ requires 333.1662); 355.1490 [M+Na]⁺ (C₁₄H₂₄N₂O₇Na requires 355.1481).

**43**

5-*N*-Acetamido-2,3-didehydro-2,3,4,5-tetradeoxy-4-*N*-ethylamino-D-glycero-D-talo-non-2-ulopyranosonic acid (**43**)

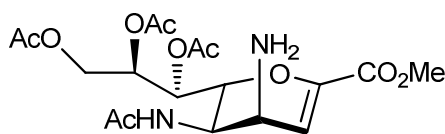
A 0.5 M aqueous solution of sodium hydroxide (5 drops) was added to a solution of the 4-*epi-N*-ethylamino Neu5Ac2ene (**124**) (100 mg, 0.3 mmol) in water (3.0 mL) at 4 °C and the solution left to warm to room temperature (2h). The solution was then neutralized (Dowex 50WX8, H⁺ form), filtered and the filtrate concentrated *in vacuo* to afford the 4-*epi-N*-ethylamino Neu5Ac2ene (**43**) as a yellow solid (110 mg, quantitative). m.p. 30 °C (hygroscopic). ¹H NMR (400 MHz, CD₃OD): δ 1.33 (t, 3H, $J = 7.4$ Hz, NHCH₂CH₃); 2.06 (s, 3H, NHC(O)CH₃); 3.20 (t, 2H, NHCH₂CH₃); 3.61 – 3.69 (m, 2H, H-7, H-9); 3.77 – 3.82 (m, 2H, H-8, H-9'); 4.20 (t, 1H, $J_{3,4} = 3.9$ Hz, H-4); 4.49 (br dd, 1H, $J_{6,7} = 2.8$, $J_{5,6} = 7.5$ Hz, H-6); 4.64 – 4.67 (m, 1H, H-5); 5.70 (d, 1H, $J_{3,4} = 3.9$ Hz, H-3). ¹³C NMR (100 MHz, CD₃OD): δ 10.11 (NHCH₂CH₃); 21.49 (NHC(O)CH₃); 40.92 (NHCH₂CH₃); 44.48 (C-5); 51.28 (C-4); 63.32 (C-9); 69.84 (C-7); 70.53 (C-8); 75.29 (C-6); 95.30 (C-3); 151.53 (C-2); 166.96 (C-1); 173.03 (NHC(O)CH₃). $[\alpha]_D^{20} = -47.9$ (c 0.15, H₂O). HRMS (ESI -ve) m/z 317.1347 [M-H]⁻ (C₁₃H₂₁N₂O₇ requires 317.1349).

**128**

Methyl 5-*N*-acetamido-7,8,9-tri-*O*-acetyl-4-azido-2,3-didehydro-2,3,4,5-tetradeoxy-D-glycero-D-talo-non-2-ulopyranosidonate (**128**)

Tris(dibenzylideneacetone) dipalladium (332 mg, 0.36 mmol) and triphenylphosphine (190 mg, 0.73 mmol) were added to a solution of oxazoline (**99**) (1.5 g, 3.63 mmol) in tetrahydrofuran (15.0 mL) at room temperature and heated to 50 °C. After 30 min azidotrimethylsilane (1.91 mL, 14.5 mmol) was added and the solution was stirred at

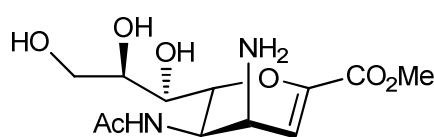
this temperature overnight. The solution was then filtered over Celite[®] and the filtrate concentrated *in vacuo*. The crude mixture was purified by flash chromatography (EtOAc:Pet Ether 7:3 → EtOAc:Pet Ether 9:1) to afford the per-*O*-acetylated-4-epi-azido Neu5Ac2ene (**128**) as a white solid (496 mg, 30%). ¹H NMR (400 MHz, CDCl₃): δ 1.97 (s, 3H, NHC(O)CH₃); 2.05, 2.07, 2.09 (3s, 9H, C(O)CH₃); 3.82 (s, 3H, OCH₃); 4.13 – 4.19 (m, 3H, H-4, H-6, H-9); 4.50 (dt, 1H, $J_{4,5} = 4.3$, $J_{5,6} = 10.5$ Hz, H-5); 4.69 (br dd, 1H, $J_{8,9'} = 2.3$, $J_{9,9'} = 12.1$ Hz, H-9'); 5.30 – 5.33 (m, 1H, H-8); 5.45 (dd, 1H, $J_{7,8} = 2.3$, $J_{6,7} = 5.1$ Hz, H-7); 5.66 (br d, 1H, NH); 6.15 (d, 1H, $J_{3,4} = 5.9$ Hz, H-3). ¹³C NMR (100 MHz, CDCl₃): δ 20.66, 20.75, 20.88 (C(O)CH₃); 23.20 (NHC(O)CH₃); 44.80 (C-5); 52.67 (OCH₃); 54.80 (C-4); 62.08 (C-9); 67.56 (C-7); 71.25 (C-8); 73.56 (C-6); 104.47 (C-3); 146.32 (C-2); 161.47 (C-1); 169.84 (NHC(O)CH₃); 169.98, 170.19, 170.56 (C(O)CH₃). HRMS (ESI +ve) m/z 457.1564 [M+H]⁺ (C₁₈H₂₅N₄O₁₀ requires 457.1571); 479.1379 [M+Na]⁺ (C₁₈H₂₄N₄O₁₀Na requires 479.1390). Spectroscopic data are analogous to those reported in the literature.¹⁵⁶

**127**

Methyl 5-*N*-acetamido-7,8,9-tri-*O*-acetyl-4-*N*-amino-2,3-didehydro-2,3,4,5-tetradeoxy-D-glycero-D-talo-2-nonulopyranosidonate (**127**)

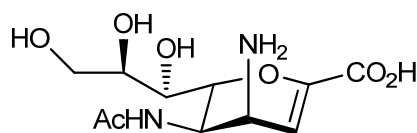
1,3-Propanedithiol (0.22 mL, 2.15 mmol) and triethylamine (0.3 mL, 2.15 mmol) were added to a solution of per-*O*-acetylated-4-epi-azido Neu5Ac2ene (**128**) (197 mg, 0.43 mmol) in methanol (4 mL) at 4 °C and stirred for 5 min after which the solution was allowed to warm to room temperature (2h). Acetic acid was added until pH 3 and then the solution was concentrated *in vacuo*. Flash chromatography (EtOAc:Pet Ether 9:1) afforded the per-*O*-acetylated-4-epi-amino Neu5Ac2ene (**127**) as a white solid (118 mg, 63%). m.p. 30 °C (hygroscopic). ¹H NMR (400 MHz, CDCl₃): δ 1.95 (s, 3H, NHC(O)CH₃); 2.05, 2.06, 2.10 (3s, 9H, C(O)CH₃); 3.43 - 3.49 (m, 1H, H-4); 3.78 (s, 3H, OCH₃); 4.02 (br dd, 1H, $J_{6,7} = 2.7$, $J_{5,6} = 10.5$ Hz, H-6); 4.17 (dd, 1H, $J_{8,9} = 7.4$, $J_{9,9'} = 12.1$ Hz, H-9); 4.28 (td, 1H, $J_{4,5} = 4.7$, $J_{5,6} = 10.2$ Hz,

H-5); 4.74 (dd, 1H, $J_{8,9'} = 2.8$, H-9'); 5.30 – 5.34 (m, 1H, H-8); 5.43 (dd, 1H, $J_{7,8} = 4.3$ Hz, H-7); 6.06 (d, $J_{5,\text{NHAc}} = 10.2$ Hz, 1H, NH); 6.11 (d, $J_{3,4} = 5.4$ Hz, H-3). ^{13}C NMR (100 MHz, CDCl_3): δ 20.79, 20.82, 20.95 ($\text{C}(\text{O})\text{CH}_3$); 23.44 ($\text{NHC}(\text{O})\text{CH}_3$); 43.75 (C-4); 45.91 (C-5); 52.40 (OCH_3); 62.32 (C-9); 68.21 (C-7); 71.77 (C-8); 73.48 (C-6); 111.82 (C-3); 143.81 (C-2); 162.35 (C-1); 169.90 ($\text{NHC}(\text{O})\text{CH}_3$); 170.20, 170.40, 170.60 ($\text{C}(\text{O})\text{CH}_3$). HRMS (ESI +ve) m/z 431.1715 $[\text{M}+\text{H}]^+$ ($\text{C}_{18}\text{H}_{27}\text{N}_2\text{O}_{10}$ requires 431.1666); 453.1543 $[\text{M}+\text{Na}]^+$ ($\text{C}_{18}\text{H}_{26}\text{N}_2\text{O}_{10}\text{Na}$ requires 453.1485).

**132**

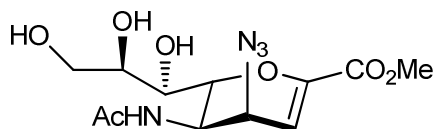
Methyl 5-*N*-acetamido-4-*N*-amino-2,3-didehydro-2,3,4,5-tetraoxo-D-glycero-D-talo-non-2-ulopyranosidionate (**132**)

A 0.5 M solution of sodium methoxide solution in methanol (0.04 mL) was added to a solution of the per-*O*-acetylated-4-*epi*-amino Neu5Ac2ene (**127**) (158 mg, 0.37 mmol) in methanol (4 mL) at 4 °C and the solution stirred at room temperature (2h). The solution was then neutralized (Dowex 50WX8, H^+ form), filtered and the filtrate concentrated *in vacuo*. Flash chromatography ($\text{EtOAc} \rightarrow \text{EtOAc}:\text{MeOH}$ 8:2) afford the 4-*epi*-amino-Neu5Ac2ene (**132**) as a white solid (62.3 mg, 54%). m. p. 65 - 70 °C. ^1H NMR (400 MHz, CD_3OD): δ 2.04 (s, 3H, $\text{NHC}(\text{O})\text{CH}_3$); 3.55 – 3.60 (m, 2H, H-4, H-7); 3.66 (br dd, 1H, $J_{8,9} = 5.5$, $J_{9,9'} = 11.3$ Hz, H-9); 3.77 (s, 3H, OCH_3); 3.83 (br dd, 1H, $J_{8,9'} = 2.8$ Hz, H-9'); 3.88 – 3.92 (m, 1H, H-8); 4.15 – 4.22 (m, 2H, H-5, H-6); 6.10 (d, $J_{3,4} = 5.1$ Hz, H-3). ^{13}C NMR (100 MHz, CD_3OD): δ 21.27 ($\text{NHC}(\text{O})\text{CH}_3$); 43.78 (C-4); 47.65 (C-5); 51.31 (OCH_3); 63.49 (C-9); 68.97 (C-7); 70.12 (C-8); 72.38 (C-6); 111.14 (C-3); 143.63 (C-2); 163.27 (C-1); 172.70 ($\text{NHC}(\text{O})\text{CH}_3$). HRMS (ESI +ve) m/z 305.1375 $[\text{M}+\text{H}]^+$ ($\text{C}_{12}\text{H}_{21}\text{N}_2\text{O}_7$ requires 305.1349); 327.1196 $[\text{M}+\text{Na}]^+$ ($\text{C}_{12}\text{H}_{20}\text{N}_2\text{O}_7\text{Na}$ requires 327.1168).

**126**

5-*N*-Acetamido-4-*N*-amino-2,3-didehydro-2,3,4,5-tetradeoxy-D-glycero-D-talo-non-2-ulopyranosonic acid (**126**)

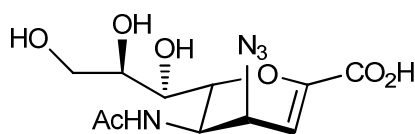
A 0.5 M aqueous solution of sodium hydroxide (1 drop) was added to a solution of the 4-*epi*-amino Neu5Ac2ene (**132**) (24.0 mg, 0.08 mmol) in water (0.6 mL) at 4 °C and the solution left to warm to room temperature (1h). The solution was then neutralized (Dowex 50WX8, H⁺ form), filtered and the filtrate concentrated *in vacuo* to afford the 4-*epi*-amino-Neu5Ac2ene (**126**) as a white solid (23 mg, quantitative). ¹H NMR (500 MHz, D₂O): δ 2.02 (s, 3H, NHC(O)CH₃); 3.60 – 3.90 (m, 4H, H-7, 8, 9, 9'); 4.17 (br s, 1H, H-4); 4.43 – 4.50 (m, 2H, H-5, H-6); 5.69 (d, *J*_{3,4} = 4.0 Hz, H-3). ¹³C NMR (125 MHz, D₂O): δ 21.98 (NHC(O)CH₃); 44.84 (C-4); 44.97 (C-5); 62.91 (C-9); 68.83 (C-7); 69.92 (C-8); 72.05 (C-6); 98.48 (C-3); 151.00 (C-2); 168.57 (C-1); 174.71 (NHC(O)CH₃). HRMS (ESI -ve) *m/z* 289.1001 [M-H]⁻ (C₁₁H₁₇N₂O₇ requires 289.1036).

**130**

Methyl 5-*N*-acetamido-4-azido-2,3-didehydro-2,3,4,5-tetradeoxy-D-glycero-D-talo-non-2-ulopyranosidonate (**130**)

A 0.5 M solution of sodium methoxide solution in methanol (0.08 mL) was added to a solution of the per-*O*-acetylated-4-*epi*-azido Neu5Ac2ene (**128**) (279.3 mg, 0.61 mmol) in methanol (8.0 mL) at 4 °C and the solution stirred for 2h at room temperature. The solution was then neutralized (Dowex 50WX8, H⁺ form), filtered and the filtrate concentrated *in vacuo* to afford 4-*epi*-azido-Neu5Ac2ene (**130**) as a light brown solid (183 mg, 92%). m. p. 145 – 147 °C. ¹H NMR (400 MHz, CD₃OD): δ 2.02 (s, 3H, NHC(O)CH₃); 3.62 (d, 1H, *J*_{6,7} = 10.2 Hz, H-7); 3.67 (dd, 1H,

$J_{8,9} = 5.4$ $J_{9,9'} = 11.3$ Hz, H-9); 3.80 (s, 3H, OCH₃); 3.80 – 3.84 (m, 1H, H-9'); 3.88 – 3.99 (m, 1H, H-8); 4.28 (d, 1H, $J_{5,6} = 11.0$ Hz, H-6); 4.35 (t, 1H, $J_{3,4} = 5.9$ Hz, H-4); 4.41 (dd, 1H, $J_{4,5} = 3.9$ Hz, H-5); 6.12 (d, 1H, H-3). ¹³C NMR (100 MHz, CD₃OD): δ 21.01 (NHC(O)CH₃); 46.61 (C-5); 51.60 (OCH₃); 54.39 (C-4); 63.40 (C-9); 68.23 (C-7); 69.85 (C-8); 72.74 (C-6); 104.42 (C-3); 145.92 (C-2); 162.57 (C-1); 172.35 (NHC(O)CH₃). HRMS (ESI +ve) m/z 331.1283 [M+H]⁺ (C₁₂H₁₈N₄O₇ requires 331.1254); 353.1087 [M+Na]⁺ (C₁₂H₁₈N₄O₇Na requires 353.1073).

**131**

5-*N*-Acetamido-4-azido-2,3-didehydro-2,3,4,5-tetradexoy-D-glycero-D-talo-non-2-ulopyranosonic acid (**131**)

A 0.5 M aqueous solution of sodium hydroxide (2 drops) was added to a solution of 4-epi-azido Neu5Ac2ene (**130**) (27.0 mg, 0.08 mmol) in water (0.5 mL) at 4 °C and the solution left to warm to room temperature (1h). The solution was then neutralized (Dowex 50WX8, H⁺ form), filtered and the filtrate concentrated *in vacuo* to afford 4-epi-azido Neu5Ac2ene (**131**) as a light yellow solid (27.8 mg, quantitative). ¹H NMR (400 MHz, D₂O): δ 1.88 (s, 3H, NHC(O)CH₃); 3.44 – 3.50 (m, 2H, H-7, H-9); 3.69 (br dd, 1H, $J_{8,9'} = 2.7$, $J_{9,9'} = 12.1$ Hz, H-9'); 3.74 – 3.79 (m, 1H, H-8); 4.08 (dd, 1H, $J_{6,7} = 0.8$, $J_{5,6} = 10.6$ Hz, H-6); 4.19 – 4.25 (m, 2H, H-4, H-5); 5.99 (d, 1H, $J_{3,4} = 5.9$ Hz, H-3). ¹³C NMR (100 MHz, D₂O): δ 21.63 (NHC(O)CH₃); 46.35 (C-5); 54.23 (C-4); 62.87 (C-9); 67.84 (C-7); 69.76 (C-8); 72.03 (C-6); 104.92 (C-3); 146.15 (C-2); 165.73 (C-1); 174.05 (NHC(O)CH₃). $[\alpha]_D^{20} = -229.3$ (c 0.08, H₂O). HRMS (ESI -ve) m/z 315.0938 [M-H]⁻ (C₁₁H₁₅N₄O₇ requires 315.0941).

11.3 Biology

11.3.1 Inhibition of influenza neuraminidase

The kinetics studies were performed by following the changes in UV/vis absorbance at a wavelength of 400 nm, in a PerkinElmer Lambda 25 equipped with a circulating Jubalo F10 water bath, maintaining the cells at a temperature of 37 °C. Cells of 1 cm path length were employed for all experiments. The buffer employed was 56 mM Tris.HCl, pH 7.2, containing 4 mM CaCl₂. The time dependent inactivation of influenza neuraminidase by the 7-*N,N*-diethylamino derivative (**39**) was monitored by incubation of the enzyme under the above conditions in the presence of several concentrations (0.1, 0.25 and 2.5 mM) of the inhibitor. Residual enzyme activity was determined at specific time points by the addition of an aliquot (20 µL) of the inactivation mixture to an assay solution (150 µL) containing 4-nitrophenol-sialic acid (100 µM).

11.3.2 Inhibition of *Trypanosoma cruzi* trans-sialidase

11.3.2.1 IC₅₀ determination

The enzyme activity was determined using purified TcTS and the activity measured as a factor of the transfer of sialic acid from 1 mM sialyl- α -(2→3)-lactose to 12 µM [D-glucose-1-¹⁴C]lactose (55 mCi/mmol), in 30 µL containing 0.5 ng of TcTS, 20 mM Hepes-Na (pH 7.5), 0.2% BSA and 30 mM NaCl. After 30 min at 25 °C the reaction was stopped by dilution with 1mL of water, QAE-Sephadex was added, and the resin washed twice with water. Negatively charged compounds were eluted with 0.8 mL of 1M NaCl and quantified in a WinSpectral 1414 liquid scintillation counter.²²³ The inhibition of the TcTS will cause a lower transfer of sialic acid to the ¹⁴C radio labelled lactose. The amount of ¹⁴C radio labelled lactose was measured with a scintillation counter.

11.3.2.2 Inhibition of the infection of cells by trypomastigotes

Vero cells were inserted in a 24-well plate (10^4 cells/well) fitted with a sterile 12-mm-diameter glass cover slip in 500 μ L 10% FBS-MEM and used after 24h of growth. Before infection, the medium was removed and the cells were washed twice with PBS. Different concentrations of inhibitor were added followed by 0.2% BSA-MEM. Prior to incubation, trypomastigotes (100 parasites/cell) were added and the plate was examined under a microscope to ensure that both cells and parasites were viable, and that the introduction of the inhibitor did not produce secondary effects, such as death of the cells and/or parasites. Once the inspection was complete, the plate was incubated for 20h, at a constant temperature of 37 °C under 5% CO₂. The plate was re-examined before changing the medium to ensure that both cells and parasites were alive after the incubation period and that the inhibitor was not cytotoxic. After removing the parasites, the wells were washed with PBS and maintained with 3% FBS-MEM. After the changing of the medium, the plate was examined again with the microscope to certify that the cells were not removed during the procedure. The plate was incubated for a final 72h period. After 72h incubation, the medium was removed and the wells washed with PBS to remove any free particles (*e.g.* dead cells, some parasites that survived the previous wash) several times. After the washings, the glass plates were conditioned for visualisation by the addition of dyes, firstly may-Grünwald (250 μ L). It was left to stand for 5 min, after which water (250 μ L) was added and left to stand for a further 1 min. After removal of the liquid another dye, Giemsa (1/4 dilution with water, 600 μ L) was added and left to stand for 5 min. The role of the dyes is to stain and fix the cells and amastigotes (present in the cytoplasm), and ultimately to close the cell membrane, making it impermeable. After this time the glass support was carefully removed, dipped in water to remove the excess of dye and dried. The plate supports were mounted with DPX mountant onto a glass support plate. The number of infected cells was counted (by eye) and the results expressed as the average of the percentage of infected cells with respect to healthy ones.

Chapter 12 - References

- (1) Traving, C.; Schauer, R. *Cell. Mol. Life Sci.* **1998**, *54*, 1330.
- (2) Lamari, F. N.; Karamanos, N. K. *J. Chromatogr., B: Anal. Technol. Biomed. Life Sci.* **2002**, *781*, 3.
- (3) Chen, X.; Varki, A. *ACS Chem. Biol.* **2010**, *5*, 163.
- (4) Blix, F. G.; Gottschalk, A.; Klenk, E. *Nature* **1957**, *179*, 1088.
- (5) Schauer, R. *Glycoconjugate J.* **2000**, *17*, 485.
- (6) Dekan, G.; Gabel, C.; Farquhar, M. G. *Proc. Natl. Acad. Sci. U. S. A.* **1991**, *88*, 5398.
- (7) El Maarouf, A.; Petridis, A. K.; Rutishauser, U. *Proc. Natl. Acad. Sci. U. S. A.* **2006**, *103*, 16989.
- (8) Johnson, C. P.; Fujimoto, I.; Rutishauser, U.; Leckband, D. E. *J. Biol. Chem.* **2005**, *280*, 137.
- (9) Rutishauser, U. *Nat. Rev. Neurosci.* **2008**, *9*, 26.
- (10) Varki, A. *Trends Mol. Med.* **2008**, *14*, 351.
- (11) Weinhold, B.; Seidenfaden, R.; Roeckle, I.; Muehlenhoff, M.; Schertzinger, F.; Conzelmann, S.; Marth, J. D.; Gerardy-Schahn, R.; Hildebrandt, H. *J. Biol. Chem.* **2005**, *280*, 42971.
- (12) Katopodis, N.; Glantz, M. J.; Kim, L.; Dafni, U.; Wu, J. K.; Perides, G. *Cancer* **2001**, *92*, 856.
- (13) Fukuda, M. *Cancer Res.* **1996**, *56*, 2237.
- (14) Gorelik, E.; Galili, U.; Raz, A. *Cancer Metastasis Rev.* **2001**, *20*, 245.
- (15) Wang, P.-H. *J. Cancer Mol.* **2006**, *2*, 107.
- (16) Williams, T. I.; Toups, K. L.; Saggese, D. A.; Kalli, K. R.; Cliby, W. A.; Muddiman, D. C. *J. Proteome Res.* **2007**, *6*, 2936.
- (17) Miyagi, T.; Wada, T.; Yamaguchi, K. *Biochim. Biophys. Acta* **2008**, *1780*, 532.
- (18) Kakugawa, Y.; Wada, T.; Yamaguchi, K.; Yamanami, H.; Ouchi, K.; Sato, I.; Miyagi, T. *Proc. Natl. Acad. Sci. U. S. A.* **2002**, *99*, 10718.
- (19) Henrissat, B.; Sulzenbacher, G.; Bourne, Y. *Curr. Opin. Struct. Biol.* **2008**, *18*, 527.
- (20) Varki, A. *Glycobiology* **1993**, *3*, 97.

-
- (21) Herscovics, A. *Biochim. Biophys. Acta, Gen. Subj.* **1999**, 1473, 96.
- (22) Matthews, B. W. *C. R. Biol.* **2005**, 328, 549.
- (23) Swallow, D. M. *Nutr. Res. Rev.* **2003**, 16, 37.
- (24) Henrissat, B. *Biochem. J.* **1991**, 280, 309.
- (25) <http://www.cazy.org/>, 15/03/10, 2010.
- (26) Davies, G.; Henrissat, B. *Structure* **1995**, 3, 853.
- (27) Henrissat, B.; Bairoch, A. *Biochem. J.* **1993**, 293, 781.
- (28) Henrissat, B.; Bairoch, A. *Biochem. J.* **1996**, 316 (Pt 2), 695.
- (29) Heightman, T. D.; Vasella, A. T. *Angew. Chem., Int. Ed.* **1999**, 38, 750.
- (30) Stütz, A. E. *Angew. Chem., Int. Ed.* **1996**, 35, 1926.
- (31) Koshland, D. E., Jr. *Biol. Rev. Camb. Phil. Soc.* **1953**, 28, 416.
- (32) Balter, M. *Science* **1997**, 278, 1014.
- (33) Service, R. F. *Science* **1997**, 277, 1217.
- (34) Service, R. F. *Science* **1997**, 278, 1015.
- (35) Withers, S. G. *Carbohydr. Polym.* **2001**, 44, 325.
- (36) Sinnott, M. L. *Chem. Rev.* **1990**, 90, 1171.
- (37) Withers, S. G.; Street, I. P. *J. Am. Chem. Soc.* **1988**, 110, 8551.
- (38) Wang, Q.; Graham, R. W.; Trimbur, D.; Warren, R. A. J.; Withers, S. G. *J. Am. Chem. Soc.* **1994**, 116, 11594.
- (39) Lemieux, M. J.; Mark, B. L.; Cherney, M. M.; Withers, S. G.; Mahuran, D. J.; James, M. N. G. *J. Mol. Biol.* **2006**, 359, 913.
- (40) Groopman, J. E. *Rev. Infect. Dis.* **1990**, 12, 908.
- (41) Laver, W. G.; Bischofberger, N.; Webster, R. G. *Sci. Am.* **1999**, 280, 78.
- (42) Treadway, J. L.; Mendys, P.; Hoover, D. J. *Expert Opin. Invest. Drugs* **2001**, 10, 439.
- (43) Zitzmann, N.; Mehta, A. S.; Carrouee, S.; Butters, T. D.; Platt, F. M.; McCauley, J.; Blumberg, B. S.; Dwek, R. A.; Block, T. M. *Proc. Natl. Acad. Sci. U. S. A.* **1999**, 96, 11878.
- (44) Lillelund, V. H.; Jensen, H. H.; Liang, X.; Bols, M. *Chem. Rev.* **2002**, 102, 515.
- (45) Asano, N. *Glycobiology* **2003**, 13, 93R.
- (46) de Melo, E. B.; Gomes, A. d. S.; Carvalho, I. *Tetrahedron* **2006**, 62, 10277.
- (47) Rempel, B. P.; Withers, S. G. *Glycobiology* **2008**, 18, 570.
- (48) Vodovozova, E. L. *Biochemistry* **2007**, 72, 1.

-
- (49) Halazy, S.; Berges, V.; Ehrhard, A.; Danzin, C. *Bioorg. Chem.* **1990**, *18*, 330.
- (50) Halazy, S.; Danzin, C.; Ehrhard, A.; Gerhart, F. *J. Am. Chem. Soc.* **1989**, *111*, 3484.
- (51) Withers, S. G.; Aebersold, R. *Protein Sci.* **1995**, *4*, 361.
- (52) Withers, S. G.; Street, I. P.; Bird, P.; Dolphin, D. H. *J. Am. Chem. Soc.* **1987**, *109*, 7530.
- (53) Braun, C.; Brayer, G. D.; Withers, S. G. *J. Biol. Chem.* **1995**, *270*, 26778.
- (54) Hart, D. O.; He, S.; Chany, C. J., II; Withers, S. G.; Sims, P. F. G.; Sinnott, M. L.; Brumer, H., III *Biochemistry* **2000**, *39*, 9826.
- (55) Zhang, R.; McCarter, J. D.; Braun, C.; Yeung, W.; Brayer, G. D.; Withers, S. G. *J. Org. Chem.* **2008**, *73*, 3070.
- (56) Ferrer, M.; Golyshina, O. V.; Plou, F. J.; Timmis, K. N.; Golyshin, P. N. *Biochem. J.* **2005**, *391*, 269.
- (57) Watts, A. G.; Damager, I.; Amaya, M. L.; Buschiazzo, A.; Alzari, P.; Frasch, A. C.; Withers, S. G. *J. Am. Chem. Soc.* **2003**, *125*, 7532.
- (58) Gebler, J. C.; Aebersold, R.; Withers, S. G. *J. Biol. Chem.* **1992**, *267*, 11126.
- (59) He, S.; Withers, S. G. *J. Biol. Chem.* **1997**, *272*, 24864.
- (60) Miao, S.; McCarter, J. D.; Grace, M. E.; Grabowski, G. A.; Aebersold, R.; Withers, S. G. *J. Biol. Chem.* **1994**, *269*, 10975.
- (61) Berkowitz, D. B.; Karukurichi, K. R.; de la Salud-Bea, R.; Nelson, D. L.; McCune, C. D. *J. Fluorine Chem.* **2008**, *129*, 731.
- (62) Ly, H. D.; Howard, S.; Shum, K.; He, S. M.; Zhu, A.; Withers, S. G. *Carbohydr. Res.* **2000**, *329*, 539.
- (63) Miao, S. C.; Ziser, L.; Aebersold, R.; Withers, S. G. *Biochemistry* **1994**, *33*, 7027.
- (64) de la Barrera, C. A.; Reyes-Teran, G. *Arch. Med. Res.* **2005**, *36*, 628.
- (65) Lewis, D. B. *Annu. Rev. Med.* **2006**, *57*, 139.
- (66) Potter, C. W. *J. Applied Microbiol.* **2001**, *91*, 572.
- (67) Sullivan, S. J.; Jacobson, R. M.; Dowdle, W. R.; Poland, G. A. *Mayo Clin. Proc.* **2010**, *85*, 64.
- (68) http://www.who.int/csr/disease/avian_influenza/ai_timeline/en/index.html, 16/03/10, 2010.
- (69) Peiris, J. S. M.; Tu, W.-w.; Yen, H.-l. *Eur. J. Immunol.* **2009**, *39*, 2946.

- (70) Dharan, N. J.; Gubareva, L. V.; Meyer, J. J.; Okomo-Adhiambo, M.; McClinton, R. C.; Marshall, S. A.; St. George, K.; Epperson, S.; Brammer, L.; Klimov, A.; Bresee, J. S.; Fry, A. M. *JAMA, J. Am. Med. Assoc.* **2009**, *301*, 1034.
- (71) Presti, R. M.; Zhao, G.; Beatty, W. L.; Mihindukulasuriya, K. A.; Travassos da Rosa, A. P. A.; Popov, V. L.; Tesh, R. B.; Virgin, H. W.; Wang, D. *J. Virol.* **2009**, *83*, 11599.
- (72) Clouthier, S. C.; Rector, T.; Brown, N. E. C.; Anderson, E. D. *J. Gen. Virol.* **2002**, *83*, 421.
- (73) Pinto Da Silva, E. V.; Travassos Da Rosa, A. P. A.; Nunes, M. R. T.; Diniz, J. A. P.; Tesh, R. B.; Cruz, A. C. R.; Vieira, C. M. A.; Vasconcelos, P. F. C. *Am. J. Trop. Med. Hyg.* **2005**, *73*, 1050.
- (74) <http://phil.cdc.gov/phil/home.asp>, 15/03/10, 2010.
- (75) Peiris, J. S. M.; de Jong Menno, D.; Guan, Y. *Clin. Microbiol. Rev.* **2007**, *20*, 243.
- (76) Webster, R. G.; Bean, W. J.; Gorman, O. T.; Chambers, T. M.; Kawaoka, Y. *Microbiol. Rev.* **1992**, *56*, 152.
- (77) von Itzstein, M. *Nat. Rev. Drug Discovery* **2007**, *6*, 967.
- (78) Hilleman, M. R. *Vaccine* **2002**, *20*, 3068.
- (79) Bullough, P. A.; Hughson, F. M.; Skehel, J. J.; Wiley, D. C. *Nature* **1994**, *371*, 37.
- (80) Carr, C. M.; Kim, P. S. *Cell* **1993**, *73*, 823.
- (81) Fuller, S. *Structure* **1994**, *2*, 903.
- (82) De Clercq, E. *Nat. Rev. Drug Discovery* **2006**, *5*, 1015.
- (83) Matrosovich, M. N.; Matrosovich, T. Y.; Gray, T.; Roberts, N. A.; Klenk, H.-D. *J. Virol.* **2004**, *78*, 12665.
- (84) Ohuchi, M.; Asaoka, N.; Sakai, T.; Ohuchi, R. *Microbes Infect.* **2006**, *8*, 1287.
- (85) Suzuki, Y. *Biol. Pharm. Bull.* **2005**, *28*, 399.
- (86) Van Reeth, K. *Vet. Res.* **2007**, *38*, 243.
- (87) <http://news.bbc.co.uk/1/hi/health/8021958.stm>, 08/08/10, 2010.
- (88) Zambon, M. C. *Rev. Med. Virol.* **2001**, *11*, 227.
- (89) Hayden, F. G. *N. Engl. J. Med.* **2006**, *354*, 785.
- (90) Bright, R. A.; Medina, M.-j.; Xu, X.; Perez-Oronoz, G.; Wallis, T. R.; Davis, X. M.; Povinelli, L.; Cox, N. J.; Klimov, A. I. *Lancet* **2005**, *366*, 1175.

- (91) De Clercq, E.; Neyts, J. *Trends Pharmacol. Sci.* **2007**, 28, 280.
- (92) Beigel, J.; Bray, M. *Antiviral Res.* **2008**, 78, 91.
- (93) Smee, D. F.; Hurst, B. L.; Wong, M.-H.; Bailey, K. W.; Morrey, J. D. *Antimicrob. Agents Chemother.* **2009**, 53, 2120.
- (94) Smee, D. F.; Hurst, B. L.; Wong, M.-H.; Bailey, K. W.; Tarbet, E. B.; Morrey, J. D.; Furuta, Y. *Antimicrob. Agents Chemother.* **2010**, 54, 126.
- (95) Furuta, Y.; Takahashi, K.; Kuno-Maekawa, M.; Sangawa, H.; Uehara, S.; Kozaki, K.; Nomura, N.; Egawa, H.; Shiraki, K. *Antimicrob. Agents Chemother.* **2005**, 49, 981.
- (96) Kiso, M.; Takahashi, K.; Sakai-Tagawa, Y.; Shinya, K.; Sakabe, S.; Le, Q. M.; Ozawa, M.; Furuta, Y.; Kawaoka, Y. *Proc. Natl. Acad. Sci. U. S. A.* **2010**, 107, 882.
- (97) von Itzstein, M.; Dyason, J. C.; Oliver, S. W.; White, H. F.; Wu, W.-Y.; Kok, G. B.; Pegg, M. S. *J. Med. Chem.* **1996**, 39, 388.
- (98) von Itzstein, M. *Curr. Opin. Chem. Biol.* **2008**, 12, 102.
- (99) Colman, P. M.; Varghese, J. N.; Laver, W. G. *Nature* **1983**, 303, 41.
- (100) Varghese, J. N.; Laver, W. G.; Colman, P. M. *Nature* **1983**, 303, 35.
- (101) Taylor, N. R.; von Itzstein, M. *J. Med. Chem.* **1994**, 37, 616.
- (102) Chong, A. K. J.; Pegg, M. S.; Taylor, N. R.; Von Itzstein, M. *Eur. J. Biochem.* **1992**, 207, 335.
- (103) Patrick, G. L. *An Introduction to Medicinal Chemistry*; 3rd ed.; Oxford University Press: Oxford, 2005.
- (104) von Itzstein, M.; Wu, W. Y.; Kok, G. B.; Pegg, M. S.; Dyason, J. C.; Jin, B.; Phan Tho, V.; Smythe, M. L.; White, H. F. *Nature* **1993**, 363, 418.
- (105) Woods, J. M.; Bethell, R. C.; Coates, J. A. V.; Healy, N.; Hiscox, S. A.; Pearson, B. A.; Ryan, D. M.; Ticehurst, J.; Tilling, J. *Antimicrob. Agents Chemother.* **1993**, 37, 1473.
- (106) Calfee, D. P.; Peng, A. W.; Cass, L. M.; Lobo, M.; Hayden, F. G. *Antimicrob. Agents Chemother.* **1999**, 43, 1616.
- (107) Gaur, A. H.; Bagga, B.; Barman, S.; Hayden, R.; Lamprey, A.; Hoffman, J. M.; Bhojwani, D.; Flynn, P. M.; Tuomanen, E.; Webby, R. *N. Engl. J. Med.* **2010**, 362, 88.
- (108) Kidd, I. M.; Down, J.; Nastouli, E.; Shulman, R.; Grant Paul, R.; Howell David, C. J.; Singer, M. *Lancet* **2009**, 374, 1036.

- (109) Wallace, A. C.; Laskowski, R. A.; Thornton, J. M. *Protein Eng.* **1995**, *8*, 127.
- (110) Gubareva, L. V.; Matrosovich, M. N.; Brenner, M. K.; Bethell, R. C.; Webster, R. G. *J. Infect. Dis.* **1998**, *178*, 1257.
- (111) Reece, P. A. *J. Med. Virol.* **2007**, *79*, 1577.
- (112) Hurt, A. C.; Holien, J. K.; Parker, M.; Kelso, A.; Barr, I. G. *J. Virol.* **2009**, *83*, 10366.
- (113) Jones, M.; Del Mar, C. *Expert Opin. Drug Saf.* **2006**, *5*, 603.
- (114) Monto, A. S. *Vaccine* **2003**, *21*, 1796.
- (115) Vorwerk, S.; Vasella, A. *Angew. Chem., Int. Ed.* **1998**, *37*, 1732.
- (116) Kim, C. U.; Lew, W.; Williams, M. A.; Wu, H.; Zhang, L.; Chen, X.; Escarpe, P. A.; Mendel, D. B.; Laver, W. G.; Stevens, R. C. *J. Med. Chem.* **1998**, *41*, 2451.
- (117) Kim, C. U.; Lew, W.; Williams, M. A.; Zhang, L.; Liu, H.; Swaminathan, S.; Bischofberger, N.; Chen, M. S.; Tai, C. Y.; Mendel, D. B.; Laver, W. G.; Stevens, R. C. *J. Am. Chem. Soc.* **1997**, *119*, 681.
- (118) Shi, D.; Yang, J.; Yang, D.; LeCluyse, E. L.; Black, C.; You, L.; Akhlaghi, F.; Yan, B. *J. Pharmacol. Exp. Ther.* **2006**, *319*, 1477.
- (119) The PyMOL Molecular Graphics System, Version 1.2r3pre, Schrödinger, LLC.
- (120) Bowles, S. K.; Lee, W.; Simor Andrew, E.; Vearncombe, M.; Loeb, M.; Tamblyn, S.; Fearon, M.; Li, Y.; McGeer, A. *J. Am. Geriatr. Soc.* **2002**, *50*, 608.
- (121) Fuyuno, I. *Nature* **2007**, *446*, 358.
- (122) Hurt, A. C.; Holien, J. K.; Parker, M. W.; Barr, I. G. *Drugs* **2009**, *69*, 2523.
- (123) Smith, J. R.; Sacks, S. *Int. J. Clin. Pract.* **2009**, *63*, 596.
- (124) McKimm-Breschkin, J.; Sahasrabudhe, A.; Blick, T.; McDonald, M. *Int. Congr. Ser.* **2001**, *1219*, 855.
- (125) McKimm-Breschkin, J. L. *Antiviral Res.* **2000**, *47*, 1.
- (126) Baranovich, T.; Saito, R.; Suzuki, Y.; Zaraket, H.; Dapat, C.; Caperig-Dapat, I.; Oguma, T.; Shabana, I. I.; Saito, T.; Suzuki, H. *J. Clin. Virol.* **2010**, *47*, 23.
- (127) Bantia, S.; Arnold, C. S.; Parker, C. D.; Upshaw, R.; Chand, P. *Antiviral Res.* **2006**, *69*, 39.
- (128) Kiso, M.; Kubo, S.; Ozawa, M.; Le, Q. M.; Nidom, C. A.; Yamashita, M.; Kawaoka, Y. *PLoS Pathog.* **2010**, *6*, 1.

- (129) MacDonald, S. J. F.; Watson, K. G.; Cameron, R.; Chalmers, D. K.; Demaine, D. A.; Fenton, R. J.; Gower, D.; Hamblin, J. N.; Hamilton, S.; Hart, G. J.; Inglis, G. G. A.; Jin, B.; Jones, H. T.; McConnell, D. B.; Mason, A. M.; Nguyen, V.; Owens, I. J.; Parry, N.; Reece, P. A.; Shanahan, S. E.; Smith, D.; Wu, W.-Y.; Tucker, S. P. *Antimicrob. Agents Chemother.* **2004**, *48*, 4542.
- (130) MacDonald, S. J. F.; Cameron, R.; Demaine, D. A.; Fenton, R. J.; Foster, G.; Gower, D.; Hamblin, J. N.; Hamilton, S.; Hart, G. J.; Hill, A. P.; Inglis, G. G. A.; Jin, B.; Jones, H. T.; McConnell, D. B.; McKimm-Breschkin, J.; Mills, G.; Nguyen, V.; Owens, I. J.; Parry, N.; Shanahan, S. E.; Smith, D.; Watson, K. G.; Wu, W.-Y.; Tucker, S. P. *J. Med. Chem.* **2005**, *48*, 2964.
- (131) <http://www.nexbio.com/>, 30/03/10, 2010.
- (132) Triana-Baltzer, G. B.; Gubareva, L. V.; Nicholls, J. M.; Pearce, M. B.; Mishin, V. P.; Belser, J. A.; Chen, L.-M.; Chan, R. W. Y.; Chan, M. C. W.; Hedlund, M.; Larson, J. L.; Moss, R. B.; Katz, J. M.; Tumpey, T. M.; Fang, F. *PLoS One* **2009**, *4*, 1.
- (133) Malakhov, M. P.; Aschenbrenner, L. M.; Smee, D. F.; Wandersee, M. K.; Sidwell, R. W.; Gubareva, L. V.; Mishin, V. P.; Hayden, F. G.; Kim, D. H.; Ing, A.; Campbell, E. R.; Yu, M.; Fang, F. *Antimicrob. Agents Chemother.* **2006**, *50*, 1470.
- (134) Nicholls, J. M.; Aschenbrenner, L. M.; Paulson, J. C.; Campbell, E. R.; Malakhov, M. P.; Wurtman, D. F.; Yu, M.; Fang, F. *J. Antimicrob. Chemother.* **2008**, *62*, 426.
- (135) Triana-Baltzer, G. B.; Gubareva, L. V.; Klimov, A. I.; Wurtman, D. F.; Moss, R. B.; Hedlund, M.; Larson, J. L.; Belshe, R. B.; Fang, F. *PLoS One* **2009**, *4*, 1.
- (136) Amaya, M. F.; Watts, A. G.; Damager, I.; Wehenkel, A.; Nguyen, T.; Buschiazzi, A.; Paris, G.; Frasch, A. C.; Withers, S. G.; Alzari, P. M. *Structure* **2004**, *12*, 775.
- (137) Watts, A. G.; Withers, S. G. *Can. J. Chem.* **2004**, *82*, 1581.
- (138) Watts, A. G.; Oppezzo, P.; Withers, S. G.; Alzari, P. M.; Buschiazzi, A. *J. Biol. Chem.* **2006**, *281*, 4149.
- (139) Lew, W.; Chen, X.; Kim, C. U. *Curr. Med. Chem.* **2000**, *7*, 663.
- (140) Meindl, P.; Bodo, G.; Palese, P.; Schulman, J.; Tuppy, H. *Virology* **1974**, *58*, 457.
- (141) Gijzen, H. J. M.; Qiao, L.; Fitz, W.; Wong, C.-H. *Chem. Rev.* **1996**, *96*, 443.
- (142) Lin, C.-C.; Lin, C.-H.; Wong, C.-H. *Tetrahedron Lett.* **1997**, *38*, 2649.

- (143) Beliczey, J.; Kragl, U.; Liese, A.; Wandrey, C.; Hamacher, K.; Coenen, H. H.; Tierling, T.; (Forschungszentrum Jülich G.m.b.H., Germany). Application: US US, 2002, p 11 pp
- (144) Excoffier, G.; Gagnare, D.; Utille, J. P. *Carbohydr. Res.* **1975**, *39*, 368.
- (145) Dax, K.; Albert, M.; Ortner, J.; Paul, B. J. *Carbohydr. Res.* **2000**, *327*, 47.
- (146) Tewson, T. J.; Welch, M. J. *J. Org. Chem.* **1978**, *43*, 1090.
- (147) Michalik, M.; Hein, M.; Frank, M. *Carbohydr. Res.* **2000**, *327*, 185.
- (148) Ágoston, K.; Dobó, A.; Rákó, J.; Kerékgyártó, J.; Szurmai, Z. *Carbohydr. Res.* **2001**, *330*, 183.
- (149) Gerstenberger, M. R. C.; Haas, A. *Angew. Chem., Int. Ed.* **1981**, *93*, 659.
- (150) Stolz, F.; Reiner, M.; Blume, A.; Reutter, W.; Schmidt, R. R. *J. Org. Chem.* **2004**, *69*, 665.
- (151) Palese, P.; Compans, R. W. *J. Gen. Virol.* **1976**, *33*, 159.
- (152) Smith, P. W.; Starkey, I. D.; Howes, P. D.; Sollis, S. L.; Keeling, S. P.; Cherry, P. C.; von Itzstein, M.; Wu, W. Y.; Jin, B. *Eur. J. Med. Chem.* **1996**, *31*, 143.
- (153) Schroven, A.; Meinke, S.; Ziegelmueller, P.; Thiem, J. *Chem.-Eur. J.* **2007**, *13*, 9012.
- (154) Holzer, C. T.; Von Itzstein, M.; Jin, B.; Pegg, M. S.; Stewart, W. P.; Wu, W. Y. *Glycoconjugate J.* **1993**, *10*, 40.
- (155) Schreiner, E.; Zbiral, E.; Kleineidam, R. G.; Schauer, R. *Carbohydr. Res.* **1991**, *216*, 61.
- (156) Schreiner, E.; Zbiral, E.; Kleineidam, R. G.; Schauer, R. *Liebigs Ann. Chem.* **1991**, 129.
- (157) Tsuji, J. *Palladium Reagents and Catalysts: New Perspectives for the 21st Century*; John Wiley & Sons, Ltd: West Sussex, 2004.
- (158) Chang, C.-W.; Norsikian, S.; Beau, J.-M. *Chem.-Eur. J.* **2009**, *15*, 5195.
- (159) Resende, R.; Glover, C.; Watts, A. G. *Tetrahedron Lett.* **2009**, *50*, 4009.
- (160) von Itzstein, M.; Jin, B.; Wu, W. Y.; Chandler, M. *Carbohydr. Res.* **1993**, *244*, 181.
- (161) McDonough, M. J.; Stick, R. V.; Tilbrook, D. M. G.; Watts, A. G. *Aust. J. Chem.* **2004**, *57*, 233.
- (162) Smith, B. J.; McKimm-Breshkin, J. L.; McDonald, M.; Fernley, R. T.; Varghese, J. N.; Colman, P. M. *J. Med. Chem.* **2002**, *45*, 2207.

- (163) <http://www.cdc.gov/flu/weekly/weeklyarchives2008-2009/weekly15.htm>, 31/03/10, 2010.
- (164) Anonymous *Wkly. Epidemiol. Rec.* **2009**, 84, 299.
- (165) Russell, R. J.; Haire, L. F.; Stevens, D. J.; Collins, P. J.; Lin, Y. P.; Blackburn, G. M.; Hay, A. J.; Gamblin, S. J.; Skehel, J. J. *Nature* **2006**, 443, 45.
- (166) Oakley, A. J.; Barrett, S.; Peat, T. S.; Newman, J.; Streltsov, V. A.; Waddington, L.; Saito, T.; Tashiro, M.; McKimm-Breschkin, J. L. *J. Med. Chem.* **2010**, 53, 6421.
- (167) Withers, S. G.; Rupitz, K.; Street, I. P. *J. Biol. Chem.* **1988**, 263, 7929.
- (168) Lineweaver, H.; Burk, D. *J. Am. Chem. Soc.* **1934**, 56, 658.
- (169) Umezawa, E. S.; Stolf, A. M.; Corbett, C. E.; Shikanai-Yasuda, M. A. *Lancet* **2001**, 357, 797.
- (170) Castro, J. A.; Montalto de Mecca, M.; Bartel, L. C. *Hum. Exp. Toxicol.* **2006**, 25, 471.
- (171) Barrett, M. P.; Burchmore, R. J. S.; Stich, A.; Lazzari, J. O.; Frasc, A. C.; Cazzulo, J. J.; Krishna, S. *Lancet* **2003**, 362, 1469.
- (172) Colli, W. *FASEB J.* **1993**, 7, 1257.
- (173) <http://www.flickr.com/photos/ajc1/3330648286/>, 24/05/10, 2010.
- (174) Coura, J. R.; De Castro, S. L. *Mem. Inst. Oswaldo Cruz* **2002**, 97, 3.
- (175) <http://pathmicro.med.sc.edu/lecture/trypanosomiasis.htm>, 15/03/10, 2010.
- (176) Norris, K. A. *Infect. Immun.* **1998**, 66, 2460.
- (177) <http://www.spectroscopynow.com/coi/cda/detail.cda?id=1687&type=Feature&chId=10&page=1>, 15/03/10, 2010.
- (178) Marr, J. J.; Docampo, R. *Rev. Infect. Dis.* **1986**, 8, 884.
- (179) Maya, J. D.; Bollo, S.; Nunez-Vergara, L. J.; Squella, J. A.; Repetto, Y.; Morello, A.; Perie, J.; Chauviere, G. *Biochem. Pharmacol.* **2003**, 65, 999.
- (180) Viotti, R.; Vigliano, C.; Lococo, B.; Bertocchi, G.; Petti, M.; Alvarez, M. G.; Postan, M.; Armentis, A. *Ann. Intern. Med.* **2006**, 144, 724.
- (181) Marin-Neto, J. A.; Rassi, A.; Morillo, C. A.; Avezum, A.; Connolly, S. J.; Sosa-Estani, S.; Rosas, F.; Yusuf, S. *Am. Heart J.* **2008**, 156, 37.
- (182) Andrade, A. L. S. S.; Martelli, C. M. T.; Oliveira, R. M.; Silva, S. A.; Aires, A. I. S.; Soussumi, L. M. T.; Covas, D. T.; Silva, L. S.; Andrade, J. G.; Travassos, L. R.; Almeida, I. C. *Am. J. Trop. Med. Hyg.* **2004**, 71, 594.

- (183) Maguire James, H. *N Engl J Med* **2006**, 355, 760.
- (184) Silveira, C. A.; Castillo, E.; Castro, C. *Rev. Soc. Bras. Med. Trop.* **2000**, 33, 191.
- (185) Solari, A.; Ortiz, S.; Soto, A.; Arancibia, C.; Campillay, R.; Contreras, M.; Salinas, P.; Rojas, A.; Schenone, H. *J. Antimicrob. Chemother.* **2001**, 48, 515.
- (186) Sosa Estani, S.; Segura, E. L.; Ruiz, A. M.; Velazquez, E.; Porcel, B. M.; Yampotis, C. *Am J Trop Med Hyg* **1998**, 59, 526.
- (187) Sgambatti de Andrade, A. L.; Zicker, F.; de Oliveira, R. M.; Almeida Silva, S.; Luquetti, A.; Travassos, L. R.; Almeida, I. C.; de Andrade, S. S.; de Andrade, J. G.; Martelli, C. M. *Lancet* **1996**, 348, 1407.
- (188) Maya, J. D.; Cassels, B. K.; Iturriaga-Vasquez, P.; Ferreira, J.; Faundez, M.; Galanti, N.; Ferreira, A.; Morello, A. *Comp. Biochem. Physiol., Part A: Mol. Integr. Physiol.* **2007**, 146A, 601.
- (189) Diaz de Toranzo, E. G.; Castro, J. A.; Franke de Cazzulo, B. M.; Cazzulo, J. *J. Experientia* **1988**, 44, 880.
- (190) Docampo, R. *Chem. Biol. Interact.* **1990**, 73, 1.
- (191) Urbina, J. A.; Docampo, R. *Trends Parasitol.* **2003**, 19, 495.
- (192) Maya, J. D.; Rodriguez, A.; Pino, L.; Pabon, A.; Ferreira, J.; Pavani, M.; Repetto, Y.; Morello, A. *Biol. Res.* **2004**, 37, 61.
- (193) Romanha, A. J.; Alves, R. O.; Murta, S. M. F.; Silva, J. S.; Ropert, C.; Gazzinelli, R. T. *J. Infect. Dis.* **2002**, 186, 823.
- (194) Turrens, J. F.; Watts, B. P., Jr.; Zhong, L.; Docampo, R. *Mol. Biochem. Parasitol.* **1996**, 82, 125.
- (195) Cerecetto, H.; Gonzalez, M. *Current Topics in Medicinal Chemistry (Hilversum, Netherlands)* **2002**, 2, 1187.
- (196) Croft, S. L.; Barrett, M. P.; Urbina, J. A. *Trends Parasitol.* **2005**, 21, 508.
- (197) Frasc, A. C. C. *Parasitol. Today* **2000**, 16, 282.
- (198) Schenkman, S.; Eichinger, D.; Pereira, M. E. A.; Nussenzweig, V. *Annu. Rev. Microbiol.* **1994**, 48, 499.
- (199) Previato, J. O.; Andrade, A. F. B.; Pessolani, M. C. V.; Mendonca-Previato, L. *Mol. Biochem. Parasitol.* **1985**, 16, 85.
- (200) Zingales, B.; Carniol, C.; De Lederkremer, R. M.; Colli, W. *Mol. Biochem. Parasitol.* **1987**, 26, 135.

- (201) Harth, G.; Haidaris, C. G.; So, M. *Proc. Natl. Acad. Sci. U. S. A.* **1987**, *84*, 8320.
- (202) Parodi, A. J.; Pollevick, G. D.; Mautner, M.; Buschiazso, A.; Sanchez, D. O.; Frasch, A. C. C. *EMBO J.* **1992**, *11*, 1705.
- (203) Schenkman, S.; Pontes de Carvalho, L.; Nussenzweig, V. *J. Exp. Med.* **1992**, *175*, 567.
- (204) Uemura, H.; Schenkman, S.; Nussenzweig, V.; Eichinger, D. *Embo J.* **1992**, *11*, 3837.
- (205) Buscaglia, C. A.; Campo, V. A.; Frasch, A. C. C.; Di Noia, J. M. *Nat. Rev. Microbiol.* **2006**, *4*, 229.
- (206) Colman, P. M.; Smith, B. J. *Structure* **2002**, *10*, 1466.
- (207) Tribulatti, M. V.; Mucci, J.; Van Rooijen, N.; Leguizamon, M. S.; Campetella, O. *Infect. Immun.* **2005**, *73*, 201.
- (208) Todeschini, A. R.; Nunes, M. P.; Pires, R. S.; Lopes, M. F.; Previato, J. O.; Mendonca-Previato, L.; DosReis, G. A. *J. Immunol.* **2002**, *168*, 5192.
- (209) Mucci, J.; Hidalgo, A.; Mocetti, E.; Argibay, P. F.; Leguizamon, M. S.; Campetella, O. *Proc. Natl. Acad. Sci. U. S. A.* **2002**, *99*, 3896.
- (210) Chuenkova, M. V.; Pereira, M. A. *Mol. Biol. Cell* **2000**, *11*, 1487.
- (211) Damager, I.; Buchini, S.; Amaya, M. F.; Buschiazso, A.; Alzari, P.; Frasch, A. C.; Watts, A.; Withers, S. G. *Biochemistry* **2008**, *47*, 3507.
- (212) Neres, J.; Bryce, R. A.; Douglas, K. T. *Drug Discov. Today* **2008**, *13*, 110.
- (213) Buschiazso, A.; Amaya, M. F.; Cremona, M. L.; Frasch, A. C.; Alzari, P. M. *Mol. Cell* **2002**, *10*, 757.
- (214) Cazzulo, J. J.; Frasch, A. C. C. *FASEB J.* **1992**, *6*, 3259.
- (215) Paris, G.; Cremona, M. L.; Amaya, M. F.; Buschiazso, A.; Giambiagi, S.; Frasch, A. C. C.; Alzari, P. M. *Glycobiology* **2001**, *11*, 305.
- (216) Neres, J.; Bonnet, P.; Edwards, P. N.; Kotian, P. L.; Buschiazso, A.; Alzari, P. M.; Bryce, R. A.; Douglas, K. T. *Bioorg. Med. Chem.* **2007**, *15*, 2106.
- (217) Paris, G.; Ratier, L.; Amaya, M. F.; Nguyen, T.; Alzari, P. M.; Frasch, A. C. *C. J. Mol. Biol.* **2005**, *345*, 923.
- (218) Harrison, J. A.; Kartha, K. P.; Turnbull, W. B.; Scheuerl, S. L.; Naismith, J. H.; Schenkman, S.; Field, R. A. *Bioorg. Med. Chem. Lett.* **2001**, *11*, 141.
- (219) Vandekerckhove, F.; Schenkman, S.; Pontes de Carvalho, L.; Tomlinson, S.; Kiso, M.; Yoshida, M.; Hasegawa, A.; Nussenzweig, V. *Glycobiology* **1992**, *2*, 541.

- (220) Agusti, R.; Paris, G.; Ratier, L.; Frasch, A. C. C.; de Lederkremer, R. M. *Glycobiology* **2004**, *14*, 659.
- (221) Busse, H.; Hakoda, M.; Stanley, M.; Streicher, H. *J. Carbohydr. Chem.* **2007**, *26*, 159.
- (222) Buchini, S.; Buschiazzo, A.; Withers, S. G. *Angew. Chem., Int. Ed.* **2008**, *47*, 2700.
- (223) Paris, G.; Ratier, L.; Amaya, M. F.; Nguyen, T.; Alzari, P. M.; Frasch, A. C. *C. J. Mol. Biol.* **2004**, *345*, 923.
- (224) Nakajima, T.; Hori, H.; Orui, H.; Meguro, H.; Ido, T. *Agri. Biol. Chem.* **1988**, *52*, 1209.
- (225) Burkart, M. D.; Zhang, Z.; Hung, S.-C.; Wong, C.-H. *J. Am. Chem. Soc.* **1997**, *119*, 11743.
- (226) Marra, A.; Sinay, P. *Carbohydr. Res.* **1989**, *190*, 317.
- (227) Okamoto, K.; Kondo, T.; Goto, T. *Bull. Chem. Soc. Jpn.* **1987**, *60*, 631.